SIMULATION AND OPTIMISATION OF INDUSTRIAL STEAM REFORMERS

Development of models for both primary and secondary steam reformers and implementation of optimisation to improve both the performance of existing equipment and the design of future equipment.

Austin James DUNN BEng

submitted for the degree

of Doctor of Philosophy

Department of Chemical Engineering

University of Bradford

2004

Abstract

Traditionally the reactor is recognised as the 'heart' of a chemical process system and hence the focus on this part of the system is usually quite detailed. Steam reforming, however, due to the 'building block' nature of its reaction products is unusual and generally is perceived as a 'utility' to other reaction processes and hence the focus is drawn towards the 'main' reaction processes of the system. Additionally as a 'mature' process, steam reforming is often treated as sufficiently defined for the requirements within the overall chemical process.

For both primary and secondary steam reformers several models of varying complexity were developed which allowed assessment of issues raised about previous models and model improvements; drawing on the advancements in modelling that have not only allowed the possibility of increasing the scope of simulations but also increased confidence in the simulation results. Despite the complex nature of the steam reforming systems, a surprisingly simplistic model is demonstrated to perform well, however, to improve on existing designs and maximise the capability of current designs it is shown that more complex models are required.

After model development the natural course is to optimisation. This is a powerful tool which must be used carefully as significant issues remain around its employment. Despite the remaining concerns, some simple optimisation cases showed the potential of the models developed in this work and although not exhaustive demonstrated the benefits of optimisation.

Acknowledgements

I would like to acknowledge all those who have supported my research and made my time in Bradford very enjoyable.

I am greatly indebted to my supervisor Dr. Iqbal Mujtaba for his guidance, expertise and support during my research. Also I would like to acknowledge the other members of the Computational Process Engineering Group who added an extra dimension to life in Bradford with our varied cultural and national diversities. Specifically I would like to offer my thanks to Michael Greaves for our years of friendship and academic discussions and Javier Yustos and Franklin Akwei who I had the pleasure of supervising during their projects in Bradford. I must also thank Process Systems Enterprise and Computational Dynamics for supporting my research by supplying free academic licenses for gPROMS and StarCD respectively. Also my thanks our extended to my friends at Synetix, specifically to Bill Cotton as a source not only of data, but also fruitful discussions.

Last but not least, I would like to thank my parents and my brother who have been constantly supportive and a great source of encouragement throughout my education. I would also like to thank the many friends I have known in Bradford for making my time enjoyable, specifically I should mention Ada, Adrian, Carolina, Chedley, Fr. Chris, Christine, Conin, David, Fr. Dennis, Dennis, Elvira, Emelyn, Fiona, Fr. Gerard, Javier, Jamie, Jim, Joanne, John, Lan, Lisa, Michael, Mark, Matt, Khim, Olivia, Pete, Siobhan, Sukainah, Vishal and Yasuhiro.

Table of contents

Chapter 1

Computer Modelling

Computer modelling is a ubiquitous expression in the field of engineering, which incorporates several forms, defined either by their task or their method of operation. However, the extent of the employment of computer modelling should not be taken as a reflection of its simplicity but as a reflection of the potential of computer modelling. This chapter will introduce several common problems encountered in computer modelling and explain the techniques available to resolve them. These issues of computer modelling are demonstrated in the simulation studies described in later chapters.

1.1 Introduction

Mathematical modelling is a mathematical description of a system, which encompasses anything from a one-line linear equation to the most complicated expressions. The model can yield various information apart from the obvious prior assessment of the viability and safety of operating conditions, also the model can assist in understanding how the system operates or is not operating correctly and can infer operational values where there is no measurement. With this potential, mathematical models are employed for several systems not only in industrial processes but also in the wider world, such as for the dunking of digestive biscuits and the shape of teapot spouts ! For steam reforming as for any reaction process, various mathematical models have been developed with various levels of success.

For both of the process equipment items under consideration, the primary and secondary reformers, the phenomena of interest, e.g. fluid flow and reaction kinetics, can be described mathematically by integral, partial differential, ordinary differential and algebraic equations (IPDAEs), see figure 1.1.1.

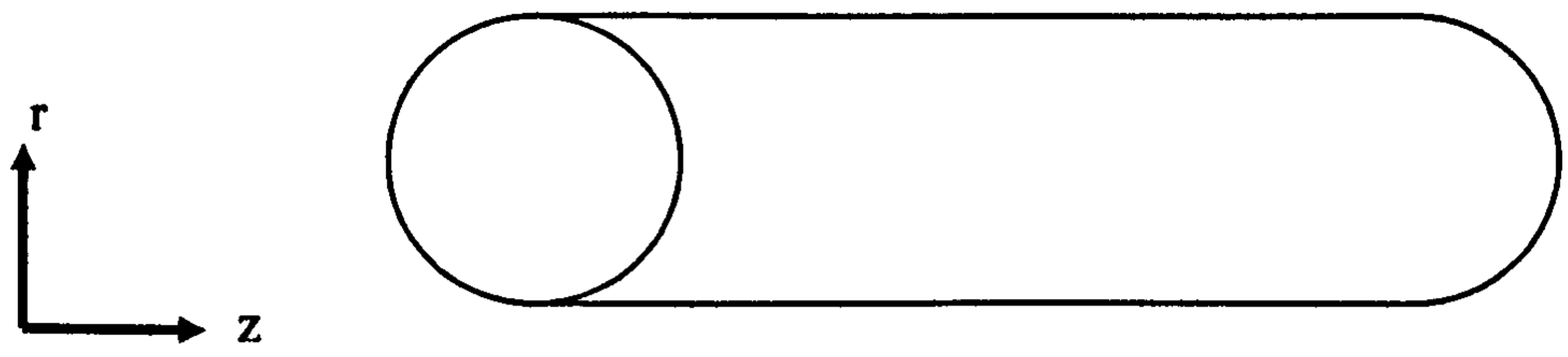

$$\frac{\partial c_i}{\partial t} = -u\frac{\partial c_i}{\partial z} + \varepsilon D_z \frac{\partial^2 c_i}{\partial z^2} + \varepsilon D_r \frac{\partial^2 c_i}{\partial r^2} + \varepsilon D_r \frac{1}{r}\frac{\partial c_i}{\partial r} + \rho_b Nu_i r$$

Figure 1.1.1 Two dimensional dynamic concentration profile for a tubular reactor

As these equations cannot be solved exactly, a numerical solution technique must be implemented to modify the equations into a solvable form. The numerical solution of integral, partial differential, ordinary differential and algebraic equations has been studied for a considerable time and from this several methods have developed including,

- Collocation
- Finite Element
- Finite Difference
- Finite Volume
- Runge-Kutta

The advantages and disadvantages are well discussed by several authors including Press et al. (1992), Zwillinger (1989), Villadsen and Michelsen (1978), Fletcher (1984), Finlayson (1972), Collatz (1966), Pipilis (1990), Duffy (1986) and Versteeg and Malalasekera (1995). There is no one ideal technique considering accuracy and solution time, so often the preference is determined by non-mathematical advantages. For one form of process modelling called computational fluid dynamics (CFD), Versteeg and Malalasekera (1995) highlighted that the Finite Volume technique is adopted for the "clear relationship between the numerical algorithm and the underlying physical conservation principle".

Ultimately, apart from the fact that numerical techniques represent an inexact solution, the accuracy can be influenced by the application of these methods. For example with the finite methods, the system is represented by a number of cells that form a mesh structure, see figure 1.1.2.

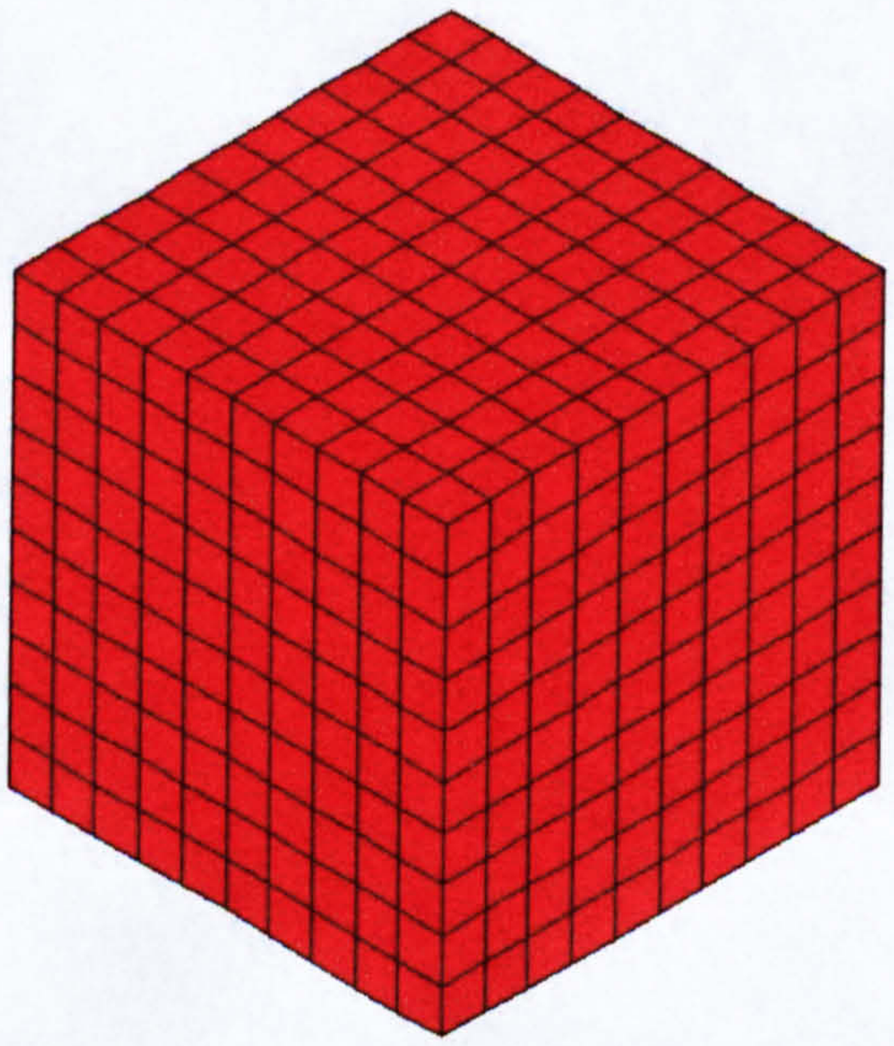

Figure 1.1.2 Mesh structure for a cube system

Ideally, the mesh should contain an infinite number of cells; however, as each cell represents a full set of system variables for that location there is a solution time penalty for each additional cell, hence a trade-off forms between solution time and accuracy. Although the overall density of the mesh is crucial also the distribution of the cells is equally significant as, especially in turbulent flow fields, the distribution can over step the detail of the flow field and not capture the whole field in its solution, see figure 1.1.3.

For all meshes, whether with or without model partitions, the mesh structure is either based on direct experience of the system or by forming a mental picture and then adjusting the mesh as required.

This phenomenon of defining a mesh structure such that it is independent of the final solution is often referred to as 'mesh independence'. This is a key issue for computational fluid dynamics and is demonstrated and further discussed in chapter 4. An infamous example of the trade-off between solution accuracy and time occurred in the UK in October 1987 [MET OFFICE (2004)], when the mesh structure for the MET office weather simulations, predetermined by the capability of the MET office machines, was such that the simulation failed to predict a major storm which caused significant damage in the United Kingdom.

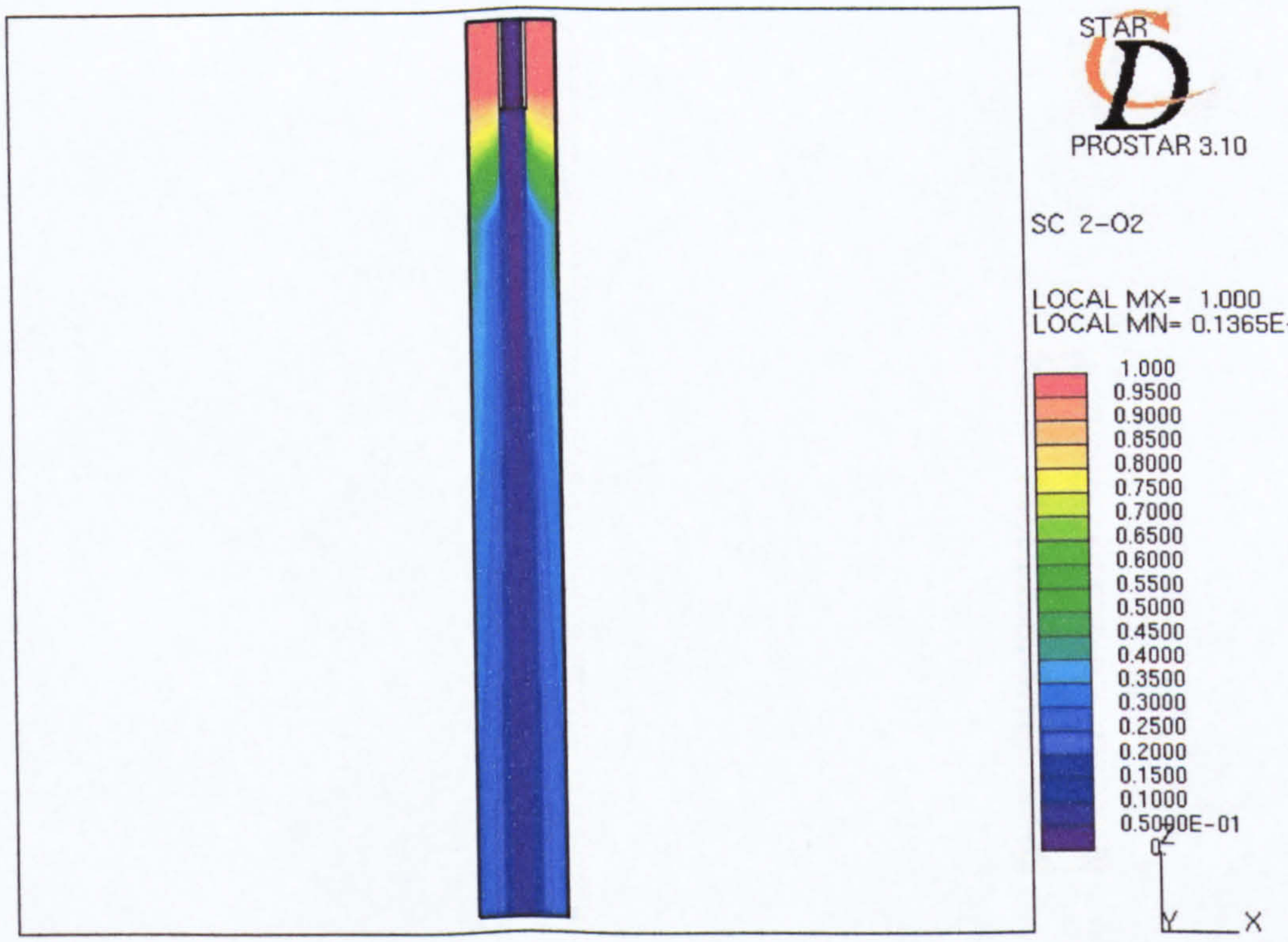

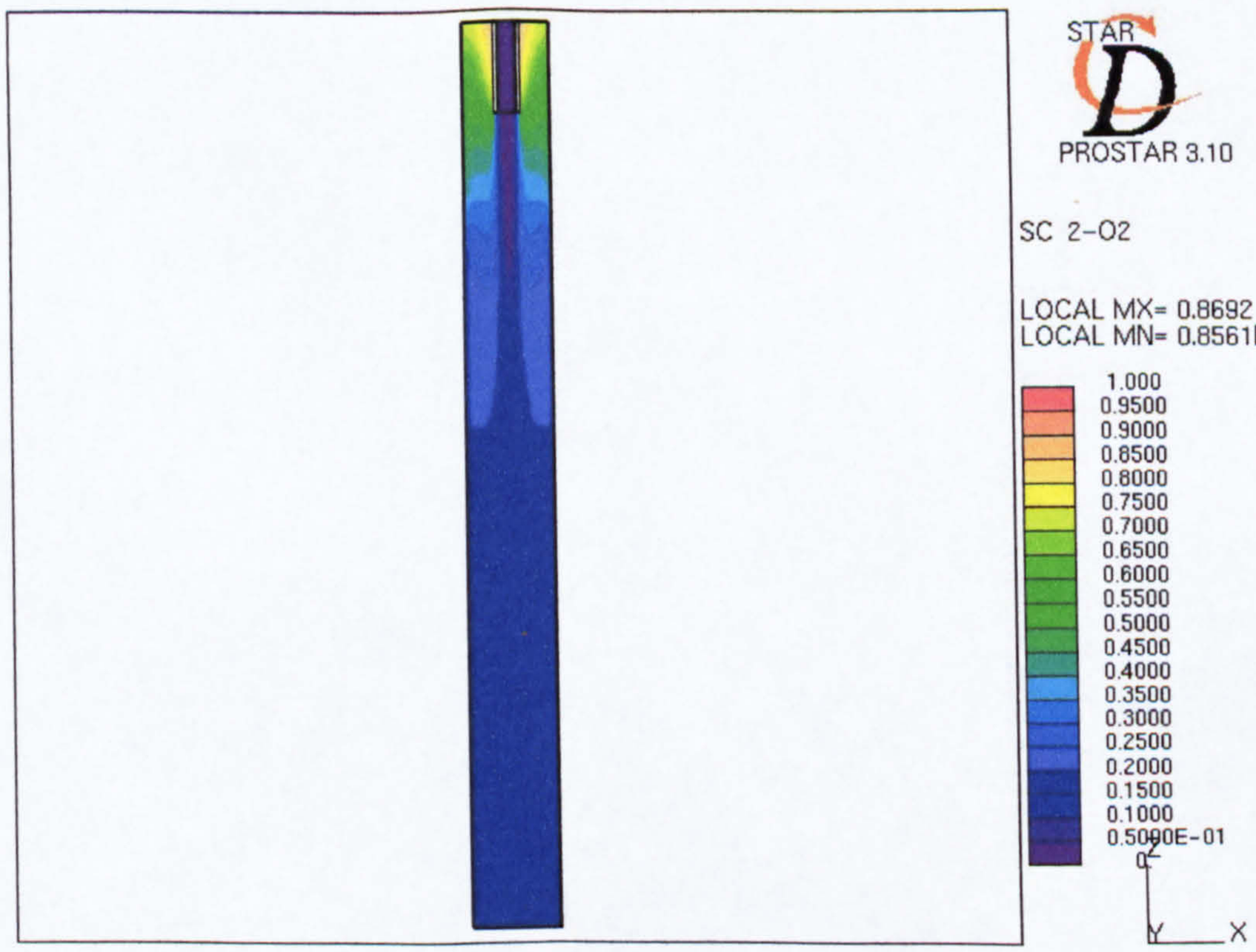

Figure 1.1.3 Alternative meshes with the same number of cells

Another potential source of inaccuracy is the conditions prescribed at the boundaries of the system. The form of presentation for differential equations, ubiquitous in mathematical text, of both the equation and the relevant boundary conditions is the same for IPDAEs, for example,

$$\frac{\partial c_i}{\partial t} = -u\frac{\partial c_i}{\partial z} + \varepsilon D_z \frac{\partial^2 c_i}{\partial z^2} + \varepsilon D_r \frac{\partial^2 c_i}{\partial r^2} + \varepsilon D_r \frac{1}{r}\frac{\partial c_i}{\partial r} + \rho_b Nu_i r \qquad (1)$$

$$c_i = 0 \text{ at } t = 0 \qquad (2)$$

$$\frac{\partial c_i}{\partial z} = 0 \text{ at } z = 0 \qquad (3)$$

$$\frac{\partial c_i}{\partial r} = 0 \text{ at } r = 0 \qquad (4)$$

$$c_i = 0 \text{ at } r = R \qquad (5)$$

Either by defining the incorrect type of boundary, such as setting the mass flux instead of the heat flux, or applying an incorrect magnitude for the condition, the potential inaccuracy is almost limitless to beyond the point of a physically realisable situations. Misappropriate conditioning is as serious a modelling issue as implementing a misappropriate expression in the model, such as laminar flow equations for a turbulent system.

Further to the issues of solution accuracy, the solution attainability can also require techniques external to the numerical solution. Due to the nature of numeric form within a computer system and the nature of these solution methods a significant variation in the magnitude of some key variables can deceive the solver; a suitable variation of magnitude is between 0.1 and 0.9. By redefining the system equations the dimensional nature of the system equations can be removed and the magnitude of all the variables can be harmonised, as demonstrated in Equations 6 to 11.

$$\Sigma (F.c_p)dT / dz = A \,.\, \rho_{catalyst} \,.\, r_{reaction}.\Delta H_r + \pi DQ \qquad (6)$$

$$T = T_{in} \text{ at } z = 0 \qquad (7)$$

$$t' = T / T_{in} \qquad (8)$$

$$dt'/dz = dt'/dt \times dt/dz = (1/T_{in}) \times dt/dz \qquad (9)$$

$$\Sigma (F.cp)\, dt'/dz = 1/T_{in} \times (A \,.\, \rho_{catalyst} \,.\, r_{reaction}.\Delta H_r + \pi DQ) \qquad (10)$$

$$t' = 1 \text{ at } z = 0 \qquad (11)$$

Alternatively instead of redefining the complete system, either the variables can be independently scaled or the system can be partitioned and scaled into regions of similar variable magnitudes; for a heterogeneous reactor simulation a typical model partition is defined between the catalyst pores and the bulk external fluid. Kosek et al. (2001) demonstrate this multi-scale nature of heterogenous reactor modelling and confirm the suitability of the modular approach. Ng (2001) interestingly illustrates this approach on a plant wide basis.

A further solution attainability problem finds its roots in that all the solvers are essentially searching for the solution to the problem and this search must be 'initialised' from a predefined location. This forms a similar problem to that of the boundary definition problem in that if the initial solver conditions are irrelevant to the system then the solver could fail to converge on the solution. However, if the initialisation employs meaningful values, essentially the solver is started 'off on the right foot' which will both increase the chance of a fully converged solution and the speed of solution.

Consider a system, which is defined by Equations 12 to 15,

$$f_1(x_1,x_2,x_3,x_4) = 0 \qquad (12)$$

$$f_2(x_1,x_2,x_3,x_4) = 0 \qquad (13)$$

$$f_3(x_1,x_2,x_3,x_4) = 0 \qquad (14)$$

$$f_4(x_1,x_2,x_3,x_4) = 0 \qquad (15)$$

Linearizing the Equations 12 to 15,

$$f_1'(x_1)\,\delta_1 + f_1'(x_2)\,\delta_2 + f_1'(x_3)\,\delta_3 + f_1'(x_4)\,\delta_4 = -f_1 \qquad (16)$$

$$f_2'(x_1)\,\delta_1 + f_2'(x_2)\,\delta_2 + f_2'(x_3)\,\delta_3 + f_2'(x_4)\,\delta_4 = -f_2 \qquad (17)$$

$$f_3'(x_1)\,\delta_1 + f_3'(x_2)\,\delta_2 + f_3'(x_3)\,\delta_3 + f_3'(x_4)\,\delta_4 = -f_3 \qquad (18)$$

$$f_4'(x_1)\,\delta_1 + f_4'(x_2)\,\delta_2 + f_4'(x_3)\,\delta_3 + f_4'(x_4)\,\delta_4 = -f_4 \qquad (19)$$

or in Matrix form

$$\begin{bmatrix} f_1'(x_1) & f_1'(x_2) & f_1'(x_3) & f_1'(x_4) \\ f_2'(x_1) & f_2'(x_2) & f_2'(x_3) & f_2'(x_4) \\ f_3'(x_1) & f_3'(x_2) & f_3'(x_3) & f_3'(x_4) \\ f_4'(x_1) & f_4'(x_2) & f_4'(x_3) & f_4'(x_4) \end{bmatrix} \begin{bmatrix} \delta_1 \\ \delta_2 \\ \delta_3 \\ \delta_4 \end{bmatrix} = \begin{bmatrix} -f_1 \\ -f_2 \\ -f_3 \\ -f_4 \end{bmatrix} \quad (20)$$

This system of equations is essentially, J . $\underline{\delta}$ = - $\underline{f}$, where J is the Jacobian matrix, $\underline{\delta}$ is the correction vector ($\delta_i = x_i^{n+1} - x_i^n$) and $\underline{f}$ is the vector of functions; the values of x_i^0 are the initialisation of the system. This demonstrates the key role of the initialisation.

For complex systems involving several physical phenomena, the 'initialisation' can be split into several stages to form a 'solution strategy', if the standard initialisation of predefining the variables as fixed parameters is not adequate to solve the system. The next logical step is to stage the process, with the first stage replacing the relevant equations for a number of key variables with a fixed variation, e.g. a polynomial expression for temperature variation along a length $T(z) = \alpha z^2 + \beta z + \chi$, and adopting the solution of this system as the initialisation for the full system. Although this method will yield a more appropriate variation in the magnitude of the key variables for the initialisation, due to the de-coupling of some of the system equations the Jacobian matrix does not hold the exact mathematical representation of the system. If this de-coupling process is unproductive, an alternative strategy is the system equations associated with the solution of the key variables could be scaled over a staged implementation. For example if the key variable chosen to be manipulated is the operating temperature, the heat balance could be adjusted by the introduction of a scaled reaction energy, see Equation 21.

$$\Sigma\,(F.c_p)dT / dz = A\,.\,\rho_{catalyst}\,.\,S_{factor}.\,r_{reaction}.\Delta H_r + \pi DQ \qquad (21)$$

The scaling factor S_{factor}, can be increased over a number of stages till its magnitude equals unity. For each stage of this solution strategy although the magnitude of the key variables may differ from the final solution no de-coupling is required and the Jacobian matrix remains mathematically fully representative. These strategies endorse Pantelides (1988) and Brown et al. (1998) amongst others views that the choice of initial values should be controlled by the system requiring initialisation and further limit the casualness of the choice. In the same spirit to the proposed solution strategy, Vieira and Biscaia Jr. (2001) recommend the employment of "simple and effective initialisation techniques".

Finally, due to the number of equations in a model, the solution technique can often track its own changes and skim over a solution as all equations are considered equal, however, block decomposition organizes the dependent equations to develop a solution strategy.

For example, considering the following system of equations and variables,

$$x_1^2 - x_3 + 15 = 0 \qquad (22)$$

$$x_1x_3 - x_2x_4 + 3 = 0 \qquad (23)$$

$$x_1 - x_2 + x_4 + 2 = 0 \qquad (24)$$

$$x_1x_3^2 - 5 = 0 \qquad (25)$$

Now Equations 22 and 25 can be solved as a 'block' for x_1 and x_3 and equations 23 and 24 can be solved as another 'block' with the solutions of x_1 and x_3 used as constants.

The computer code for several of the favourable numerical solution techniques are available in published literature, such as by Press et al. (1992), Zwillinger (1989) and Villadsen and Michelsen (1978). However, quite often the techniques are "built-in" to commercial computer packages, such as general simulation packages MATLAB and gPROMS and specific packages Star-CD, but still a choice of scheme and settings are user-defined. Modelling with IPDAEs should not be preconceived as possessing a 'black box' solution.

1.2 General Simulation

Almost all instances of simulation of process equipment require the use of differential equations to achieve a reasonable degree of modelling accuracy. With the increase in computer power, the potential modelling accuracy has improved by allowance for other process complexities, e.g. partial differential equations and process discontinuities, in a more viable time-scale.

The recent techniques available in general simulation packages include,

- Dynamic and steady-state simulation
    - continuous and batch processes
    - process discontinuities e.g. laminar/turbulent flow
    - complex operating procedures e.g. start-up
    - distributed systems e.g. tubular reactors
    - Real time applications
- Dynamic and steady-state optimisation. Allows simultaneous optimisation of equipment sizes and operating procedures.
- Dynamic and steady-state parameter estimation

In addition to these modelling techniques the general simulation packages have also developed other features, based on object orientation, to improve other issues than modelling accuracy.

To assist the usability of the general packages a sophisticated natural language has replaced the limited letter protocol and mathematical functions are sectioned into actions, see Figure 1.2.1.

```
# Mass balance

FOR i = 1 to N DO

        DHP(i) = Fin*Xin(i) – Fout*X(i) +TV*SUMR

END # For
```

```
# Mass balance

FOR i = 1 to NoComp DO

    $Holdup(i)    =    ReactorFlowin*Xin(i)    –    ReactorFlowout*X(i)    +
TotalReactorVolume *SIGMA(StochiometricCoefficient(i,)*ReactionRate);

END # For
```

Figure 1.2.1 Typical code and sophisticated language

Also the model code is structured into sections which perform a specific task, to improve the ease of understanding both by increased organisation and by limiting the amount of reproduction and hence the amount of code. So for example a distillation column model is sectioned into a model for a plate, the re-boiler, the condenser and an overall model instead of writing a full model specifying the equation for each plate.

To improve the functionality the general simulation packages have adopted a modular basis, where the one model can not only have multiple applications, such as laboratory parameter estimation and full plant simulation, but also a model can be developed with the evolution of the process, see figure 1.2.2.

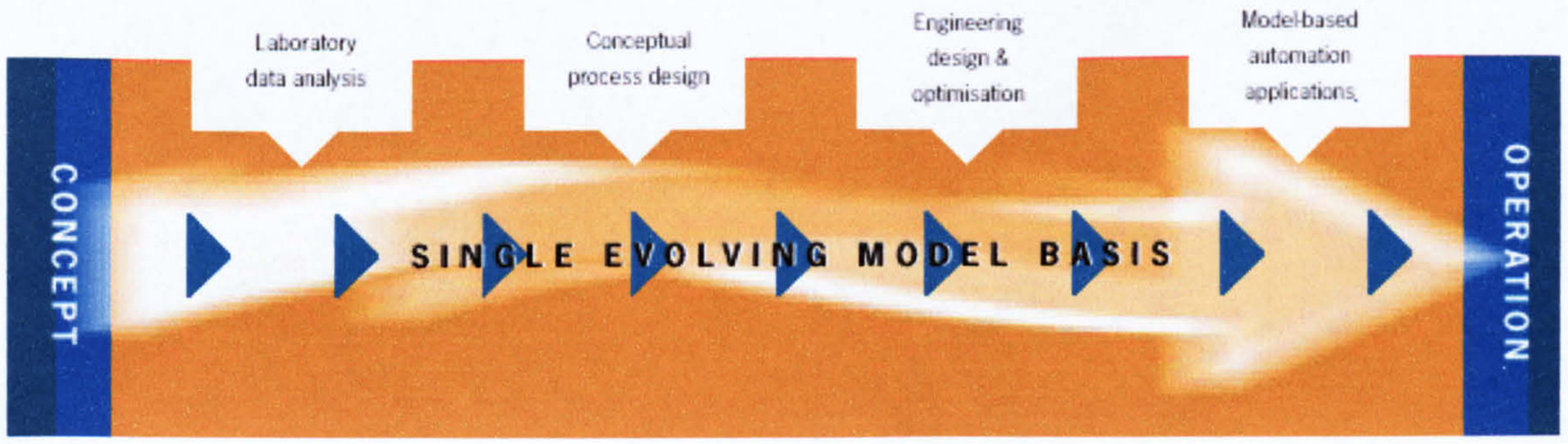

Figure 1.2.2 Evolution of model development (Process Systems Enterprise, 2002)

Incorporated with the modularization are 'open interfaces' to different types of simulation packages. This is often described as 'best-in-class' or "best-of-breed" applications where the modelling can be distributed over several packages depending on their capabilities. One software vendors' vision is "You can run the model on a Unix system, obtain data from a Windows system, and display results on your Palm Pilot".

The general simulation package gPROMS offers such advances in model complexity and hence is adopted for this research. gPROMS was developed by Process Systems Enterprise, based at Imperial College, and its customer base includes several international and multinational process companies. The use of gPROMS is becoming more extensive, e.g. Smith and Pantelides (1995), and is utilised for some of the simulation work presented in chapter 4.

1.3 Computational Fluid Dynamics

Instead of general simulation packages, specific modelling packages can be used to simulate some phenomena. Such is the case for fluid flow analysis, where Computational Fluid Dynamics (CFD) packages have been developed. Computational Fluid Dynamics (CFD) is an umbrella title given to modelling which incorporates fundamental fluid flow equations based on the Navier-Stokes equations.

As discussed before, to simulate a system requires the system volume to be divided into a mesh structure; generally for CFD all three dimensions are considered hence the mesh structure consists of cubical cells of a small volume. For each cell in the mesh, a value exists for each variable e.g. velocity, pressure and temperature. Fundamental fluid flow equations for conservation of mass and momentum, based on the Navier-Stokes equations, are linked to time-averaged turbulence models to describe fluid flow,

$$\rho\frac{Du}{Dt}=-\frac{\partial p}{\partial x}+\frac{\partial}{\partial x}\left[2\mu\frac{\partial u}{\partial x}+\lambda div\,\mathbf{u}\right]+\frac{\partial}{\partial y}\left[\mu\left(\frac{\partial u}{\partial y}+\frac{\partial v}{\partial x}\right)\right]+\frac{\partial}{\partial z}\left[\mu\left(\frac{\partial u}{\partial z}+\frac{\partial w}{\partial x}\right)\right]+S_{Mx} \quad (26)$$

$$\rho\frac{Dv}{Dt}=-\frac{\partial p}{\partial y}+\frac{\partial}{\partial x}\left[\mu\left(\frac{\partial u}{\partial y}+\frac{\partial v}{\partial x}\right)\right]+\frac{\partial}{\partial y}\left[2\mu\frac{\partial v}{\partial y}+\lambda div\,\mathbf{u}\right]+\frac{\partial}{\partial z}\left[\mu\left(\frac{\partial v}{\partial z}+\frac{\partial w}{\partial y}\right)\right]+S_{My} \quad (27)$$

$$\rho\frac{Dw}{Dt}=-\frac{\partial p}{\partial x}+\frac{\partial}{\partial x}\left[\mu\left(\frac{\partial u}{\partial z}+\frac{\partial w}{\partial x}\right)\right]+\frac{\partial}{\partial y}\left[\mu\left(\frac{\partial v}{\partial z}+\frac{\partial w}{\partial y}\right)\right]+\frac{\partial}{\partial z}\left[2\mu\frac{\partial w}{\partial x}+\lambda div\,\mathbf{u}\right]+S_{Mz} \quad (28)$$

Other phenomena such as radiation and conduction can be included in the simulation with the utilisation of the relevant equations. The numerical solution of such systems is essentially the same as for IPDAEs; by an appropriate approximation technique. Versteeg and Malalasekera (1995) state Finite Volume as the "most well-established and thoroughly validated general purpose CFD technique" used by "four of the five main commercially available CFD codes".

In addition to the modelling issues highlighted for IPDAEs, CFD also has its own specific mood points; namely turbulence, thermal radiation and chemical reaction which will be discussed in depth in chapter 4.

Turbulence modelling is the major issue of computational fluid dynamics and hence considerable research and discussion has been dedicated to this topic and is still ongoing. Turbulence is a chaotic process and it is unrealistic to expect an 'exact' representation via mathematical equations but the need for simulation of flow fields is obvious. Within published literature there are several established models, all based on time-averaged Reynolds equations, however, Versteeg and Malalasekera (1995), Foumeny (1996) and Computational Dynamics (1998a) identify the mixing length and $\kappa-\varepsilon$ models as the most popular and hence most validated. Additionally, the situation is further complicated in the 'near-wall' region where the flow field formation is distinct due to the interaction of the wall.

Thermal radiation is itself the most complicated form of heat transfer but unlike the turbulence the simulation is, as Oran and Boris (2001) state, "straightforward, but horrendous". A zonal method is one of the most popular representations for the radiative transfer as it incorporates absorption, emission and scattering.

Reactive flow is relatively new to CFD simulations and hence the issue is not as well researched as turbulence itself although it shares the same fundamental problem of modelling chaos. Ultimately to develop an 'exact' representation the modelling would have to be taken to a molecular level; which is currently unreachable. There are two main approaches a probability distribution function model and an eddy break-up model where the rate of reaction is assumed controlling.

As for the general simulation packages the CFD packages over a suite of standard facilities, however, for CFD this not only includes coded solvers, but also mesh generation and post processing tools. The operation and features are similar for most commercial CFD packages; the features include,

- Dynamic and steady-state simulation
- Laminar and turbulent
- Chemical Reaction
- Distributed resistances to represent porous media.
- Rotation e.g. for mixers
- Multiphase flow

Recently CFD packages, in contrast to the general simulation packages, have focused on developing the modelling capability of packages rather than the usability.

As discussed the mathematical representation of turbulence is a key enigma for CFD and obviously a major stumbling block in its more wide spread application. Alternative to the time-averaged approach, turbulence is separated in two regimes of large and small scales. The large scales are hypothesised to contain most of the turbulent energy; hence this approach is named Large-Eddy Simulation. The Large-Eddy Simulation approach is in terms of accuracy closer than time averaging to the ideal of direct numerical simulation. Deen et al. (2001) demonstrate the aptitude of Large-Eddy Simulation turbulence modelling.

As postulated with reference to the mesh structure for IPDAEs, if fluid flow analysis is included in the modelling phenomena not only does a trade-off form between solution time and accuracy but also the principle that the key is both the number of cells and the relevance of their position. Until recently the common approach to 'mesh independence' is the ambiguous technique of doubling the mesh density until there is an 'insignificant change' in the simulation results. This makes no allowance for cell location and the eight-fold increase in the number of cells for each stage can become unworkable. The new technique is an 'adaptive' refinement based on a directional estimation of truncation errors. Consider the following equation,

$$\frac{dy}{dx} = f(x, y) \tag{69}$$

If Euler's approximation is implemented, $y_{i+1} = y_i + f(x_i, y_i)h$ (70)

The full representation however is,

$$y_{i+1} = y_i + f(x_i, y_i)h + \frac{f`(x_i, y_i)}{2!}h^2 + \ldots + \frac{f^{(n-1)}(x_i, y_i)^{(n)}}{n!}h^n \quad (71)$$

Hence the truncation error of the approximation is,

$$Error = \frac{f`(x_i, y_i)}{2!}h^2 + \ldots + \frac{f^{(n-1)}(x_i, y_i)^{(n)}}{n!}h^n \quad (72)$$

Alternatively the truncation error is approximated to the second order expression,

$$Error \approx \frac{f`(x_i, y_i)}{2!}h^2 \quad (73)$$

Conveniently this approximation actually over estimates the truncation error, as the other order terms will only reduce its magnitude.

The truncation error can be estimated after each iteration of the numerical solver and can be applied in an optimisation routine to automatically generate a mesh with the minimum error, for a fixed number of cells, while solving the numerical simulation. By removing the complications and mundane nature of mesh development not only is the mesh development time significantly improved but also as Nithiarasu and Zienkiewicz (2000) discuss the adaptive approach produces "a mesh which represents the nature of the problem".

As an alternative to the more obvious totalitarian strategy of increasing the computational power, parallel computation has greatly increased the scope of the maximum number of cells in a mesh structure. Incorporated in the CFD packages are management facilities that section the simulation task into related parts in a similar fashion to the technique of block decomposition. The capabilities of the management facilities are such that rather than distribute the parts amongst a fixed number of machines they can search a network for idle computers and exploit their computational resources. If a machine in the network is required the management facility cancels the relevant part of the task and reissues it to another machine. The potential of parallel computing is shown in Figure 1.3.1.

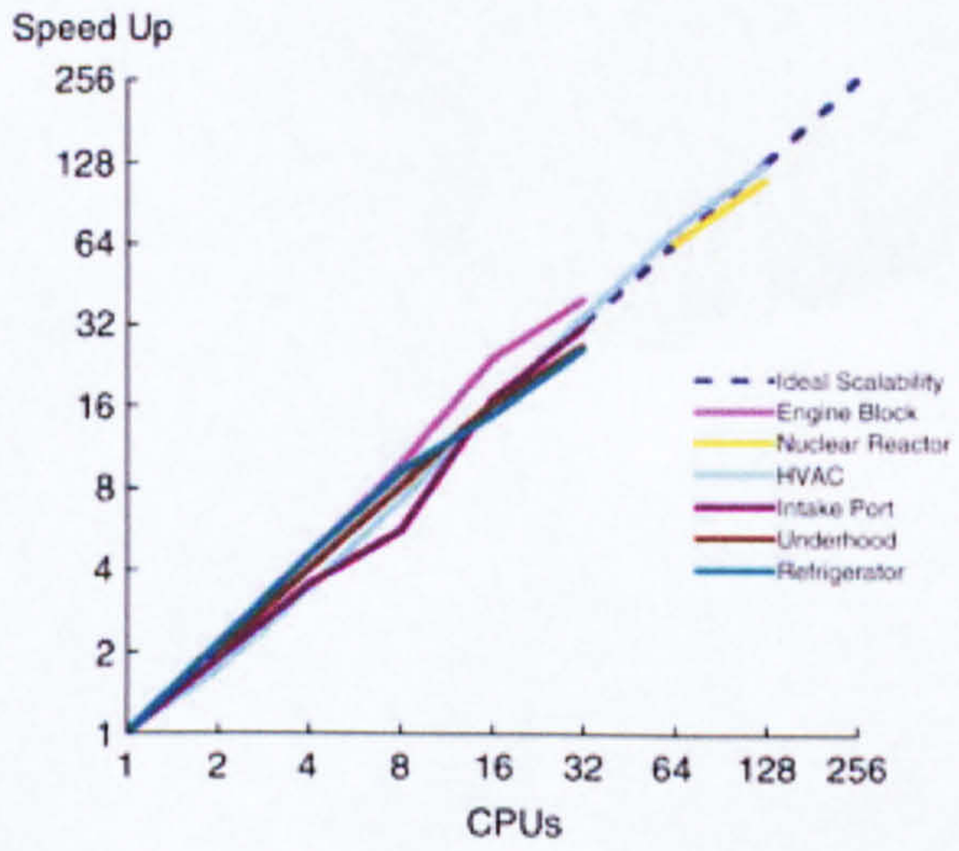

Figure 1.3.1 Parallel computing of CFD (Computational Dynamics, 2002)

As for the general simulation packages "open interfaces" are now a ubiquitous feature. CFD will either represent a "best-in-class" package, for a general simulation, or as is becoming more popular be inter-linked with a Finite Element Analysis package so that both stress and flow analysis can be performed in tandem.

Originally, CFD packages were developed primarily for the aerospace and automotive disciplines to analyse aerodynamics, such as demonstrated in Slooff and Schmidt (1994 a and b), Ucer (1994), Binder (1997), Knight (1997), Svenningsen et al. (1996) and Gani and Rajan (1999). However, not only is CFD becoming more popular as a design tool, most famously by Noble (1998) for the Thrust-SSC, but also due to the inclusion of other phenomena, the scope of application in process engineering is expanding, such as,

- Bubble column – Pandiella (1996)
- Chimney Stacks – Craig et al. (1999)
- Combustion – Yossefi et al. (1995)
- Fluidised Beds – Hoomans et al. (1998)
- Jet mixers – Holiday (1996 a and b)
- Reactors – Maggioris et al. (1998), McKenna (1998), Harris et al. (1996) and Ferschneider (1993)
- Reformers – LeBlanc (1996), Christensen et al.(1994), Farnell (1992) and Blanchard and LeBlanc (1993)
- Sprays – Dombrowski et al. (1996) and Pierce and Moin (1998)
- Stirred Tanks – Jaworski and Dudczak (1998)
- Structured packed beds – Gulijk (1998) and Fradette et al. (1998)

The commercial forms of CFD packages include most if not all of the features introduced in this section; such as the Star-CD package used in my research. Star-CD was developed by Computational Dynamics and its customer base includes several international and multinational engineering companies.

1.4 Conclusions

Although computer modelling is a very powerful tool, this potential does not come without some pitfalls and challenges. The numerous numerical solution techniques for IPDAEs and their potential application errors are a testament to the level of complexity. Additionally, further complexities arise with more specific applications of computer modelling. However, with not only the advancement of computer power but also greater understanding of the issues from both increased levels of research and more widespread application the problems are being successfully addressed.

Chapter 2

Optimisation

The term optimisation is freely used to describe the complete spectrum of techniques from the basic multiple run approach of trial and error to highly complex numerical strategies. This assortment stems from the fact that optimisation is not idyllic in the real world but there are a lot of issues which require a practical approach. However, the potential benefit is huge and hence it is the next logical step after developing a model. So to avoid the numerous pitfalls it must not be flippantly treated or downsized in complexity! This chapter will introduce several common problems encountered in optimisation and explain the techniques developed which attempt to resolve them. These issues of optimisation are demonstrated not only in a number of selected examples but also in the optimisation studies described in later chapters.

2.1 Introduction

As for the solution of differential and partial differential equations, optimisation techniques have been studied for a considerable time and research is still ongoing, such as Smith and Pantelides (1995) and Wujek and Renaud (1998 a and b). From this research several techniques have been developed which can be ideologically sectioned into direct methods, that generally employ search techniques, and indirect methods, that utilise gradient-based information. These techniques and their advantages and disadvantages are well discussed by several authors including Gill (1981), Dennis and

Schnabel (1983), Reklaitis et al. (1983), Bunday (1985), Fletcher (1987) and Press et al. (1992). Again there is no 'black-box' solution as there is no ideal technique considering robustness and solution time. The choice of an optimisation technique is limited by the nature of the system to be optimised.

The computer code for several of the favourable techniques are available in published literature, such as by Press et al. (1992). However, as for the solvers, optimisation techniques are "built-in" to commercial computer packages, such as the general simulation package gPROMS, but still a choice of scheme and settings are still user-defined.

All optimisation studies can be classified as either unconstrained or constrained single or multiple parameter optimisation. Although this classification does in some way categorise the optimisation techniques there is considerable 'common ground'. To introduce optimisation, first single and then multiple parameter optimisation are discussed.

2.1.1 Single Parameter

After developing a model the most natural instinct is to utilise its full potential. Usually, validation follows model development; included in this stage is the adjustment of operating parameters as part of a sensitivity analysis to confirm that the model reflects other known operating conditions. Although it is not formally considered as such, sensitivity analysis is a form of optimisation.

The 'multiple run' form of optimisation is effectively the first form of optimisation and is generally limited over 'suitable' operating conditions i.e. the optimisation is constrained within bounds of either operational confidence or physical limits. However, this optimisation may only yield a 'pseudo-optimum' as the ultimate optimal operating conditions, or global optimum, could be overlooked either because they are located outside of the constraints [Figure 2.1.1(a)], or more fundamentally due to the discrete nature of the multiple runs not all conditions are tested so the optimum may have been overstepped especially if the system response is complex [Figure 2.1.1(b)]. Both these scenarios fail to yield the global optimum. Traditionally if the pseudo-optimum is an optimum within a region of the operating conditions it is termed as a local optimum.

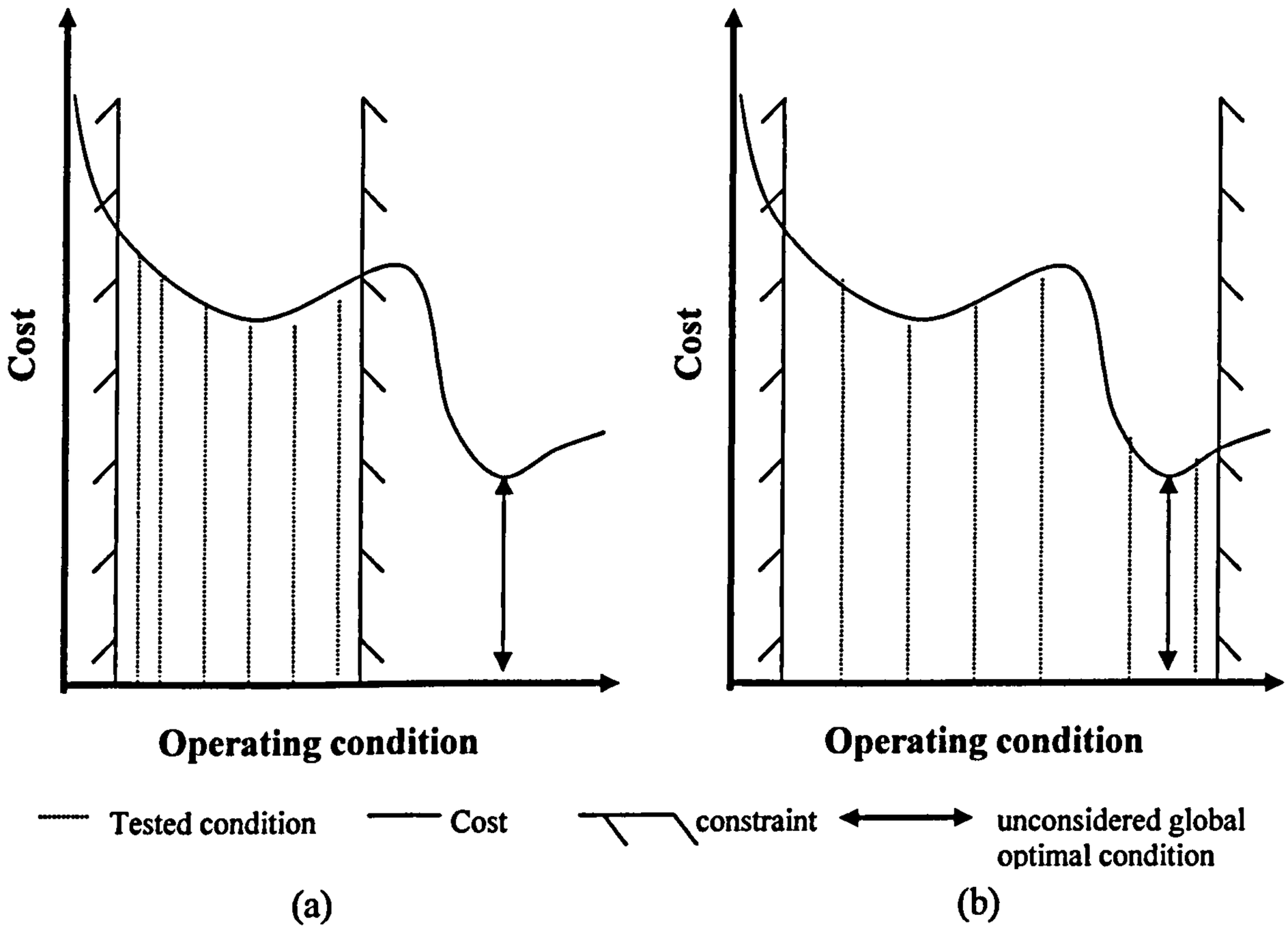

Figure 2.1.1 failings of multiple run optimisation with constraints

Apart from a standard bisection, potentially there are several rules which can be implemented to predetermine, for the 'multiple run' optimisation, the next operating condition for consideration. The most popular form is the golden section search technique, discussed by Press et al. (1992), which implements the 'golden ratio' to determine the next operating conditions for consideration. Another popular strategy also discussed by Chapra and Canale (1998), is to approximate the function evaluations with a second-order polynomial representation, yield the optimal point for the approximation and then recalculate the polynomial approximation and optimal position.

After early beginnings of repetitive simulation the next logical step is to offer more guidance to the optimisation by using the information of the system. This form of guidance from the system is to incorporate not only the magnitude of the optimised function but also the relevant rates of change or gradient. Although the term optimisation is often used loosely in engineering, this approach is probably the academic perception when referring to optimisation. The two fundamental strategies are Newton-Raphson method $X_{i+1} = X_i - f(X_i) / f'(X_i)$ or alternatively Newton's method $X_{i+1} = X_i - f'(X_i) / f''(X_i)$. However, the increase of topographical information in the optimiser will not guarantee the global optimum, considering the problems discussed for the multiple runs.

The aim of each of these strategy developments is the reduction in the function evaluation count as each function evaluation represents an extension to the time requirement of optimisation. An optimiser is considered to have improved 'efficiency' if the strategy reduces the function evaluation count. If no exact derivative exists then extra function evaluations are required; this will discussed in depth in section 2.1.4.

Even at this basic level of optimisation the main problems of optimisation can be clearly demonstrated. As for the solution of the model equations, misappropriate boundary conditions have a catastrophic potential, that can render the optimisation useless either by locating the optimal condition outside the boundaries or by saturating the optimiser with too many potential conditions that will increase the likelihood of a pseudo-optimum condition. Also as for the model equations initialisation is a key consideration. Optimisation is a search for the optimal conditions, if the optimiser is initialised from a poor set of conditions the global optimum may elude the optimiser or prolong the optimisation. Murphy's law of "a shortcut is the longest distance between two points" is very apt, with the 'shortcut' representing the lack of consideration or poor selection of the initialising values. Unlike the solvers, for optimisation there is not the same extent of potential strategies for initialisation. The golden rule is that the initialisation points should be varied to confirm system optimum. If the optimal results vary for each initialisation then this is a clear indicator that the response of the system is not simplistic and more consideration is required.

Poor formulation of the optimisation problem is equivalent to the implementation of irrelevant equations in a model as highlighted in section 1.1. For every optimisation study the benefit or detriment to a system is expressed as a formula to be maximised or minimised; traditionally this formula is known as the objective function. Typical objective functions include expressions of various costs of a unit and deviation from a desired operating condition or production condition. As for the solvers if the expression is irrelevant either a pseudo optimum will be reached or the optimiser will fail to reach any optimal conditions depending on the inappropriateness of the expression. The proverb "ask a stupid question ... get a stupid answer" is probably the best way to

consider this optimisation problem. As profit is usually dictatorial in a project this commonly forms the objective function, however, profit expressions can exhibit complex responses to the system. An illustration of this phenomenon is given in figure 2.1.2; if this represented a reactor which required an optimised temperature, the performance response could be expected to have a reasonably smooth trend, however, the number of possible options on the utility sources will be reflected in the cost function response. Additionally, as Edgar and Himmelblau (1989) discuss, the term 'profitability' is not clear cut and "will depend on the specific corporate environment in which you find yourself and the problem to be solved". Also it should be noted that profit expressions can exhibit high sensitivity to price fluctuations, so for any employment of a profit objective function this must be considered.

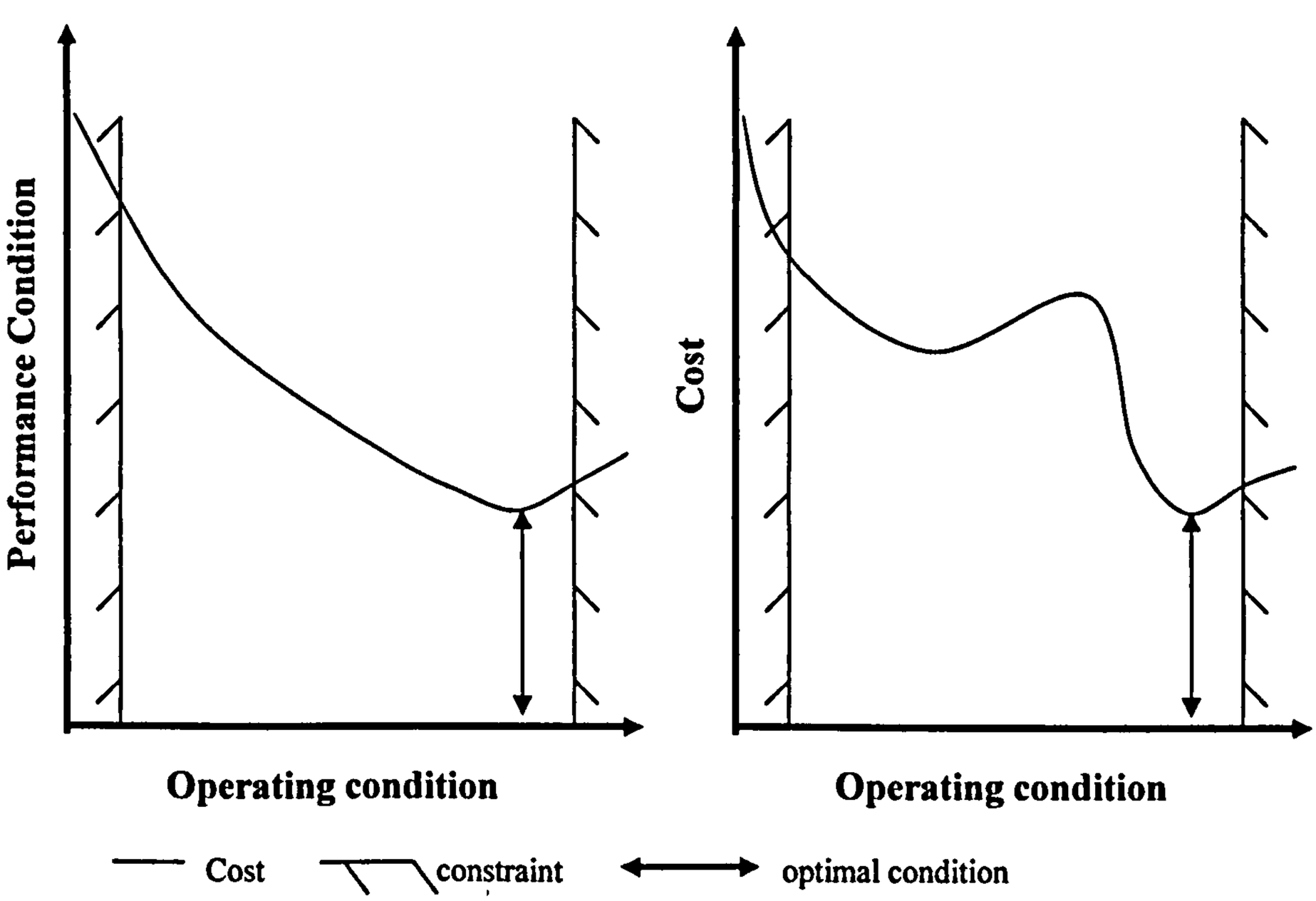

Figure 2.1.2 Alternative objective function expressions

2.1.2 Multiple Parameter

In the real world it is rare that the optimisation problem will be single parameter, more likely is that the problem will be a compromise of design settings and operational conditions. At the most basic level the strategies use pattern information of the objective function derived from function evaluations. Amongst the many variations the downhill simplex method and Powell's method are probably the best known of these pattern techniques. The downhill simplex method attributed by Press et al. (1992) to Nelder and Mead, starts with a set of function evaluations that form a simplex and then steps to the next evaluation position via a series of rules. The most common step is to reflect the evaluation through the simplex from the highest function value to a lower value. Powell's method is based on conjugate directions, which have the advantage that instead of following a series of small steps they will focus on the direction of the optimum, see figure 2.1.3. Edgar & Himmelblau (1989), however, admit "indirect methods have been demonstrated to be more efficient than direct methods on all experimental testing of algorithms".

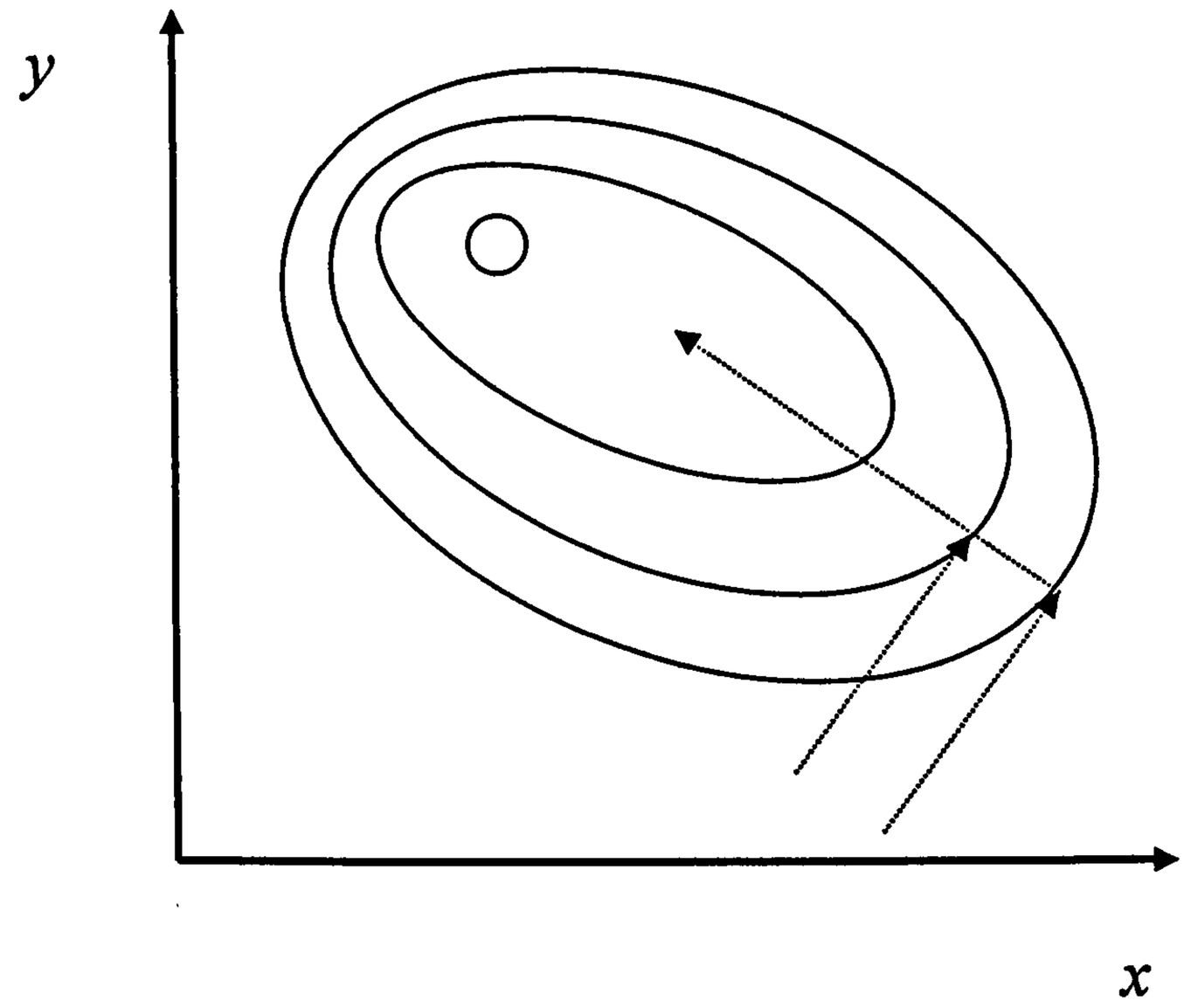

Figure 2.1.3 conjugate directions

As for single parameter, more advanced optimisation strategies employ gradient information, however, as stated by Press et al. (1992) " a common beginner's error is to assume that any reasonable way of incorporating gradient information should be about as good as any other". As in Powell's method conjugate techniques offer an improved efficiency but for multiple parameters a conjugate gradient technique is adopted, such as for Fletcher-Reeves. Due to the impracticality of Newton Method's requiring the computation of a full set of second derivatives for each iteration, a Quasi-Newton approach is adopted where alternatively the Hessian is approximated. There are two primary Quasi-Newton strategies, the Davidson- Fletcher-Powell and the Broyden-Fletcher-Goldfarb-Shanno algorithms. Chapra and Canale (1998) state that "Broyden-Fletcher-Goldfarb-Shanno is generally accepted as being superior in most cases". Edgar and Himmelblau (1989) offers these words of caution, to "keep in mind that usually the second-order information may be only approximate as it is based not on second derivatives themselves but approximates to second derivatives."

The observations and conclusions of the numerous researchers give generally good agreement, however, both agreement and certainty are not complete. Reklaitis (1983) found from a comparison of optimisation methods on two test functions that a Fletcher-Reeves/Cubic combination, a conjugate gradient method, performed preferably to quasi-Newton methods. But this is highlighted in the text as unusual as results for Fletcher-Reeves are "more successful than previously reported".

Both Fletcher (1987) and Reklaitis (1983) argue that there is no replacement for actual "experimentation" with optimisation techniques.

2.1.3 Constrained Multiple Parameter

Also realistically, the optimisation problem will be constrained by physical and operational limits. Unfortunately the inclusion of constraints in a multiple parameter optimisation problem is more complex than for single parameter.

If we consider a system where x1 and x2 are operating parameters in a system and the optimisation problem is defined as,

$$\text{Profit} = 5x1 + 7.5x2 \qquad (2.1)$$

$$x1 + x2 \Rightarrow 4 \qquad (2.2)$$

$$3x1 + 6x2 \leq 18 \qquad (2.3)$$

$$x1, x2 \Rightarrow 0 \qquad (2.4)$$

As both the objective function and the constraints are linear, a linear programming approach can be adopted to solve the optimisation problem, see figure 2.1.4.

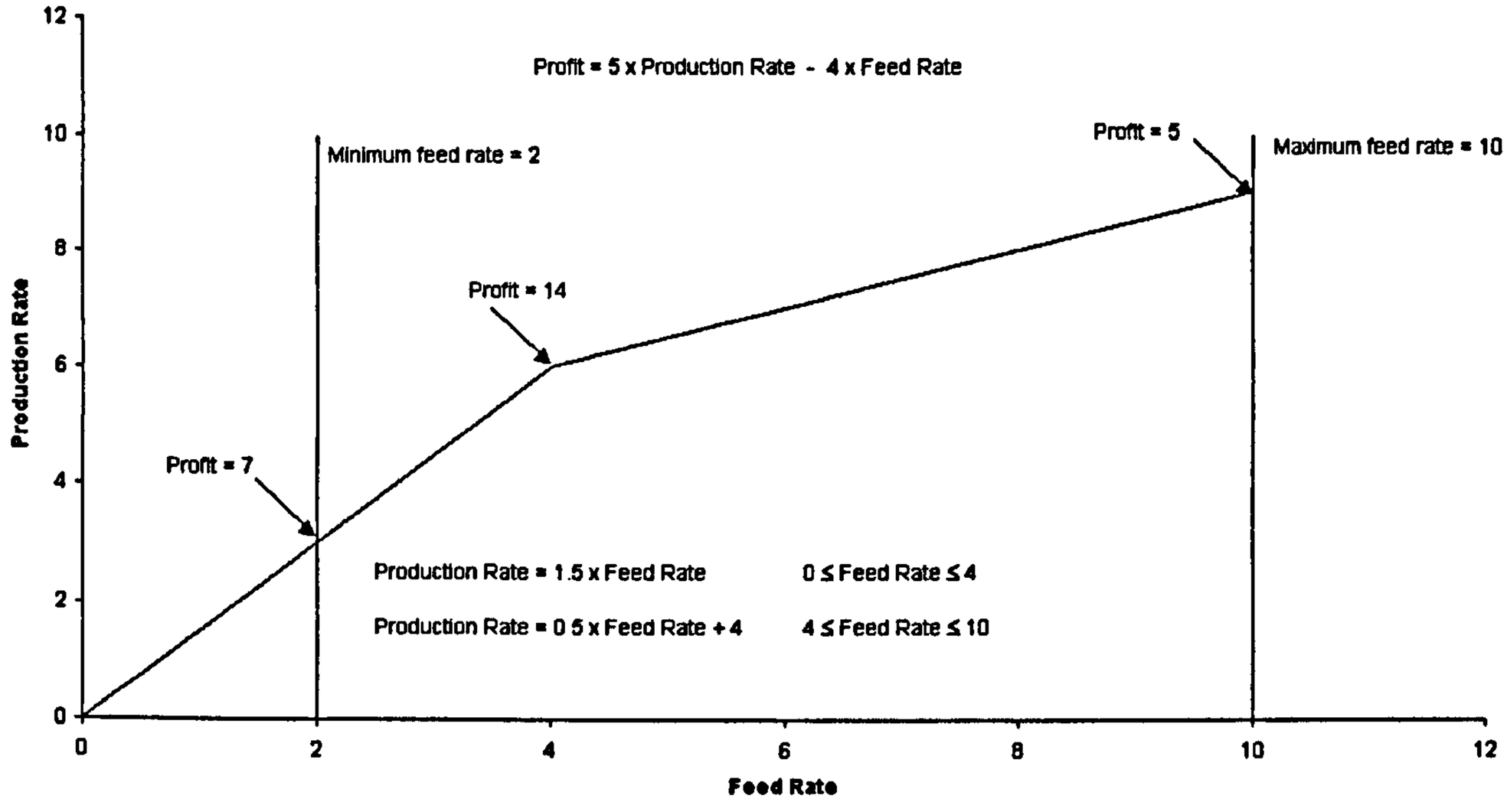

Figure 2.1.4 Linear Programming

For linear programming the constraints define a feasible region within which exist an infinite number of operating conditions. The constraints of the defining region are known as binding constraints whilst any external constraints are considered non-binding. As is demonstrated in figure 2.1.4, the optimum point for linear programming problems exists on the exterior of the feasible region at a juncture of constraints. Either all these points could be determined and then evaluated or more efficiently, especially for greater than two parameters, the simplex method is implemented which will guide the optimisation.

If any of the equations 2.1 to 2.4, defining the optimisation problem were of a quadratic rather than linear form then a linear programming approach would be inapplicable.

As an alternative to the linear programming approach of employing the constraints within the optimisation strategy, penalty functions marshal the constraints to convert the problem to an unconstrained optimisation problem. The optimisation constraints are added to the objective function with a penalty weighting such that the constraints become stigmatised. The moot point with penalty functions is that the values of the penalty weighting are both to some extent ambiguous and determine the efficiency of the optimisation. Due to the weighting issues of the penalty functions alternative approaches have gained prevalence.

As for penalty functions, the generalised reduced gradient search strategy converts the optimisation to an unconstrained optimisation, which allows the employment of the unconstrained strategies such as conjugate gradients or quasi-newton. The generalised reduced gradient approach first predetermines the active constraints, then defines the reduced sub-space by the active constraints, then evaluates the objective function and maintains feasibility. Chen (1988) states that due to the requirement of feasible points "an inefficiency may occur in following the boundary of the active constraints" and if a feasible region does not exist at a certain state the optimisation can suffer from "repeatedly adding and dropping the same constraints" and "converging to a non-optimal point". Alternatively, for successive quadratic programming, at each optimisation step an approximation subproblem is generated, the solution of which yields a search direction. Chen (1988) considers the "major difficulties of this method are that a quadratic programming subproblem may not always be well-defined and it is

not easy to ensure global convergence". Positively, Hoek and Schittkowski (1981) demonstrate that successive quadratic programming is one of the most efficient optimisation methods in terms of function evaluations, which as Chen (1988) observes for "chemical processes are generally expensive".

Generalised reduced gradient and successive quadratic programming are shown to perform comparatively, with Edgar and Himmelblau (1989) observing from a study of several optimisation techniques that both techniques "surpassed all the others quite clearly". The general simulation package gPROMS employs the successive quadratic programming technique and is utilised for some of the optimisation work presented in chapter 5.

2.1.4 What no exact derivative?

As highlighted in section 2.1.1 for Newton-Raphson method, $X_{i+1} = X_i - f(X_i) / f'(X_i)$, and Newton's Method, $X_{i+1} = X_i - f'(X_i) / f''(X_i)$, the issues of the lack of exact derivatives requires further discussion. In fact for the majority of optimisation problems an exact derivative deficiency is almost ubiquitous.

Consider a system of an ideal continuously stirred tank reactor operating at steady state, for which the volume does not change with reaction, the concentration is defined as,

$$c_a = \frac{c_{a0}}{1 + k\left(V / v_0\right)} \tag{2.5}$$

where the objective function of the optimisation is simply defined as to maximise the yield. With limited mathematics some exact first and second derivatives can be derived.

Alternatively for a more complex system or as some would term more realistic, reconsider the system to be a tubular reactor, the concentration profile is defined as,

$$\frac{\partial c_i}{\partial t} = -u\frac{\partial c_i}{\partial z} + \varepsilon D_z \frac{\partial^2 c_i}{\partial z^2} + \varepsilon D_r \frac{\partial^2 c_i}{\partial r^2} + \varepsilon D_r \frac{1}{r}\frac{\partial c_i}{\partial r} + \rho_b Nu_i r \qquad (2.6)$$

Which design or operational parameters for this system will yield an exact first derivative? and the second derivative ? As was highlighted in section 2.1.1, this form of objective function is quite simplistic, so for more complicated forms the possibility of an exact derivative will only further decrease.

Nevertheless, the issue can not be avoided as Edgar & Himmelblau (1989) state "indirect methods have been demonstrated to be more efficient than direct methods on all experimental testing of algorithms". More specifically, Fletcher (1987) states that "even when no derivatives are available to the minimisation method, then the estimation of first derivatives by finite differences, combined with quasi-Newton method, has provided the currently most efficient method" which is confirmed by Gill (1981).

To estimate a derivative by finite differences there are three approaches, forward, backward and central differencing. Recall the Taylor's series expression for a function,

$$f(x_{i+1}) = f(x_i) + f'(x_i)h + \frac{f''(x_i)}{2!}h^2 + \ldots + \frac{f^{(n)}(x_i)}{n!}h^n \qquad (2.7)$$

or alternatively the first derivative is expressed as,

$$f'(x_i) = \frac{\left(f(x_{i+1}) - \left(f(x_i) + \frac{f''(x_i)}{2!}h^2 + \ldots + \frac{f^{(n)}(x_i)}{n!}h^n \right) \right)}{h} \tag{2.8}$$

for a first-order approximation, the first derivative is truncated to,

$$f'(x_i) \approx \frac{(f(x_{i+1}) - f(x_i))}{h} \tag{2.9}$$

which is more commonly named as a first forward difference approximation. The first backward difference approximation, equation (2.10), the first central difference approximation, equation (2.11), and all the other forms of higher derivative difference approximation are developed from the Taylor series.

$$f'(x_i) \approx \frac{(f(x_i) - f(x_{i-1}))}{h} \tag{2.10}$$

$$f'(x_i) \approx \frac{(f(x_{i+1}) - f(x_{i-1}))}{2h} \tag{2.11}$$

A graphical representation of these first-order approximations is shown in figure 2.1.5. It is apparent that of the first-order approximations, the central difference form is the most accurate representation of the derivative.

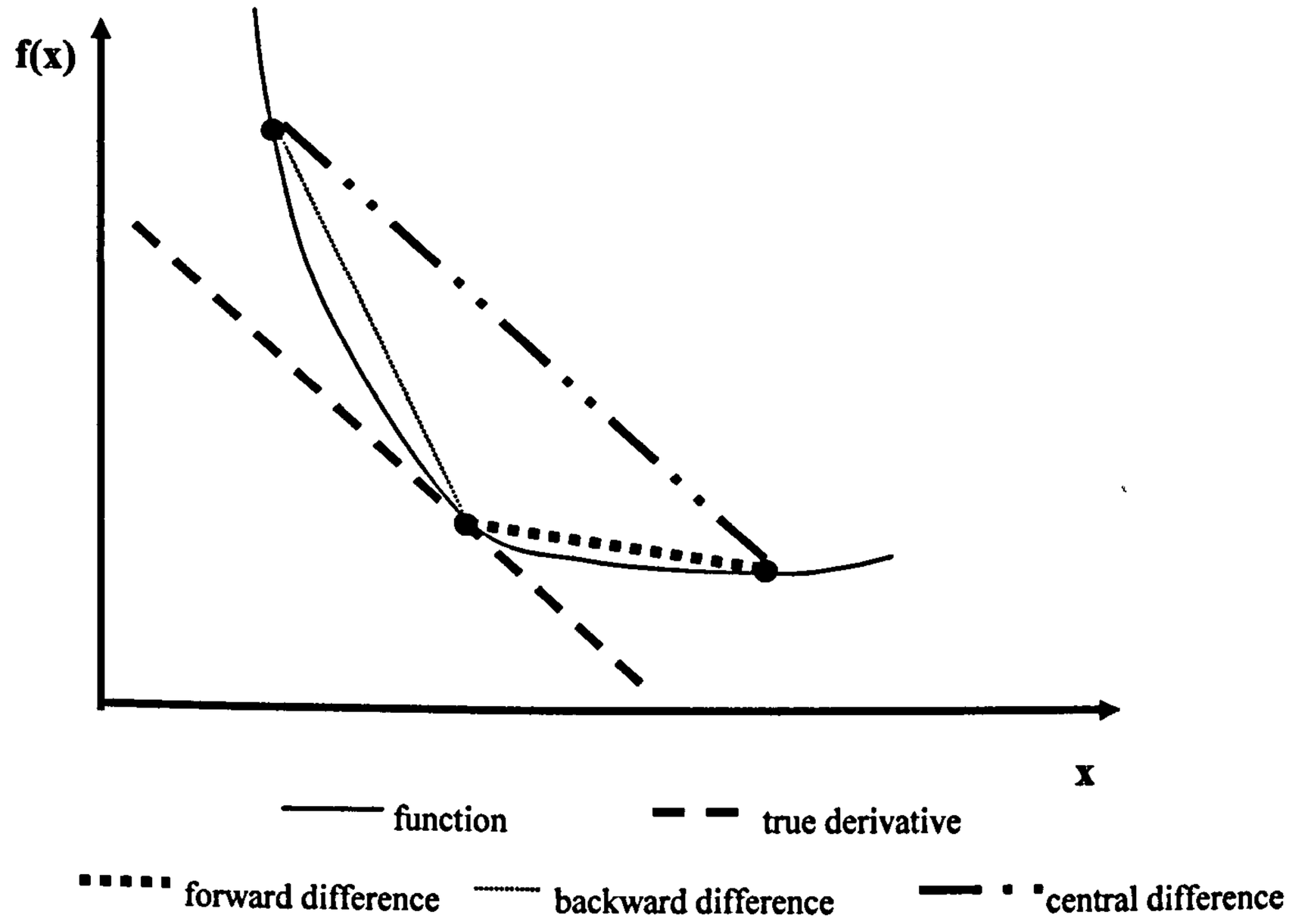

Figure 2.1.5 backward, central and forward differencing

Unfortunately, all these difference approximations suffer from two key forms of error, that originating from the truncated form of derivative and that originating from the round-off by the computer of numbers. Edgar and Himmelblau (1989) identify these truncation and round-off errors as the "main difficulty" for optimisation as they can "cause an algorithm to fail to converge or cause it to converge to the wrong solution". The source of the problems is the difference in magnitude of the errors and the convergence criteria; the size of the errors should not exceed the convergence criteria.

The magnitude of the truncation error for all forms of the difference approximations can be reduced by alternatively retaining the second order terms from the Taylor series expression. So for a second-order approximation, the first derivative is truncated to,

$$f'(x_i) \approx \frac{-f(x_{i+2}) + 4f(x_{i+1}) - 3f(x_i)}{2h} \tag{2.12}$$

As is more often than not, this improved accuracy is in fact no 'free meal' as the improved accuracy requires extra function evaluations. For the first derivative, the first-order expressions of both the forward and backward difference equations require only one additional function evaluation to the known $f(x_i)$, while the first-order central difference and the second-order forward and backward difference expressions require two additional function evaluations. The key is the cost of these additional function evaluations, which as Chen (1988) observes for "chemical processes are generally expensive". The expense of these function evaluations is particularly steep for complex modelling such as CFD, as is demonstrated in chapter 5. This is not a 'win-win' situation, but purely another form of the fundamental balance of accuracy and practicality that occurs throughout engineering!

As a compromise Fletcher (1987) suggests forward difference initially, but near the optimal solution "preferably" use central difference, while Gill (1981) recommends forward difference unless the error is too large and suggests a switch only in local area of difficulties. This concurs with Edgar and Himmelblau (1989) statement that "the values of the derivatives, or the approximates, near the solution of the problem, that are of importance. Errors in the derivatives at the start of the minimisation have little effect"

As was highlighted in section 2.1.3, from a study by Schittkowski, discussed by Reklaitis et al. (1983), successive quadratic programming was found to be the most "efficient" method for constrained optimisation. Reklaitis et al. (1983) agrees with this result but found that with linear constraints there was no "significant improvement over the successive linear programming approaches". Also as acknowledged in section 2.1.3, these statements only highlight favourable methods; both Fletcher (1987) and Reklaitis (1983) argue that there is no replacement for actual "experimentation" with optimisation techniques. For cases with no exact derivative Rosen and Luus (1991) argues that the best approach "will depend on the type of problem" and recommends "for implementation purposes" employment of multiple methods as a crosscheck. Strategies for optimisation when no exact derivative is available are utilised for some of the optimisation work presented in chapter 5.

2.2 Appraisal of optimisation studies

Even though, the modelling of steam reforming is extensively studied, optimisation is limited. However, within published literature there are several optimisation studies of other industrial reactors and processes, which demonstrate interesting techniques.

2.2.1 Steam reformers

Within published literature there is lack of both optimisation studies for steam reformers or any reference to unpublished studies; this is also highlighted by Rajesh et al. (2000) as a "contrast" to the modelling and simulation work. A possible reason for this deficiency, is the limited range of published data on operational reformers, highlighted in chapter 4, due to unwillingness in industry not only to publish data but also to adjust operational set points. Hence, values outside an area of knowledge are associated with considerable uncertainty.

The simplest reported optimisation study for steam reforming is by Hossain (1988). The author performs an optimisation by Golden Section search of some of the operating parameters to maximise the carbon monoxide yield. Although this technique is popular, its capability is limited and not really applicable beyond the simplistic nature of the associated modelling.

Zhang (1995) carried out a minimum energy optimisation study for a primary and secondary reformer in ammonia plant. However, only a few operating parameters were varied and no geometric parameters, and the optimisation used the "method of variable transformations" from the method of multipliers, demonstrated less efficient by Schittkowski in Reklaitis et al. (1983).

Kvamsdal et al. (1999) maximise the conversion of methane in a primary steam reformer by altering the feed flow rate. The sequential quadratic programming techniques available in the gPROMS package are employed for the optimisation study.

However, as the author discusses, the simulation accuracy of the variable for the key constraint is questionable and requires further study.

Rajesh et al. (2000) claim to perform the "first attempt to study steam reforming optimisation using multiple-objective functions and constraints". The optimisation objectives are to minimise inlet methane flow and maximise carbon monoxide production for a fixed hydrogen production, employing a Nondominated Sorting Genetic Algorithm. In addition to the cautions expressed in section 2.2.2 on Genetic Algorithms, the authors admit that the "results were dependent to a good extent on the choice of some of the computational parameters". However, probably an understated benefit of genetic algorithms indicated in this paper is that they can yield multiple 'preferred solutions'; although a preference is ultimately required which could become a protracted process. In a subsequent paper Oh et al. (2001), two sets of objectives were studied, maximising hydrogen and steam production only and minimising the steam reformer heat duty while maximising hydrogen and steam production.

2.2.2 Reactors

Although in other reactors steam reforming may not occur, there is notable similarity in both the reactor designs and operational issues. Moreover, the optimisation problems will be similar in nature to steam reforming.

Cuthrell and Biegler (1987 and 1989) maximised the utility production from a packed bed reactor while minimising the reactor length with and without hotspots and optimised the feed rate profiles. The optimisation method converted the problem to a set of non-linear equations via finite-element collocation and solved them with a successive quadratic programming technique. Vasantharajan and Biegler (1990) improved the technique by addition of more general element adjustment, with the same packed bed reactor case and also an ammonia reactor. Logsdon and Biegler (1992) introduced further improvements with a structured decomposition algorithm demonstrated on a batch distillation. However, for the method of approximating via finite element collocation, from a large number of finite elements a complex non-linear problem is developed, which is difficult to solve.

Upreti and Deb (1997) criticises the optimisation of an ammonia reactor by Vasantharajan and Biegler (1990) as appearing to not "do justice to the not-so smooth reactor profiles" leaving an "uncertainty of the globality of the obtained optimum solution". Although this study offers several improvements to previous research the optimisation utilises genetic algorithms, which suffer some controversy. Morton (1998) highlights that genetic algorithms do not guarantee a global optimum and severely criticised their use, however, their use is becoming more popular, such as by Venkatasubramanian et al. (1995). To combine the advantages of both gradient-based techniques and genetic algorithms, Maskan et al. (2001) recommend a sequential employment of these techniques, genetic algorithms followed by gradient-based techniques. Nagy et al. (2001) demonstrate this combined approach but hypothesise that sequential employment is not the only choice, also parallel employment yields benefits from both techniques, however in a different manner.

2.2.3 Reactors systems

Steam reforming is often a mid-stream process in a wider chemical plant and can be arranged as a reactor system. Hence an understanding of typical consequences of optimisation within a wider process is interesting.

Biegler and Hildebrandt (1995) and Feinberg (1999) performed optimisation on a series of reactor network examples, both by the construction of attainable regions and embedding their principles into optimisation formulations. Attainable regions are the state space of achievable production from all permitted design configurations, as demonstrated by Omtveit et al. (1994) for steam reforming. However, Biegler and Hildebrandt (1995) state "the theory behind the attainable region still needs to be developed" and highlight that optimisation formulations suffer from localisation.

The problem of localization may be resolved by the use of partial solutions, suggested by Fraga (1998) for automated network design tools.

2.2.4 Computational Fluid Dynamics (CFD)

The key issue of balancing the accuracy and practicality swamps all other issues of CFD optimisation. Although due to the nature of some of the systems, convenient compromises can be developed, the issues for reactive flow systems are completely portable.

Ucer (1994) chaired a conference on turbomachinery design using computational fluid dynamics. Several of the papers discussed the use of optimisation, in general they agreed that more work is required on improving their convergence time and operational difficulty. The optimisation techniques included numerical optimisation combined with mean-line prediction, search techniques and evolution strategy which seems similar to genetic algorithms.

The Haack-Adams theoretical minimum-drag body was chosen by Cheung et al. (1995) to demonstrate optimisation. The optimisation used sequential quadratic programming and a quasi-Newton algorithm with a finite difference approximation for the gradient of common interval, which agrees with the appraisal of optimisation techniques (section 2.1). However, Cheung et al. (1995) demonstrate that care must be taken in choosing the interval, which agrees with Dennis and Schnabel (1983). Further to this, Cheung et al. (1995), highlight the other main issue of efficient use of CFD and optimisation, that of grid refinement. The key is to "choose a sufficiently coarse grid so that the cumulative CPU time does not become excessive, yet a fine enough grid to locate a physically valid optimum". The technique of using trials to determine the grid density does not guarantee mesh independence of the results. However, for small changes in geometry as in this case this may not be a problem.

Holiday (1996) and Holiday et al. (1996) performed optimisation on a jet mixer, using the Golden Search, Modified Downhill Simplex and Powell's method discussed by Press et al. (1992). For both studies, the optimisation problem failed to converge on a sensible result and the author associated this with difficulties in specifying the problem, however, as discussed in section 2.1.4, there is general agreement that a gradient-based

optimisation technique with finite difference approximation is more efficient than a search technique. Mesh independence, see section 1.3, 4 and 5, was claimed by doubling the mesh density in all three co-ordinates until there was no difference in the simulation results. The author validates the simulation, using data from Razinsky and Brighton (1971), however, Yule et al. (1993) demonstrate that the validation set must not be for fully developed pipe flow but instead for the actual system of confined jet formation.

Svenningsen et al. (1996) chose a two-dimensional symmetric diffuser for optimisation. Sequential linear programming with adaptive move limits is selected "based on experience gained in the field of structural optimisation". With a semi-analytical method implemented, instead of finite difference, to reduce computational time for the sensitivity analysis. However, the optimisation is "restricted to laminar flows only".

Knight (1997) performs a brief review of optimisation and CFD, and gives examples of automated design. The author introduces the gradient techniques of method of steepest descent, conjugate gradient, sequential quadratic programming and control theory, and the stochastic techniques of simulated annealing and genetic algorithms. Control theory is identified as more efficient than finite difference approximation of the gradient, and both stochastic techniques are labelled as possibly unsuitable due to the required "evaluation of a large number of designs". However, the author notes from the examples that the genetic algorithm was "somewhat more efficient" than sequential quadratic programming, but not all techniques discussed were utilised. The author associates this result with design space discontinuity.

Craig et al. (1999) minimised the pollution due to Chimney Stacks using a dynamic trajectory method, penalty function and move limits with a forward finite difference for gradient approximation. However, Penalty functions are notoriously difficult to set-up, the authors state this "received a lot of attention" which agrees with the general comments from optimisation, and according to Morton (1998) the move for constraints is toward trust regions instead, as less case specific. Further to this the authors solely used forward finite difference to approximate the gradient, which was criticised in section 2.1.3, but found a very clever use of "restart field" option available in Star-CD. Finally, due to the nature of the problem the optimal arrangement was "less grid dependent", hence a coarse grid could be used throughout the optimisation and independence verified on end result, hence avoiding the issue.

Gani and Rajan (1999) improved the life of a structure considering fracture mechanics. The authors used the method of feasible directions, highlighted by Reklaitis (1983) as suffering from "weaknesses", with the sensitivity approximated solely by forward difference method, which was criticised in section 2.1.3. However, the authors thoroughly discuss the issues of mesh generation and regeneration and states that for shape optimal design "the choice of remeshing scheme becomes very important". An automated mesh generator is used and recommends localised patch remeshing instead of global as less storage space requirements, no alteration required of the automated mesh generator, patch compatibility is preserved and operates independently of user intervention.

Dadone and Grossman (2000) optimised a series of two-dimensional design problems over the transonic, subsonic and supersonic flow regimes. The authors develop a discussion of many of the issues and techniques highlighted in section 2.1.4 from a review of current research. A sequential quadratic programming technique is employed with discrete adjoint formulation to compute the sensitivity derivatives. Distinct to previous approaches rather than adopting a serial methodology of fully solving the model and then updating the derivatives, the authors develop what is termed as a "progressive" algorithm where the model is continuously solved and optimised in parallel for a series of progressively finer mesh densities; where the mesh density is purely doubled in every direction at each stage. As the authors admit this is only "a plausible" methodology as it has not been fully optimised and although they conclude "there appears to be no impediment" to extending to "three-dimensional flows with complex geometries". From the comments of Rosen and Luus (1991) it is clear that efficiency of gradient approximations is case specific and developing the complexity of the flow system to be optimised may shift this balance.

As previously discussed in section 2.2.2 the popularity of genetic algorithms is growing, one such example for computational fluid dynamics is offered by Poloni (2001), for the optimisation of the insulation of a refrigeration system. The optimisation is reported to have found "the best compromise between a conflicting set of design parameters". Apart from the concerns expressed in the previous comments on genetic algorithms, additionally as this case includes fluid flow modelling the confidence in the simulation result must be quantified to check that it does not dwarf the benefit of the optimisation.

2.3 Conclusions

Although optimisation suffers from fewer issues than mathematical modelling, their magnitudes are incomparable, but the potential benefit of optimisation is immense. With not only the increased calculation capacity but also the advancement in mathematical techniques, numerous optimisation methods have been developed and the research is still continuous. While admittedly progress has been made from this research to improving the optimisation efficiency and increasing the understanding of the issues of optimisation, still no idyllic method exists. For any engineering optimisation, a pragmatic cost-benefit approach must be adopted, however, this philosophy must be checked, as from too harsh a form sprouts ideas such as genetic algorithms and the general discouragement of any numerical form of optimisation. It should be remembered that trial and error was often the norm for what we now consider suitable optimisation problems. The difference between then and now is that both the modelling has improved so the confidence in the simulation result no longer dwarfs the estimated benefit of the optimisation and the cost in financial and time terms has reduced greatly.

Despite this overriding fact that both the nature of the system and the modelling type significantly affect the choice and employment style of optimisation techniques, some general conclusions can be drawn for steam reformers. For a fully comprehensive constrained optimisation with a limited penalty for function evaluations, the successive quadratic programming and generalised reduced gradient techniques are equally suitable. If the function evaluation penalty is more severe then a staged approach is required, with an initial employment of alternative indirect approaches that are less complex, to develop an understanding of the objective function response.

Chapter 3

Steam Reforming

Steam reforming is an industrially important chemical reaction process, applied in several production schemes including ammonia, hydrogen, methanol and oxoalcohols. Hydrocarbons, predominately methane in the current economic climate, and steam react to form a mixture of hydrogen and carbon oxides, which are major chemical building blocks. This chapter will introduce the steam reforming process and the issues related to the process in the sense of both design and operation. The information gleamed from the identification of the key process issues and the decipherment of published research is used as the groundwork for the model development in later chapters.

3.1 Introduction

Steam reforming is used to produce hydrogen and carbon oxides from hydrocarbons and steam. The predominant hydrocarbon feed for steam reforming is natural gas, however, as mentioned by Siminiceanu and Ungureanui (1997) and Twigg (1997); alternative feeds include methanol and other heavier hydrocarbons. Traditionally, the mixture of hydrogen and carbon monoxide is called synthesis gas or syngas.

Other processes for the production of syngas include partial oxidation and gasification, however, Goff and Wang (1985) demonstrate the economic disadvantages of these alternatives. In fact Soliman et al. (1988) states that for Saudi Arabia and Egypt the percentage production of syngas via steam reforming is "almost 100%".

Christensen and Primdahl (1994) state that syngas "is a major route from hydrocarbons to many important bulk chemicals", see figure 3.1.1, these include ammonia, methanol and hydrogen, the uses include fertilisers, synthetic gasoline and raising the octane number of gasoline. This importance is confirmed by LeBlanc et al. (1995) quoting 75-80% of world's production of ammonia and 80-85% for methanol. Also, for hydrogen Alatiqi et al. (1989), Alatiqi and Meziou (1991) and Barbieri and Di Maio (1997) confirm steam reforming's importance, with Barbieri and Di Maio (1997) claiming 50% world demand of hydrogen.

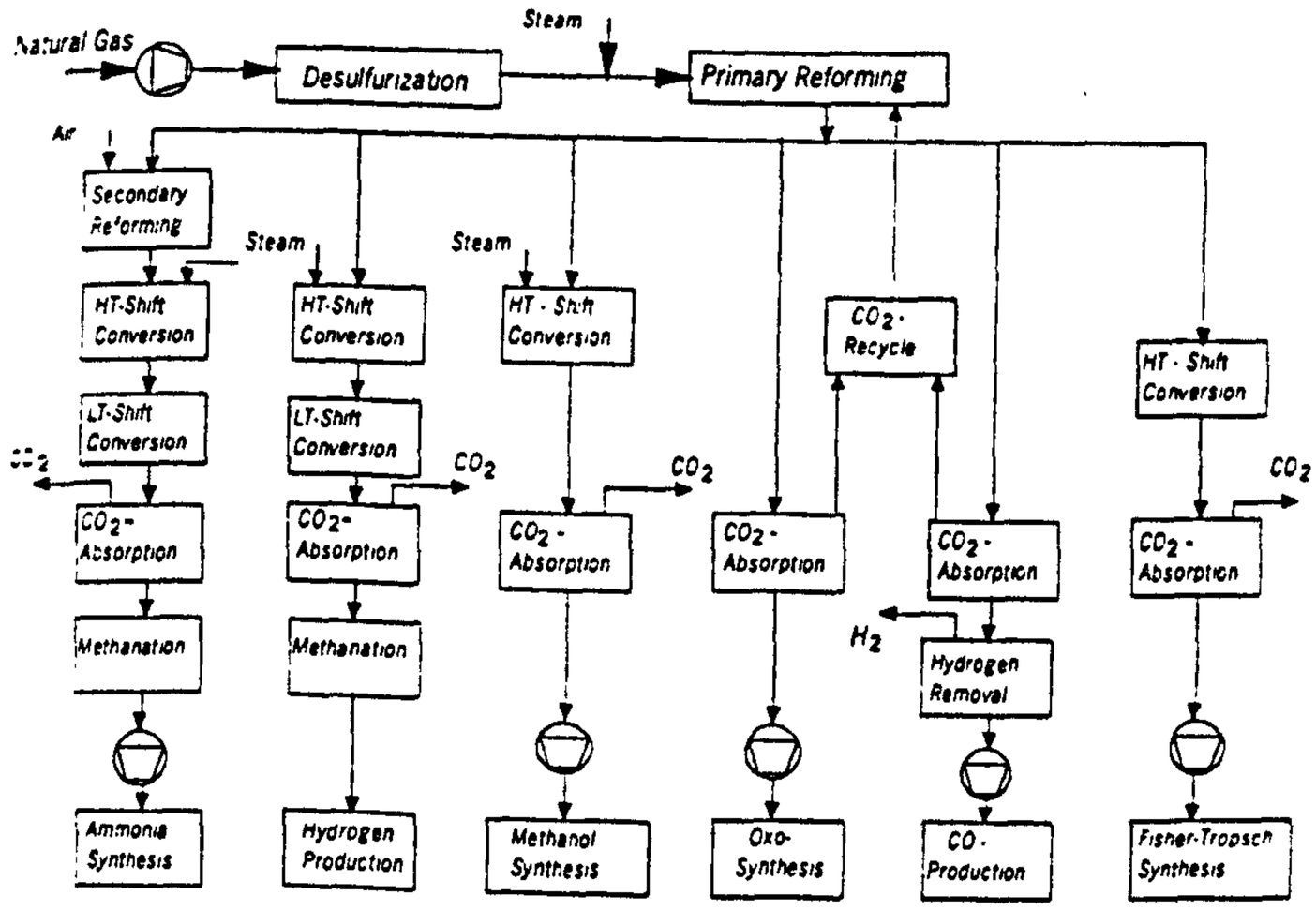

Figure 3.1.1: Block diagram showing different applications of Steam Methane Reforming [Adris et al. (1996)]

Although, traditionally, steam reforming has had an economic advantage, Rosen (1991 and 1996) identifies particularly for hydrogen production that there are other process routes under development, mainly non-hydrocarbon-based. Rosen (1996) demonstrates that these alternative processes can offer improved energy and exergy efficiencies.

However, Adris et al. (1996) refers to the prediction by Scott in 1987 that steam reforming "will dominate in the production of hydrogen for at least three decades and be important for more than fifty years"

Rostrup-Nielsen (1975) and Twigg (1997) give a thorough review of steam reforming, from both a historical and industrial basis.

3.2 Steam reforming reactions

Wagner and Froment (1992) reported Mond and Langer in 1888 as the first to study the kinetics of steam reforming. There have been several other investigations since and, periodic surveys, which include Van Hook in 1980, Rostrup-Nielsen et al. (1988), Elnashaie et al. (1988) and Twigg (1997) which are reviewed in chapter 4.

Within a steam reformer there are several reactions, which can be grouped into those related to the production of syngas and those related to carbon formation/removal. Most authors simplify the reaction scheme over reformer catalyst beds to,

for syngas production

$CH_4 + H_2O \Leftrightarrow CO + 3H_2$	Steam Reforming
$CH_4 + 2H_2O \Leftrightarrow CO_2 + 4H_2$	Steam Reforming
$CO + H_2O \Leftrightarrow CO_2 + H_2$	Water-Gas Shift
$CH_4 + CO_2 \Leftrightarrow 2CO + 2H_2$	Carbon dioxide reforming

for carbon formation

$$2CO \Leftrightarrow C + CO_2 \qquad \text{Boudouard Reaction}$$

$$CH_4 \Leftrightarrow C + 2H_2 \qquad \text{Thermal Cracking}$$

$$CO + H_2 \Leftrightarrow C + H_2O \qquad \text{Carbon monoxide reduction}$$

Notwithstanding the almost universal adoption of this reaction scheme, there is disagreement amongst some authors about the occurrence of the water-gas shift reaction which Froment et al. (1982) and Elnashaie et al. (1992) have gone some way to resolve. Additionally there is the issue for the syngas reactions, of the approach to the existence of higher hydrocarbons in the system, which is discussed in more depth in chapter 4. Despite this for higher hydrocarbons it should be noted that the products of the process remain as only carbon dioxide, carbon monoxide, hydrogen, methane and steam. The kinetics of carbon formation/removal are covered in Trimm (1997) but are not always included in reformer simulations, instead assessment is often carried out on an equilibrium basis; this issue is also developed in chapter 4.

Despite the amount of research for steam reforming and relative consensus for the reaction scheme, as Elnashaie et al. (1992) states "a number of discrepancies exist between the rate expressions available in the literature", the authors identify the sign of the order of the rate of methane disappearance upon steam as the most interesting discrepancy. Additionally, some authors lump an assumed constant effectiveness factor into the rate constant, which is contentious as "the rate of steam reforming is not controlled only by the kinetics of the reaction, but they are also affected by the rate of diffusion through the pores of the catalyst" (Elnashaie et al., 1988). Xu and Froment (1989b) claim to have modelled this successfully by their approach.

3.3 Operating parameters

As was discussed in section 3.1, steam reforming is used in several processes with differing product requirements from the reforming process. In the main, no design parameter alterations are required to match the change of product requirements, but this does not hold for all situations and in fact some extreme situations require additional units. Nevertheless, as explained in more detail in section 3.5, reformers are designed process-specific and rarely are used for another process. Hence, any change in product requirements would only be minimal, so only the operating parameters would require adjustment.

The key operating parameters for reformers are,

- Hydrocarbon composition
- Steam to Carbon Ratio
- Operating Temperatures
- Operating Pressures
- Oxygen to Carbon Ratio

A thorough discussion of the effects of these operating parameters and an explanation of their industrial values are given by several authors including Snyder et al. (1986), Hossain (1988), Christensen and Primdahl (1994), Dybkjaer (1995), Adris et al. (1996) and Twigg (1997). The freedom of setting these parameters, however, is limited, as reforming is often either an initial or a midstream process and this is reflected in the reasoning. Further to this the interaction of the operating parameters is very complex.

- The hydrocarbon feed is predetermined by the feedstock availability, however, if the process requires a low hydrogen to carbon-monoxide ratio then carbon-dioxide can be added to the feed.
- Carbon formation not only deactivates the catalyst, but also causes a heat imbalance in the tube, which can lead to metal failure. A high steam to carbon ratio is required to guarantee carbon removal, which improves the steam reforming and water-gas shift equilibria for hydrogen, but steam production is expensive. Although, as discussed by Elnashaie et al. (1988) and Trimm (1997) research is ongoing into catalysts which can operate with lower ratios, see section 3.4.
- Steam reforming is a highly endothermic reaction, hence high operating temperatures are required. However, the physical properties of the containing metal, carbon formation and in certain situations the properties of the catalyst are limiting.
- Although a high pressure is detrimental to the steam reforming equilibrium, considering the overall process economics, a high pressure improves heat recovery and avoids compression downstream.
- As for the operating temperature, the oxygen to carbon ratio is limited by the metal structures, risk of carbon formation and catalyst structure. Additionally, the combustion of valuable product for reformers which ignite part of the feed.

Basini and Piovesan (1998) performed an economic analysis on reducing steam to carbon and oxygen to carbon ratios by improved catalyst technology for steam reforming and discovered significant cost reductions. Further to this, Hossain (1988)

performed an optimisation, by Golden Section search (see chapter 2), of some of the operating parameters to maximise the carbon monoxide yield.

3.4 Steam reforming catalyst

There are not only several companies who produce catalyst, but also they offer a range of catalyst types, and could be said to "come in all shapes and sizes". However, the two main industrial catalyst companies for steam reforming are Haldor-Topsoe and Synetix, part of the ICI group formerly known as ICI Katalco. Although the topic of catalyst formulation and shape is particularly industrially sensitive, most reactor design texts discuss the key requirements of the catalyst.

Several transition metals are suitable as a catalyst for steam reforming, however, nickel has traditionally been used as it is "much cheaper and sufficiently active to enable suitable catalysts to be produced economically" (Twigg, 1997). The nickel is either precipitated or impregnated on to a catalyst support, such as a mixture of aluminium and magnesium oxides or alumina, respectively. However, Twigg (1997) identifies that "most commercial natural gas catalyst are now of the impregnated type" for amongst other reasons "impregnated catalysts are generally stronger".

At a glance it is obvious that the catalyst support should at least be able to withstand the conditions in the reactor and not be detrimental to the activity of the nickel. Further to this, several authors including Elnashaie et al. (1988), Trimm (1997) and Twigg (1997), have reported that the choice of support can reduce carbon formation, and both

Elnashaie et al. (1988) and Trimm (1997) recommend that the role of the support is researched further.

Many shapes and sizes have been developed for steam reforming catalyst, see figure 3.4.1, as the structural design is essentially a balance between chemical performance and mechanical behaviour; discussed thoroughly by many authors including Twigg (1997). For steam reforming, due to the steep concentration gradient, the catalyst activity must be distributed close to, or be on the surface. Considering both catalyst strength and pressure drop for the optimisation of the surface area, commercial designs have developed into a cylindrical pellet with a number of cylindrical holes.

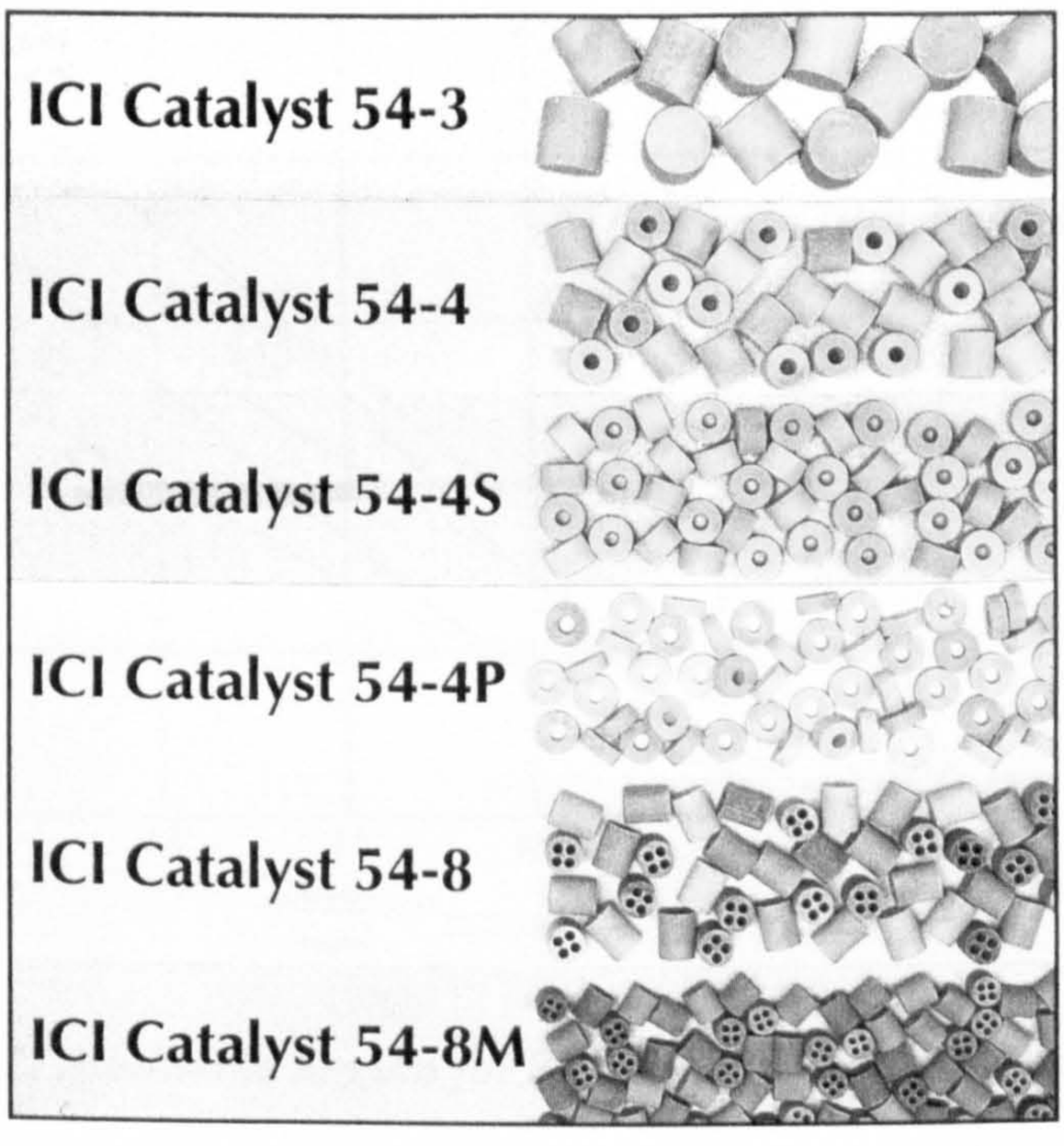

Figure 3.4.1: Various shapes of steam reforming catalyst supplied by ICI

[Operating Manual ICI Secondary Reforming Catalysts]

3.5 Reactors

Omtveit et al. (1994) studied the steam reforming system at 1050 K by using the attainable region technique, see figure 3.5.1, 'line 1' for ideal plug-flow (PFR) and 'line 4' continuously stirred tank (CSTR) reactors. This study confirms the industrial practice of fixed catalyst beds for the steam reformers, as this yields the maximum conversion of methane, 'point B'. However, other than traditional reactor configurations, Adris et al. (1996) discuss alternative reactor designs under development for steam reforming.

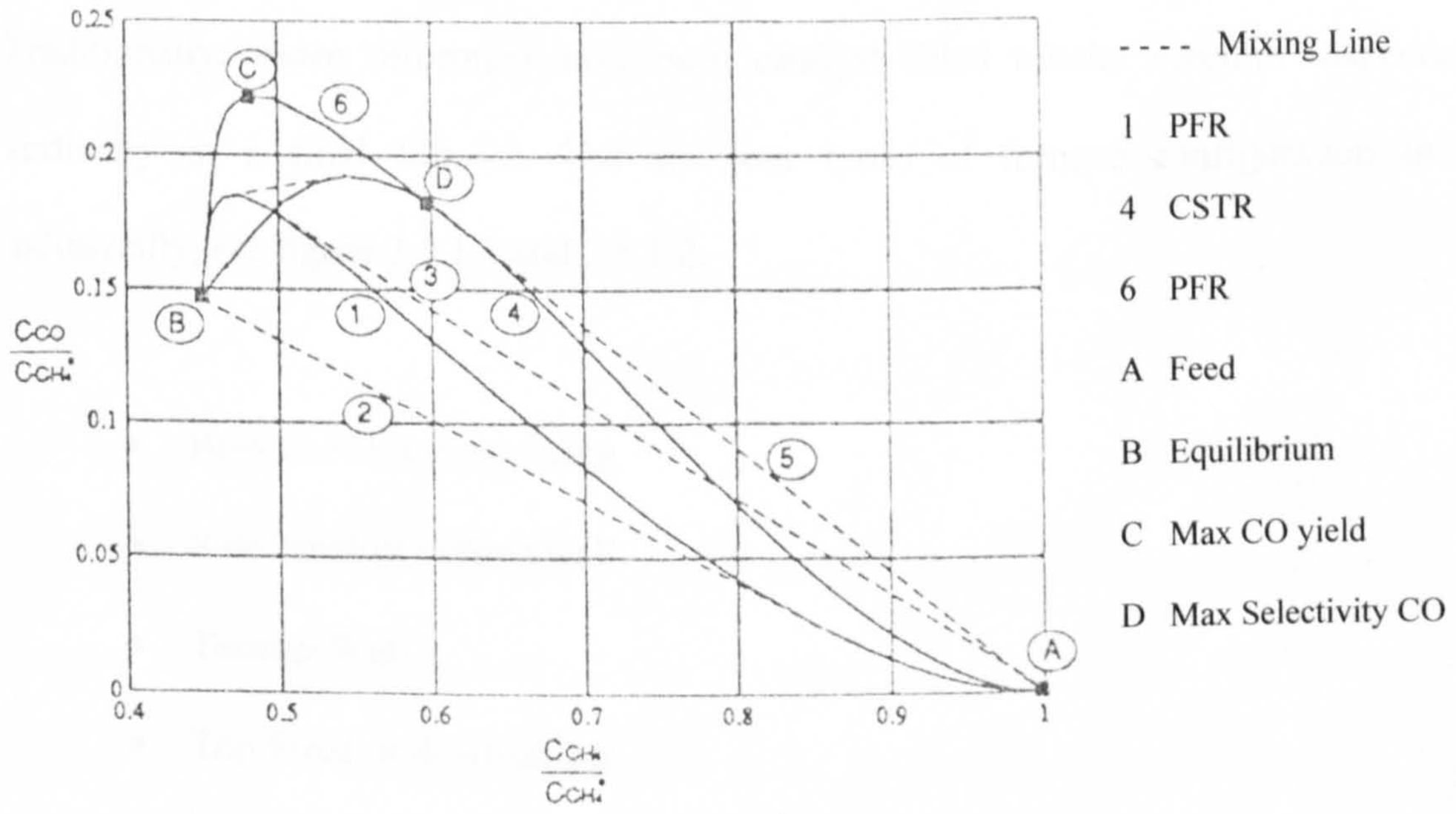

Figure 3.5.1: Attainable Region for Steam Reforming Reactions at 1050K

[Omtveit et al. (1994)]

As for the catalyst, there is no single standard design for reformers and these are discussed by several authors. However, there can be considered three main industrial types, primary, secondary or autothermal, and combined.

The relative merits of the reformer configurations and combinations is debated by several authors including Goff and Wang (1985), Orphanides (1993), Chritensen and Primdahl (1994), Seddon (1994), Dybkjaer (1995) and Basini and Piovesan (1998), however, there is no universal preference. This debate is also repeated for debottlenecking by Synder et al. (1986), Singh and Patel (1995) and Koenig et al. (1997).

3.5.1 Primary reformers

Traditionally, steam reformers have been catalyst filled tubular reactors suspended vertically in a fired furnace. The are four types of furnace configuration used industrially, see figure 3.5.1.1 and 3.5.1.2,

- Bottom Fired or up-firing
- Side Fired or radiant wall
- Terrace Wall
- Top Fired or down-firing

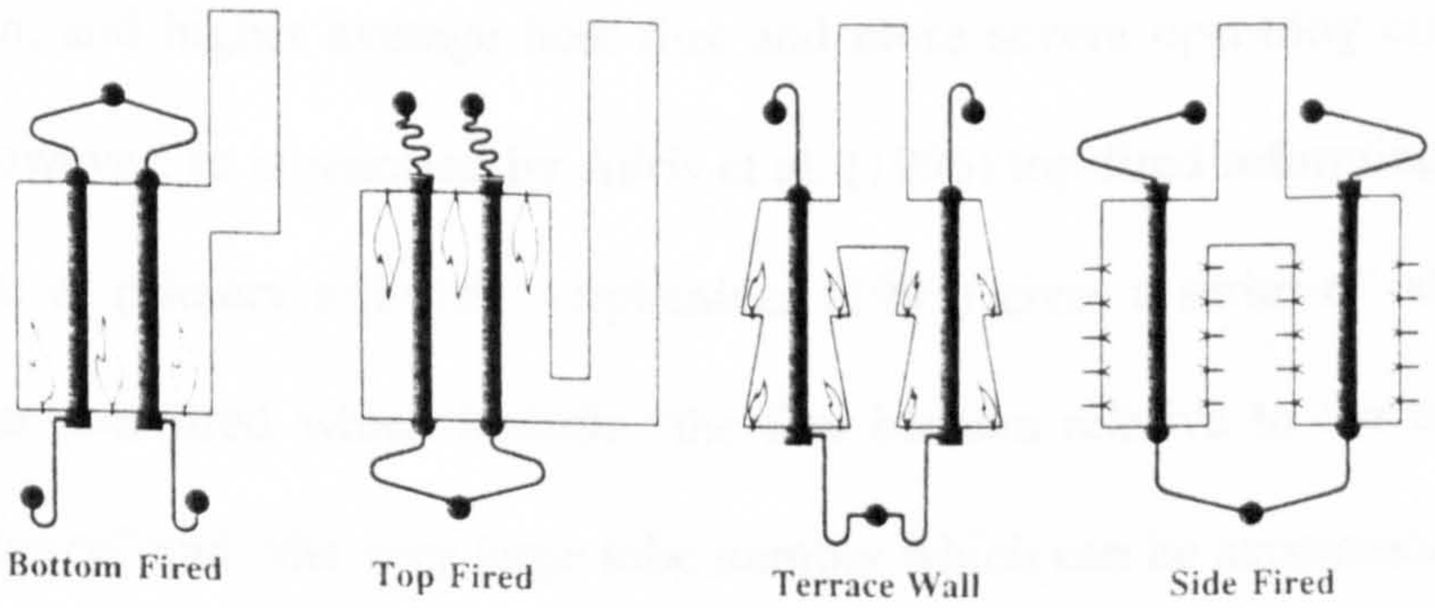

Figure 3.5.1.1: Furnace configurations for Primary Reformers [Dybkjaer (1995)]

The relative merits of the reformer configurations and combinations is debated by several authors including Goff and Wang (1985), Orphanides (1993), Chritensen and Primdahl (1994), Seddon (1994), Dybkjaer (1995) and Basini and Piovesan (1998), however, there is no universal preference. This debate is also repeated for debottlenecking by Synder et al. (1986), Singh and Patel (1995) and Koenig et al. (1997).

3.5.1 Primary reformers

Traditionally, steam reformers have been catalyst filled tubular reactors suspended vertically in a fired furnace. The are four types of furnace configuration used industrially, see figure 3.5.1.1 and 3.5.1.2,

- Bottom Fired or up-firing
- Side Fired or radiant wall
- Terrace Wall
- Top Fired or down-firing

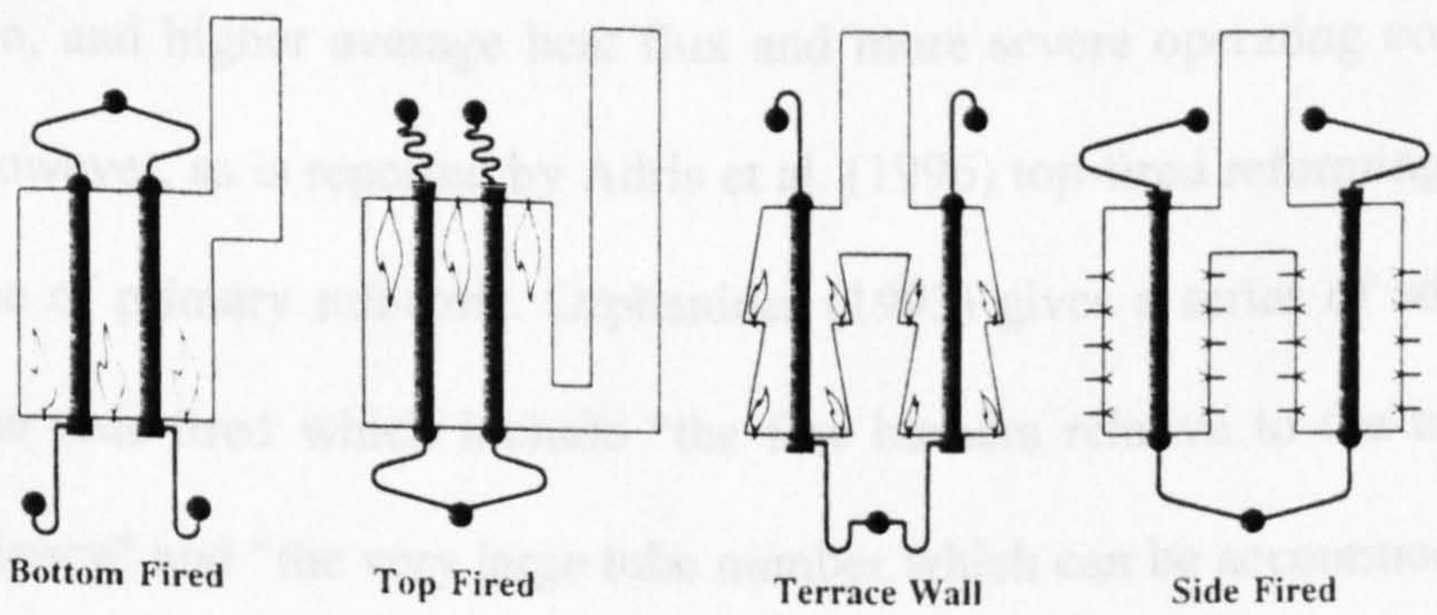

Figure 3.5.1.1: Furnace configurations for Primary Reformers [Dybkjaer (1995)]

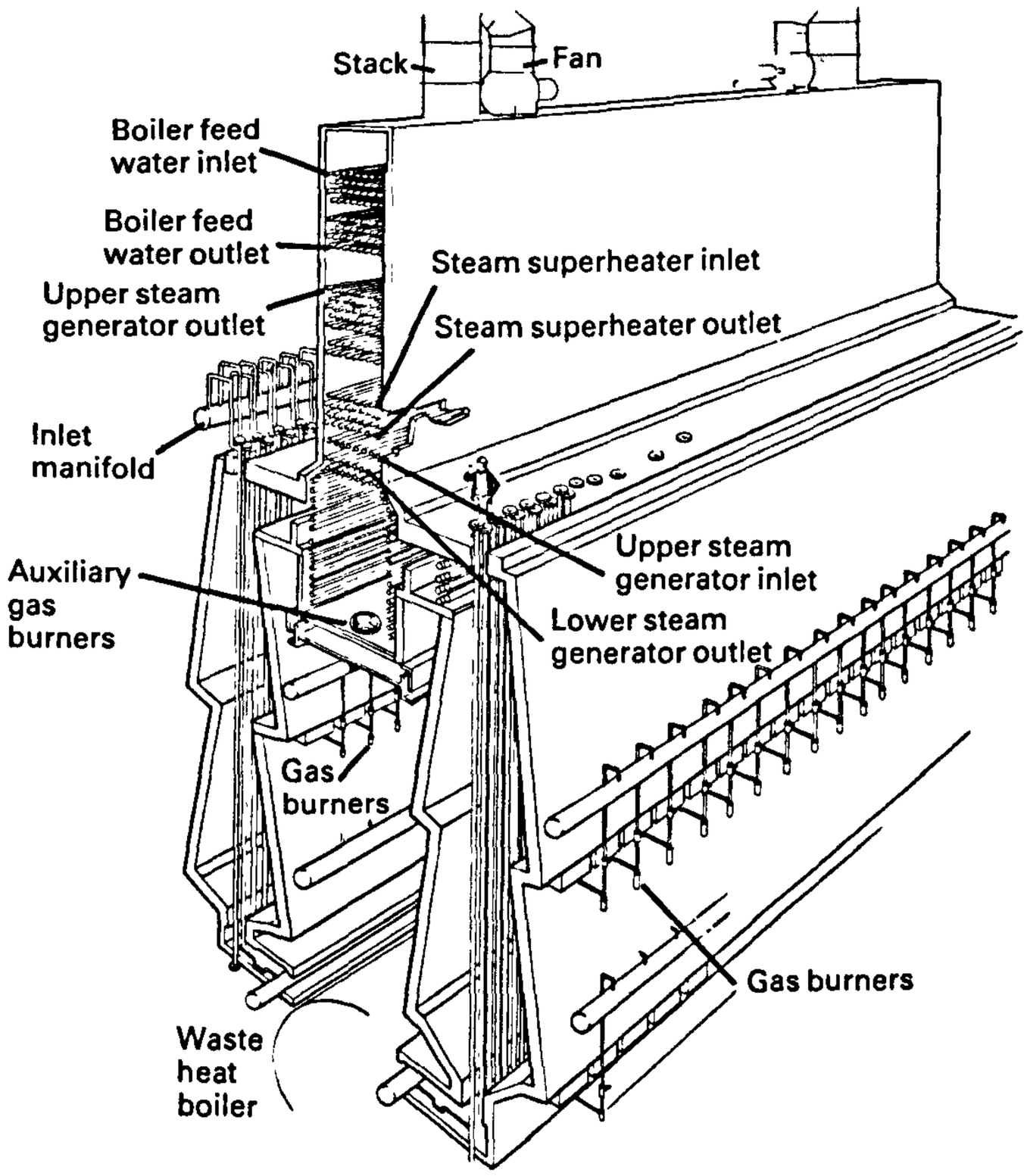

Figure 3.5.1.2: Schematic arrangements of Terrace-Wall Furnaces and Top-Fired

[Twigg (1997)]

The different arrangements of the burners in the furnace produce different heating patterns and hence temperature profiles, see figure 3.5.1.3. Dybkjaer (1995) contends that a side-fired arrangement is the most suitable as it "offers more flexibility in design and operation, and higher average heat flux and more severe operating conditions are possible". However, as is reported by Adris et al. (1996) top-fired reforming is the most common type of primary reformer. Orphanides (1993) gives a series of advantages of top-fired over side-fired which include "the few burners relative to the tubes, higher radiant efficiency" and "the very large tube number which can be accommodated in one radiant box".

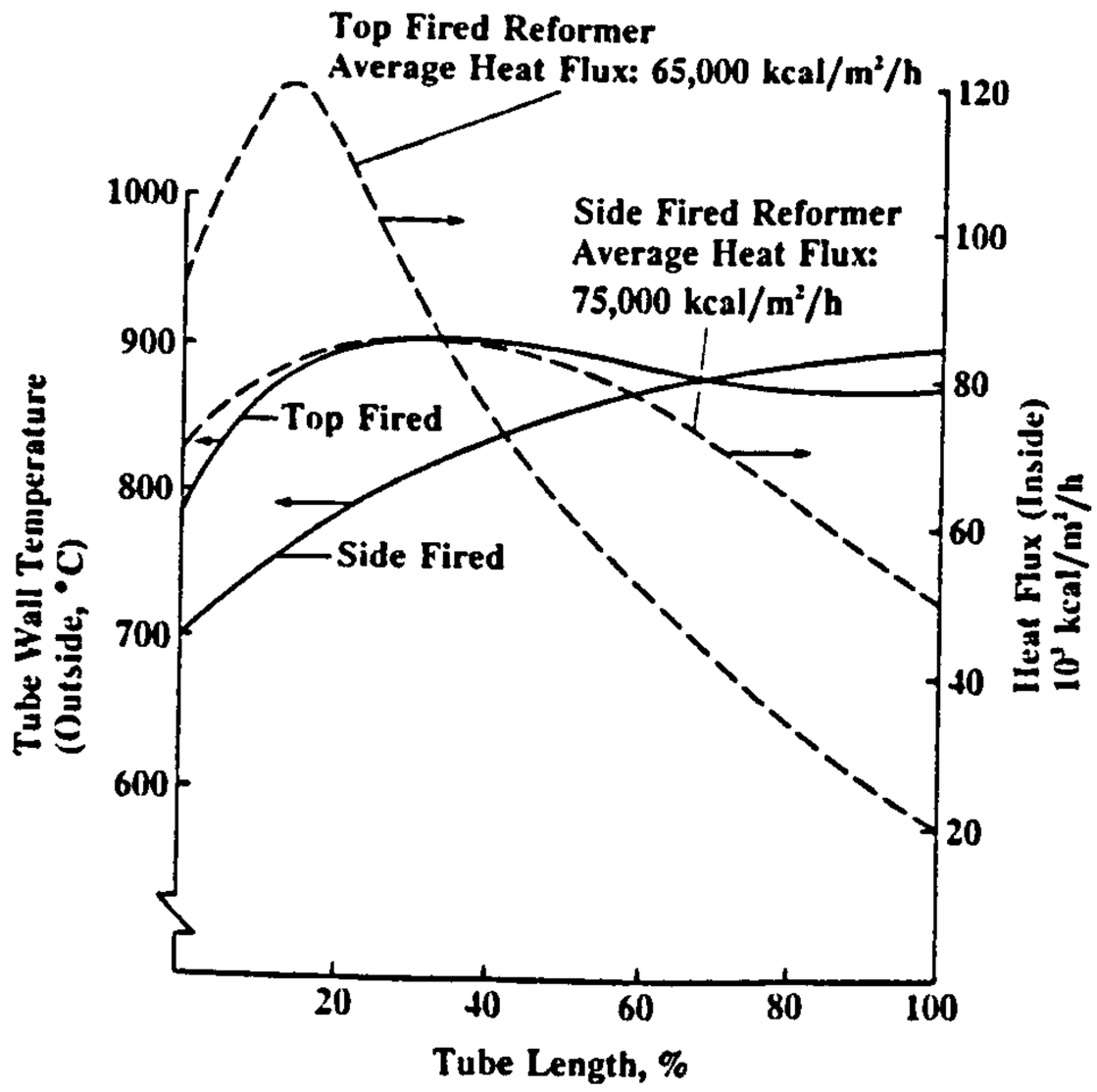

Figure 3.5.1.3: Tube temperature and heat flux profiles. Side and top fired reformers. Start of run [Dybkjaer (1995)]

Adris et al. (1996) detail typical features of 40 to 400 tubes of internal tube diameter range 70 to 160 mm, tube wall thickness 10 to 20 mm and length 6 to 12m. The tubes are high alloy nickel chromium steel and are either supported from the floor or the ceiling.

Typical operating conditions of a primary reformer for Ammonia and Methanol plants are listed in table 3.5.1.1.

Ammonia Plant

	Inlet primary reformer	Exit primary reformer	Exit secondary reformer
Pressure/bar	35	30	29
Temperature/°C	525	790	971
CH_4/%	91.9	9.4	0.2
C_2H_6/%	2.9	0.0	0.0
C_3H_8/%	0.6	0.0	0.0
C_4H_{10}/%	0.2	0.0	0.0
C_5H_{12}/%	0.1	0.0	0.0
C_6H_{14}/%	0.1	0.0	0.0
CO_2/%	0.3	11.6	8.8
N_2/%	1	0.5	22.1
CO/%	0.0	8.3	11.5
H_2/%	2.9	70.2	57.1
A/%	0.0	0.0	0.3

Methanol Plant

	Inlet primary reformer	Exit primary reformer
Pressure/bar	23.0	20.4
Temperature/°C	514	850
CH_4/%	89.1	4.5
C_2H_6/%	3.3	0.0
C_3H_8/%	1.2	0.0
CO_2/%	0.1	8.1
N_2/%	2.3	0.6
H_2/%	4.0	73.1
CO/%	0.0	13.7

Table 3.5.1.1: Typical operating conditions for primary reformers on Ammonia and Methanol plants (dry gas analysis) [Twigg (1997)]

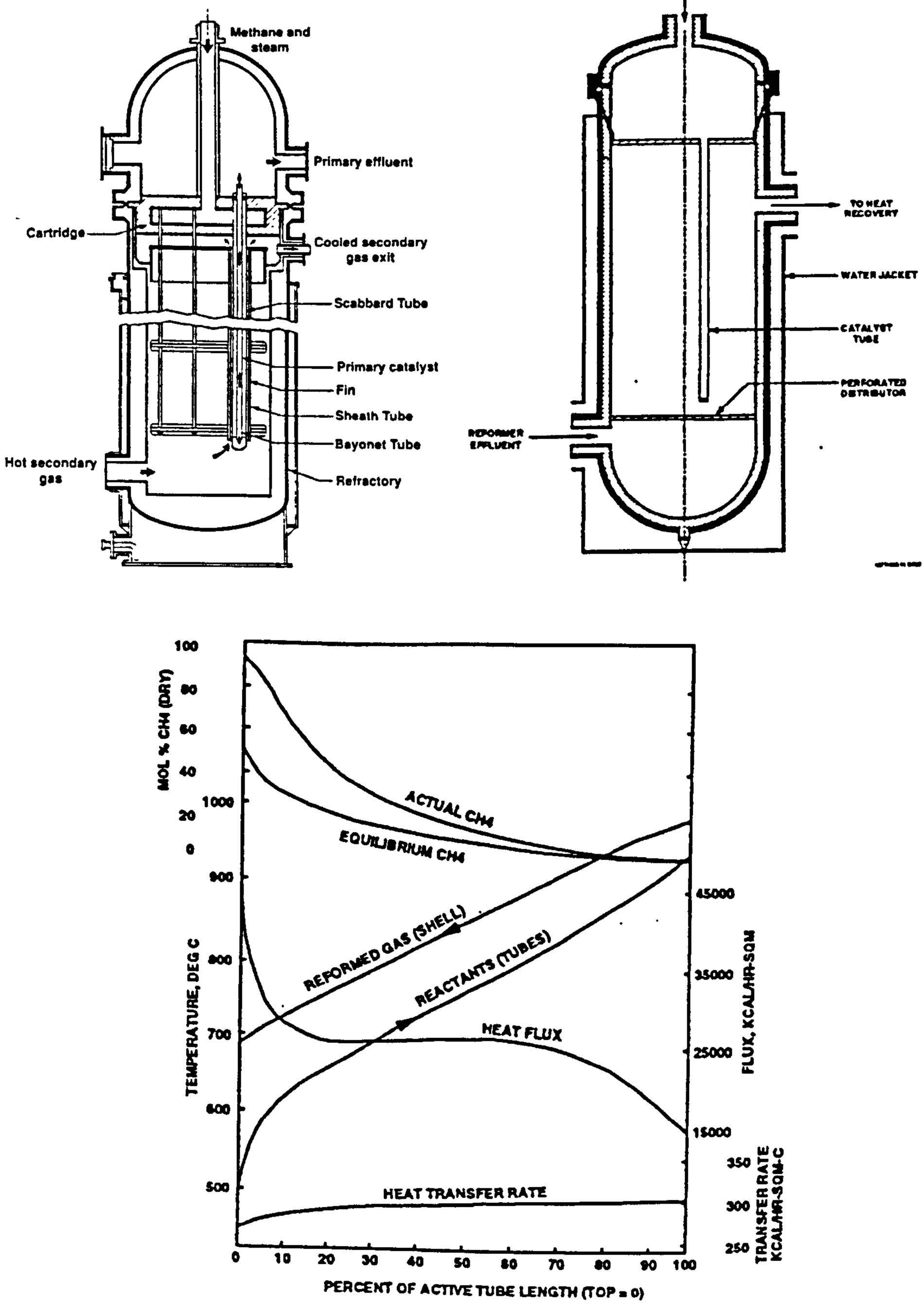

Figure 3.5.1.4: KRES and GHR reformers layout and KRES performance profile [Orphanides (1993), LeBlanc et al. (1996)]

Within industry, however, there is a shift away from the fired furnaces towards designs which could be considered as catalyst filled heat exchangers, see figure 3.5.1.4. The failings of the fired heaters are reported by several authors including Orphanides (1993), Dybkjaer (1995), Adris et al. (1996) and LeBlanc et al. (1996), as heat transfer limitations, large and complex heat recovery systems, long and costly start up periods and nitrous oxides from burners. Miyasugi (1984), Orphanides (1993), Dybkjaer (1995) and LeBlanc et al. (1996), see figure 3.5.1.4, introduce and discuss various heat exchanger designs for steam reformers and all claim progress in resolving the problems. Adris et al. (1996) identifies further failings of industrial designs of steam reformers, and discusses the various alternative designs which have attempted to improve performance. However, apart from the heat exchanger style reformers the designs are in the "laboratory, pilot or demonstration stage of development".

Generally for primary reformers, however, there are similar design considerations which include,

- Tube life – Orphanides (1993) states the tubes are "the most critical item in a fired reformer", also Adris et al. (1996) adds that the tubes "account for a large part of the reformer cost" and "the reliability of the tubes is also important because tube failures could result in long down-periods for re-tubing and hence loss of production". Tillack and Guthrie (1999) indicate that "seldomly" is one alloy suitable for all the system requirements, so "compromises" are required. Ultimately, the tubes will suffer creep, however, this can be accelerated by several conditions discussed by Orphanides (1993) such as uneven flow in tubes, uneven heating of tubes,

catalyst deterioration, many start-ups and shut-downs and over-firing during start-up.

- Tube corrosion – Oxidation, sulfidation, carburization, nitridation and halogen corrosion are potential corrosion mechanisms in a steam reformer. However, carburization in the form of "Metal dusting" is the predominant corrosion concern for steam reforming. Dybkjaer (1995) discusses this "catastrophic corrosion" which occurs when carbon monoxide-rich gas contacts metals at high temperatures. The corrosion products are more brittle and can easily be eroded forming holes in the material similar to pitting, see figure 3.5.1.5. A number of techniques to control "metal dusting" are discussed by Hohmann (1996).
- Heat transfer performance – a fired furnace has only a thermal efficiency of about 50%, LeBlanc et al. (1996).
- Pressure drop – as indicated in section 3.3, a high pressure is operated on the basis of overall process economics.
- Catalyst life – carbon formation and catalyst sintering and poisoning are the most important effects on catalyst life. From these further problems can develop that could shorten the catalyst life and affect the operation of the reformer. Teixeira and Giudici (1999) studied, and simulated, steam reforming catalyst sintering at process conditions.

Finally, the reformers once operational must be monitored as the performance will change with time. A major periodic survey of a reformer is recommended to give "an accurate assessment of catalyst performance, reformer operation, tube life estimation and identification of operating limits" which can be "used to identify suitable reformer

optimisation and uprate strategies" (Farnell 1996). Rase (1990) develops an expert system of stream reformers for such reactor diagnostics. These techniques can be used during the start up of a primary reformer to assess the quality and precision in catalyst loading, for which the methods and related problems are discussed in Cromarty and Farnell (1993) and Twigg (1997).

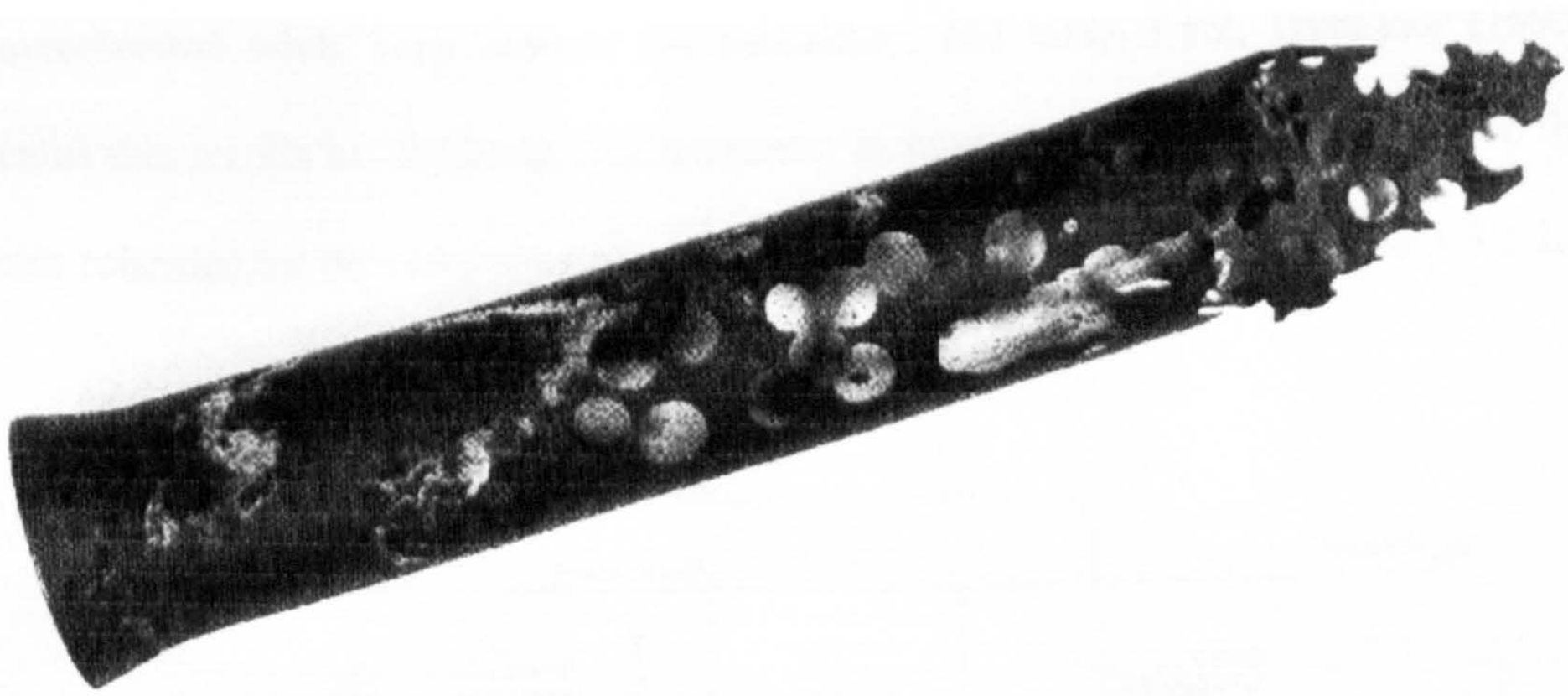

Figure 3.5.1.5: Alloy800 Boiler Ferrule which has suffered Metal Dusting in Steam Reformed Gas at ca 600°C [Richardson (1983)]

3.5.2 Autothermal or secondary reformers

Elvers et al. (1989b) states that autothermal and secondary reformers are employed for,

- High equilibrium temperatures, hence, low methane concentration
- Ability to operate at high pressures and high temperatures, impractical in fired reformers
- Ammonia Synthesis, as the point of introduction of elemental nitrogen

Part of the feedstock is oxidised to supply the energy required for the steam reforming reactions, catalytic oxidation for autothermal reformers and thermal oxidation for secondary reformers. There are some discrepancies in the literature on the combustion reaction schemes for both types of reactors, which is discussed in chapter 4.

Due to the distinct application of autothermal and secondary reformers, full conversion for autothermal while only closure for secondary, see table 3.5.2, Dybkjaer (1995) indicates this results in "different requirements for burner and reactor design". Also the process schemes for the reforming section are different, see figures 3.5.2.1 and 3.5.2.2.

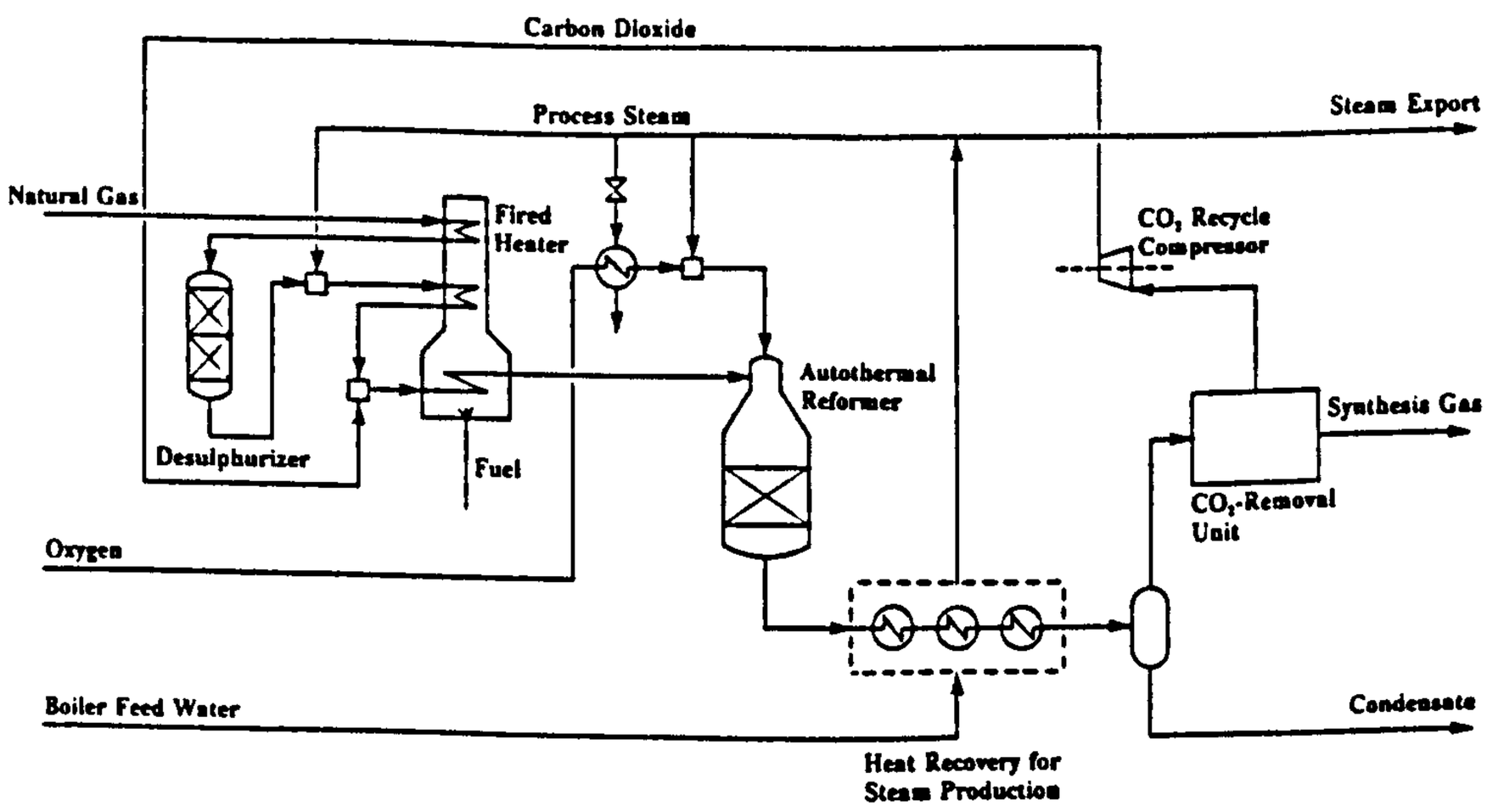

Figure 3.5.2.1: Typical process flow diagram for autothermal reforming. Production of synthesis gas with hydrogen-carbon monoxide ratio 2.0 [Dybkjaer (1995)]

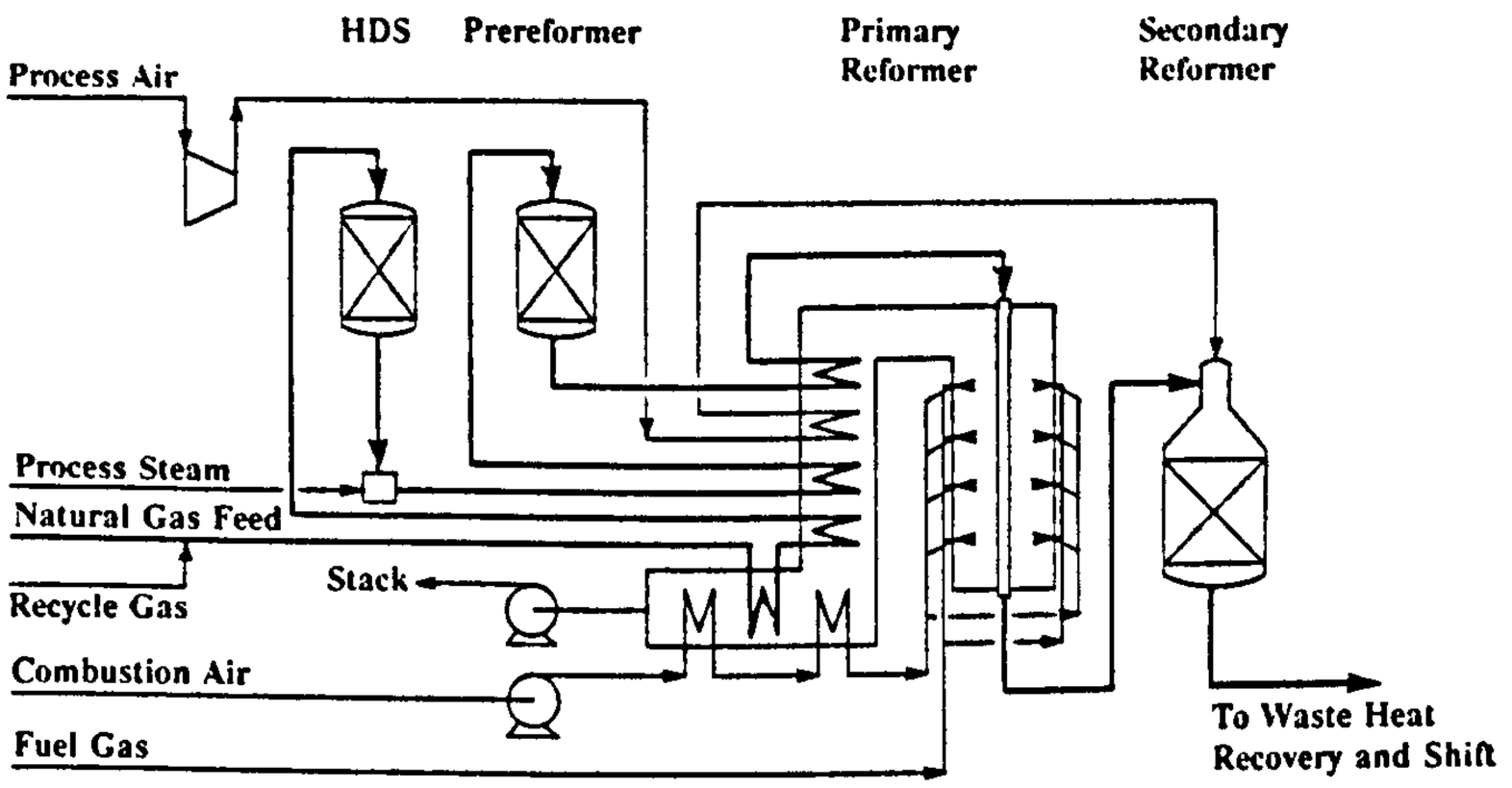

Figure 3.5.2.2: 'State-of-the-art' reforming section for production of ammonia synthesis gas [Dybkjaer (1995)]

Despite the differences as Dybkjaer (1995) indicates essentially, "both consist of a compact refractory-lined pressure vessel with a burner, a combustion chamber and a catalyst bed". This system is often described as four zones, a burner for feed mixing, a turbulent combustion flame or combustion zone, a thermal zone in which reforming, the shift and several other homogenous reactions occur, and a catalytic zone or catalyst bed with the same reaction scheme as the primary reformer. Several authors, including Dybkjaer (1995) identify the burner as "the key element of the autothermal and secondary reforming technology". The burner style represents the greatest variation between the designs, see figure 3.5.2.3.

		Methane tail gas reforming with oxygen addition	Reforming with air addition and precombustion (secondary reformer)
Gas for reforming	Composition,vol %		
	CO_2		7.11
	CO	3.90	4.25
	H_2	1.80	34.32
	CH_4	80.0	3.90
	C_2H_4	0.25	
	C_2H_6	0.05	
	N_2	1.70	
	Ar	12.30	
	H_2O		50.42
	Flow rate, m^3/h	55000	160000
	Pressure, MPa	3.0	3.04
	Temperature, °C	500	780
Oxygen or air	Flow rate, kg/h	27725	30400
	Temperature, °C	240	550
Steam	Flow rate, kg/h	113100	
	Temperature, °C	485	
Reformed gas (dry)	Composition,vol %		
	CO_2	13.23	10.59
	CO	16.99	11.67
	H_2	63.23	55.52
	CH_4	1.08	0.19
	N_2	0.65	21.77
	Ar	4.82	0.26
	Flow rate, m^3/h	148400	109000
Reformed gas (moist)	Flow rate, m^3/h	251450	196000
	Pressure, MPa	2.65	2.97
	Temperature, °C	925	965

Table 3.5.2: Data for two reformed gases obtained by autothermal reforming [Elvers et al. (1989a)]

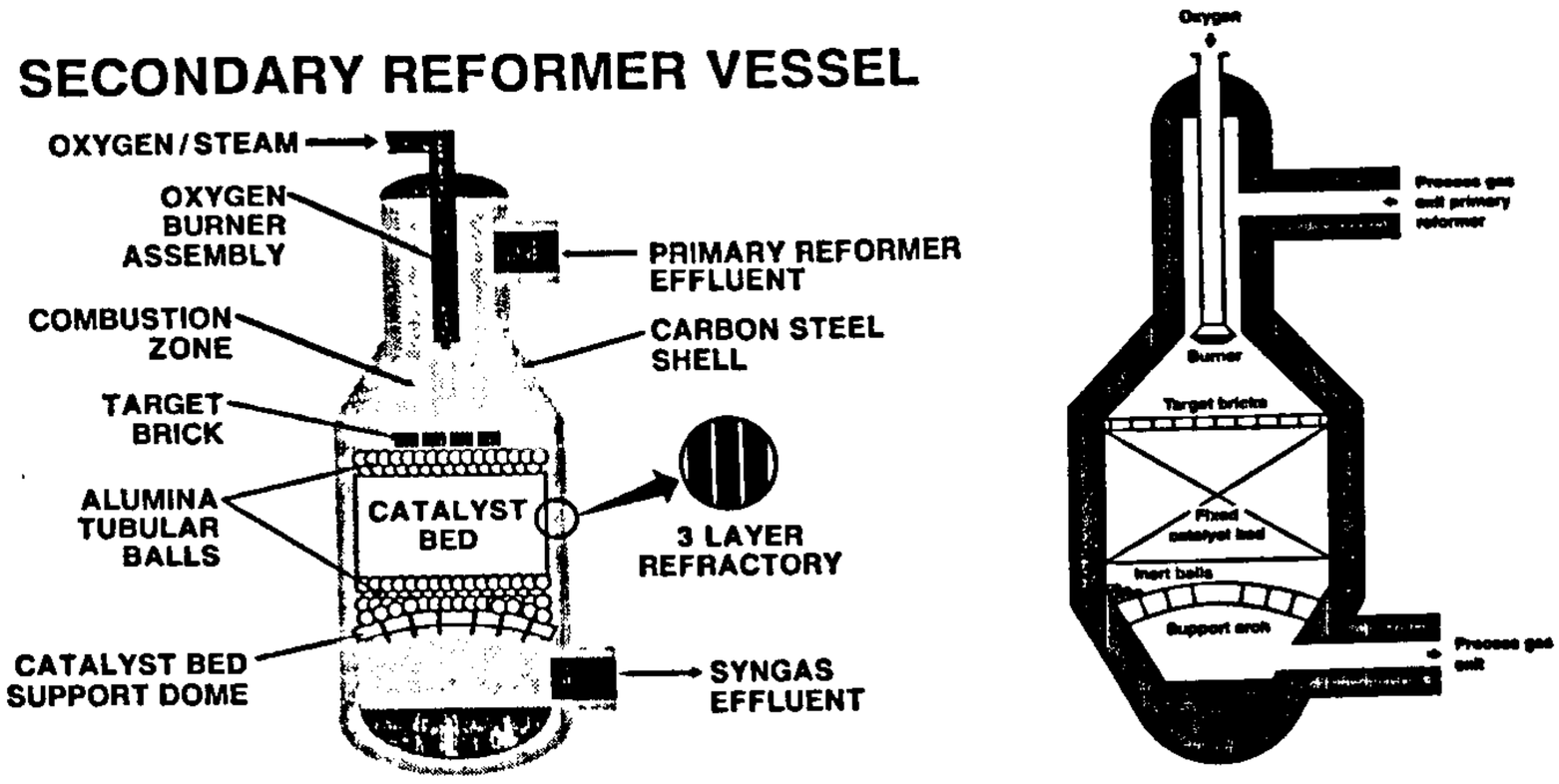

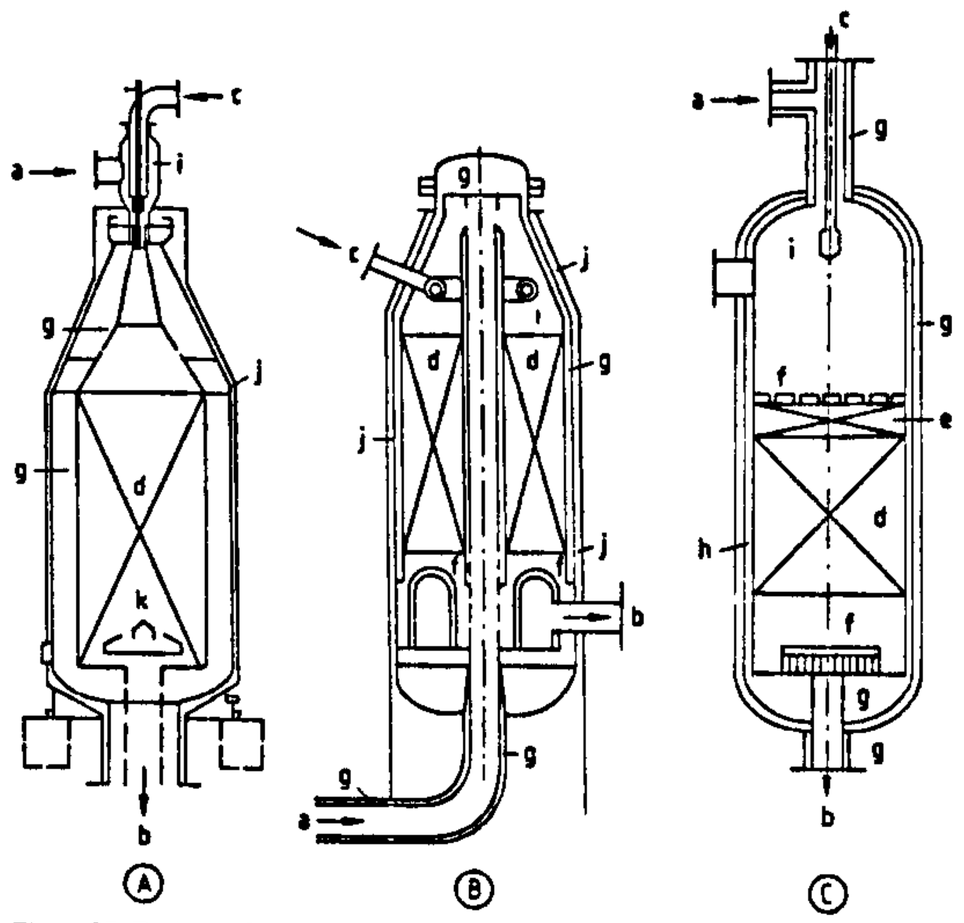

Figure 25. Designs of secondary (autothermal) reformers
A) Water-cooled jacket reactor with burner for methane-rich gases
B) Secondary reformer with toric oxygen or air supply device [4 42]
C) Secondary reformer with water-cooled tip without water jacket [4 55]
a) Raw gas inlet; b) Reformed gas outlet; c) Air, oxygen, and steam inlet; d) Catalyst; e) High-temperature catalyst, f) Inert material; g) Internal insulation; h) Multiple layers insulation; i) Burner; j) Water jacket

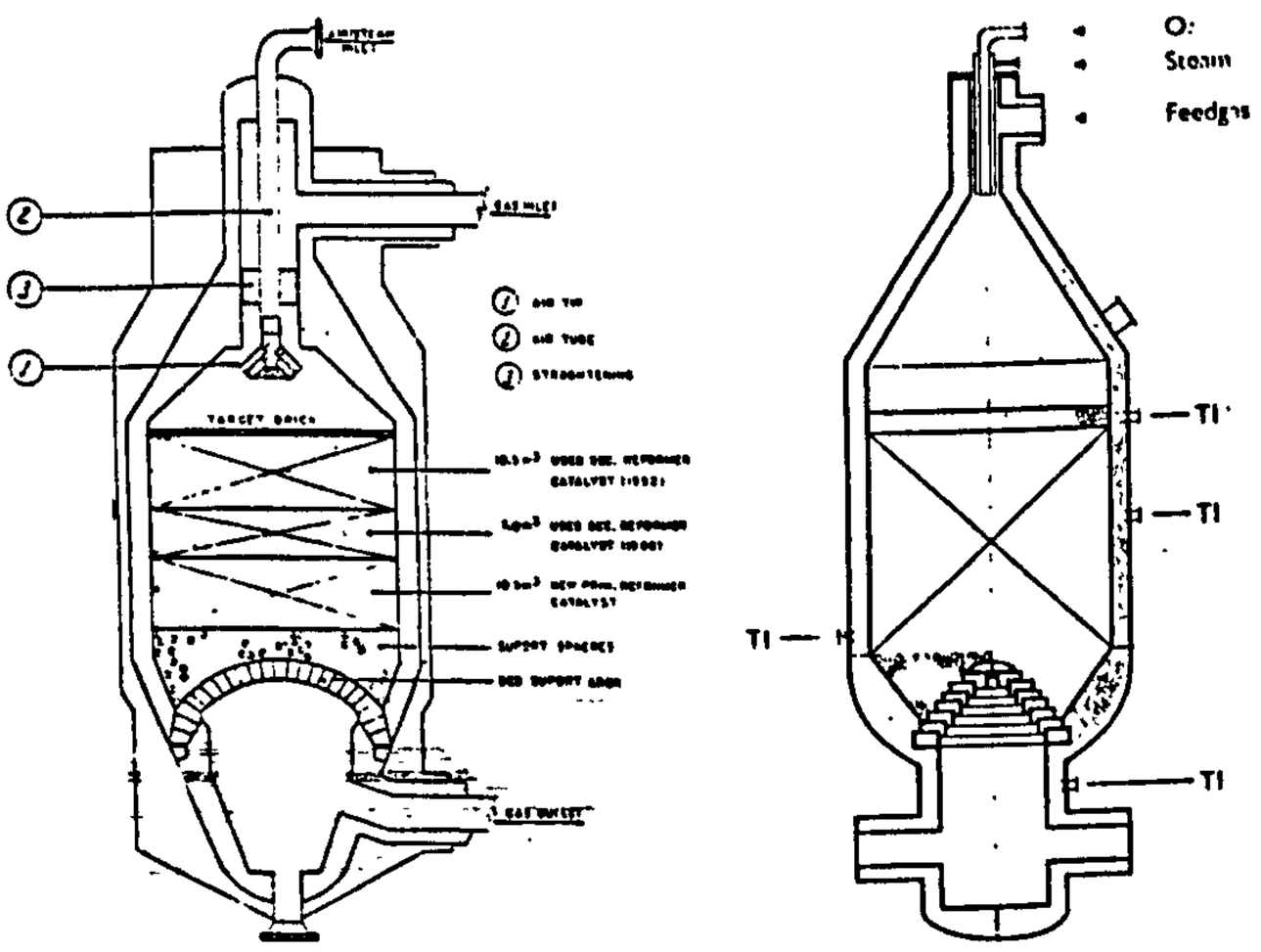

Figure 3.5.2.3: Various arrangements for autothermal and secondary reformers

[Synder et al. (1994), Elvers et al. (1989a and b), Farnell (1993), Rocha de Avila and Neto (1993), Shaw et al. (1994)]

In the literature there is only one comparison of burner designs, by Christensen et al. (1994), however, the styles of the burners are not shown, and as is the case in most of the literature the authors claim best performance. Christensen et al. (1994) discuss burner design and state "until recently, burner design was largely an empirical exercise, and new developments were to a large extent based on stepwise improvements of existing designs", confirmed by comments of Singh and Patel (1996) and equipment sketches by Orphanides (1993). Singh and Patel (1996) also demonstrate the comment of Christensen et al. (1994) that "designs based on this type of approach tend to be conservative, and it is generally difficult to extrapolate to new process conditions." To improve burner development and design there is a general consensus in the literature that additional design tools should be used, specifically computational fluid dynamics, see section 2.3. However, Farnell (1992) argues that with underlying knowledge of combustion systems, together with design experience it is no longer necessary to use CFD to diagnose every problem. Further to this, most authors suggest overall some form or ring burner with nozzles as the most suitable burner, however, Blanchard and LeBlanc (1993) state such devices are "particularly prone to metallurgical failure at high temperatures, which can result in performance deterioration, premature shutdowns, and degradation and reduced life of the catalyst charge". Ultimately though, there is no indication given in the literature of automated optimization and most authors seem to suggest a repetitive simulation strategy with the initial start point derived from fundamental fluid dynamics knowledge such as Thring and Newby (1953) and Beer and Chigier (1972).

Jet mixing in confined flows, as is the case for autothermal and secondary reformers, is often applied in conjunction with other mixing aids. For the process gas a set of straightening plates are installed above the burner, to produce fully developed laminar flow which maximizes the jet mixing. Due to the temperature of operation, between the burner and the catalyst bed, inclusion of thermally robust materials is almost impossible or uneconomical. Finally, swirling vanes could also be added to the air, however, there is no indication in the literature of this being used.

Obviously, the dimensions of reformers vary not only due to the different operation conditions and performance requirements, see table 3.5.2, but also due to distinct choice of burner. Within the literature there is less information than for primary reformers so dimensions must be gleamed from several authors. The rough dimensions for an autothermal or secondary reformer are about 13m in height and a maximum diameter of 5m, some idea of scale can be understood when compared to a primary reformer, see figure 3.5.2.4.

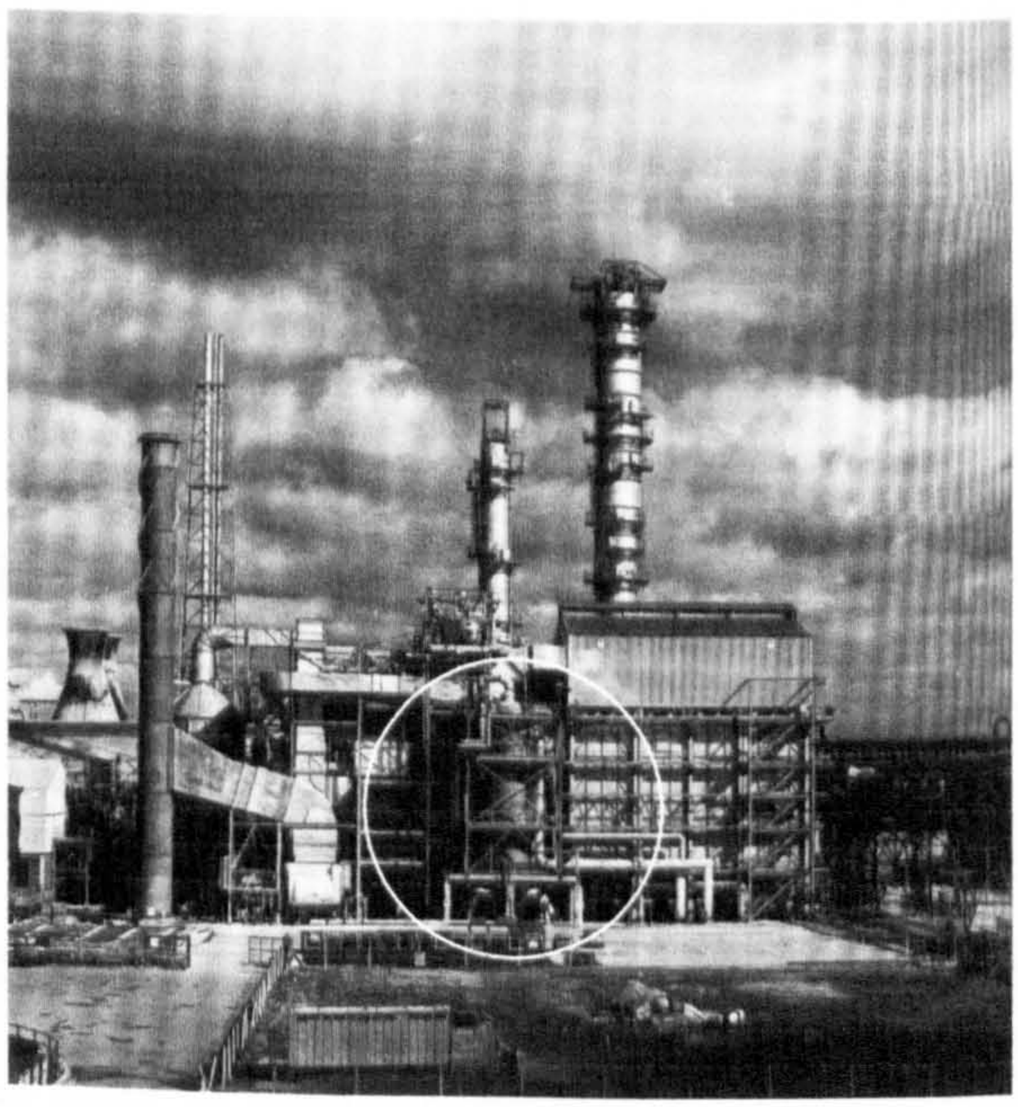

Figure 3.5.2.4: The top-fired reformer on ICI's No.4 ammonia plant at Billingham

[Twigg (1997)]

Despite the differences for autothermal and secondary reformers there are similar design considerations which include,

- Burner Style – Several authors discuss the requirements of burner; these include the requirement to limit the temperature on the metal of the burner, provide enough mixing for soot-free combustion, guarantee all the oxygen is combusted and generate a suitable flow pattern for the other flow-field dependent considerations. Also, Shaw et al. (1994) illustrate that the burner must limit the sensitivity to vibration by choice of construction material and Christensen et al. (1994) discuss how shape can limit erosion and corrosion, hence maintenance.
- Temperature and concentration variation across the top of the catalyst bed – Farnell (1992) states "the major requirement from a process performance point of view is the production of an evenly-mixed gas stream for entry into the catalyst bed. The gas must have a uniform concentration and temperature at the top of the catalyst bed in order to ensure that the catalyst bed is fully utilized, giving the lowest possible methane concentration at the outlet." [Confirmed by McKetta and Cunningham (1977), Blanchard and LeBlanc (1993), Christensen and Primdahl (1994) and Christensen et al. (1994)].
- Refractory temperature – Excessive temperatures on the refractory are discussed by Christensen et al. (1994). Initially damage will be caused to the refractory which will fall as debris on top of the catalyst bed and potentially inflict further damage. Ultimately even if excessive temperatures are not maintained this can lead to damage to the pressure vessel and catastrophic failure. The need to limit the refractory temperature is also highlighted by several other authors.

- Temperature on top of the catalyst bed – Christensen et al. (1994) associates excessive temperatures with catalyst destruction and sintering.
- Magnitude of velocity across the top of the catalyst bed – "the velocity gradient exiting the combustion chamber is reduced to an appropriate low value at the catalyst bed surface so that milling and degradation is minimised" is identified by Blanchard and LeBlanc (1993) as a design consideration. However, there is no other mention of this in the literature, the only other comment to approach the subject of the velocity is by Christensen et al. (1994) on requiring even flow direction and magnitude.
- Pressure drop – as indicated in section 3.3, a high pressure is operated on the basis of overall process economics.
- Refractory lining material – The lining is identified by McKetta and Cunningham (1977) and McKetta (1994) as "a potential source of compounds that could deactivate downstream catalysts or foul heat exchanger surfaces." Such an industrial example is given by Shaw et al. (1994).
- Soot formation – The risk of soot formation is very low, however, Christensen and Primdahl (1994) and Christensen et al. (1994) report that catalyst converts the soot and its precursors into "non-fouling compounds, which can be observed in the process condensate". However it should be noted that the source of formation may be external to the secondary reformer design, as reported by Murdoch and Still (1996).
- Metal dusting – As described in section 3.5.1 this can occur in both autothermal or secondary reformers, such an occurrence is described by Shaw et al. (1994).

These design considerations must be taken into account when determining the geometric design parameters for autothermal and secondary reformers. The geometric parameters are the diameter of the process gas inlet, height of the burner above the bed, angle of the cone, diameter of the catalyst bed and shape of the burner. As is mentioned earlier, there is no indication of automated optimisation for the design of autothermal or secondary reformers, even though the difficulty of predicting the effect of these parameters on the design considerations is evident. This difficulty is highlighted for the scale-up of secondary reformers, reported by Shaw et al. (1994) and Singh and Patel (1996).

The operation of secondary reformers and autothermal reformers in industry has often suffered problems due to burner design. Christensen et al. (1994) categorises them into "catastrophic failure, malperformance with increased production cost and mechanical wear". An industrial example of catastrophic failure is described by Shaw et al. (1994) where fragments generated by metal dusting lodged in the burner and promptly the refractory and shell failed, see figure 3.5.2.1. Malperformance is well reported in the literature; examples include catalyst support dome failure by Connaughton and Clark (1984), catalyst deformation and volatilization and lower shroud failure by Vick (1987), case studies of poor burner design by Farnell (1992) and burner failure by Rocha de Avila and Neto (1993).

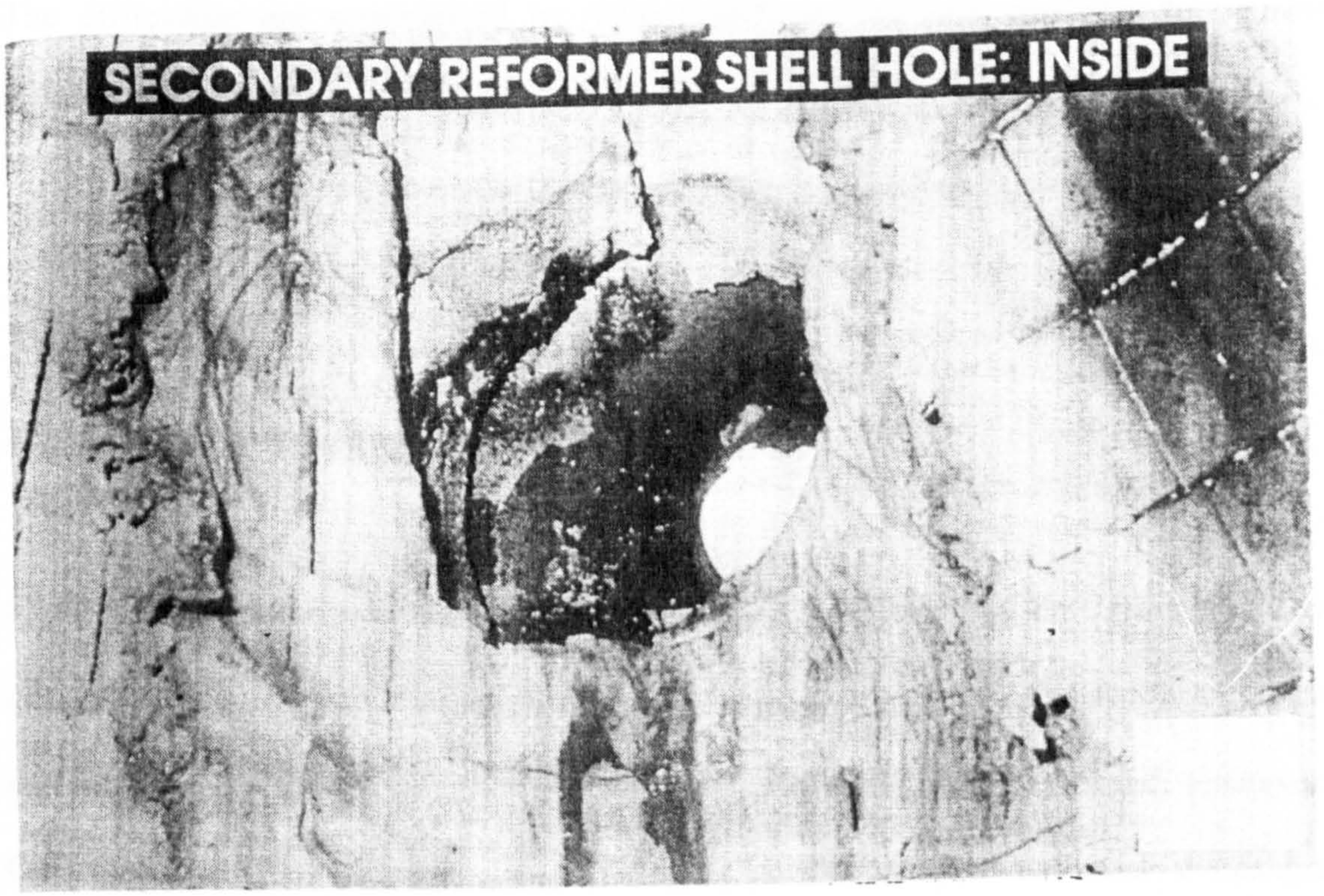

Figure 3.5.2.1: Secondary reformer shell hole: inside [Shaw et al. (1994)]

An ICI Secondary Reforming Catalysts manual states that "operating problems are difficult to interpret because of lack of reliable operating records and in particular, the difficulty in measuring accurately the high temperature". This is confirmed in the industrial examples. The only suggestion by ICI is to maintain "regular readings of gas compositions, bed temperature and pressure drop". Other methods proposed were by Shaw et al. (1994), of burner vibration monitoring to determine crack propagation and shell temperature measurements with optical fibre, and by Twigg (1997) using the exit carbon monoxide concentration to verify the exit temperature. The limits of the measurement accuracy should be remembered, as Rocha de Avila and Neto (1993) discovered that "as usual, bed temperature profile was not reliable" due to the length of the thermocouple and its positioning relative to the problem region.

The difficulties are summarised by Vick (1987) as "an easy catalytic duty under difficult mechanical conditions. This disparity can result in extended intervals between comprehensive vessel inspections, further aggravating mechanical problems."

3.5.3 Combined reformers

Orphanides (1993) describes a demonstration unit developed by the Uhde company named a Combined Autothermal Refomer (CAR), figure 3.5.3.1, in which both a heat exchanger type primary reformer and an autothermal reformer are housed. However, Orphanides (1993) indicates that a simpler model of just the heat exchanger arrangement is under development for operation with an autothermal or conventional reformer and states that "ICI, MWKellogg and others are following the same route." The CAR, apart from suffering from the flaw identified by Orphanides (1993) of "part of the feed gas is only partially oxidised, without undergoing a subsequent secondary steam reforming", also seems to increase the difficulty in debottlenecking the reforming section and the likelihood of the effect of a failure transmitting to the other reforming stage.

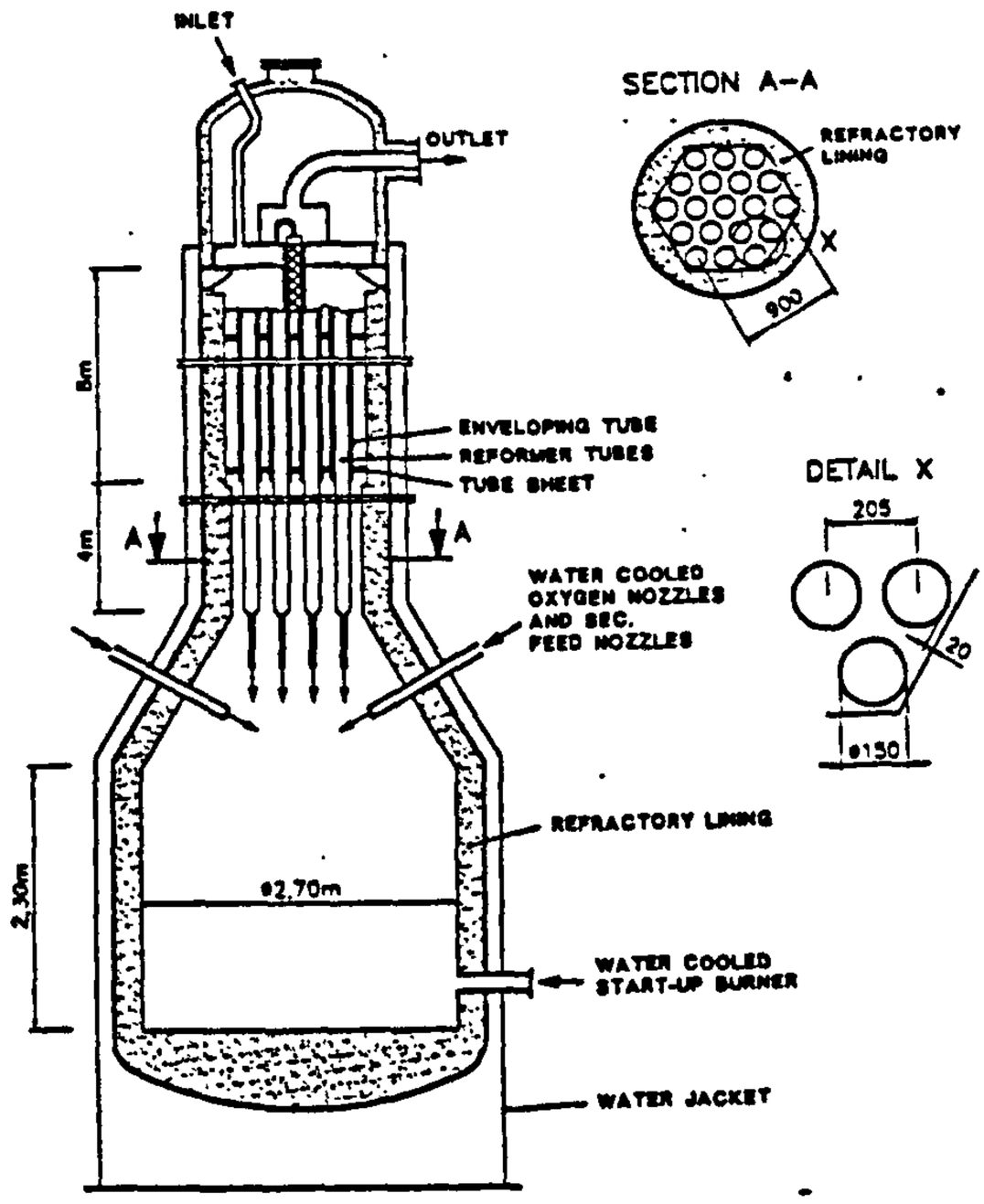

Figure 3.5.3.1: CAR demonstration reactor [Orphanides (1993)]

3.6 Models of reactors

3.6.1 Primary reformers

There have been several attempts to model primary reformers at various levels of complexity, not only to improve performance of the primary reformer but also for other purposes, such as to develop control schemes.

Roesler (1967) discussed the simulation of a top-fired primary reformer furnace, with the complexities of the tube side modelling ignored. The author suggests that the furnace simulation should be segregated on a radiation field basis, using the method of Schuster-Schwarzschild, as a more "straight-forward" approach to the geometrical

'zoning' method, presented by Hottel and collaborators. Both the tube and the burners are assumed to be uniformly distributed, so that the geometry of the furnace can be defined by four parameters. Also the flow for most of length is defined as plug flow, however, in the flame region an allowance is made for the turbulence. For the heat transfer, conduction and convection from the furnace gas to the tube skin are both ignored, and only two types of radiation are presumed, "band radiation" or "window radiation". Essentially the author regards the reformer as a "multi-stream exchanger".

As is common amongst primary reformer simulations, Hyman (1968) considers only the internals of the reformer tubes and ignores the furnace modelling by using a typical tube wall temperature profile. Also, as for several other authors, only one tube is simulated, which is considered to be representative of all, and no radial gradients are deemed to be "sufficiently significant". The kinetics of Moe and Gerard from 1965, were adopted, which use an empirical relationship for the ratio of carbon dioxide to monoxide to represent the water-gas shift kinetics. For heavier hydrocarbons than methane instantaneous hydocracking is assumed at the inlet leading to a "methane equivalent". The side-fired reformer simulation compared well with a series of industrial data and yielded logical results from a sensitivity analysis.

The main focus of the optimisation study by Davies and Lihou (1971) was tube geometry and furnace operation. The simulation, however, included no reaction kinetics and an approximate temperature difference across the wall of the reformer tube had to be assumed. Despite this, the authors claim that the optimal case "agrees with published data" and that the model explains several disadvantages of high temperature operation.

Singh and Saraf (1979 and 1981) proposed a side-fired reformer model. The authors adapted reaction kinetic data and expressions from previous publications to account for the "significant pore diffusion resistance". For the furnace heat transfer, the radiation from the furnace gas and the flames to the tubes were separated and the heat loss through the furnace walls was assumed equal to the furnace gases' conduction and convection. The simulation was proven to produce "close agreement" for several sets of industrial data, however, for one set the difference is significant which is associated by the authors with measurement error.

A major commercial use for steam reforming for the future is fuel cell systems. Murray and Snyder (1985) developed a model for such a unit, but due to the difference in the scale of operation to the primary steam reformer, the assumptions vary for the simulations. Although essentially the same chemical system is under consideration, the physical situation contrasts to an extent that the simulation offers almost no relevance to primary steam reformers. The statement by Alatiqi et al. (1989) that no radiation was included, suggests that this difference has not been fully appreciated.

Chang and Liou (1987) use the PROCESS simulator by Simulation Sciences Inc. for a hydrogen plant. An approach to equilibrium of 20 to 50 °F for steam reforming and 0 °F for water-gas shift is assumed. The authors state “excellent agreement was obtained” when compared to plant data and “the model can be used as the hydrogen plant design basis”. However, the model can be considered very simplistic when compared to the issues discussed in section 3.5.1.

Elnashaie et al. (1988) apart from reviewing several issues involving steam reformers including kinetics also discusses the complexity of simulation of steam reformers. "Two main questions arise in this respect, the first is: 'shall we use a heterogeneous model or a pseudo homogenous model?' and the second is: 'shall we use a one-dimensional model or a two-dimensional model ?'". The authors conclude that heterogeneous models should be used, however, this approach is not universally adopted so they suggest further and more rigorous research is required. Also the authors report that "many authors have suggested the use of a one dimensional model".

Soliman et al. (1988) simulated both top-fired and side-fired furnace arrangements and performed model verification with industrial and published data. The authors developed a one-dimensional heterogeneous model with intraparticle diffusional resistances and the kinetics expressions developed by Xu and Froment (1989a), highlighted in section 3.2 and discussed in more depth in chapter 4. The solution technique used was a modified orthogonal collocation, see chapter 1. However, for the side-fired furnace the authors assume a "well-stirred enclosure having a mean temperature which is different from the exit temperature" and for the top-fired furnace a fraction of fuel combusted along the reformer is assumed.

Xu and Froment (1989b) relate the diffusional limitations to the tortuosity factor, with the tortuosity being determined by fitting simulated to experimental values. The same model type and solution technique as Soliman et al. (1988) is adopted. However, to compute the external tube temperature profile a zone model by Rao in 1988 is adapted for the furnace and coupled to the reactor.

Alatiqi et al. (1989) use a one dimensional heterogeneous model, as for the previous two authors but a fourth-order Runge-Kutta solution method, to trial two kinetic expressions by Moe and Gerhard in 1965 and a first order expression. To eliminate "the ambiguity of extensive radiation and convection calculations" a heat flux polynomial dependent on fuel gas fuel rate, fuel gas specific gravity, unit efficiency and length is developed. Data from two different industrial scale reformers show "excellent accuracy" for both kinetic expressions, but the first order expression gave "unrealistic sensitivity results", and "accurately simulated" by the empirically derived polynomial. However this author identifies assumptions made by some authors but not identified in the prior papers, that "all tubes in the reformer are considered to behave similarly" and "no carbon deposition is assumed to occur in the reformer".

Plehiers and Froment (1989) maintain that "present-day simulation and design of a steam reforming furnace requires the coupling of the reactor and furnace simulations" instead of imposing a tube wall or heat flux profile "without the guarantee that it can be satisfactorily achieved in the given firebox". The authors implement the model of Xu and Froment (1989b) and solution technique, but give a more in-depth description of the workings of the zone model. "Excellent agreement" was achieved with industrial data, and "it should be stressed here that the simulation does not involve any adaptable parameters". However, for convection "if desired, an approximation of the flue gas flow pattern in the firebox can be generated". The work of Plehiers and Froment is discussed in greater detail by Froment and Bischoff (1990) as part of a major reactor analysis and design text.

Ravi et al. (1989) model a primary reformer as part of an energy optimisation of the reforming section of an ammonia plant. The authors make the assumptions that a single tube is representative of all other tubes, fixed bed and only one dimensional concentration and temperature variation. Kinetics developed by Singh and Saraf in 1979 and 1981 were adopted and an outer tube wall temperature profile assumed. "Close agreement" between the plant data and simulation was obtained. However, apart from not mentioning several important modelling considerations for steam reforming and choosing some very simplifying assumptions, the kinetic scheme has been previously criticised; highlighted in section 3.2 and discussed in more depth in chapter 4.

Alatiqi and Meziou (1991) developed a dynamic model based on overall reaction kinetics to "design and test the need for a programmed adaptive control scheme". The authors use a previous steady-state simulation, Alatiqi et al. (1989), as a basis for the dynamic model but with a solution technique of a combination of finite difference and fourth-order Runge-Kutta. The simulation "has shown good agreement with actual plant performance and "can be used later for more advanced studies" for "as long as the steam-to-carbon ratio is large enough to prevent appreciable catalyst activity deterioration". However, the authors do not attempt to reduce the assumptions highlighted by Alatiqi et al. (1989).

Rosen (1991 and 1996) uses the Aspen Plus simulation package modules but limited discussion on the implications of the settings is given. Further to this, as for the previous simulation package based model, the simulation can be considered very simplistic when compared to the issues discussed in section 3.5.1.

Wagner and Froment (1992) based a model of a steam/CO_2 reformer on the model presented by Froment and Bischoff (1990) to assess the methods predicting carbon formation. The equilibrium-based approach is successfully demonstrated to be "conservative" when compared to the kinetic approach, which can affect the optimisation of the operating parameters. Further to this, the authors criticise the practice of using graphite data for carbon deposition, as coke formation and not graphite formation is the condition. Instead of an overall furnace simulation, as performed in Froment and Bischoff (1990), the authors use an assumed inside heating profile as the emphasis of their research is on coke formation and not on overall furnace operation.

Again a one dimensional heterogeneous model is chosen, for top and side fired furnaces, by Elnashaie et al. (1992), with two approximations for effective diffusivities and inclusion of the modified collocation solution technique. Xu and Froment (1989a) kinetics were also adopted and the authors assumed an outer wall temperature profile. The model derived from Stefan-Maxwell gives a higher accuracy but the author states that "more efficient steam reformers which operate even further from thermodynamic equilibrium will require a more rigorous model (the dusty gas model)". The authors argue that as good accuracy is obtained both close to and relatively far from thermodynamic equilibrium that "the models can thus be used with a reasonable to high degree of confidence in the simulation, design and optimisation of these reactors". However, apart from the tube profile assumption the authors also assume that any reformer tube is "representative of any other tube in the furnace" irrespective of the location of the burners or furnace walls.

Omtveit et al. (1994) demonstrate graphical targeting procedures for steam reforming with Xu and Froment (1989a) kinetics. Other issues discussed above on steam reforming modelling are not introduced.

Zhang and Yu (1995) as for Ravi et al. (1989) attempt an optimisation of the reforming section of an ammonia plant. The authors criticise Plehiers and Froment (1989) for the model being "rather complicated and the calculation was rather time-consuming" so the authors suggest the Schuster-Schwarzschild method, as implemented by Roesler (1967). "Good agreement" is claimed, however, no comparison of this technique with that of Plehiers and Froment (1989) is reported and from the explanation in the paper, the benefits of the alternative technique are not very apparent.

Farnell (1996) reports on an industrially developed model, which is based on the work of Roesler (1967). As the model has been "licensed to many reformer designers" it has a "substantial validation base" and claims to "cover the full range of feedstocks and catalysts" and be "suitable" for "all furnace geometries". Although detailed information on the model is lacking the author highlights some key issues. For a detailed simulation of steam reformers the model must "consider the physical and chemical processes occurring both inside and outside the reformer tubes". Additionally, "basic furnace modelling" is only suitable for "preliminary assessment tools". In a subsequent paper, Farnell (1999), the author develops a two dimensional Monte Carlo simulation of the lower regions of the reformer furnace focusing on the region in proximity to the tunnels; validated against "actual designs". This model is essentially an 'add-on' to the previous model, developed to account for "higher than predicted" temperatures reported at the base of several steam reformers.

Barbieri and Di Maio (1997) simulate a catalytic Pd-membrane reactor, with the assumptions of steady-state operation, plug-flow, no polarisation boundary layer on membrane surface, isothermal and isobaric conditions and use Xu and Froment (1989a) kinetics with a fourth order Runge-Kutta solver. "Good agreement" is reported for experimental data from both traditional and membrane reactors. However, the authors attribute the differences "to the model simplification assumptions, in particular to the plug flow hypothesis".

Levent et al. (1998) used Xu and Froment (1989a) kinetics and estimated mass and heat transfer distribution, outside and within the catalyst particles. This is only a qualitative study to develop understanding and there is no attempt made of direct comparison to experimental data.

Oh and Yeo (1998) used the dynamic model of Alatiqi et al. (1989) and Alatiqi and Meziou (1994), to assess linear and bilinear control algorithms. For both simulated and plant data the bilinear model reproduces the steam reformer dynamics "more accurately" than the linear model for change of disturbances. However, as for Alatiqi and Meziou (1994) the authors make no attempt to reduce the assumptions highlighted by Alatiqi et al. (1989).

Goldstone and Malik (1999) simulated a primary reformer burner with a CFD model. To simulate the reaction the authors used a multi-step Eddy Break-up model and for the radiation a discrete-transfer method was implemented. The simulation results although not compared directly with measured data demonstrated the 'observed' flame deflection from the burner.

Cotton (1999) studies the unusual flow pattern discovered in some top-fired steam reformers. The non-uniform upflow reported in these furnaces is demonstrated to produce significant operational variation across the furnace. The author develops a computational fluid dynamics model, however, "in order to make the modelling manageable a series of simplifying assumptions were made". These simplifications include, only one tube row is modelled, a non-rigorous form of combustion modelling is employed and no tube heat transfer is included. The author hypothesises that the model, although "slightly inaccurate", still allows prediction of furnace flow patterns and reports that "dry powder tests agreed with the model in terms of flow patterns".

Kvamsdal et al. (1999) presented a dynamic pseudo-homogenous two-dimensional model for a side-fired primary reformer, adopting the kinetics of Xu and Froment (1989a). For each burner level, the furnace is sectioned into ideal mixed stages, but the same temperature is assumed for each stage, as no data are available. Three expressions for the internal wall heat transfer coefficient and four conditions for the effective radial conductivity were applied to determine the most accurate combination, however, without industrial or experimental data the selection was limited. Nevertheless the authors demonstrated that the effect of the choice of correlations on the conversions is limited but is significant for the tube wall temperatures. From both the dynamic simulations of various process disturbances and optimisation, the authors also illustrated the importance of the external tube wall temperature constraint.

Rajesh et al. (2000) develops a side-fired steam reformer model employing the kinetics of Xu and Froment (1989a), a non-iterative form of the furnace model of Singh and Saraf (1979) and the calculation approach of Elnashaie et al. (1992) for effective diffusivities. The authors report "a very good match is observed between the results obtained from our simulation and published industrial data". In a subsequent paper Oh et al. (2001), by some of the same authors, the model is developed to include ethane, butane and propane, and replace the fixed furnace gas temperature with a quadratic expression of the heat flux. Although the inclusion of higher alkanes than methane in the reaction scheme is an improvement, as "suitable rate expressions and kinetic data" for these heavier alkanes for the relevant catalyst formulation "could not be found" the simulation results should be treated with caution. The inclusion of heavier hydrocarbons will be discussed in more depth in chapter 4.

Wesenberg et al. (2001) employ a two-dimensional model adapted from Kvamsdal et al. (1999) for a "convective steam reformer". This steam reformer from the description given, appears to be of the modern style "heat exchanger design" discussed in section 3.5.1. The aim of this study was to assess the suitability of a number of wall heat transfer coefficient expressions. The authors conclude that two of the expressions "are both in good agreement with practical experience", however, as several authors discuss the accuracy of pseudo-homogeneous assumption is questionable.

3.6.2 Secondary reformers

Davies and Lihou (1971) proposed a simple model for a secondary reformer, as part of reformer section simulation. No reaction kinetics were included for either the combustion or steam reforming and the heat loss through the reformer walls is assumed negligible. However, the authors conclude that consideration must be given to the effect of local hot spots at the entrance to the catalyst bed although not included in the simulation.

Singh and Saraf (1981) considered that the kinetics of hydrogen combustion was significantly greater than for the carbon monoxide and the methane, however, the justification for this assumption was not given. The catalyst bed section is based upon the primary reformer model by Singh and Saraf (1979), however, the rate of steam reforming is considered to be limited by diffusion to the catalyst surface. The authors claim that the simulation compares "very well" for previous published data from a secondary reformer and industrial data for the ammonia process.

Ravi et al. (1989) model a secondary reformer as part of an energy optimisation of the reforming section of an ammonia plant. The authors adapt the primary reformer model they developed in the paper, see section 3.6.1, for the secondary reformer. However, the choice of combustion reactions is controversial, as highlighted in section 3.5.2 and discussed in more depth in chapter 4, and for combustion no kinetics are used as instantaneous reaction is assumed. Also due to the choice of kinetic expressions for the

reactions over the catalyst bed an additional mass transfer resistance must be lumped into the reaction rate, see chapter 4. Apart from this no spatial variation or flow pattern is considered which is key to most of the design considerations for a secondary reformer, see section 3.5.2.

Farnell (1992) covered a number of case studies of industrial secondary reformers all suffering performance difficulties. The author uses a commercial CFD package, see section 2.3, with an "add-on package" for the combustion chemistry to simulate the reformers. As the author states model verification is impossible by measurement so "simplified combustion models have been carried out which can be checked against well proven classic jet theory and also against experience in fluid flow and combustion". Further to this "correct prediction of effects such as hot zones on the catalyst bed, or generally poor performance, which can be verified by inspection or operating data, also add to the validation of the techniques used". However, the author admits that kinetic models are available currently but have not been implemented, also not all the design considerations from section 3.5.2 seem to have been taken into account. The same techniques seem to have been employed by Farnell (1999b) for a proceeding study that concentrates on the burner locale.

Blanchard and LeBlanc (1993) used the FLUENT CFD package with incorporated hydrogen combustion kinetics, to design a secondary reformer. The authors choose CFD as this allows "a more exhaustive analysis of the combustion chamber design than empirical correlations and cold-flow modelling". The results of this study are "consistent with expectations" with the earlier cold-flow modelling work and finite element modelling. Although the authors account for more design considerations from

section 3.5.2, than previous models still not all are covered. However, the authors cause confusion concerning the reaction model as further to the initial remark of "incorporating" hydrogen combustion kinetics they use a reaction model including the exothermic combustion of methane by oxygen plus the endothermic reforming reaction, which neither mentions hydrogen combustion or kinetics.

Christensen et al. (1994) compared the performance of two industrially operated burners with both CFD and isothermal physical modelling. The authors use the CFDS-FLOW3D CFD package and validated the simulation by comparing the results with those of "other modelling and experimental techniques, and against process performance". The isothermal modelling performed was hydraulic modelling which unlike CFD "can be used for studies of transient and local phenomena such as turbulent flow eddies and local recirculations", but the combustion is given a peculiar representation of the "mixing of acid and alkali" with "the selection of a proper indicator creates a visual picture of the flame". The operating characteristics of both burners are successfully demonstrated and "the match between the two modelling techniques has been excellent", however, the combustion modelling for both techniques is not thoroughly explained and again there is a lack of design considerations, see section 3.5.2.

Zhang and Yu (1995) as reported above attempted a system similar to Ravi et al. (1989). "Good agreement" is claimed, however, no discussion of the model development or principals is given by the authors. The only assumption that can be made is that the model by Ravi et al. (1989) is adopted with no changes, so comments above still apply.

3.6.3 CFD models of reactors

The simulation issues for most reactive flow systems are consistent and hence are a potential source of simulation techniques and performance information for any reaction process.

Harris et al. (1996) give a through discussion of CFD and chemical reactions not only from a viewpoint of current capabilities and recent developments, but also the "future needs and expectations of the chemical processing industry with respect to CFD modelling". A similar reactor system to reformers is discussed and the authors conclude that mean value model (MV) and probability density function model (PDF) can both be used in the comparative studies of promising reactor geometries, but as the computational cost of the MV is smaller and the difference in predictions for the reactors studied was found to be very small "it was recommended to use the MV with the refinement of the PDF model to be used as a check at the end". The authors identify a lack of multiphase flow modelling with CFD and chemical reactions even though there are industrial examples "that are of particular importance" which suffer difficulty in design.

Yossefi et al. (1995 and 1997) simulate the early stages of combustion by a multiple reaction scheme. However, the discussion by the authors emphasises relevant points on kinetic modelling of combustion and ignition, both important for autothermal and secondary reformer simulation.

Zhang and Frankel (1998) argue that instead of a full reaction scheme, a reasonable accuracy can be achieved with simpler chemical schemes. An eddy break-up model is implemented for a global two-step scheme with the "limiting process" of the reaction and mixing kinetics adopted as "turbulent combustion rate". The kinetic expressions were taken from Westbrook and Dryer (1981) and Yetter et al. (1986), but unlike in elemental reactions, the authors adopt a temperature-dependent activation energy.

Ha and Zhu (1998) implement the three step reaction scheme from Westbrook and Dryer (1981), as a single step global mechanism over predicts the extent of reaction and adiabatic flame temperature. The turbulent combustion rate is simulated by the slower of either the chemical kinetics or the turbulent mixing.

Manickam et al. (1998) implemented both a 'mixed is burnt' and an eddy break-up model. For the eddy break-up model the slowest of the mixing and chemical kinetics are adopted, however, the chemical kinetics are derived using Chemkin [Kee et al. (1990)]. The authors demonstrate the eddy break-up model to be superior to the 'mixed is burnt' mode, for inlet composition and operating conditions similar to the autothermal and secondary reformers.

Srinivasan et al. (1998) and Kulasekaran et al. (1999) considered fluidized bed combustion, for carbon monoxide and hydrogen combustion kinetics were taken from Dryer and Glassman (1973) and Westbrook and Dryer (1981). However, the authors consider combustion behaviour as "more complex" than simple schemes.

3.7 Conclusion

The industrial importance of the steam reforming process is unquestionable and due to the process versatility this importance can be expected to continue for some time. Despite the significant variations in the design and operation, all share a common set of complications with only limited disparity. Current simulation research has approached some of these complications with relative success, however, both for the primary and secondary reformer there is room for further development.

The areas focused on in the remaining chapters are the reaction kinetics and schemes for the steam reforming process; covering inclusion of heavier alkanes than methane and coke formation. Specifically for the primary reformer, furnace modelling and operational issues are developed and for the secondary, reactive flow analysis, radiation modelling and overall reactor simulation are developed. The topic of performance optimisation for both stages of the steam reforming process is also approached.

Chapter 4

Primary Steam Reformers

As was highlighted in the previous chapters, both the operation and design of primary steam reformers is far from trivial. Despite this the most basic form of a primary steam reformer model, which could be considered reasonably accurate, is surprisingly simplistic. This model is fundamentally based on the assumption that the exit conditions of the reactor tubes are at equilibrium conditions, hence reaction kinetics can be ignored, and the only relevant reactions considered are the methane steam reforming and water gas shift reactions,

$$CH_4 + H_2O \Leftrightarrow CO + 3H_2 \qquad \text{Steam Reforming}$$

$$CO + H_2O \Leftrightarrow CO_2 + H_2 \qquad \text{Water-Gas Shift}$$

Additionally, the model assumes no carbon deposition / removal and ignores the furnace side of the primary steam reformer. From these two equilibrium relationships develop two simultaneous equations in terms of temperature, pressure and molar compositions, of the form,

$$K_{\text{reforming}} = \frac{P^2\left[(x_1 - x_2)(3x_1 + x_2)^3\right]}{\left[(x_a - x_2)(x_b - x_1 - x_2)(x_a + x_2 + x_c + 2x_1)^2\right]} \qquad (4.1)$$

Hossain (1988) employs such a model and several authors including Froment and Bischoff (1990) demonstrate that this equilibrium assumption is not absurd. However, this model overlooks several issues for the primary steam reformer and is effectively redundant as model development has evolved with computer capabilities.

4.1 General Primary Steam Reformer Model

- 'DUNN, A.J. and GREAVES, M.A., 2000, Modern CAPE Techniques, IChemE East Pennine Centre, Bradford, UK

To initiate the current research and form a foundation from which to advance, a model is developed based on previously published research by several authors. From the previous studies a model approach which could be considered as a `consensus` view is adopted as a suitable level to start tackling some of the simulation issues for primary steam reformers. As is indicated in chapter 3, the fundamentals of such an approach are still employed in current research although their remains scope for investigation.

In this work, using the model reported by Ravi et al. (1989) as a basis, various improvements have been implemented to the model. The improvements include a representation for carbon deposition / removal, improved physical property expressions and an improved furnace modelling approach. Model validation is performed against industrial data from a number of steam reformers.

The general purpose modelling package of gPROMS is used in this work, which includes several features highlighted in chapter 1. Of particular interest for primary steam reformer simulation is the range of numerical solution techniques and the open architecture for model definition, which removes the tedious development of a solution technique.

A sensitivity analysis is performed varying the key operating parameters of temperature, pressure, steam to carbon ratio and tube wall temperature. These results compared well with previous observations of sensitivity analyses.

4.1.1 Model description

The construction of primary steam reformers leads the system to be considered as two domains, that of the steam reformer tubes and that of the furnace. The model description includes a section for both of these domains and also for the physical property expressions used for the steam reformer tube section and numerical solution of the model. Although only the key equations are discussed in the model description a full listing is included in Appendix 3.

Steam Reformer Tubes

Prior to the development of any chemical reactor model, the reaction scheme and associated kinetic expressions are defined. Within a primary steam reformer tube there are two groups of reactions, those associated with the production of synthesis gas and those relating to carbon formation / removal.

For the synthesis gas group, the variation of opinion on the reaction scheme is not too controversial and the extent of the discrepancies has been diminished with continuing research. For steam reforming of methane the two remaining reaction schemes, dictated by kinetic research, are either,

$$CH_4 + H_2O \Leftrightarrow CO + 3H_2 \qquad \text{Steam Reforming}$$

$$CO + H_2O \Leftrightarrow CO_2 + H_2 \qquad \text{Water-Gas Shift}$$

or, the previous reactions and an additional steam reforming reaction,

$$CH_4 + 2H_2O \Leftrightarrow CO_2 + 4H_2 \qquad \text{Steam Reforming}$$

However, for heavier alkanes than methane, a greater disparity exists. Several authors including Hyman (1968) and Oh et al. (2001), consider that these alkanes will hydrocrack to form methane,

$$C_kH_{2k+2} + (k\text{-}1)\,H_2 \Leftrightarrow kCH_4 \qquad \text{Hydrocracking}$$

while amongst others Twigg (1997) and ICI (1996) consider that these alkanes will undergo steam reforming,

$$C_nH_{2n+2} + nH_2O \Leftrightarrow nCO + (2n+1)H_2 \qquad \text{Steam Reforming}$$

It is not clear which reaction scheme occurs in primary steam reformer tubes, as there is no unique chemical species in either scheme, or if in fact both occur simultaneously. As successful experiments are reported for both schemes, under similar operating conditions to those within the primary steam reformer tube, this would seem a reasonable conclusion. But it is unclear as to relative performance of the reactions in a methane rich environment or in competition with other reactions.

The kinetic expressions for the steam reforming of methane employed in early models were of limited consensus. A popular set of kinetic expressions, by Moe and Gerard (1965), were employed by several authors including Hyman (1968) and more recently in the number of papers by Alatiqi et al. (1989 and 1991),

$$r_{CH_4} = k_2\left[K_2 P_{CH_4} P_{H_2O}^2 - P_{H_2}^4 P_{CO_4}\right] \qquad (4.2)$$

However, instead of a kinetic expression for the water gas shift reaction they proposed an empirical relationship proportional to the methane conversion.

Singh and Saraf (1979) suggest that the root cause of this variation in kinetic expressions was "the neglect of pore diffusional resistance" by several researchers. Based on a set of forms of kinetic expression from the catalyst company Haldor Topsoe, Singh and Saraf (1979) developed kinetic expressions for both reactions, which were employed in Singh and Saraf (1979 and 1981) and Ravi et al. (1989),

$$R_1 = 127\sqrt{P}\exp\left(\frac{-8780}{R_g T}\right)\left(x_{CH_4} - \frac{x_{H_2}^3 x_{CO} P^2}{K_{eq1} x_{H_2O}}\right) \qquad (4.3)$$

$$R_2 = \exp\left(\frac{-13880}{R_g T} + 8.23\right)\sqrt{P}\left(x_{CO} - \frac{x_{H_2} x_{CO_2}}{K_{eq2} x_{H_2O}}\right) \qquad (4.4)$$

From a more extensive study of these diffusional limitations, based on trialling various standard heterogeneous kinetic approaches, Xu and Froment (1989a) proposed that there are three fundamental reactions. Xu and Froment (1989a) derived the following kinetic expressions, the definition of which is included in Appendix 3,

$$r_1 = \frac{k_1}{p_{H_2}^{2.5}}\left(p_{CH_4} p_{H_2O} - \frac{p_{H_2}^3 p_{CO}}{K_1}\right) \Big/ (DEN)^2 \qquad (4.5)$$

$$r_2 = \frac{k_2}{p_{H_2}}\left(p_{CO} p_{H_2O} - \frac{p_{H_2} p_{CO_2}}{K_2}\right) \Big/ (DEN)^2 \qquad (4.6)$$

$$r_3 = \frac{k_3}{p_{H_2}^{3.5}}\left(p_{CH_4} p_{H_2O}^2 - \frac{p_{H_2}^4 p_{CO_2}}{K_3}\right) \Big/ (DEN)^2 \qquad (4.7)$$

To initiate the model development a compromise of convenience and complexity, from the school of "you must walk before you can run", was adopted for the intricate issue of chemical kinetics. The pseudo-homogenous kinetics, developed by Singh and Saraf (1979) were adopted in this model as they were demonstrated to perform well. To further manage this complexity it was assumed that there was negligible radial variation across the steam reformer tubes, which is in conceded by the majority of researchers.

Most authors avoid the issue of higher hydrocarbons by studying hypothetical arrangements, where they are not included, as not only is there disagreement as to the physical processes involved but also how best to represent them in a model. There are reports of kinetic studies for both reaction schemes, but as Oh et al. (2001) highlights there are no published kinetics for industrial catalyst formulas. Oh et al. (2001) introduce what they term as "suitable weighting factors" to the reported kinetic expressions for other catalyst formulas, however, there is no scientific basis for these factors nor the method they employ for estimating these parameters. The 'methane equivalent' approach proposed by Hyman (1968) is adopted in this model, where instantaneous hydrocracking is assumed at the inlet, with instantaneous reforming required to avoid negative hydrogen flow. Not only has this approach been reported by several authors to perform successfully, but also seems viable as the heavier alkanes only represent a small amount of the feed to primary steam reformers under consideration.

As for heavier alkanes than methane, for carbon formation/ removal most authors avoid the issue by removing any existence i.e. assuming no carbon deposition occurs. Although this is not an unrealistic hypothetical situation the issue should not be flippantly overlooked, particularly for optimisation studies of reactor performance, as carbon deposition is a major limit.

There is general agreement on the fundamental reactions of carbon formation/ removal and Trimm (1997) states that the process is "reasonably well understood". The reaction scheme is expressed as,

$2CO \Leftrightarrow C + CO_2$	Boudouard Reaction
$C_nH_{2n+2} \Leftrightarrow nC + (n+1)H_2$	Thermal Cracking
$CO + H_2 \Leftrightarrow C + H_2O$	Carbon monoxide reduction

The use of the term carbon formation/removal or more often 'coke' can be considered general as several authors including Cromarty (1990), Wagner and Froment (1992) and Trimm (1997) discuss that there are multiple forms of carbon formation. The two main forms are a coated layer on the catalyst surface and filament deposits. In earlier studies the carbon deposits were presumed to be solely graphitic and predictions for deposition were based on equilibrium calculations using graphite, however, as Wagner and Froment (1992) highlight neither are graphitic in nature.

Previous studies of carbon deposition are criticised by Wagner and Froment (1992) for being "limited to qualitative observations" or developing "too simplistic" forms of kinetic expressions. Although these authors recommend the use of kinetic expressions they have developed and defined in unpublished research, they suggest equilibrium style "threshold values" based on experimentation with the reactor catalyst as a preferred alternative, or if neither is available to resort to the "conservative" graphitic equilibrium calculations. As neither kinetic expressions nor quantitative experimentation exist in the public domain for the industrial catalysts, the graphitic equilibrium approach is adopted for the model.

Apart from the chemical reaction model requirements, heat transfer and fluid flow parameters require definition

For primary steam reformer tubes, neglecting the influence of fouling, the overall heat transfer coefficient is defined by Ravi et al. (1989) as,

$$\frac{1}{U} = \frac{D_i}{D_o}\frac{th}{\lambda_w} + \frac{1}{h_i} \qquad (4.8)$$

However, this equation is only suitable for a plane sheet and a more rigorous logarithmic form suitable for cylinders must be employed for steam reformer tubes,

$$\frac{1}{U} = \frac{1}{h_i} + \frac{D_i \ln\left(D_o / D_i\right)}{2\lambda_w} \qquad (4.9)$$

For typical data of a primary steam reformer tube, the discrepancy in the calculated overall heat transfer coefficient is some ten percent.

Due to the difference in the shape of modern catalysts, previously published expressions for both the internal heat transfer coefficient and the pressure drop are modified. The basis for the internal heat transfer coefficient and the pressure drop equation are Beek (1962), equation 4.10, and Robbins (1991), equation 4.11, respectively.

$$\frac{h_i D_p}{\lambda_m} = htfactor\left(2.58\,\mathrm{Re}_p^{1/3}\,\mathrm{Pr}^{1/3} + 0.094\,\mathrm{Re}_p^{0.8}\,\mathrm{Pr}^{0.4}\right) \qquad (4.10)$$

$$\frac{dP}{dz} = -3.026\cdot 10^{-7}\, Fpd\rho^3 u^2 \qquad (4.11)$$

As no published data exists for these parameters, due to commercial sensitivity, the common practise of processing the parameter values against industrial data is adopted.

Physical Properties

For completion, the model of the steam reformer tube requires several physical properties of the gaseous mixture in the tube, including heat capacity, viscosity and conductivity. Polynomial expressions for the component properties, derived from published data, are taken from Yustos (1999). The pressure dependence of these component properties is demonstrated to be negligible in the operating envelope of the steam reformer, see Appendix 1.

The heat capacity of the mixture is calculated as an average considering the molar fraction of each component, as recommended by Beaton (1989) and Alatiqi et al. (1989). However, for the viscosity and the conductivity, averaged expressions are not considered suitable.

For the viscosity of a gaseous mixture, Reid (1977) and Perry (1997) recommends an expression by Wilke:

$$\mu_m = \sum_{i=1}^{NC} \frac{x_i \mu_i}{\sum_{k=1}^{NC} x_k \phi_{ik}}, \text{ where} \qquad (4.12)$$

$$\phi_{ik} = \frac{\left[1+\left(\frac{\mu_i}{\mu_k}\right)^{0.5}\left(\frac{M_k}{M_i}\right)^{0.25}\right]^2}{\left[8\left(1+\left(\frac{M_i}{M_k}\right)\right)\right]^{0.5}} \qquad (4.13)$$

The effect of employing alternative expressions for the viscosity of a gaseous mixture is demonstrated in Appendix 2.

and for the gas conductivity, the Wassiljewa equation is also recommended by Reid (1977):

$$\lambda_m = \sum_{i=1}^{NC} \frac{x_i \lambda_i}{\sum_{k=1}^{NC} x_k A_{ik}} \qquad (4.14)$$

with the Mason and Saxena approximation: $A_{ik} = \phi_{ik}$

The effect of employing alternative expressions for the conductivity of a gaseous mixture is demonstrated in Appendix 2.

Furnace model

As an improvement to the assumed tube wall temperature profile implemented by Ravi et al. (1989), a polynomial representation of the heat flux profile proposed by Alatiqi et al. (1989) is adopted for the model. The main benefit of the heat flux profile approach is it removes the assumption that the tube wall temperature profile is static and allows for the dependence on primary steam reformer operation. Also Alatiqi et al. (1989) claim that this approach "eliminates the ambiguity of extensive radiation and convection calculations" and "eliminates the need for any assumption regarding the prevailing mode of heat transfer".

Alatiqi et al. (1989) proposes that the heat flux profile is dependent on the furnace fuel gas flow rate, the fuel gas specific gravity and the unit efficiency,

$$q = F_G SG\left(a + bz + cz^2\right)\eta \tag{4.15}$$

The authors claim that as the inner wall temperature profile "is a second order polynomial" so the heat flux profile "will be a polynomial of the same order". As is demonstrated by Dybkjaer (1995), Oh et al. (2001) and Rostrup-Nielsen (1984) the shape of the profile is actually dependent on the furnace configuration. However, the almost exponential trend reported by Alatiqi et al. (1989) is in contrast to the Rostrup-Nielsen (1984) view for side-fired furnaces of a "parabolic with a dominant peak near the entrance".

While the second order expression is suitable for side-fired furnaces, it was discovered in this model development, that a higher order is required for top-fired furnaces,

$$q = F_G SG\left(a + bz + cz^2 + dz^3 + ez^4\right)\eta \tag{4.16}$$

Other furnace configurations such as terrace or bottom-fired are not considered in this work, however, the same approach could be adapted for these alternatives. Plehiers and Froment (1989) argue that neither "imposed" tube wall nor heat flux profiles can give a guaranteed representation of the furnace and more accurate representations are required. In the same spirit as for the primary steam reformer tube, the heat flux profile approach was adopted, although not the most complicated but with reasonable accuracy.

Numerical solution

The full model of the primary reformer, results in a system of differential and algebraic equations, consisting of ninety-nine equations. Usually, the author would have to develop a solution algorithm for this system such as those discussed in chapter 1. This is not required with a generalised modelling package such as gPROMS.

The gPROMS package offers several features for simulation including, a range of numerical solution methods for discretisation, parameter estimation, optimisation and an open architecture for real time applications. Within this open architecture, the model is structured as building blocks that allow the description of composite models of complex unit operations, entire flowsheets or 'domains' in the case of the steam reformer model.

For the reported simulation, the most important capability of gPROMS is the ability to manage distributed systems. The capability of the package is such that to generate the distributed equations, the user is required to define the equations in a 'sentence' form, specify the numerical solution method for the discretisation, the order of approximation and the number of discretisation intervals. A second order orthogonal collocation method with 15 discretisation points was applied for the solution technique as this was proven to be mesh independent. Previously, gPROMS has been applied to several industrial examples, including grain drying, as reported by Sun et al. (1995) and batch plant operation, as reported by Winkel et al. (1995). These capabilities are not only appropriate for the reported primary steam reformer model, but also for further developments.

As was discussed in chapter 1, solving sets of IPDAEs such as for this primary steam reformer model is not a 'black-box' operation. Even for a relatively simple form of IPDAEs as defined by this model of a one-dimensional steady state system, solution techniques must be considered. Scaling can be considered 'best practice', so this was immediately enforced in the primary steam reformer model, however, only the temperature required scaling to achieve a solution. Block decomposition was not fundamental to solution attainability but for the model, the solution time was improved by some eight percent by employing this technique.

The difficulties of initialisation of IPDAEs for steady-state systems, highlighted in chapter 1, were confirmed in the original attempts at solving the model. The sensitivity of the initial values for the various parameters produced several failed solutions, however, a set was found which would yield a solution. From the frustration of the required manipulation a more robust initialisation approach was developed, as discussed in chapter 1, which required de-coupling the heat balance and pressure profile equations in the steam reformer tubes. The de-coupled model was solved and then the full model was initialised with this de-coupled solution. For the de-coupling stage, assumed temperature and pressure profiles were introduced based on the set of industrial data. The de-coupling of these two equations resolved the robustness issue of the initialisation for the primary steam reformer model and also gave a fixed solution sequence of two steps for this model.

4.1.2 Simulation and Model Validation

The model was validated against industrial data from top-fired and side-fired primary steam reformers within both the ammonia and methanol processes. A typical industrial top-fired steam reformer comprises 8 rows of 44 tubes and 12.6 m in length and operates at an inlet pressure and temperature of 35.94 bar and 455 oC, respectively. A typical industrial side-fired steam reformer comprises 10 rows of 6 tubes and 12.2 m in length and operates at an inlet pressure and temperature of 22.0 bar and 502.67 oC, respectively. The simulation results are presented in Table 4.1.1 and Table 4.1.2, and clearly show that the simulated data compared well to the industrial data.

Table 4.1.1: Comparison between plant and simulated data for a Top-Fired Primary Steam Reformer

		Plant data	Calculated values	Deviation (%)
Outlet T (K)		1084	1083	0.04
Outlet P (atm)		32.57	32.58	-0.03
ΔP (atm)		2.9	2.89	0.35
Dry mol %	CH_4	8.1	8.03	0.87
	CO	10.39	10.31	0.78
	CO_2	10.96	11.04	-0.69
	H_2	70.28	70.36	-0.11
	Inerts	0.270	0.267	1.13

Table 4.1.2: Comparison between plant and simulated data for a Side-Fired Primary Steam Reformer

		Plant data	Calculated values	Deviation (%)
Outlet T (K)		1141.3	1141.5	0.025
Outlet P (atm)		20.13	20.15	-0.07
ΔP (atm)		1.58	1.57	0.95
Dry mol %	CH_4	3.01	3.03	-0.66
	CO	14.83	14.81	0.13
	CO_2	8.14	8.15	-0.12
	H_2	73.9	73.88	0.03
	Inerts	0.12	0.122	-1.67

Despite the reassuring performance of the overall model with industrial data, the carbon deposition / removal component was not as successful. As stated in section 4.1, the equilibrium approach to graphite carbon deposition / removal is considered by Wagner and Froment (1992) to be "conservative" compared to kinetic calculations. However, for known 'safe' operating conditions from an industrial steam reformer this approach predicted carbon formation within three metres of the inlet to the steam reformer tube, see figure 4.1.1.

The root cause of this discrepancy was discovered to be the approach to the inclusion of higher hydrocarbons than methane of assuming instantaneous reaction at the steam reformer tube inlet. Interestingly this distance ties in with the observation of Hyman (1968) for the consumption of higher hydrocarbons.

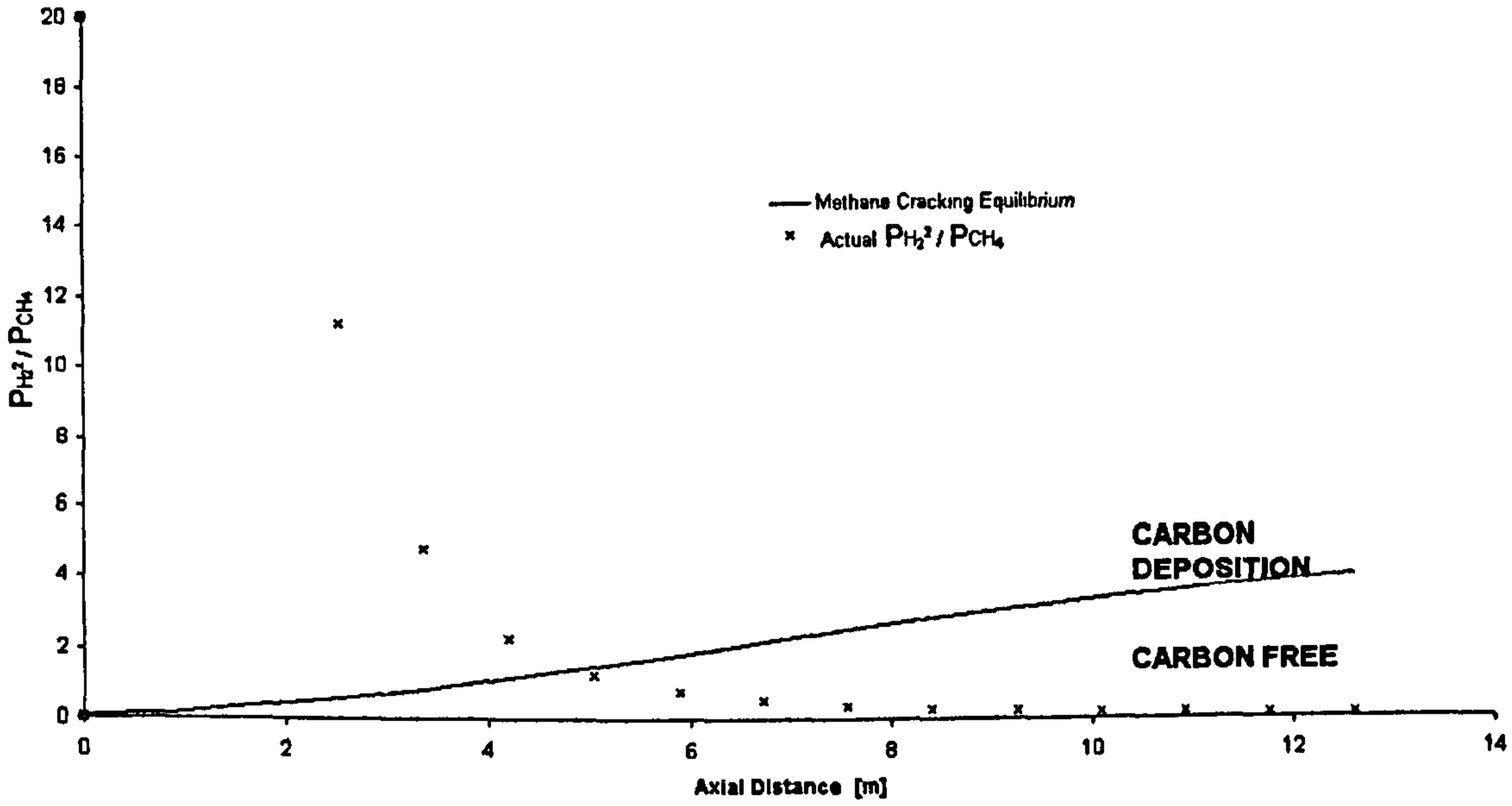

Figure 4.1.1: Prediction of Carbon formation in Primary Steam Reformer Tubes

The typical effect of this assumption on the inlet composition can be easily reckoned.

Employing data from a typical industrial steam reformer, the gas feedstock is,

CH_4 [mol/h]	C_2H_6 [mol/h]	C_3H_8 [mol/h]	C_4H_{10} [mol/h]	CO_2 [mol/h]	N_2+Inerts [mol/h]	H_2 [mol/h]	H_2O [mol/h]
1210.8	105.4	34.4	13.9	26.3	14.6	63.4	5768

Assuming instantaneous cracking, the equivalent methane is calculated as follows,

$$1210.8 + 2 \times 105.4 + 3 \times 34.4 + 4 \times 13.9 = 1580.4 \text{ mol/h}$$

The hydrogen required for the cracking of the higher hydrocarbons to methane at the inlet would be,

$$105.4 + 2 \times 34.4 + 3 \times 13.9 = 215.9 \text{ mol/h}$$

As there is only 63.4 mol/h, so the remaining 152.5 mol/h must be accounted for by assuming instantaneous methane reforming at the tube inlet. So the equivalent methane and the steam flow are reduced and the carbon monoxide flow is increased, yielding,

CH_4 [mol/h]	CO [mol/h]	CO_2 [mol/h]	N_2+Inerts [mol/h]	H_2 [mol/h]	H_2O [mol/h]
1529.567	50.833	26.3	14.6	~0	5717.167

This 'shift' in composition will be transmitted along the length of the steam reformer tube. Rostrup-Nielsen and Tottrup (1979) hypothesise that the reaction of heavier hydrocarbons than methane is completed between two to six metres. As the carbon prediction for the simulations is in agreement with reality, from around the start of this region, the simulations both offer some confirmation to this hypothesis and indicate that the effect of the composition 'shift' is limited to this region. As the more accurate expressions of carbon deposition are also based on composition, the effect of this shift would be replicated.

Apart from carbon prediction the effect on the remainder of the model seems limited as is confirmed by the overall simulation performance.

4.1.3 Sensitivity Analysis

A top-fired furnace model was employed in the sensitivity analysis, for which the inlet pressure, inlet temperature, steam to carbon ratio and feed rate were varied.

For most applications of steam reforming, the aim of a steam reformer is primarily to reduce the methane concentration and yield the required composition for downstream processing. However, the outlet of a primary steam reformer is close to chemical equilibrium, so the sensitivity of the composition is affected. The consequences of which are observable for the inlet pressure (Figure 4.1.2), steam to carbon ratio (Figure 4.1.3) and feed rate (Table 4.1.3).

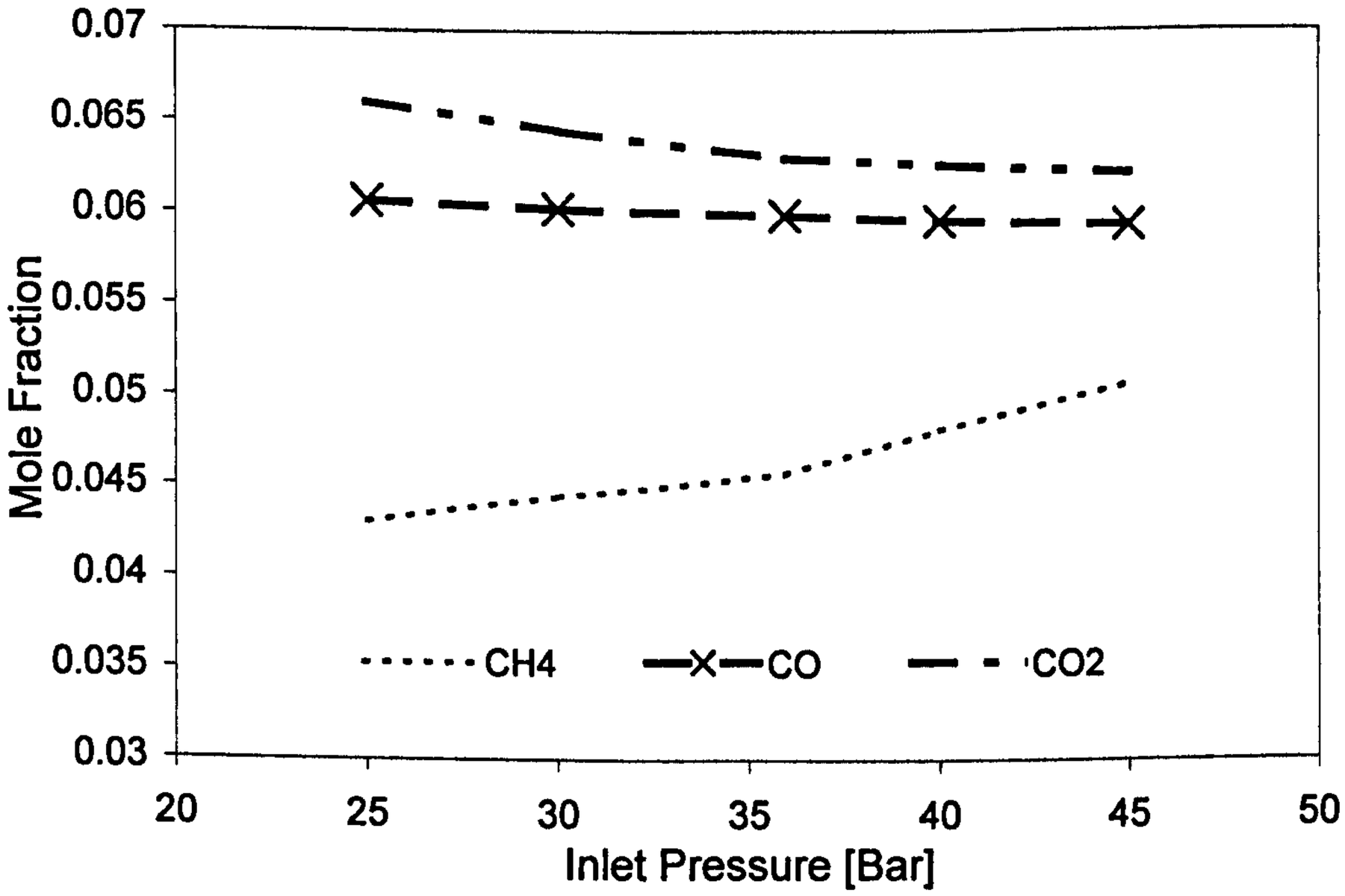

Figure 4.1.2: Influence of inlet pressure on the outlet molar fractions of CH_4, CO and CO_2

Table 4.1.3: Influence of feed rate on the outlet molar fractions of CH_4, CO, CO_2 and H_2

	Feed Rate				
	80%	90%	100%	110%	120%
X_{CH4}	0.020	0.034	0.046	0.057	0.067
X_{CO}	0.085	0.071	0.059	0.050	0.042
X_{CO2}	0.056	0.060	0.063	0.065	0.066
X_{H2}	0.452	0.428	0.404	0.383	0.364

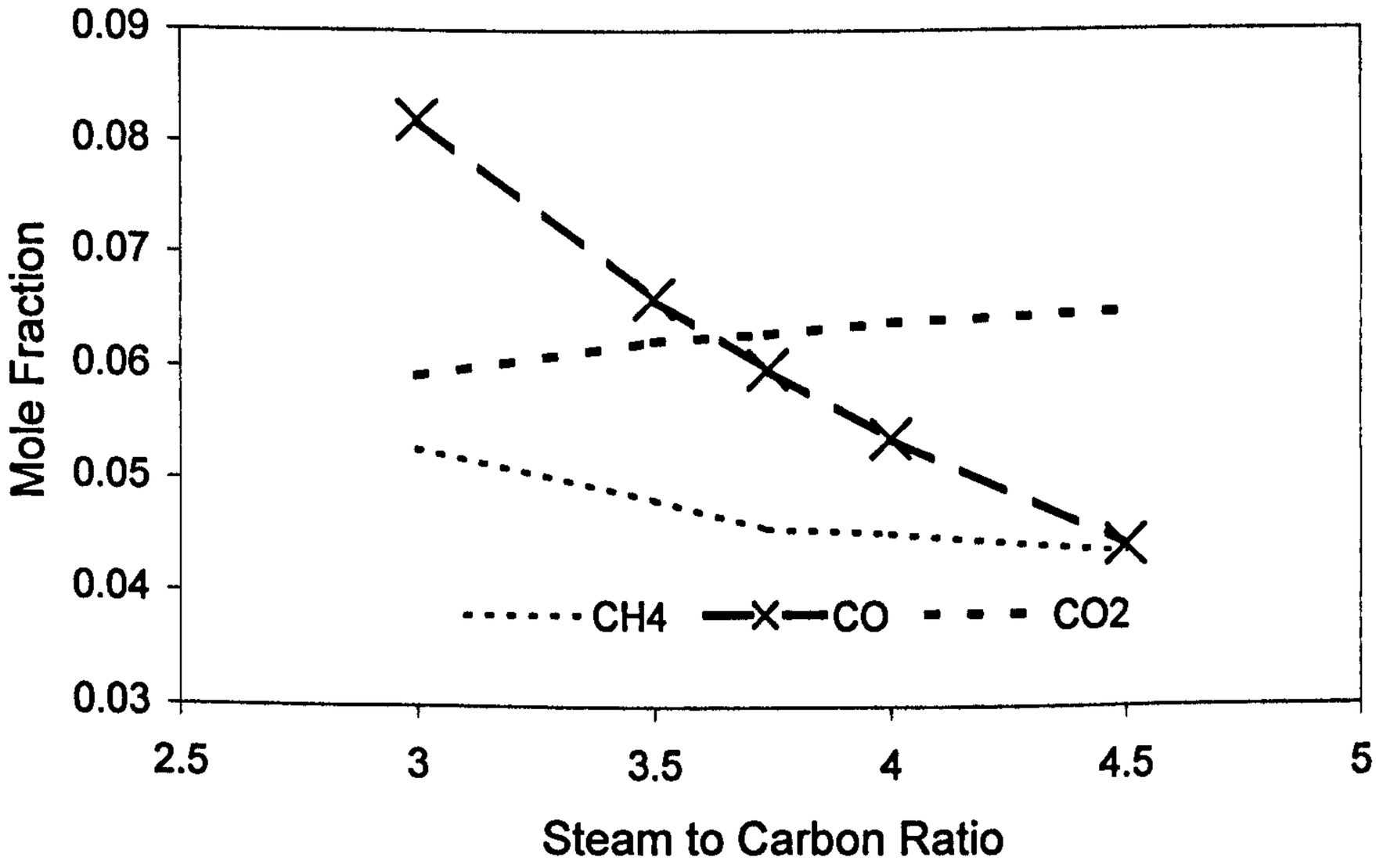

Figure 4.1.3: Influence of inlet steam to carbon ratio on the outlet dry molar fractions of CH_4, CO and CO_2

Due to the magnitude of heat supplied to the reformer tube, the sensible heat at the inlet has a limited influence on the gas temperature, especially in the region of normal operation (Table 4.1.4).

Table 4.1.4: Influence of inlet temperature on the outlet molar fractions of CH_4 and H_2

	Inlet Temperature [K]				
	648	708	728	748	808
X_{CH4}	0.055	0.048	0.046	0.044	0.038
X_{H2}	0.388	0.400	0.404	0.408	0.420

The choice of material of construction and design parameters for the reformer tube are not only constrained by the maximum heat flux but also the maximum tube temperature, hence, a suitable range of operating conditions are required. Although the effect on the reformer exit gas temperature is small with increased inlet temperature and pressure, along the tube length more significant changes occur and this is reflected in the tube wall temperature profile (Figure 4.1.4).

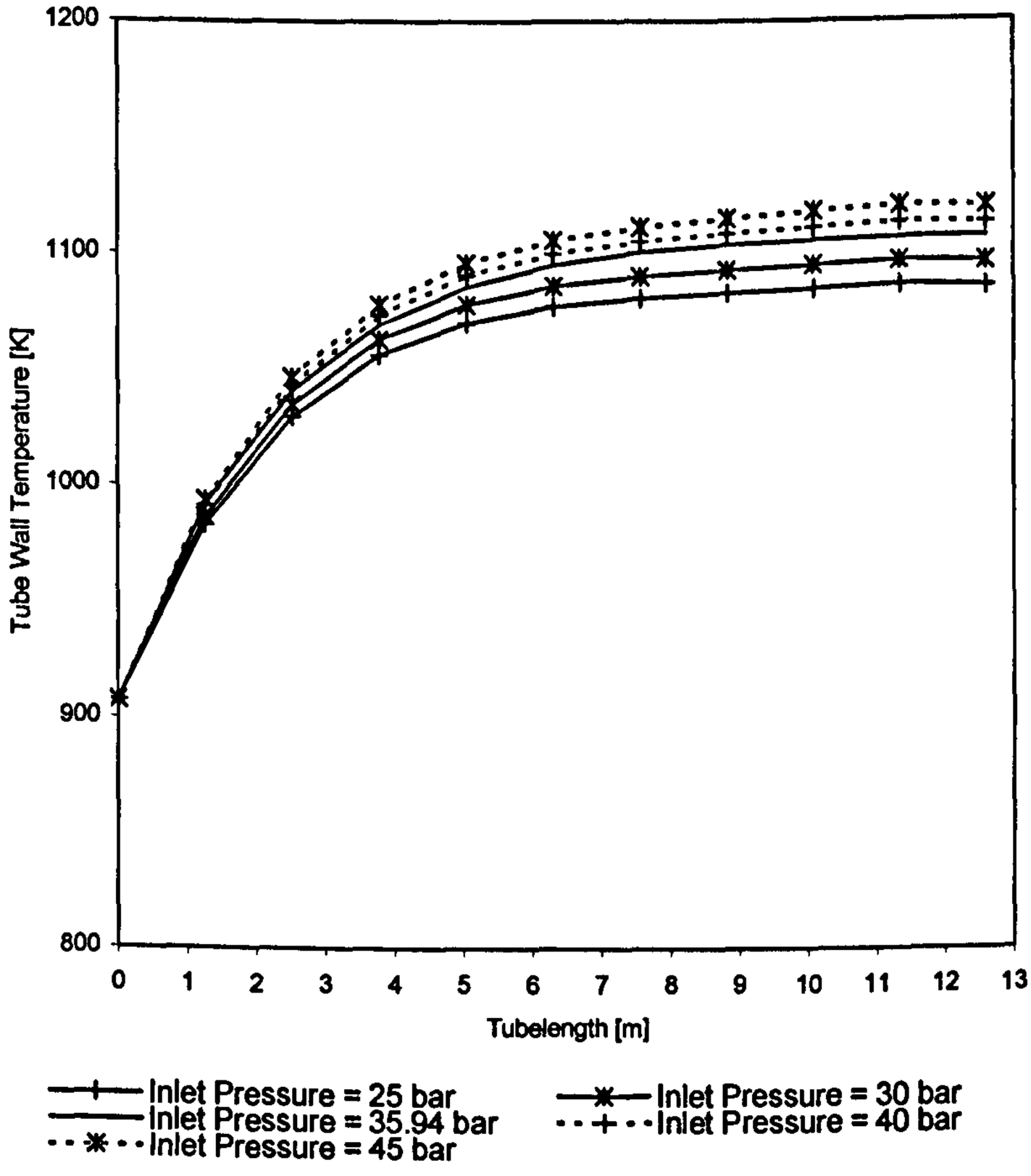

Figure 4.1.4: Influence of inlet pressure on the average tube wall temperature profile

When more steam is added (Figure 4.1.5) or the feed rate (Figure 4.1.6) is increased to the reformer tube, (independent of the increased requirement in sensible heat) the increase in reaction rate produces an increased cooling effect. This is due to the net endothermic behaviour of the steam reforming process.

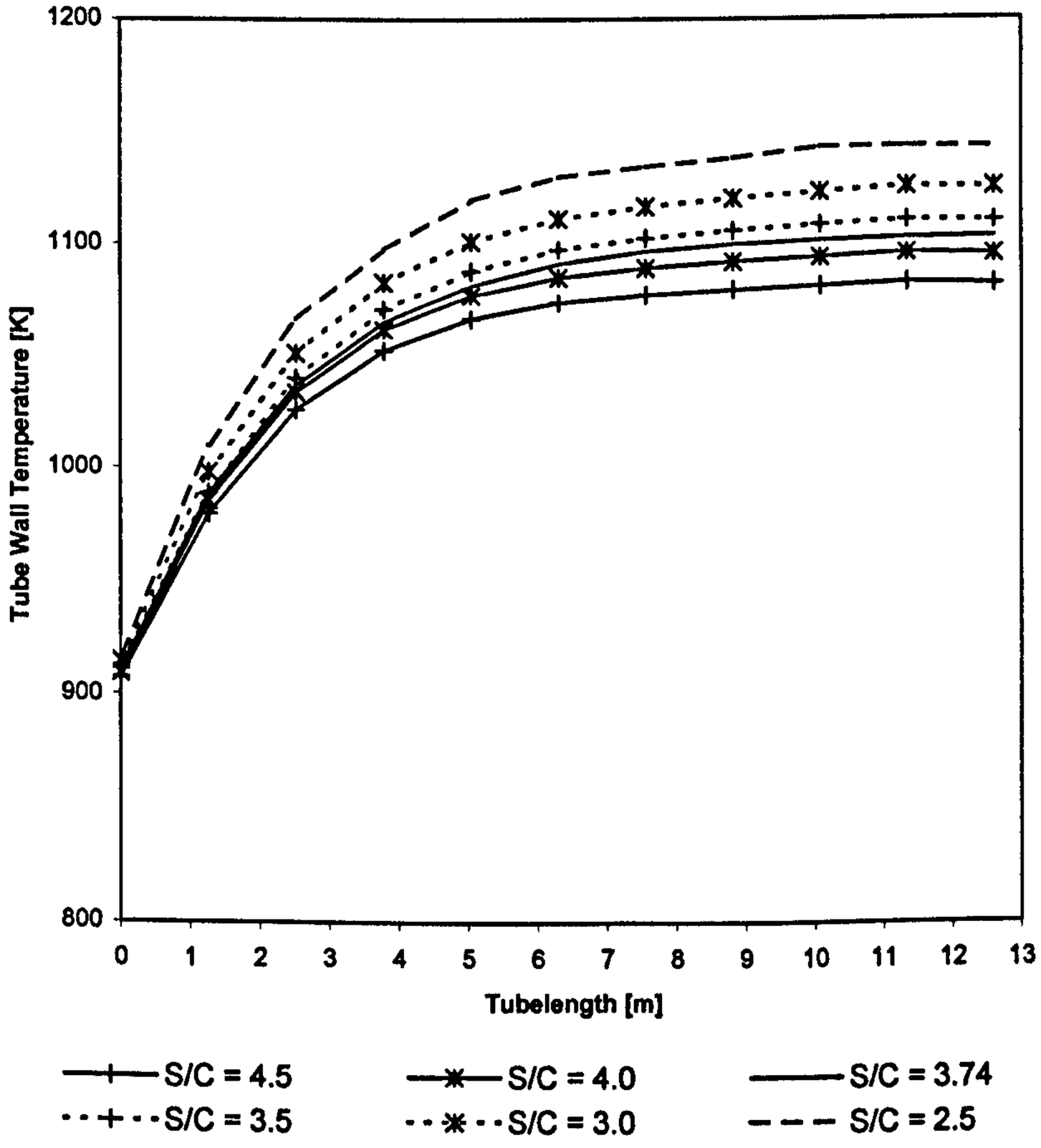

Figure 4.1.5: Influence of inlet steam to carbon ratio on the average tube wall temperature profile

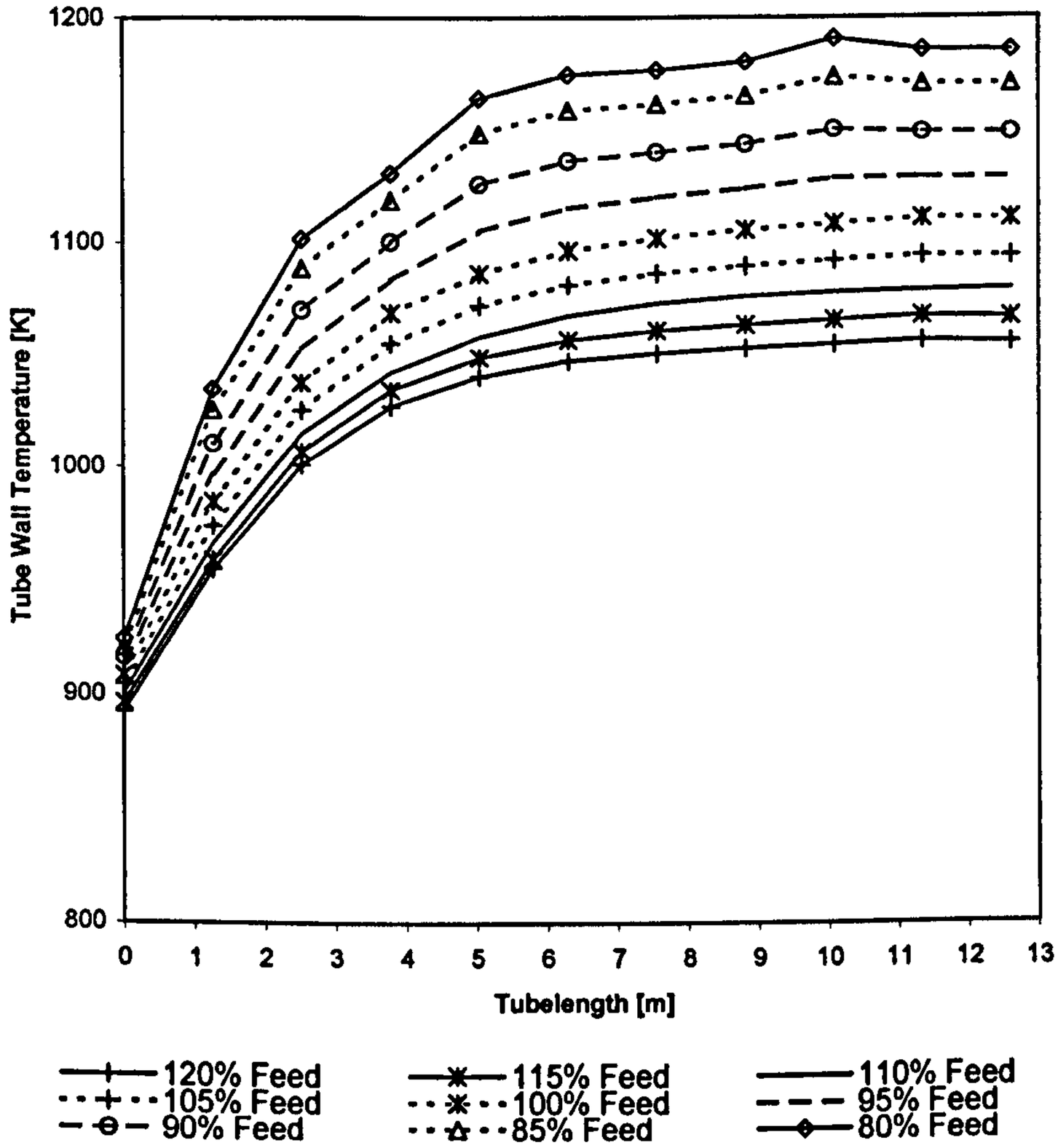

Figure 4.1.6: Influence of feed rate on the average tube wall temperature profile.

The pressure drop for the primary steam reformer is an important operational variable not only for the steam reforming section, but also for the overall process, and hence an optimal pressure drop must be determined. Due to the effect on gas density, the pressure drop increases with inlet pressure and slightly decreases with increased inlet temperature. However, when more steam is added or the overall feed rate is increased, the velocity increases and hence the pressure drop increases.

The results of the sensitivity analysis presented in this work suffer from no strange quirks or anomalies and are very similar to those reported by several authors including Alatiqi et al. (1989). Thus reinforcing the validation of the primary steam reformer model to include confidence not only at one set of steady-state conditions but also within the normal operational envelope.

Although steam reforming is often mid-stream of a process, the constraints on the system parameters still leave a scope for optimisation. Therefore, formulation of an optimisation problem with constraints on the operating parameters is essential, as repetitive simulation is tedious and does not guarantee a true optimum solution.

4.1.4 Conclusions

A 'first pass' attempt of a primary steam model was developed to initiate further research of the simulation of primary steam reformers. The model was based on previously published research but refined with a number of developments for both the model definition and the solution techniques. From this model development several of the key areas of primary steam reformer modelling were discussed and assessed, including chemical reactions and kinetics and furnace modelling.

Although the model is not the most complicated primary steam reformer model, the simulation results demonstrated close agreement to industrial plant data. Also a sensitivity analysis of the key operating parameters of outlet composition, heat flux and pressure drop was completed. The observations are comparable to those in published

literature. Further investigations are required to evaluate the benefit, in terms of accuracy and complexity of calculation of including other physical phenomena or replacing expressions from the model.

4.2 Furnace Modelling and Operation

- DUNN, A.J., MUJTABA I.M. and YUSTOS, J., 2000, Modelling and Simulation of a Top-Fired Primary Steam Reformer using gPROMS, National University Singapore, Singapore
- DUNN, A.J., MUJTABA I.M. and YUSTOS, J., 2002, Modelling and Simulation of a Top-Fired Primary Steam Reformer using gPROMS, Dev. in Chem. Eng. & Mineral Proces. Journal., Vol. 10, No. 1 & 2, pp 77 – 87

From the initial model development and associated work, came a thorough understanding of primary steam reformer modelling issues and areas of particular interest. Consistently the issue of furnace modelling was noticeably passed over by most researchers, with the main focus on the tube side model development. In fact currently only two published papers make any attempt to advance from the assumed profile representation of one tube discussed in section 4.1. The top-fired furnace arrangement was chosen as the focus of this development as for this arrangement the burner – tube configuration varies the most significantly across the furnace. Interestingly Adris et al. (1996) reports that the top-fired furnace is the "most popular" arrangement of industrial steam reformers.

In this work, using the model developed in section 4.1 as a basis, various improvements have been implemented to the model over two stages. The main improvement is the extension of the heat flux profile application, from the assumption of one tube profile representing all the tubes in the reformer to a zone approach. Due to the nature of the arrangement of top-fired furnaces, see Figure 4.2.1, tubes are situated in one of two locations, either in-between rows of burners or a row of burners and a refractory wall, hence two zones. Polynomials are developed for the differing zone heat flux profiles using the same method as Alatiqi et al. (1989). Model validation is performed against industrial data from a steam reformer within an ammonia process.

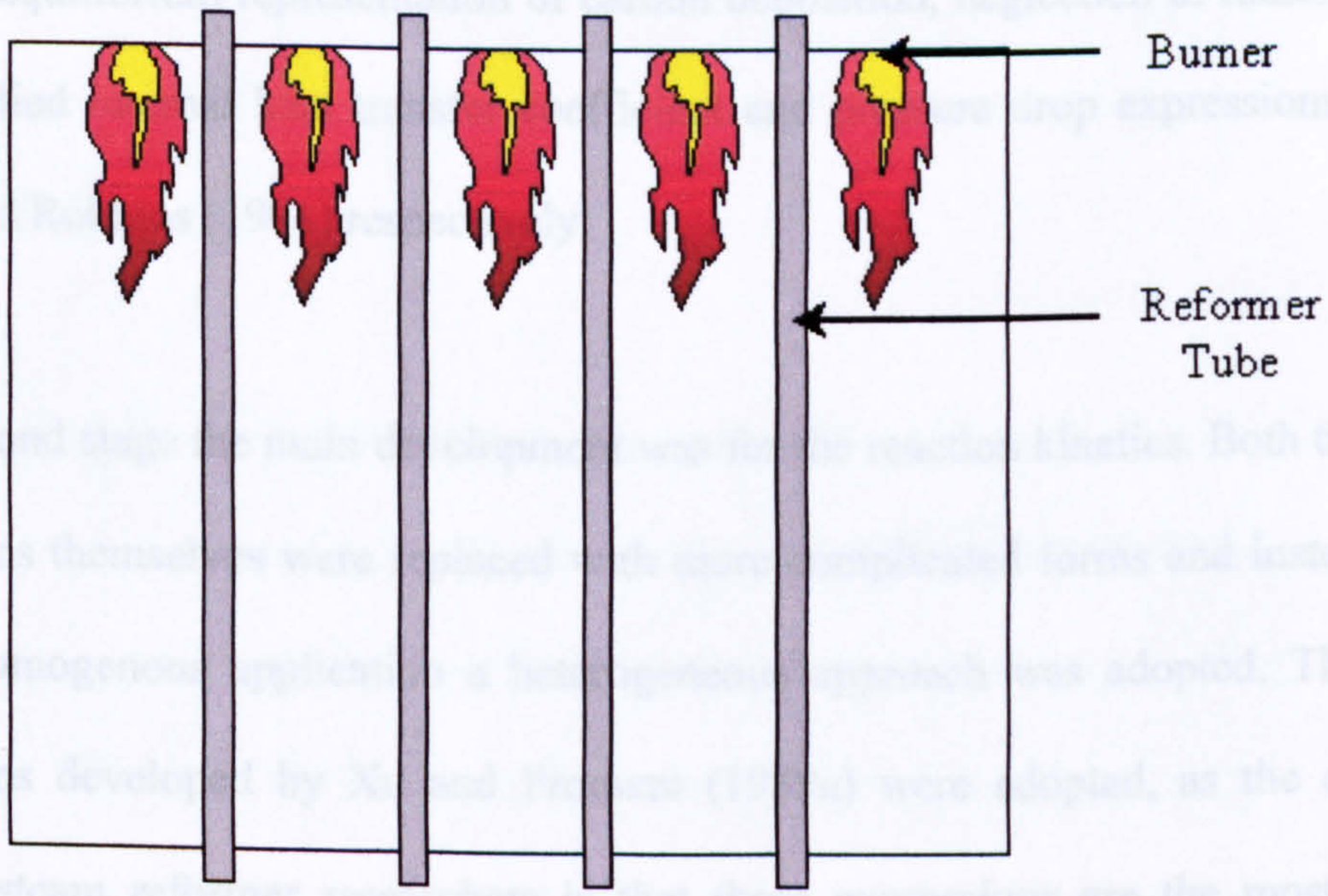

Figure 4.2.1: Layout of a Top-Fired Primary Reformer.

The general purpose modelling package of gPROMS is used in this work, which includes several features for simulation such as object-orientation, modularisation and open-interfaces. A sensitivity analysis is performed by varying the key operating parameters of temperature, pressure, steam to carbon ratio and tube wall temperature.

4.2.1 Model Description

As for the model developed in section 4.1, the model description is partitioned into, the steam reformer tubes, the furnace, the physical property expressions used for the steam reformer tube section and numerical solution of the model. Although only the key equations are discussed in the model description a full listing is included in Appendix 3.

Steam Reformer Tubes

For the first stage of development, the same steam reformer tube model was adopted as the initial model described in section 4.1. With the kinetic expressions developed by Singh and Saraf (1979), a 'methane equivalent' approach for higher hydrocarbons than methane, equilibrium representation of carbon deposition, neglection of radial variation and modified internal heat transfer coefficient and pressure drop expressions of Beek (1962) and Robbins (1991) respectively.

In the second stage the main development was for the reaction kinetics. Both the kinetic expressions themselves were replaced with more complicated forms and instead of the pseudo-homogenous application a heterogeneous approach was adopted. The kinetic expressions developed by Xu and Froment (1989a) were adopted, as the consensus amongst steam reformer researchers is that these expressions are the most accurate available [equations 4.5 to 4.7]. For these kinetics the following reaction scheme is assumed,

$$CH_4 + H_2O \Leftrightarrow CO + 3\,H_2 \qquad \text{(methane steam reforming)}$$

$$CO + H_2O \Leftrightarrow CO_2 + H_2 \qquad \text{(water-gas shift)}$$

$$CH_4 + 2H_2O \Leftrightarrow CO_2 + 4\,H_2 \qquad \text{(methane steam reforming)}$$

Although Xu and Froment (1989b) recommend a heterogeneous application of these kinetics, Kvamsdal et al. (1999) and the subsequent associated papers employ a pseudo-homogeneous form. This pseudo-homogeneous approach is contentious not only as it contradicts the authors recommendations but also "the rate of steam reforming is not controlled only by the kinetics of the reaction, but they are also affected by the rate of diffusion through the pores of the catalyst" [Elnashaie et al. (1988)]. Xu and Froment (1989b) demonstrate that contrary to the pseudo-homogeneous assumption of a constant lumped effectiveness factor for the chemical reactions, within the steam reformer tube the effectiveness factor varies greatly, see figure 4.2.2.

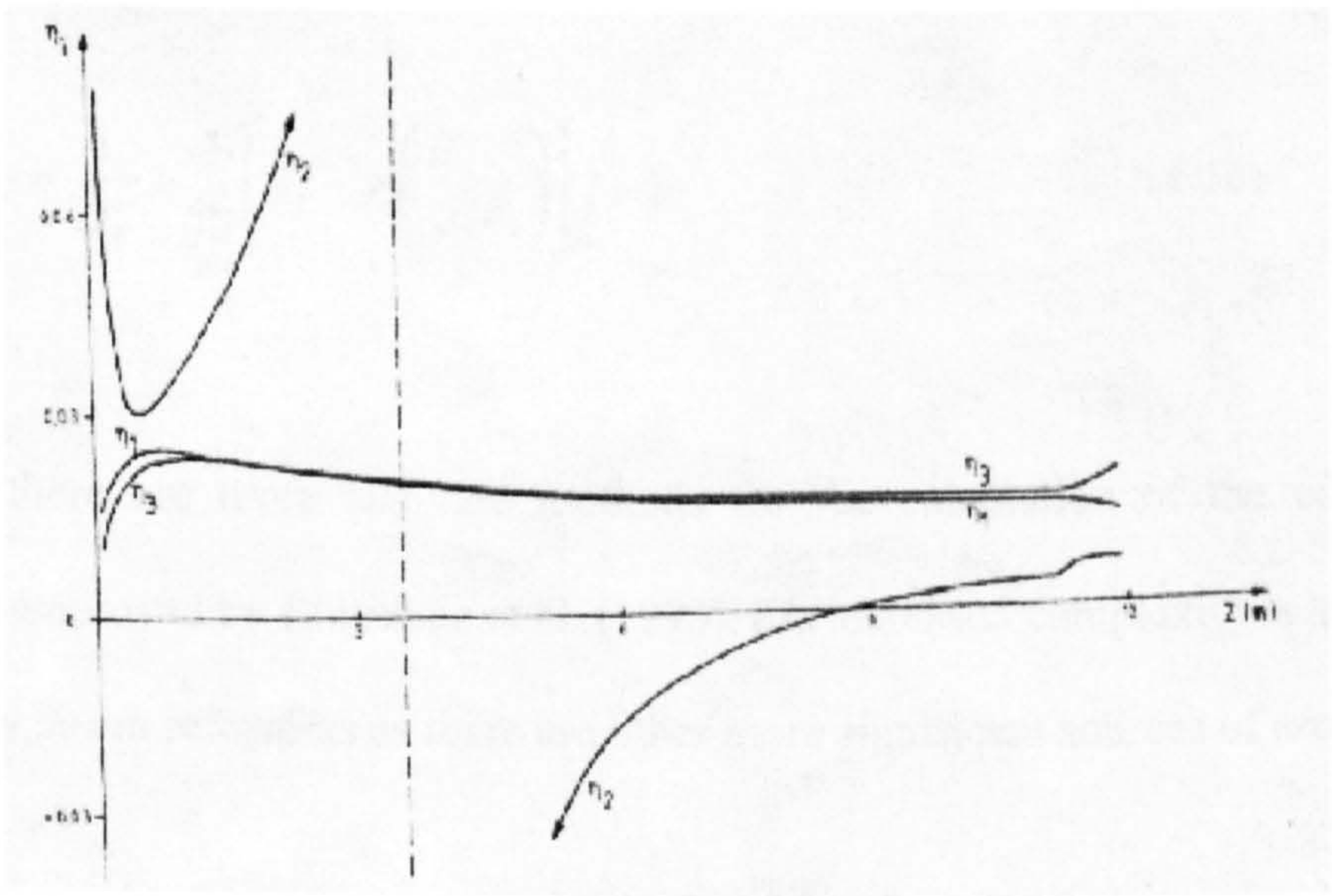

Figure 4.2.2: Evolution of effectiveness factors in a commercial steam reformer (Xu and Froment, 1989b)

A heterogeneous approach was adopted for this model, employing the calculation method recommended by Elnashaie et al. (1992) for the effectiveness factor and associated parameters. Elnashaie et al. (1992) compared the performance of this effectiveness factor calculation method with the previously preferred approach and found that when the primary steam reformer is operating near equilibrium both approaches proved to be "quite accurate and reliable". However, if the operation is far from equilibrium the recommended method of Elnashaie et al. (1992) "gives more accurate results". The key elements of this calculation method are,

$$\eta_i = \int_0^1 r_i \, d\omega / r_{ib} \tag{4.17}$$

$$\frac{1}{D_i^e} = \frac{1}{D_{ik}^e} + \sum_{\substack{j=1 \\ j \neq i}}^{n} \left[y_j - y_i \left(R_j / R_i \right) \right] \Big/ D_{ik}^e \tag{4.18}$$

Although there are more accurate methods for the calculation of the effectiveness factors, as employed by Elnashaie et al. (1993), the increased complexity is unjustifiable for primary steam reformers as there are other more significant sources of error.

The only other development apart from the kinetics and associated parameters was that with the alternative furnace modelling a representation of the distribution of reactant gas feed to the primary steam reformer tubes was required. So for the orifice plates, expressions were adopted, derived from a general energy balance assuming isothermal flow of an ideal gas,

$$G = \frac{C_D A_0}{v_2} \sqrt{\frac{2 P_1 v_1 \ln\left(\frac{P_1}{P_2}\right)}{1 - \left(\frac{v_1 A_0}{v_2 A_1}\right)^2}} \tag{4.19}$$

Physical Properties

For both stages of the development of the model the same physical property expressions were adopted as the initial model described in section 4.1. Polynomial expressions for the physical properties of the gaseous components in the reformer; heat capacity, viscosity and conductivity. With an average expression for the heat capacity of the mixture, however, for viscosity and conductivity of the mixture, the expressions by Wilke and Wassiljewa, respectively, were adopted.

Furnace model

Current reactor simulation capabilities have now extended way beyond the basic one-dimensional models, entrapped by assumptions, to integrated three-dimensional models, such as Detemmerman and Froment (1998). This enhancement encouraged not only an increased usage of reactor simulation but also more widespread applications. However, with the simulation improvements, the need to match the level of modelling complexity to the application becomes more important.

For previous steam reformer simulations the furnace modelling vary in complexity, from an assumed tube wall temperature profile, implemented by Hyman (1968), to a coupled 'zoning' model, proposed by Plehiers and Froment (1989). Although, the solution time and complexity of the 'zoning' approach are not justifiable in studies less concerned about accurate furnace modelling, the assumption that the external tube wall temperature profile is independent of process changes in the reformer tubes is flawed. As a compromise to these approaches, Alatiqi et al. (1989) proposed a polynomial representation of the heat flux profile, which was adopted in the model developed in section 4.1.

However, in a top-fired steam reformer, the heat flux profile is not equivalent for all the reformer tubes, as the tubes are either situated in-between rows of burners or a row of burners and a refractory wall, hence two zones. These zones are distinct, as the refractory wall affects the heat transfer performance, although the actual variation in external tube wall temperature is limited by furnace operation strategy. Roesler (1967) argues that the furnace should be sectioned on a radiation field basis, instead of the geometrical basis of Hottel and Sarofim (1965) implemented by Plehiers and Froment (1989). The "two-zones" theory complements both reasoning, to some extent, and offers an enhancement to the proposal of Alatiqi et al. (1989).

The "two-zones" approach was developed over both stages to allow for the different operating conditions between the zones for both the tube and furnace domains. The zonal variation of furnace conditions and conditions within the steam reformer tubes can be due to not only the burner distribution but also due to different burner operation, depending on the furnace operation strategy employed, see section 4.2.4. Due to the complexity of full fluid flow analysis of the furnace, discussed in section 4.5, the same assumption as Plehiers and Froment (1989) of a plug-flow pattern was adopted. For the steam reformer tubes the fluid flow analysis is less complex with the main consideration the fact that all of the tubes are in 'parallel' as they both feed and return to common headers. Although this "two-zone" approach is not applicable for all the primary steam reformer arrangements the approach is still portable in some form.

Numerical Solution

The full model of the primary reformer results in a system of differential and algebraic equations, consisting of sixty-eight equations for each zone. A second order orthogonal collocation finite element method with 15 discretisation points was applied for the solution technique.

As was discussed both in chapter 1 and in section 4.1, careful consideration is required to solve sets of IPDAEs. As the complexity of the model defined by the IPDAEs develops, so the requirement for increased solution consideration increases. Scaling was immediately enforced to the supplementary model equations in the primary steam reformer model, so the majority of the model variables were scaled. In contrast to the previous model and despite the employment of scaling, the increased complexity in the system of IPDAEs required the block decomposition technique to attain a valid solution.

Again the difficulties of initialisation of IPDAEs for steady-state systems were confirmed, however, the previously developed approach of de-coupling the heat balance and pressure profile equations in the steam reformer tubes failed to reach a valid solution. As this initialisation method used for the model in section 4.1 failed, a more controlled initialisation approach was developed, as discussed in chapter 1, which required employment of a scaled introduction factor for the mass and heat balances and pressure profile equations in the steam reformer tubes. The system equations associated with the solution of the key variables mole fraction, temperature and pressure were scaled over a staged implementation. For each stage of this strategy, the model was solved and the resultant solution was used to initialise the next stage with an increased scaling factor. The scaled implementation resolved the robustness issue of the initialisation for the primary steam reformer model and this technique developed is fully portable to any system of IPDAEs as it suffers from no prerequisite requirement of assumed profiles.

4.2.2 Simulation and Model Validation

The model was validated against industrial data from top-fired primary reformer within both the ammonia and methanol processes. A typical industrial top-fired reformer comprises 8 rows of 44 tubes and 12 m in length and operates at an inlet pressure and temperature of 35.94 bar and 455 °C, respectively. The simulation results are presented in Table 4.2.1, which clearly shows that the simulated data compared well to the industrial data.

Table 4.2.1: Comparison between plant and simulated data.

		Plant data	Calculated values	Deviation (%)
Outlet Temperature (K)		1084	1091	0.66
Outlet Pressure (Bar)		33	33.54	1.63
Dry Mol %	CH_4	8.10	8.15	0.62
	CO	10.39	10.36	-0.29
	CO_2	10.96	11.17	1.92
	H_2	70.28	70.05	-0.33
	Inerts	0.270	0.270	0.04
Approach to Equilibrium (K)		Reaction I		4.9
		Reaction II		0
		Reaction III		5.5

The difference between the process gas temperature and the temperature if equilibrium would have been achieved, or more commonly known as the approach to equilibrium, demonstrates the proximity of the equilibrium limit, see Table 4.2.1. Hence, further validation was required, so the heat flux profile was compared to that of an industrial simulation package (Figure 4.2.3). Overall, the profiles compare well.

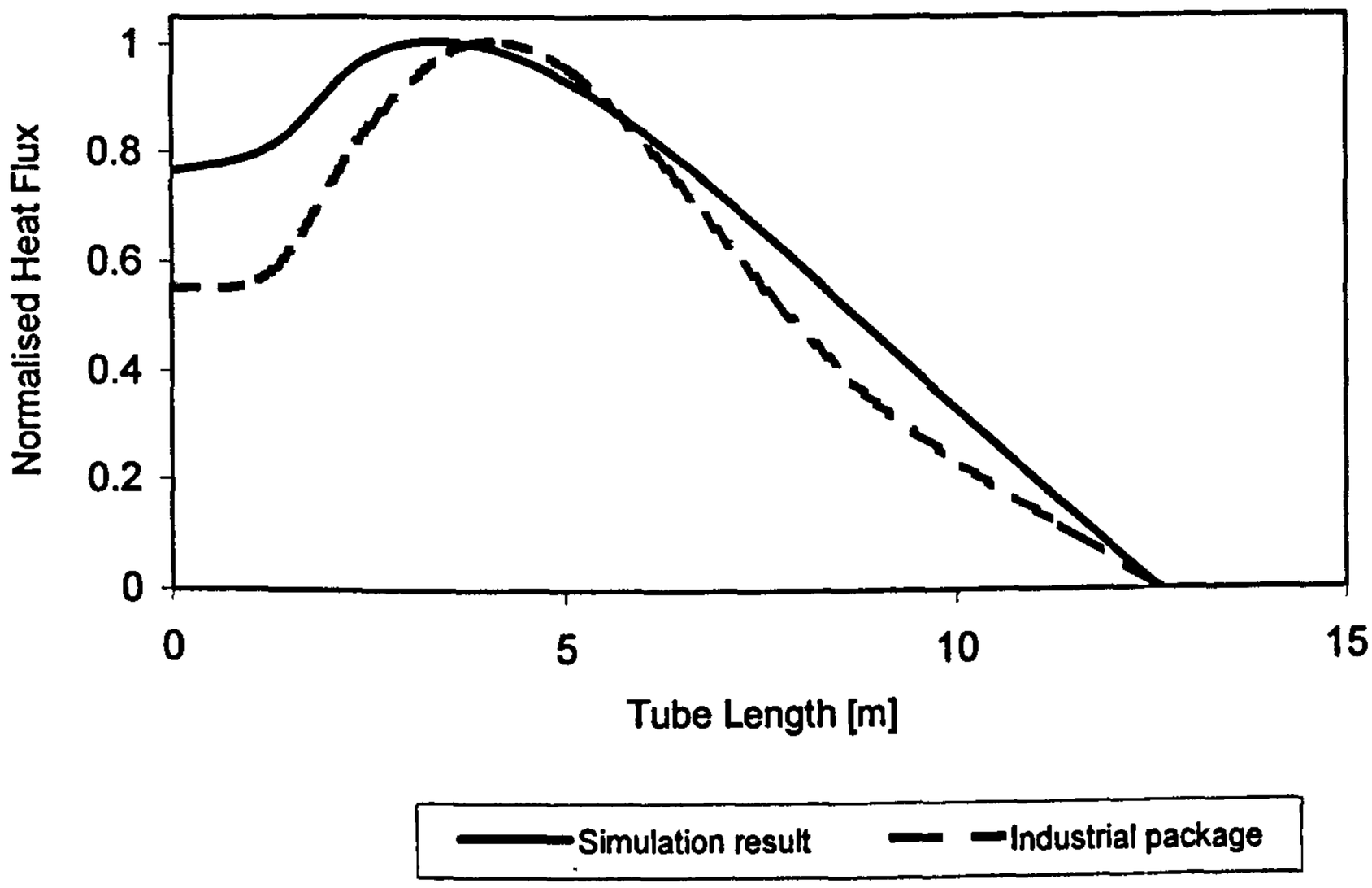

Figure 4.2.3: Comparison of Heat Flux profiles with an industrial simulation package.

4.2.3 Sensitivity Analysis

For most applications of steam reforming, the aim of a steam reformer is primarily to reduce the methane concentration and yield the required composition for downstream processing. However, the outlet of a primary steam reformer is close to chemical equilibrium, so the sensitivity of the composition is affected. The consequences of which are observable for the inlet pressure (Figure 4.2.4) and steam to carbon ratio (Figure 4.2.5).

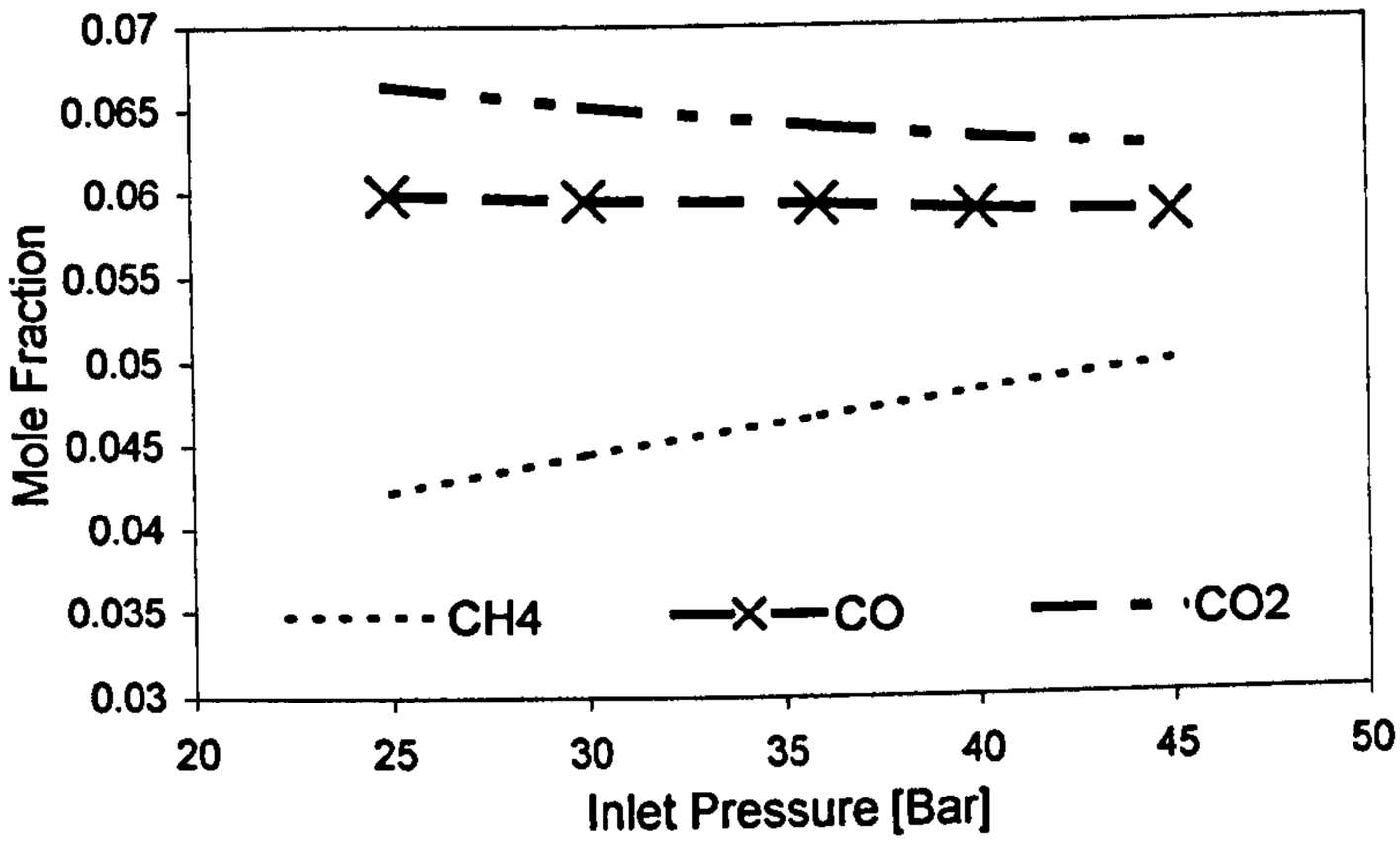

Figure 4.2.4: Influence of inlet pressure on outlet mole fractions of CH_4, CO and CO_2

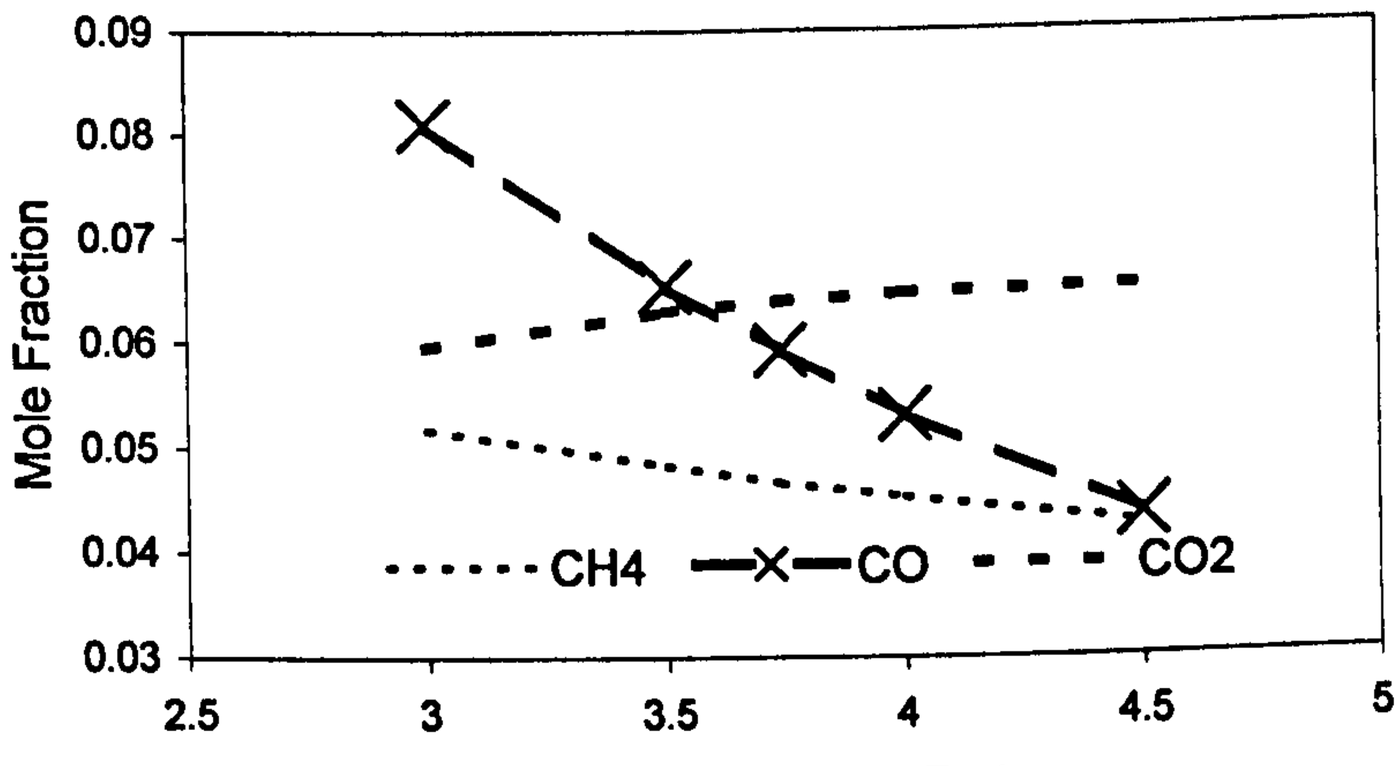

Figure 4.2.5: Influence of inlet steam to carbon ratio on outlet mole fractions of CH_4, CO and CO_2.

The choice of material of construction and design parameters for the reformer tube are not only constrained by the maximum heat flux but also the maximum tube temperature, hence, a suitable range of operating conditions are required. Although the effect on the reformer exit gas temperature is small with increased inlet temperature and pressure, along the tube length more significant changes occur and this is reflected in the tube wall temperature profile (Figure 4.2.6).

The results of the sensitivity analysis presented in this work suffer from no strange quirks or anomalies, and are very similar to those reported by several authors including Alatiqi et al. (1989). Thus reinforcing the validation of the improved primary steam reformer model, not only at steady-state but also within the normal operational envelope.

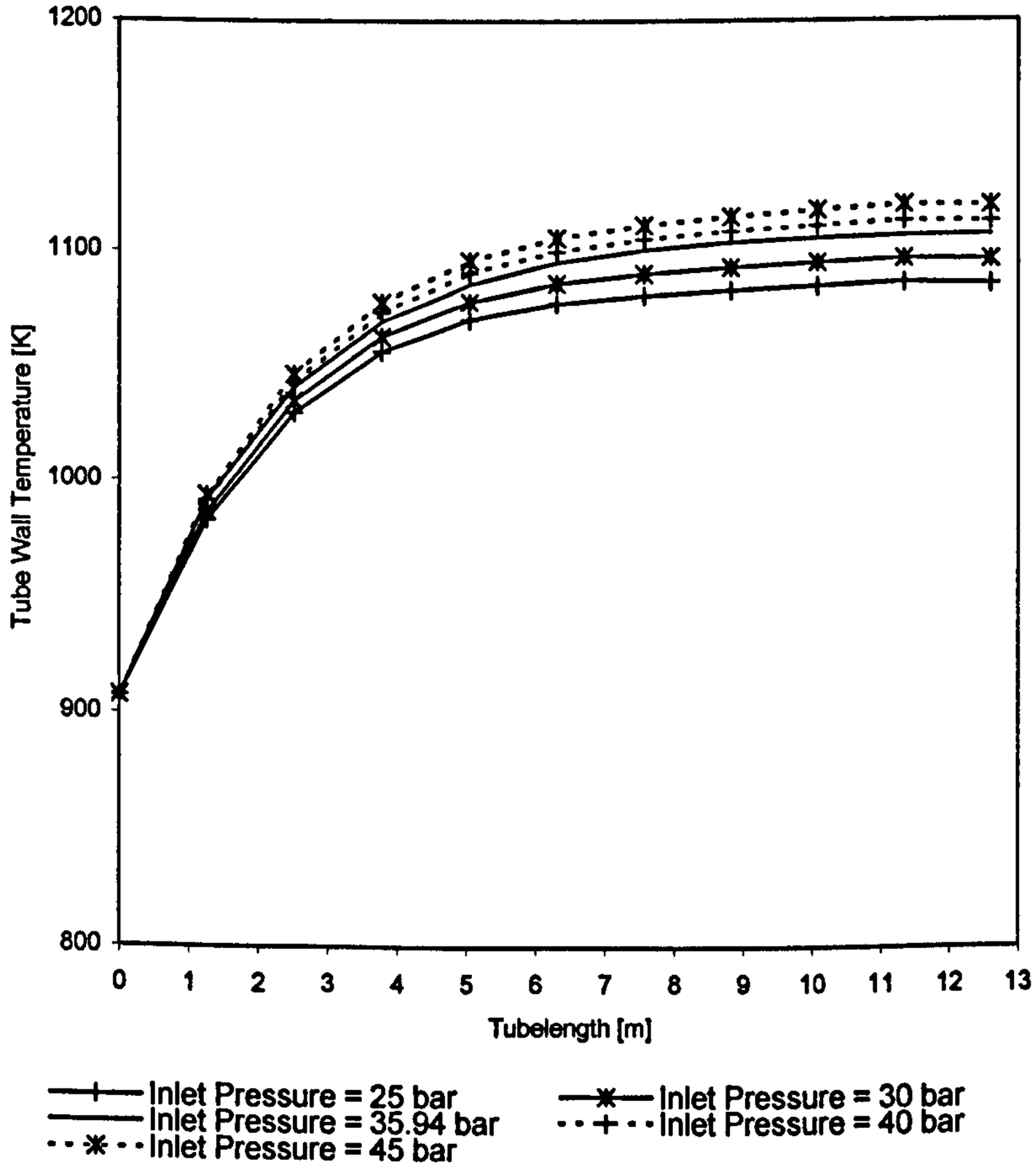

Figure 4.2.6: Influence of inlet pressure on the average tube wall temperature profile.

4.2.4 Furnace Operation

For all steam reformers, the operational lifetime of a steam reformer tube is fundamentally dependent on the maximum temperature experienced, so for ease of maintenance and avoidance of reduced capacity, the furnace should have a consistent

tube lifetime or equivalently a uniform temperature profile. Operators of top-fired steam reformers can limit the spread of temperature profiles by adjustment of the burner profile and the reactant gas distribution, or as it is more commonly called furnace balancing.

Adjustment of both the burner profile and the reactant gas distribution between the two zones, for the model, reduced the difference in the temperature profiles (Figure 4.2.7 and 4.2.8), hence enhancing the 'balance' of the furnace. The results from the zone approach are logical, but the full implications of the operational changes are not portrayed as the flow analysis of the furnace was overlooked.

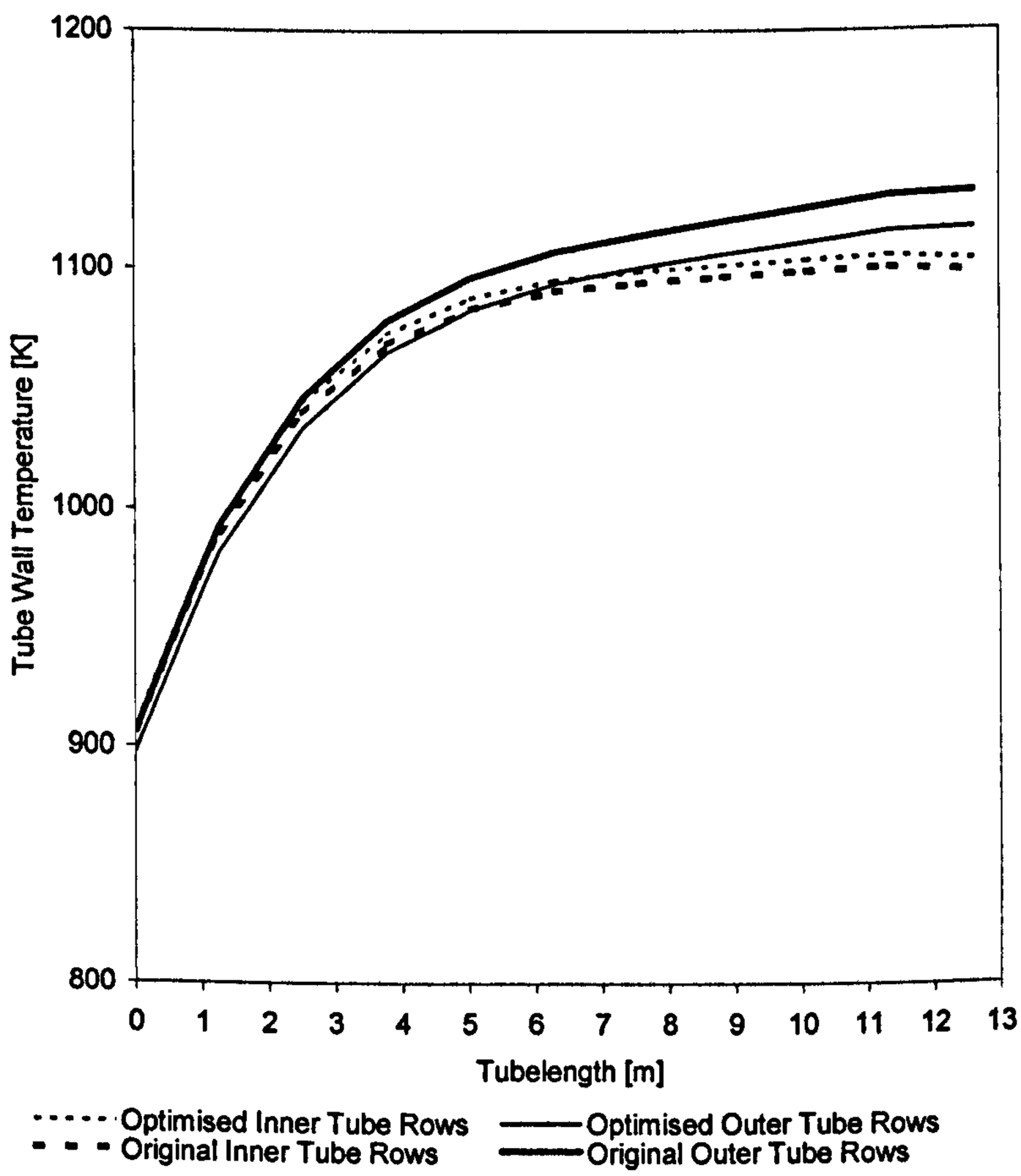

Figure 4.2.7: Comparison of inner and outer zones' tube wall temperature profiles.

Furnace balancing via adjustment of the burner profile.

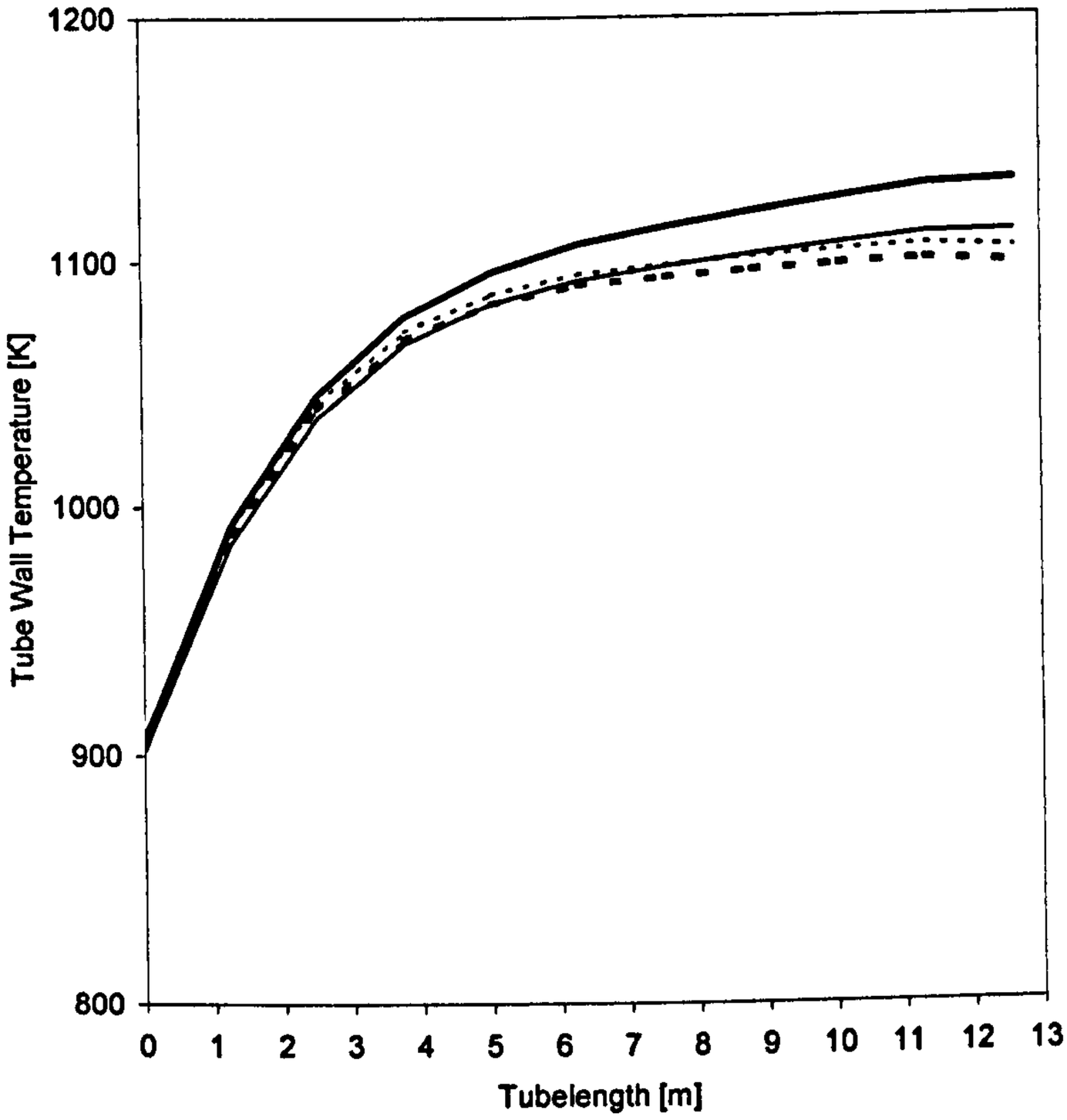

Figure 4.2.8. Comparison of inner and outer zones' tube wall temperature profiles.

Furnace balancing via adjustment of the reactant gas distribution.

4.2.5 Conclusions

A more advanced primary steam reformer model was developed with further progress for both the model definition and the solution techniques. The main model developments were the extension of the furnace model from an average tube to a zone approach that allowed for the difference in reformer tube location and the adoption of more accurate reaction expressions.

As for the initial model, in comparison to previously published simulations, the simulation results demonstrated close agreement to industrial plant data. The sensitivity analysis of the key operating parameters of outlet composition, heat flux and pressure drop was also comparable to those in published literature. Balancing the burner profile and reactant gas distribution, between the zones, was shown to reduce the difference of the tube wall temperature profiles, which is a significant operational condition overlooked by defining an average reformer tube. However, the implications of the 'balancing', particularly the furnace flow field effects require further investigation.

4.3 Dynamic modelling

- DUNN, A.J., MUJTABA I.M. and YUSTOS, J., 2001, Preliminary Optimisation of a Top-Fired Primary Steam Reformer using gPROMS, 6th World congress of Chemical Engineering, Melbourne, Australia

Although the emphasis on dynamic modelling of primary steam reformers has not been as limited as for furnace modelling, only studies of control strategy development or the effect of key operating failures exist. In reality the system of the primary steam reformer is constantly changing, predominately due to process disturbances, however, unequivocally the performance of the reactor will alter due to changes in the performance of the catalyst and reformer tubes. Previously, no attempt has been reported to simulate these effects or understand how to minimise their potential. Again the top-fired furnace arrangement was chosen as the focus for this study as the configuration is the most suitable for the study.

In this work, a dynamic model was developed from the model reported in section 4.1. The furnace model employed was the fully developed "two-zone" approach, see section 4.2, which allows for investigation of the furnace operation. Industrial data from within an ammonia process is used to validate the model. Finally, a series of operational studies were carried out for a number of situations that a primary reformer will experience.

4.3.1 Model Description

Again as for the model developed in section 4.1, the model description is partitioned into, the steam reformer tubes, the furnace, the physical property expressions used for the steam reformer tube section and numerical solution of the model. Although only the key equations are discussed in the model description a full listing is included in Appendix 3.

Steam Reformer Tubes

The steady-state model developed in section 4.1 was used as a basis for the dynamic model developed in this work. Using the following principle the equations of the previous model were converted,

If the steady-state expression is, $\frac{\partial T}{\partial Z} = \frac{A\rho_C r\Delta H + \pi D_i Q}{FC_P}$ (4.20)

Then for a dynamic conversion, $\partial T = \frac{\partial T}{\partial t}\partial t + \frac{\partial T}{\partial Z}\partial Z$ (4.21)

$$\frac{\partial T}{\partial Z} = \frac{\partial T}{\partial t}\frac{\partial t}{\partial Z} + \frac{\partial T}{\partial Z} \tag{4.22}$$

$$\frac{\partial T}{\partial t}\frac{1}{v} = \frac{A\rho_C r\Delta H + \pi D_t Q}{FC_P} - \frac{\partial T}{\partial Z} \tag{4.23}$$

$$\frac{\partial T}{\partial t} = v\left(\frac{A\rho_C r\Delta H + \pi D_t Q}{FC_P} - \frac{\partial T}{\partial Z}\right) \tag{4.24}$$

Within the primary steam reformer tube, the only chemical reactions considered are,

$CH_4 + H_2O \Leftrightarrow CO + 3\,H_2$ methane steam reforming

$CO + H_2O \Leftrightarrow CO_2 + H_2$ water-gas shift

For higher hydrocarbons than methane, a 'methane equivalent' approach is adopted and an equilibrium representation of carbon deposition is assumed.

The kinetic expressions developed by Singh and Saraf (1979) are adopted in preference to more complicated kinetics, such as adopted in section 4.2, to limit the size of the problem. Alatiqi and Meziou (1991) have demonstrated that these kinetics not only yield "excellent agreement" with reported plant records at various steady-states, but also predict the plant dynamics with "very good" agreement. Radial variation is neglected for all variables and the internal heat transfer coefficient and the pressure drop expressions of Beek (1962) and Robbins (1991) respectively, are modified to take into account the shape of modern catalyst.

As for the model in section 4.2, a representation of the distribution of reactant gas feed to the primary steam reformer tubes was required. The same orifice plates expressions as for the model in section 4.2, assuming isothermal flow of an ideal gas, were employed.

Physical Properties

Again as for the models in section 4.1 and 4.2, the same physical property expressions were adopted. Polynomial expressions for the physical properties of the gaseous components in the reformer, including heat capacity, viscosity and conductivity. With an average expression for the heat capacity of the mixture, however, for viscosity and conductivity of the mixture, the expressions by Wilke and Wassiljewa, respectively, were adopted.

Furnace model

As discussed in section 4.2, with the development in computing hardware and software, reactor simulation capabilities have extended way beyond the basic one-dimensional models, entrapped by assumptions, to integrated three-dimensional models, such as Detemmerman and Froment (1998). With this, the usage of reactor simulation has increased and diversified, however, there is now a possibility of over developing the simulation and the need to match the level of modelling complexity to the application becomes more important.

Several methods of modelling the furnace of a steam reformer have been hypothesised of different complexities; including assumed temperature and heat flux profiles and coupled `zoning`. As the "two-zone" approach developed in section 4.2, allows for investigation of the furnace operation it was adopted for this study.

Numerical Solution

The full model of the primary reformer results in a system of differential and algebraic equations, consisting of thirty-nine equations for each zone. A second order orthogonal collocation finite element method with 15 discretisation points was applied for the solution technique.

In contrast to the previous models discussed in this chapter, the model developed in this section is dynamic, however, the caution expressed previously is fully applicable to this set of IPDAEs. Scaling was previously introduced to the prerequisite model equations in the primary steam reformer model and block decomposition was automatically employed to assist the solvers.

Interestingly, initialisation was not a key issue for solving this model. Brown et al. (1998) also observed this same result, of steady-state systems rather than dynamic systems being "more sensitive to the initial guess". However, the steady-state results reported in section 4.1 were used to initialise the simulation as it improved the solution time.

4.3.2 Simulation and Model Validation

The model was validated against industrial data for a top-fired primary reformer within the ammonia process. The reformer comprises 8 rows of 44 tubes and 12 m in length. The reformer operates at an inlet pressure and temperature of 35.94 bar and 455 °C, respectively. The simulation results are presented in Table 4.3.1, which clearly shows that the simulated data compared well to the industrial data.

The proximity of the equilibrium limit at the exit of the reformer tube is demonstrated by the difference between the process gas temperature and the temperature if equilibrium would have been achieved, or more commonly known as the approach to equilibrium, see Table 4.3.1. Due to the proximity, further validation is required, so the heat flux profile is compared to that of an industrial simulation package (Figure 4.3.1). Considering the whole tube length, the profiles are considered to be comparable.

A sensitivity analysis of several key operating parameters, reported in section 4.1, suffered from no strange quirks or anomalies and was comparable to previously observations in published literature.

Table 4.3.1: Comparison between plant and simulated data

		Plant data	Calculated values	Deviation (%)
Outlet Temperature (K)		1084	1086	0.11
Outlet Pressure (Bar)		33	32.6	0.21
Mol % Dry	CH_4	8.10	7.78	3.99
	CO	10.39	10.46	0.63
	CO_2	10.96	10.96	0.03
	H_2	70.28	70.54	0.37
	Inerts	0.270	0.265	1.7
Approach to Equilibrium (K)		Reaction I		4.5
		Reaction II		0

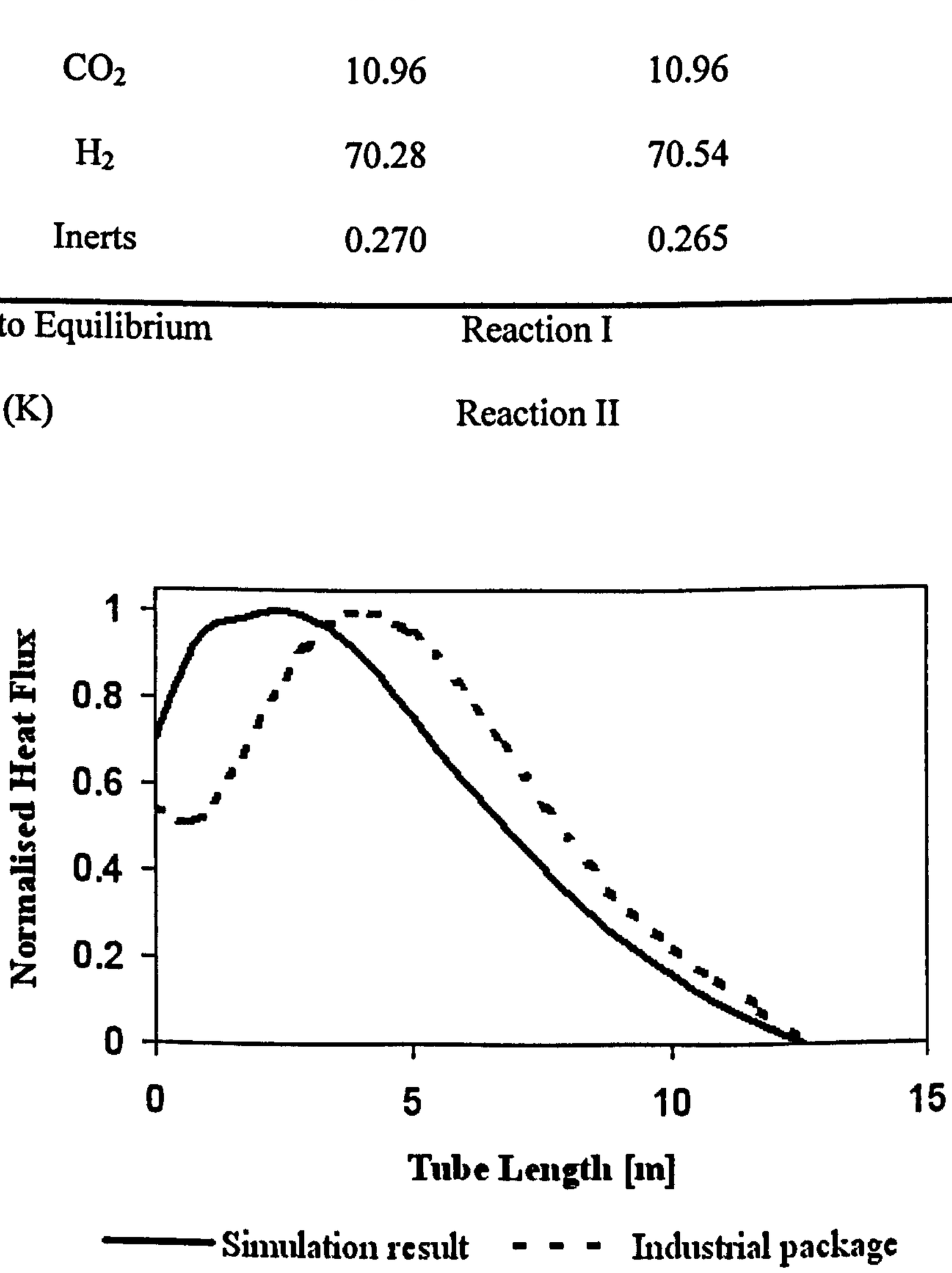

Figure. 4.3.1: Comparison of Heat Flux profiles with an industrial simulation package

4.3.3 Dynamic Response

As a primary steam reformer is a mid-stream process it has the potential to suffer from several process disturbances during operation. Typical process disturbances include, fluctuations in the steam flowrate, process gas composition and fuel gas rate.

Kvamsdal et al. (1999) have previously considered step changes to the steam and process gas feeds; which are comparable to the dynamic responses of the model proposed in this work (Figure 4.3.2 and 4.3.3). Both scenarios produce notable increases in the tube wall temperature as the change in operating conditions significantly alters the previous preferences of the reaction scheme.

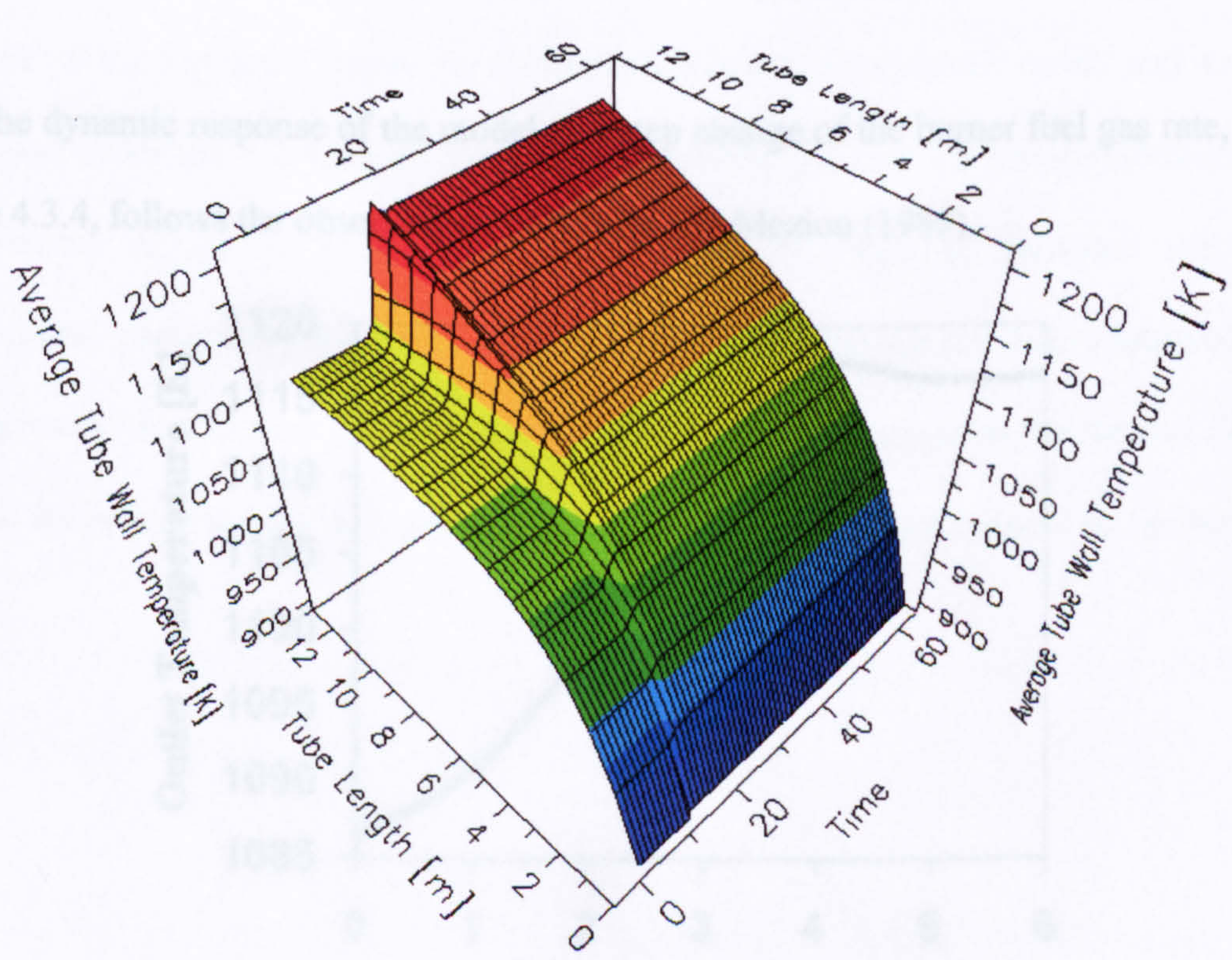

Figure 4.3.2: Dynamic response to a step up of feed steam flow rate

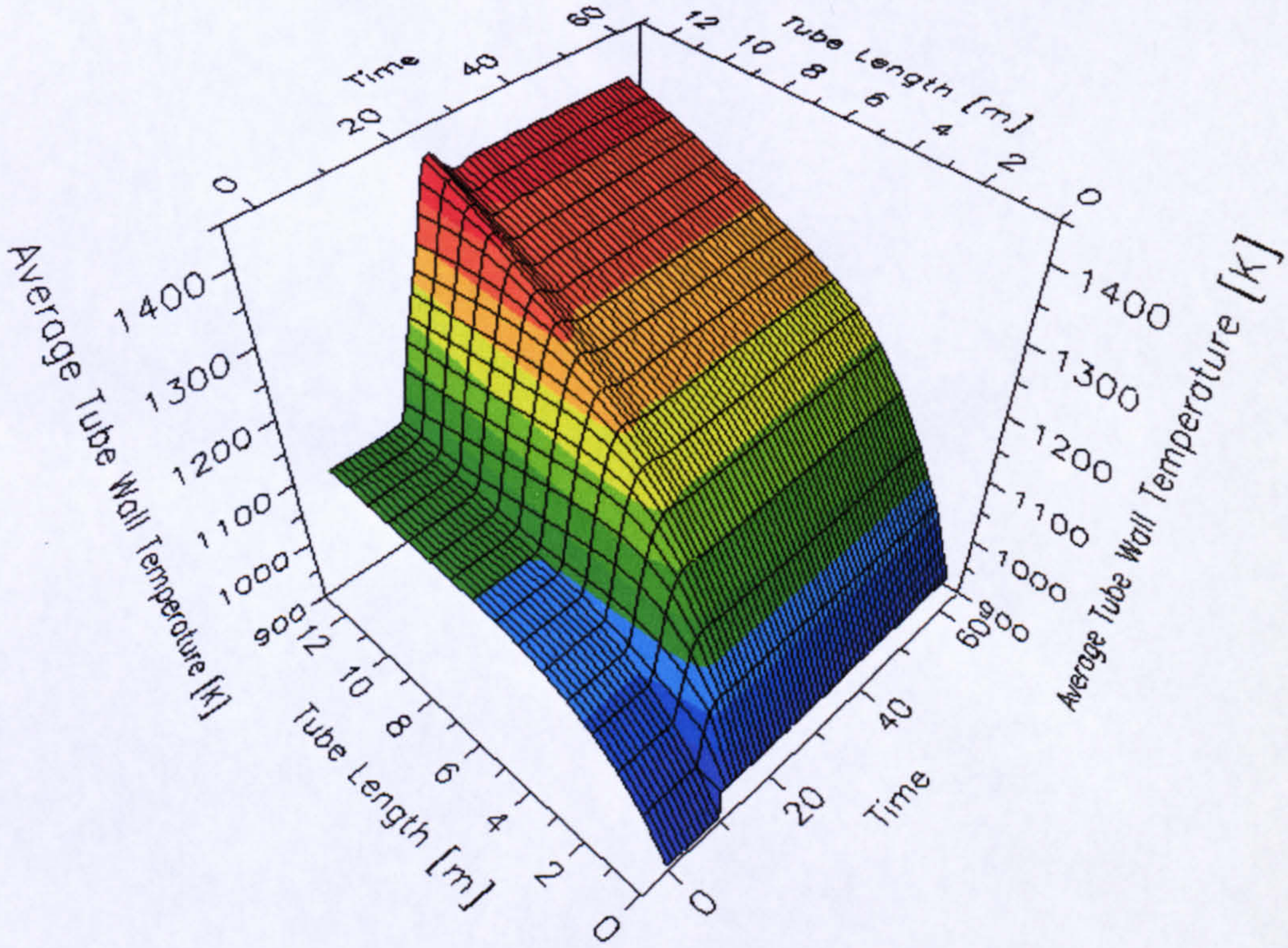

Figure 4.3.3 Dynamic response to a step change of feed gas flow rate

Also the dynamic response of the model to a step change of the burner fuel gas rate, see Figure 4.3.4, follows the observations of Alatiqi and Meziou (1989).

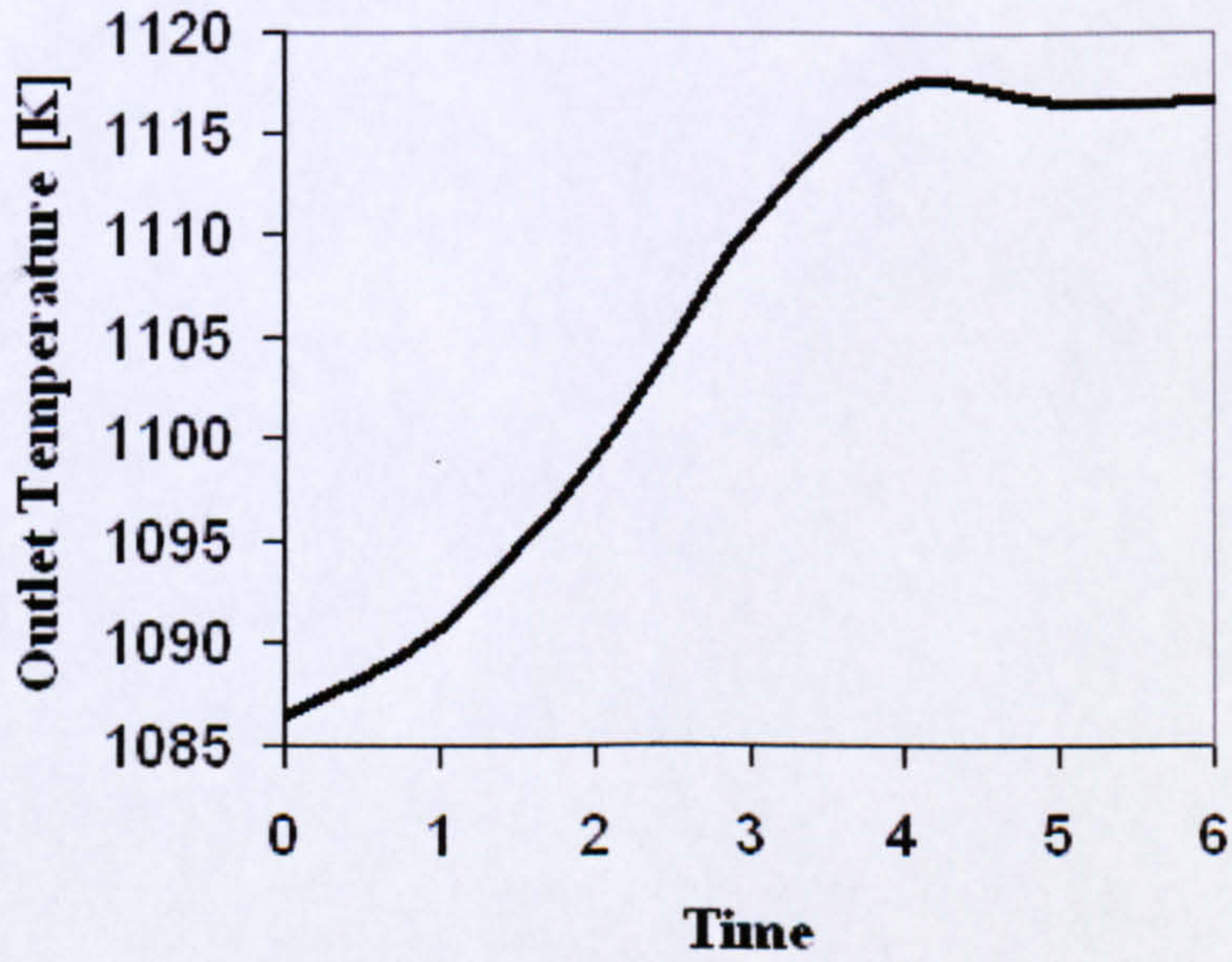

Figure 4.3.4: Dynamic response to a step change of fuel gas flow rate

4.3.4 Optimisation of Furnace Operation

Both the maximum temperature and the heat flux experienced by a steam reformer tube can significantly affect its operational lifetime. Ideally, the furnace should have a consistent tube lifetime or equivalently a uniform temperature profile, both for ease of maintenance and to avoid operating the furnace with reduced capacity which could be uneconomical.

As discussed in section 4.2.4, for top-fired steam reformers, the spread of temperature profiles can be limited by adjustment of the burner profile or the reactant gas distribution; this technique is commonly called furnace balancing. In section 4.2.4 adjustment of the burner profile and the reactant gas distribution between the two zones, was shown to reduce the difference in the temperature profiles and hence enhance the 'balance' of the furnace. Despite the differences between the dynamic model and model developed in section 4.2.4, again the results of altering the reactant gas distribution for the dynamic model are logical, see figure 4.3.5. Although as discussed the full implications, particularly the affect on the furnace flow-field are not fully portrayed by this representation. Cotton (1999) discusses the effects experienced on the furnace flow-field of an industrial top-fired primary steam reformer due to adjustment of the burner profile.

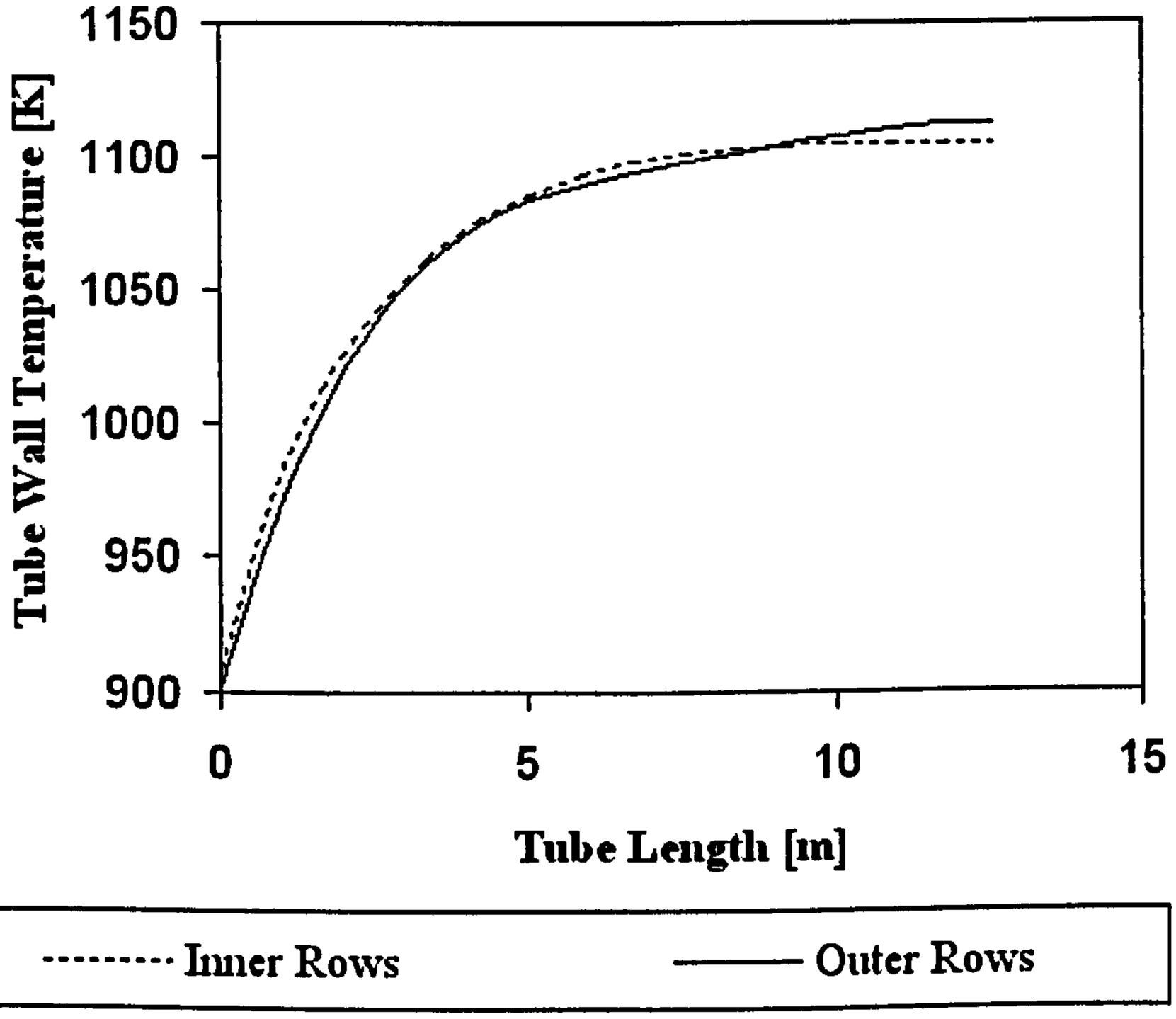

Figure 4.3.5: Comparison of inner and outer zones' tube wall temperature profiles.

Furnace balancing via adjustment of the reactant gas distribution.

Operational Cases

Over the operational life of the catalyst charge and reformer tubes, the process operators will be required to respond to several process changes. Predominately the cause will be process disturbances, however, unequivocally the performance of the reactor will alter. As is industrial practice, a furnace previously balanced via adjustment of the reactant gas distribution is employed for all the operational cases.

A major operational disturbance that could significantly affect the furnace balance is a composition change of burner feedstock. This situation could arise for a number of reasons, however, we will consider that the fuel gas is supplied from a gas field and that

the steam reformer operators have been informed of the impending step change. Over an operating period of one hour, the specific gravity can be considered to shift to a new operating condition, see figure 4.3.6.

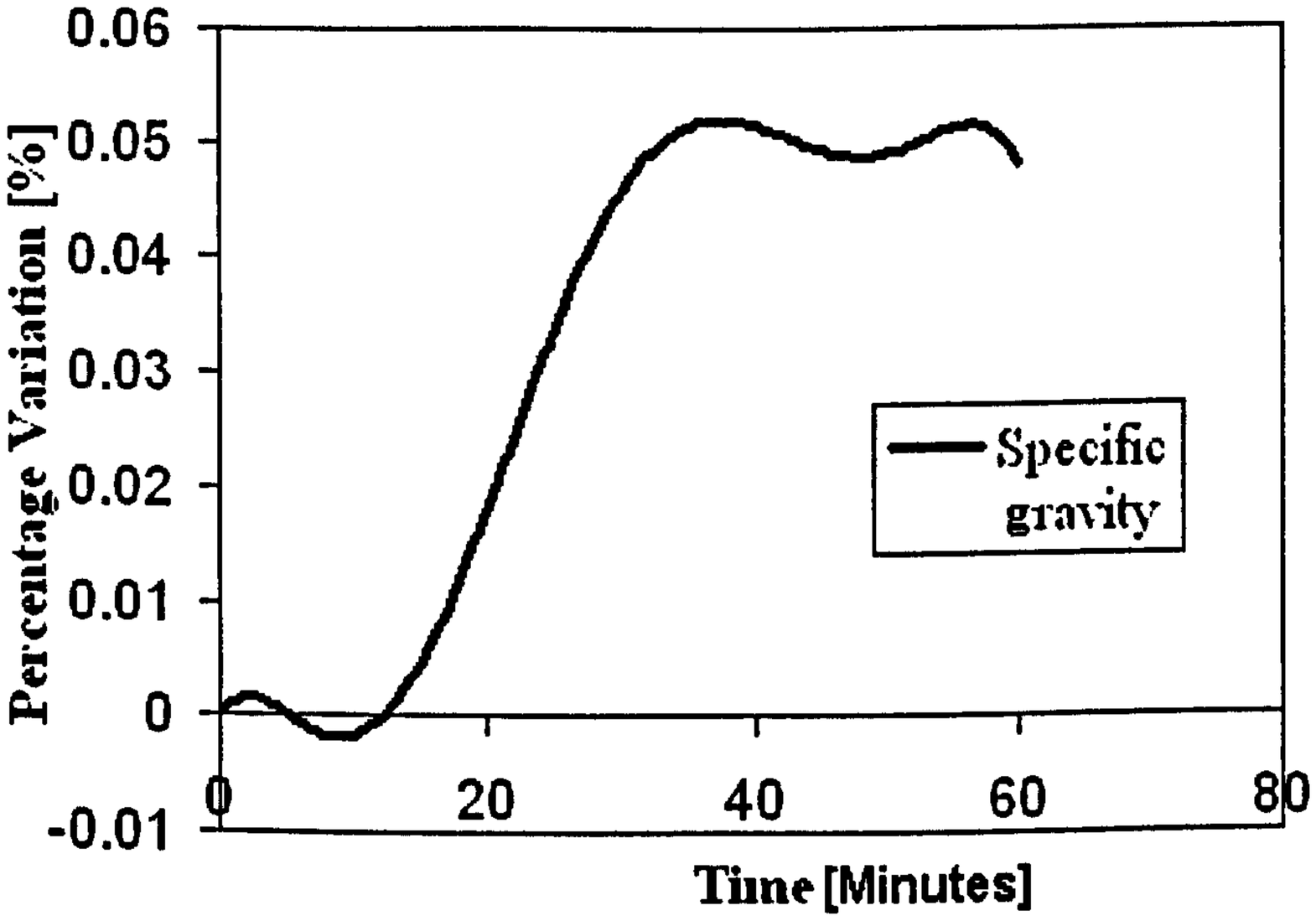

Figure 4.3.6: Burner fuel specific gravtity profile

Zidan (2001) reports that industrial practice is to respond with initially manual feedforward contol, of reducing the burner rates, followed by staged manual feedback control (Figure 4.3.7).

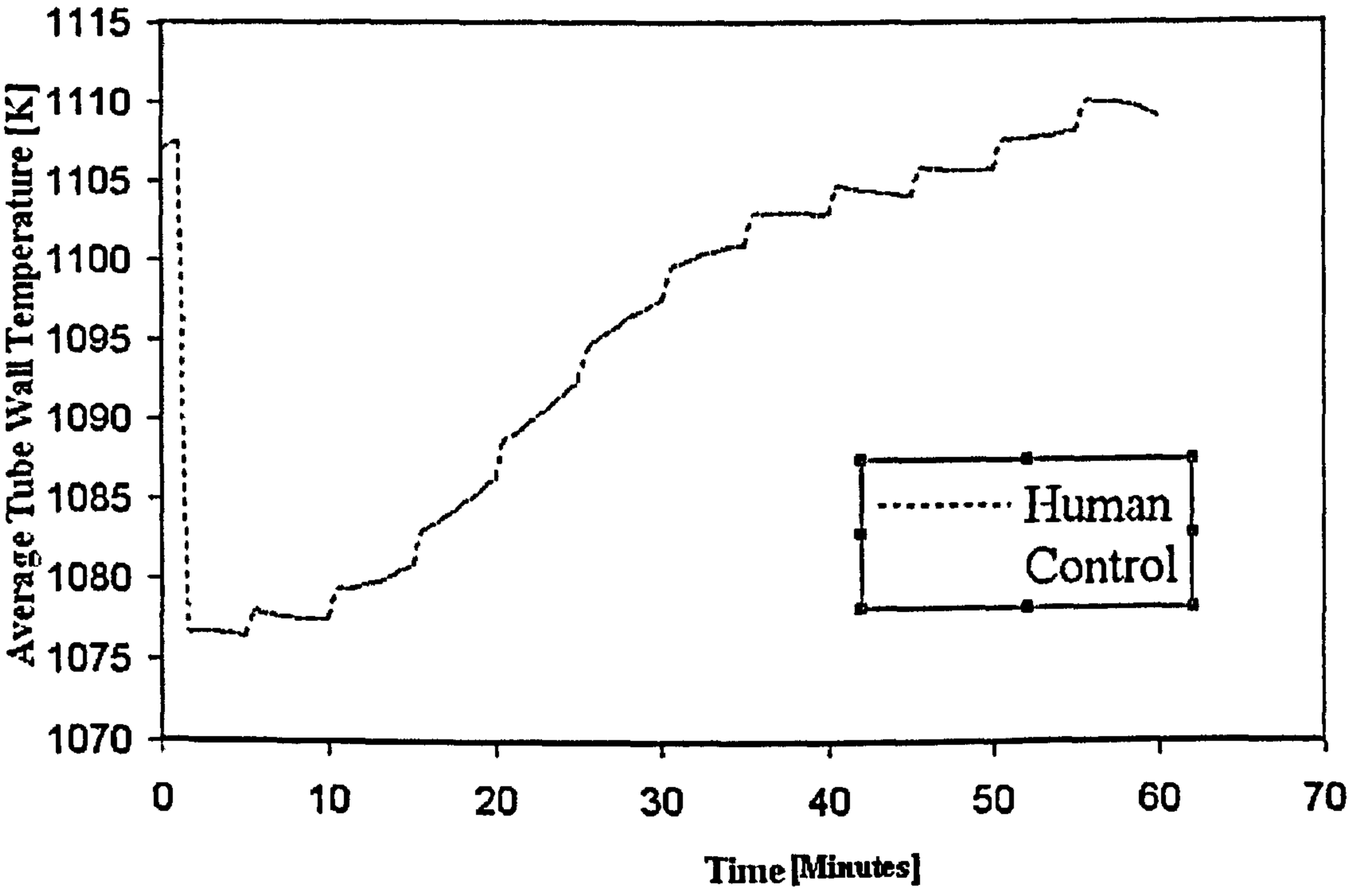

Figure 4.3.7: Response of Average Tube Wall Temperature to variation in the fuel specific gravity

The resultant effect of this strategy on the outlet composition is noticeable, see figure 4.3.8, and clearly an improved strategy is required. Throughout the period of change of burner fuel composition the 'balance' of the furnace deviates only slightly and produces a very limited scope for adjustment of the burner profile across the zones.

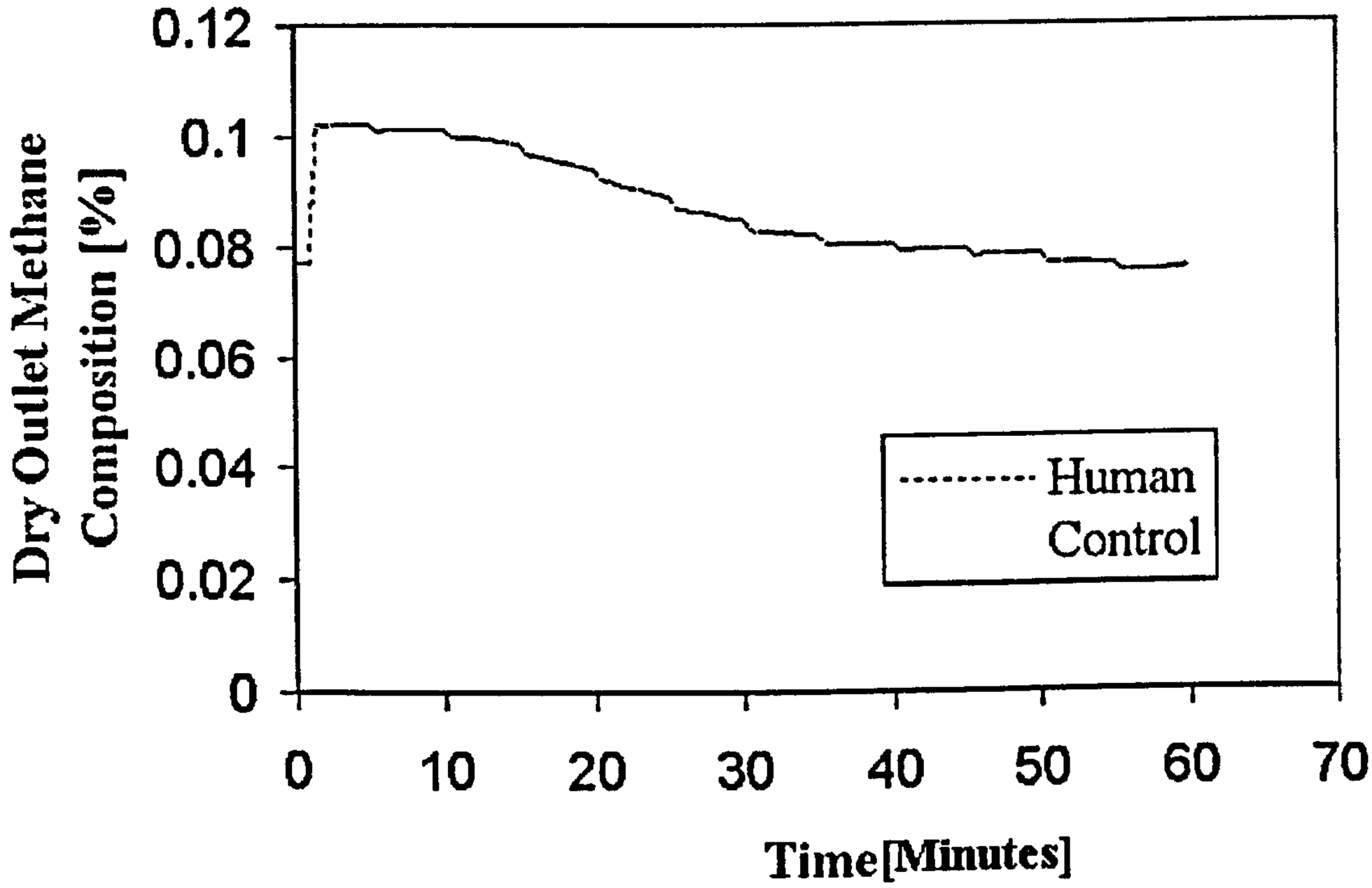

Figure 4.3.8: Response of outlet methane composition to variation in the fuel specific gravity

The main shifts in the primary reformer performance, are increased pressure drop due to structural damage of the catalyst and catalyst deactivation. Considering typical industrial observations reported by Zidan (2001) over a period of a year, both the catalyst mechanical breakdown and deactivation demonstrate a drift in process performance, see figure 4.3.9, which could be corrected periodically. As was observed for the specific gravity case, the 'balance' of the furnace only changes slightly.

4.4 Two Dimensional Model

- DUNN, A.J., MUJTABA I.M. and YUSTOS, J., 2001, Preliminary Optimisation of a Top-Fired Primary Steam Reformer using gPROMS, 2001, University of Malaya, Malaysia

As for the furnace the interest in two-dimensional models is limited for primary steam reformers. This is probably due to common belief that there are larger sources of model error than assuming no radial variation; Bird et al. (2002) consider that for a tube-to-particle diameter ratio "very large or close to unity", such as for the primary steam reformer, that the flow variation is not complex. In fact the only study of radial variation in primary steam reformers reported in published literature, Kvamsdal et al. (1999), focused on which correlations were "the most suitable", despite having no measured data, rather than considering the extent of the variation. In contrast for the wider arena of packed bed chemical reactors the topic of radial variation has been extensively researched.

In this work, a two-dimensional model was developed from the model reported in section 4.1, with the additional expressions appropriated from various literature sources. Model validation is performed against industrial data from a number of steam reformers. From this development both an assessment of the radial parameter expressions and the radial variation in primary steam reformer tubes was completed.

4.4.1 Model Description

Again the model description is partitioned into, the steam reformer tubes, the furnace, the physical property expressions used for the steam reformer tube section and numerical solution of the model. Although only the key equations are discussed in the model description a full listing is included in Appendix 3.

Steam Reformer Tubes

The steady-state model developed in section 4.1 was used as a basis for the two-dimensional model developed in this work. So within the primary steam reformer tube, the only chemical reactions considered are,

$$CH_4 + H_2O \Leftrightarrow CO + 3\,H_2 \qquad \text{methane steam reforming}$$

$$CO + H_2O \Leftrightarrow CO_2 + H_2 \qquad \text{water-gas shift}$$

For higher hydrocarbons than methane, a 'methane equivalent' approach is adopted and an equilibrium representation of carbon deposition is assumed. The kinetic expressions developed by Singh and Saraf (1979) are adopted in preference to more complicated kinetics, such as adopted in section 4.2, to limit the size of the problem. The internal heat transfer coefficient and the pressure drop expressions of Beek (1962) and Robbins (1991) respectively, are modified to take into account the shape of modern catalyst.

Although Kvamsdal et al. (1999) is inconclusive as to the most accurate representation of radial expressions, the authors highlight several of the key expressions in published literature. Froment and Bischoff (1990) offer a wider discussion including alternative approaches for two-dimensional modelling; Vortmeyer and Haidegger (1991) and Papageorgiou and Froment (1995) performed further reviews of this discussion. From assessing these reviews, clearly a range of model complexities exists from the simple model of constant porosity and plug flow to a heterogeneous model incorporating the lack of structural uniformity of the bed into the fluid flow equations.

As the focus was to ascertain the magnitude of radial variation, the same pragmatic ideal as previously of balancing complexity with accuracy was adopted. The consensus of the highlighted reviews was that an approach allowing for radial variation of porosity and velocity would deliver ample accuracy. Delmas and Froment (1988) proposed such an approach, which was adopted as a basis for this model, however, some improvements were introduced.

The main improvement was the replacement of the method for calculating voidage variations proposed by Govindarao and Froment (1986). This method has since been further developed in Govindarao and Ramrao (1988) and Govindarao et al. (1990), however, the approach by Govindarao and Ramrao (1988) was adopted for this exploratory investigation. The difference in accuracy between these approaches is demonstrated by Govindarao et al. (1990), see figure 4.4.1.

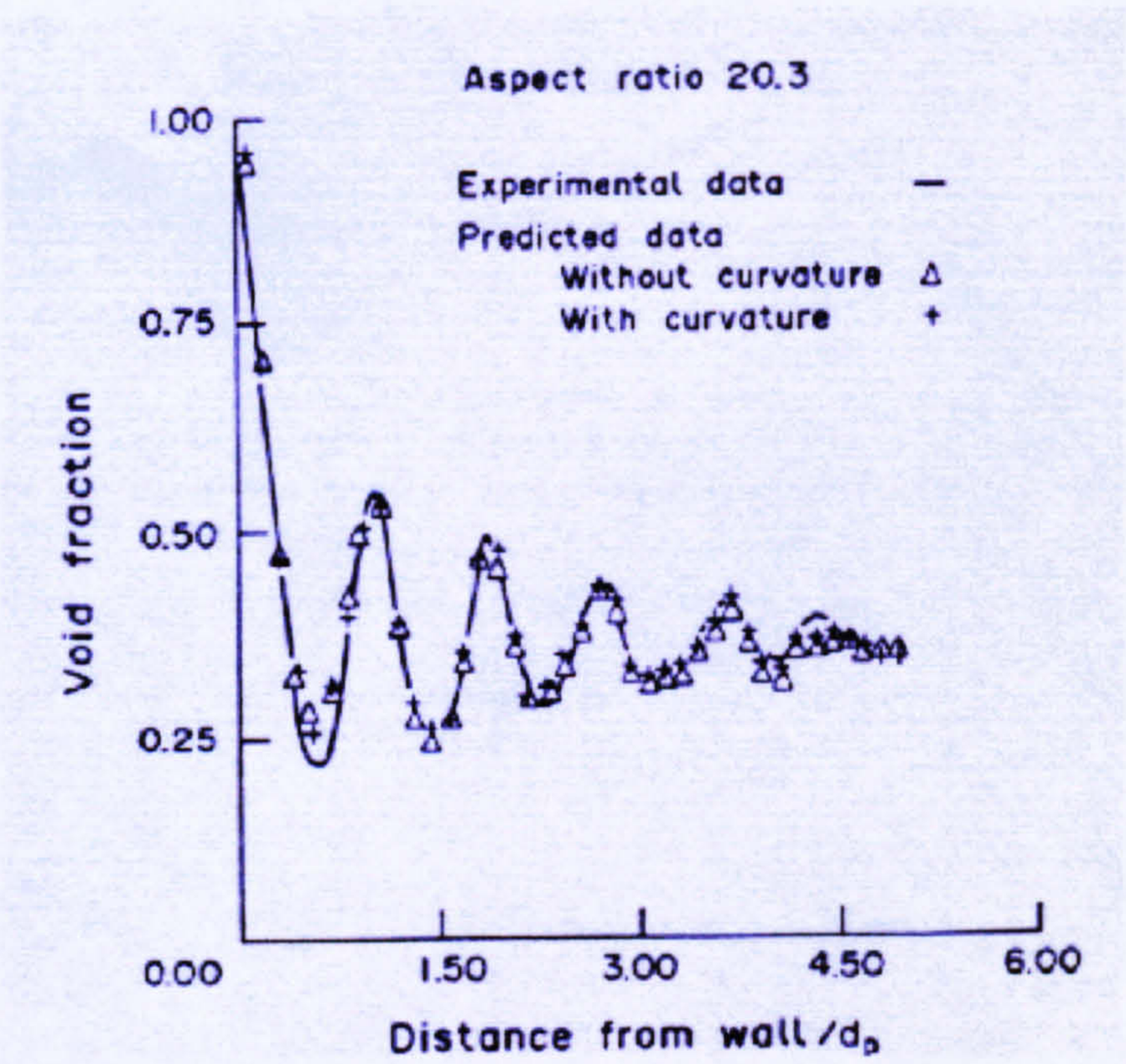

Figure 4.4.1: Comparison of experimental data with a calculated void fraction profile

[Govindarao et al. (1990)]

Due to the representation of the radial variation, essentially the tube is segregated into two regions, a near wall region of one and half times the catalyst particle diameter over which the voidage varies and a centre core of constant voidage. The model was partitioned into these sections to allow variation in mesh requirements matching the variation of the local variables.

Physical Properties

As for the models developed in section 4.1, the same physical property expressions were adopted. Polynomial expressions for the physical properties of the gaseous components in the reformer, including heat capacity, viscosity and conductivity. With an average expression for the heat capacity of the mixture, however, for viscosity and conductivity of the mixture, the expressions by Wilke and Wassiljewa, respectively, were adopted.

Furnace model

Despite the encouraging performance of the "two-zone" model, this approach has not been developed for other styles of furnace arrangement. As the focus of the model development was the assessment of the radial variation in the 'family' of primary steam reformers, the polynomial representation of the heat flux profile discussed in section 4.1 was adopted. Although not the most complicated representation of the furnace, the model delivers reasonable accuracy.

Numerical Solution

The full model of the primary reformer results in a system of differential and algebraic equations, consisting of eighty-five equations per region. The solution techniques applied along the length was a second order orthogonal collocation finite element method with 15 discretisation points. Across the radius, the method of calculating the voidage profile essentially divides the radius into two regions, so the solution techniques applied were both second order orthogonal collocation finite element methods, with 10 discretisation points and 12 discretisation points.

Both scaling and block decomposition were immediately enforced for the primary steam reformer model. Despite the potential difficulties of initialisation of IPDAEs for steady-state systems, highlighted in prior models, a relatively simple approach of initialising with a solution for no radial variation reached a valid solution. This simple approach probably will require a staged implementation for more significant radial variation.

4.4.2 Simulation and Model Validation

The model was validated against industrial data from top-fired and side-fired primary steam reformers within both the ammonia and methanol processes. A typical industrial top-fired steam reformer comprises 8 rows of 44 tubes and 12 m in length and operates at an inlet pressure and temperature of 35.94 bar and 455 oC, respectively. A typical industrial side-fired steam reformer comprises 10 rows of 6 tubes and 12.2 m in length and operates at an inlet pressure and temperature of 22.0 bar and 502.67 oC, respectively. The simulation results are presented in Table 4.4.1 and Table 4.4.2, and clearly show that the simulated data compared well to the industrial data.

Table 4.4.1: Comparison between plant and simulated data for a Top-Fired Primary Steam Reformer

		Plant data	Calculated values	Deviation (%)
Outlet T (K)		1084	1085	-0.05
Outlet P (atm)		32.57	32.56	0.02
ΔP (atm)		2.9	2.91	-0.28
Dry mol %	CH_4	8.1	8.05	0.68
	CO	10.39	10.33	0.58
	CO_2	10.96	11.03	-0.59
	H_2	70.28	70.34	-0.09
	Inerts	0.270	0.268	0.74

Table 4.4.2: Comparison between plant and simulated data for a Side-Fired Primary Steam Reformer

		Plant data	Calculated values	Deviation (%)
Outlet T (K)		1141.3	1141.0	0.029
Outlet P (atm)		20.13	20.12	0.06
ΔP (atm)		1.58	1.59	-0.759
Dry mol %	CH_4	3.01	3.03	-0.522
	CO	14.83	14.82	0.101
	CO_2	8.14	8.15	-0.100
	H_2	73.9	73.89	0.020
	Inerts	0.12	0.121	-1.11

For both these validation sets the radial variation predicted by the simulation was of a similar order, figure 4.4.2.

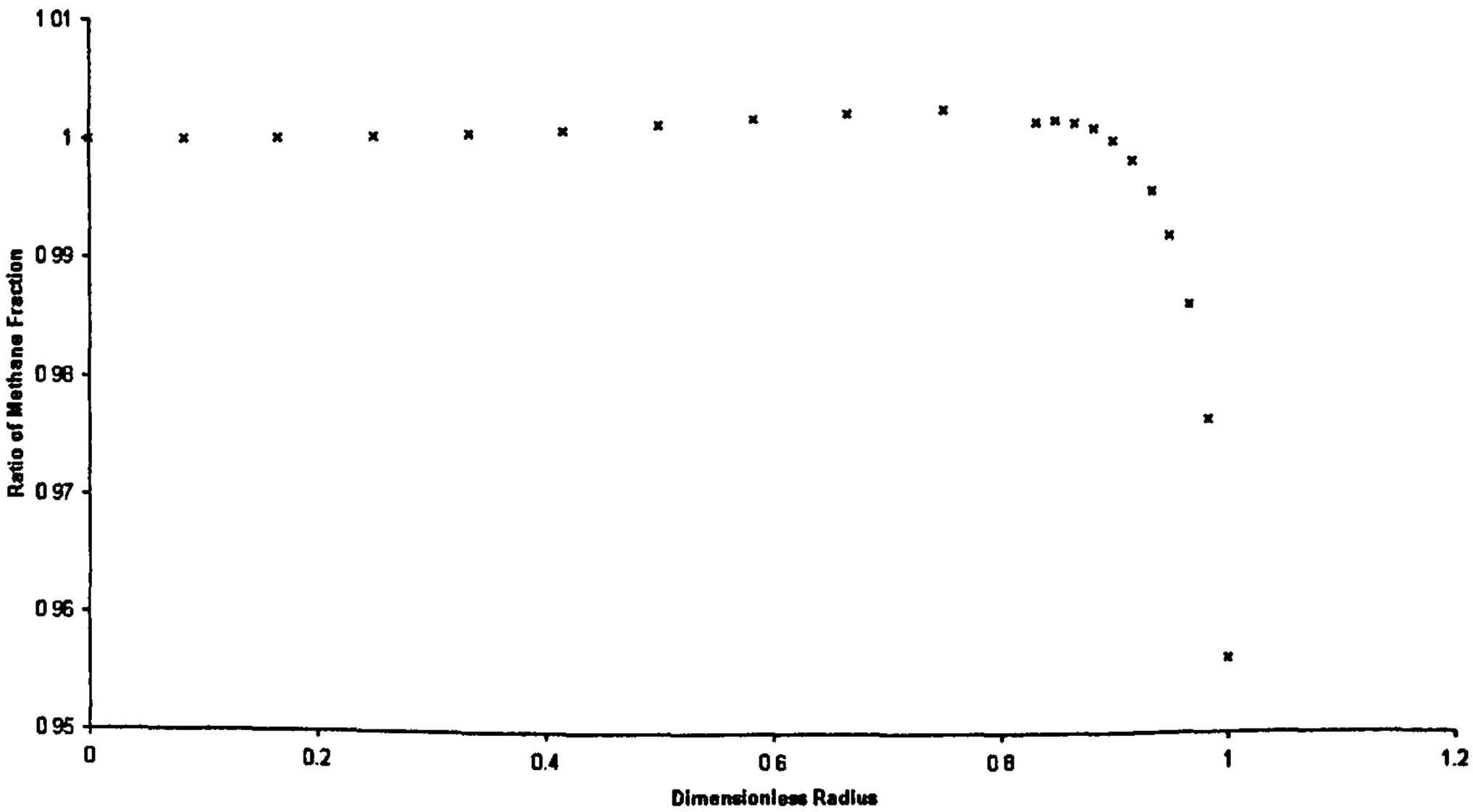

Figure 4.4.2: Radial variation across primary steam reformer tubes

As Bird et al. (2002) hypothesised, clearly the segregation across the radius of the primary steam reformer tubes is limited. Additionally the trend of the profile matches follows those reported by Froment (1990) and Govindarao and Ramrao (1988) amongst others.

4.4.3 Conclusions

Two-dimensional modelling and simulation of primary steam reformers has been carried out using gPROMS. The model demonstrated close agreement to industrial plant data. An assessment of radial parameter expressions and the magnitude of the radial variation in primary steam reformer tubes were completed. Although the trend matched those reported in previously published literature, clearly the radial variation is significantly limited. This study has demonstrated that there is a 'consensus' to the approach of modelling radial variation, despite the discrepancies in the specific equations, and that overlooking the radial variation is a reasonable assumption.

4.5 Three Dimensional Modelling

- DUNN, A.J., MUJTABA I.M. and YUSTOS, J. 2001. Preliminary Optimisation of a Top-Fired Primary Steam Reformer using gPROMS, 2001, *University of Malaya*, Malaysia

The next logical progression in model development is to extend the modelling to a three-dimensional system. Although three-dimensional modelling of chemical reactors in general has only recently become popular, due to advances in computational power,

and the lack of focus on furnace modelling, primary steam reformers have not escaped this development. Unfortunately the 'ideal' of a fully comprehensive three-dimensional coupled simulation of furnaces and reactor tubes has not been reached by models reported previously in published literature.

In this work a three-dimensional model was developed, employing the models reported in sections 4.1 to 4.4 for the tube section of the primary steam reformer. For the furnace additional expressions were appropriated from various literature sources and the previously published modelling attempts.

The aim of this development was twofold, primarily to further assess the "two-zone" approach to the furnace modelling, and from this advance the modelling of the primary steam reformers closer to the fully comprehensive ideal.

4.5.1 Model Description

The model description is partitioned into, the steam reformer tubes model, the furnace model and numerical solution of the model. As primary steam reformers are often geometrically unique, data for one of the top-fired furnaces in the validation set of section 4.1 is used for the model definition. Although only the key equations are discussed in the model description a full listing is included in Appendix 3.

Steam Reformer Tubes

Originally, the concept of this model development was to employ the most accurate expressions, however, during the development it became clear that this approach required compromise to limit the problem size to a manageable form. This limit is fully discussed in the furnace model section.

As the model developed in section 4.1 demonstrated a reasonable level of accuracy, the same expressions were employed, however, the code required converting to suite software differences between packages. By coupling a one-dimensional and a three-dimensional system, the system boundaries become skewed. To overcome this disparity, it was assumed that a geometrically averaged tube wall temperature would suffice as a link between the two systems. The same physical property expressions as for the models developed in section 4.1, were adopted i.e. polynomial expressions for the gaseous components properties and average expressions for the gaseous mixture properties except for viscosity and conductivity.

Furnace model

There are only three previously published papers on primary steam reformer furnace modelling, Roesler (1967), Plehiers and Froment (1989) and Cotton (1999), so research from other systems was drawn upon. The most comprehensive furnace modelling in published literature was reported by Detemmerman and Froment (1998) and is used as a basis for this model.

As was discussed in Chapter 1, at the core of modelling with computational fluid dynamics is an acceptance of the fundamental that an essentially chaotic process can be represented by a set of mathematical expressions. In recent years this form of modelling has gained approval and has matured from purely qualitative to an increasingly quantitative basis, as its use has become more widespread. As was highlighted in chapter 1, new approaches have been developed to simulate the turbulent phenomena, however, these methods remain unproven for a reactive flow system such as in the furnace. As the most validated, the time-averaged approach was adopted for the simulation; specifically Chen's κ–ε model [Computational Dynamics (1998a)]. Throughout the references studied, consistently for reactive flow simulations, similar κ–ε expressions were employed. Additionally, the simulation results were found to vary insignificantly for a series of alternative κ–ε models.

There is no ideal approach to flame simulation, with amongst others, both main reaction simulation techniques highlighted in chapter 1 being considered to give a reasonable accuracy for furnace burners. In fact each of the reported steam reformer simulations used a different approach, but none included the complexities of the interaction of the flow and reaction, either using assumed flow patterns or overlooking the reaction modelling. The only common 'best practice' for flame simulations is the simplification of the chemical reaction scheme from the full component inclusion,

$$O + H_2O \rightarrow OH + OH$$

$$CO + OH \rightarrow CO_2 + H$$

$$CO + O_2 \rightarrow CO_2 + O$$

$$H_2O + O_2 \rightarrow HO_2 + OH$$

$$H + O_2 \rightarrow OH + O$$

$$H_2O + M \rightarrow H + OH + M$$

$$H + O_2 + M \rightarrow HO_2 + M$$

to a more general consideration,

$$CO + \tfrac{1}{2} O_2 \rightarrow CO_2$$

By limiting the number of components, the simulation size is made more manageable. With such a limited chemical reaction scheme employed as part of a probability distribution function model, Libby and Williams (1994) report that for a simulation "mean properties of the such flames can be predicted with reasonable accuracy". Hence the same approach was adopted for this simulation. The complex issue of the representation of reactive flow will be discussed in depth in chapter 5.

In contrast to the chemical reaction representation, there is some commonality in thermal radiation with most authors basing their simulations on the zonal approach of Hottel and Sarofim (1967). For this simulation the 'Discrete transfer method' of Lockwood and Shah (1981) is employed to account for the radiation in the participating media. Additionally, as for Plehiers and Froment (1989) and Detemmerman and Froment (1998), the radiation properties are represented by correlations from a radiation band model, however, the model by Grosshandler (1993) is employed. Despite this agreement, fundamentally thermal radiation and chemical reaction do share common issues; the prediction of physical parameters for both have inherent difficulties, such as surface polishing or catalyst tortuosity, and incorrect representation of these parameters

can lead to outrageous errors. As for chemical reaction 'best practice' is usually developed from trial and error either on the same or similar systems, it just so happens that the Hottel and Saforim (1967) zonal approach appears to perform well for several systems.

Thermal conduction from the furnace is calculated using thermal conductivity data from Perry's (2000) and Beaton (1989). For the air surrounding the furnace an average air temperature of 20 °C was assumed to allow calculation of the thermal losses through the furnace walls; and the effect of inspection holes was ignored.

Apart from the radiation properties, the same physical property expressions as for the steam reformer tubes were adopted i.e. polynomial expressions for the gaseous components properties and average expressions for the gaseous mixture properties except for viscosity and conductivity. However, as is discussed later the full expressions for all the physical properties including the radiation properties are introduced in stages within 'operational envelopes' to limit the chances of destabilising the solution.

Numerical Solution

As for the other primary steam reformer models discussed in section 4.1, numerical solution required careful consideration and reassessment throughout the development of the various meshing versions. Alternatively to the previously discussed models, the StarCD computational fluid dynamic simulation package was employed in the full furnace simulations.

The StarCD package offers several features for simulation including, a mesh generation platform, a number of coded routines of various physical phenomena and physical properties and a range of numerical solution methods for discretisation and some specific to the phenomena modelled in the system. The architecture of StarCD is of a set of core compiled blocks, which allow only parametric adjustment, linked to a number of optional sub-routines coded by the user, which can supersede some of these core blocks. Often computational fluid dynamics packages such as StarCD are deemed by purists to be 'dumbing down' computational simulation as the format in which they are presented allows a quick solution to be attained with only limited consideration of modelling issues, however, for the proficient user they avoid 'reinventing the wheel'.

Despite some of the arsenal of numerical techniques discussed for the models in section 4.1 being incorporated into the package as 'best practice', such as scaling and block decomposition, the inclusion of three dimensional fluid flow simulation significantly increases the complexity of the numerical solution issues.

As highlighted in chapter 1, the finite volume approach is employed almost universally for CFD, for which the governing model equations are integrated over all the finite volumes of the system, this integral form is then converted to an algebraic form by discretisation and then this set of equations are then solved iteratively.

There are several techniques for discretisation, however for systems such as the primary reformer furnace, with both convection and diffusion, the technique must exhibit "conservativeness, boundedness and transportiveness to give physically realistic results and stable iterative solutions" [Versteeg & Malalasekera (1995)]. Additionally, the

schemes can suffer from what Versteeg & Malalasekera term as "false diffusion" when the direction of flow is not aligned to the mesh. In order to combat these failings initially the tactic has been to blend the two approaches, however, more recently the trend has been to develop higher order discretisation schemes such as QUICK and MARS [Computational Dynamics (1998b)]; there only failing being a potential lack of numerical solution stability.

As for discretisation the approaches for the solution algorithms have also evolved with their increased employment. Essentially the same predictor-corrector approach is still employed, which starts with a guessed initial pressure field, the discretised momentum equations are then solved, the pressure and velocities are then corrected through the associated corrections equations for the technique, all other transport equations are solved and convergence is checked for based on residual error calculations. There are a number of techniques available for the solution of the discretised equations but as for most packages the conjugate gradient technique is used by StarCD. The two main types of the solution algorithms are SIMPLE and PISO, the main difference being that the correction stage has two steps for the PISO algorithm. There remains some debate, as to which approach offers greater performance, however, the StarCD manufacturers recommend their SIMPISO version of the PISO algorithm for systems such as the primary steam reformer. For all solution algorithms, under-relaxation is required to ensure numerical stability of the solution, the magnitude of which must be determined by the user; under-relaxation controls the stability by blending the corrected variables on a percentage basis with the initial guess for the pressure and their values from the previous iteration for the velocities.

As is clear from this discussion there are a significant number of options that remain with the user of the computational fluid dynamics packages, although often the packages have values which are preset, these are usually there purely so a value exists in the field and often these values require redefinition. Some of these settings are set on a basis of accuracy and some require tailoring to the initialisation strategy as discussed later in this section i.e. sometimes it is better to start of with the less complicated but more stable approach.

While the amount of discussion of initialisation techniques in published literature, for the model types described earlier in section 4.1, can be described at best as limited the discussion for computational fluid dynamic modelling is even more sparse. This tendency is probably due to the fact that for most packages one of the core compiled blocks is an initialisation routine and this presumably achieves the demands of most authors. The ideology behind the pre-prescribed techniques used in commercial computational fluid dynamics packages is a predictor-corrector approach employing pressure field initialisation. As for the previous models described in section 4.1, a more considered approach was required, which followed the same principle of gradual introduction i.e. limiting for each stage of initialisation the impact on the values of each variable, so that the values remain realistic or are realistic in a model system which is using staged factorial increases.

For each of the mesh arrangements employed a common approach was found for initialising the flow field analysis. Firstly the model was solved with the SIMPLE solution technique and upwind differencing as these were found to be the most 'forgiving' or successful in achieving convergence; Jang (1985) also observed the

robustness of the SIMPLE technique when compared to other predictor-corrector routines. These results were then employed to initialise the next stage with the improved approaches of SIMPISO and higher order discretisation. Although a flow field was solved within the reformer tubes, as this system at this stage was not coupled to the external tube flow field, no consideration was given to its accuracy.

The introduction of the other physical phenomena is the area of initialisation that requires more consideration, as the approach of the pre-prescribed compiled routines appears to be only, to solve the variables associated with the flow-field analysis for a fixed number of iterations and then introduce all the other variables into the system, independent to the progress towards convergence. The philosophy for this approach presumes that a partially solved flow-field will be sufficient to initialise the other variables, however, for complex systems quite often the flow-field is far from approaching convergence when these other variables are introduced and this will often lead to divergence. The solution of the heat balance is the most sensitive to this fixed term introduction approach as the heat balance is strongly coupled to the local flow-field variables and chemical composition; particularly if chemical reaction is involved. If thermal radiation is included this coupling is further complicated as it escalates the number of variables linked to the each temperature value. Physically this means both the range of temperature can be quite large and its profile can be quite intricate.

For the primary steam reformer system the same logical principle of gradual introduction, demonstrated earlier in section 4.1, was followed with the results from the previous step employed as the initialisation data for the next step. The most robust approach to initialisation, shown earlier in section 4.1, followed the principle of

employing the key system variables i.e. velocity, temperature and chemical composition, without decoupling the system definition and then gradually introducing the effect of the relevant physical phenomena i.e. reaction rate.

Initially the model was solved as for the first step of the flow-field simulation, however, a heat balance was included with convection and conduction across the reformer tubes. The more accurate flow-field definition was introduced at the next step with the correct flow-field definition within the steam reformer tubes. Then to complete the inclusion of the key system variables, the next step is to introduce the chemical components but without chemical reaction. Once the key variables are linked, the choice is then of which physical phenomena to introduce. The reformer tube system was side lined to be resolved after the furnace, as the furnace system is more complex, the impact of gradually introducing the reformer tube system at this point will be limited and the flexibility of the user defined coding for the reformer tube section caters for this staged introduction.

Due to the sensitivity of the heat balance particularly the radiant term, the combustion reactions were introduced next, followed by thermal radiation over a number of steps. Initially, the radiation expressions were defined without the effect of a participating media between the radiating surfaces, then with participating media of constant radiation properties and finally with fully calculated radiation properties from a user coded routine. To reduce the chances of destabilising the solution, the radiation properties were set an 'operational envelope' which was calculated as the maximum possible range of these parameters for this system, outside of which the routine adopted the previously employed constant properties; this could also be considered as a form of

filtering. Unlike the previous models defined in section 4.1, as the software package does not allow as much control on decoupling system equations, instead of factoring in these equations some of the physical properties, density, conductivity, specific heat and molecular viscosity, were gradually introduced to assist the initialisation of the model. Initially the properties were assumed constant across the system definition, then for the next step they were calculated on a component concentration basis and finally as for the radiation properties they were fully calculated to allow for variation with temperature, pressure and composition via a user coded routine with 'operational envelopes' to limit the chances of destabilising the solution.

With the flexibility of user defined coding for the reformer tube system, the same approach of initialisation was possible as for the model defined in section 4.1 i.e. de-coupling the heat balance and pressure profile equations. As the external steam reformer tube temperature is the sole link between the reformer tube and the furnace systems, a precautionary step was included, before the previously defined stages, of averaging the wall temperature calculated by the model with measured profiles; essentially staggering the heat sink effect of the reformer tubes.

The fundamentals behind this logical approach to initialisation are vindicated by the fact that the general stages of initialisation are applicable to the further computational fluid dynamics simulations of a notably different system discussed in section 4.2. As these systems are different, so the impacts of each general stage will vary in magnitude, hence some stages are required to be split into small steps. The requirements for splitting into steps are found by trial and error, but once defined even for widely varying boundary definitions the same steps can be employed.

Unfortunately, these stages are not totally 'portable' to any computational fluid dynamic simulation, however, from the experience gathered in this research, the only change required is that for some systems the complexity of the flow-field system has to be initially simplified, such as by adjusting the boundary definitions, up to the stage were either all the key variables are included or once all the physical phenomena are included. This boundary condition adjustment simplifies the complexity of the flow-field by reducing the turbulence and hence the amount of mixing; diminishing the effect of recirculation patterns, jet interactions etc., with the effect of ultimately approaching laminar conditions.

Once achieved, the integrity of the solution comes into question. As indicated earlier in chapter 1 and section 4.5.1, this is a key issue in the world of computational fluid dynamics, with probably more prominence than for other modelling types due to the diversity between the 'simple' colourful nature of the results and the complexities behind achieving those results. Apart from the challenge for justifying the system of model equations and associated boundary conditions, the issue of whether the achieved solution for these equations is influenced by the number of variables employed still remains unanswered. This solution influence is generally termed as 'mesh independence' and does not consider the relevance of the model theory.

The ideology of mesh independence is to reach a solution from the system of equations and boundaries that is not affected by changes to the mesh structure employed for the system i.e. increasing the number of discretisation points. The traditional approach developed for one- and two-dimensional modelling was to double the mesh density until the results did not change significantly. Due to the convenience, this practice was adopted for the three-dimensional modelling in computational fluid dynamics, however, as more geometrically complicated systems have been modelled other approaches have been considered as the doubling will exponentially increase the solution time.

As was demonstrated in chapter 1 for the same system definition and the same number of cells, but only differing cell distribution, considerably different results of diverging accuracy can be obtained. This efficient employment of the cell resources can be based around the calculation of error estimation as demonstrated in chapter 1. This minimisation of error can be automated as part of the simulation package, however, this option was unavailable for the package employed for this research, so rather than updating the structure after each iteration instead after the simulation had solved the truncation error was estimated for each cell and the top twenty percent were refined. This process of refining was repeated either until the maximum number of cells that could be solved within the computational hardware constraints was reached or the error reached an insignificant level.

Several authors argue that fundamentally 'mesh independence' is an ideal that is unachievable. Although the technical argument behind this opinion is quite strong, on a practical level this offers no justice for simulation; "Of two evils, the less is always to be chosen (Thomas à Kempis)". Additionally the error due to meshing must be considered against all other sources of error in the simulation. The error estimation approach is more scientific than the rule of thumb approach and will guarantee, particularly for complex geometries or flow patterns that for an equal number of cells the error estimation method will yield a more accurate result.

4.5.2 Simulation and Model Validation

The basis for the simulation was an ammonia reformer, the same as used in "two-zone" work. All the geometrical detail was taken from that steam reformer, including the details of exact location of coffin inlets.

As was discussed in the model definition in section 4.5.1, Cotton (1999) is the only previously published model of a primary reformer furnace with flow field analysis. The initial work for the model development was aimed at assessing the system definition of Cotton (1999), specifically the outlet and repeating structure definitions, see figure 4.5.1. Followed by an analysis of the methods of representation of the physical phenomena, discussed in section 4.5.1, to ultimately develop a fully comprehensive model.

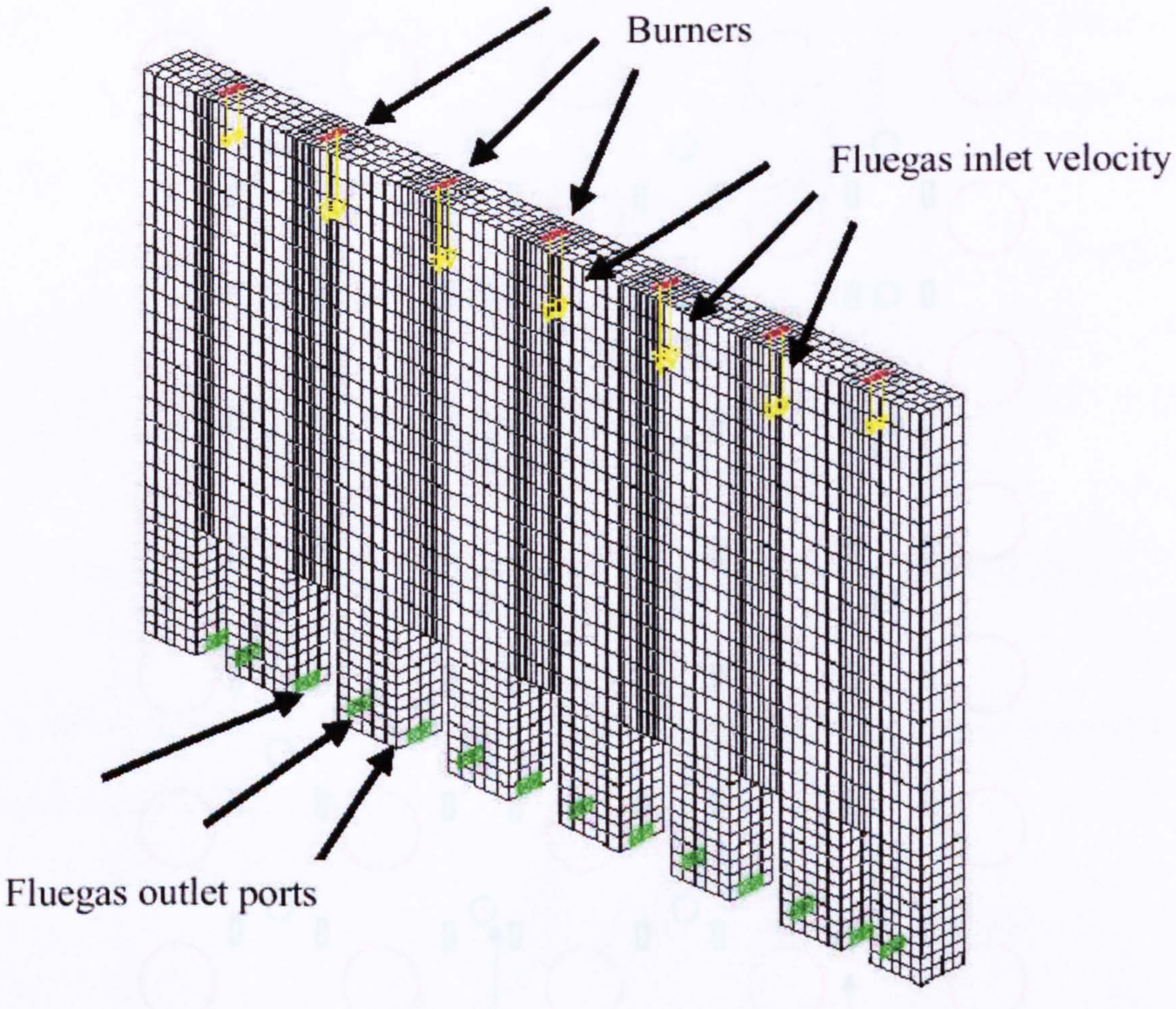

Figure 4.5.1: System definition (Cotton, 1999)

Taking a literal view of repeating patterns only one exact pattern exists in the furnace, that of a quartered section, particularly as the coffin inlets are not strictly positioned to align to the tube positioning, but are literally brick walls with a blank left every few bricks. This is demonstrated in figure 4.5.2 which shows the extremes of the pattern compared to those assumed by Cotton (1999).

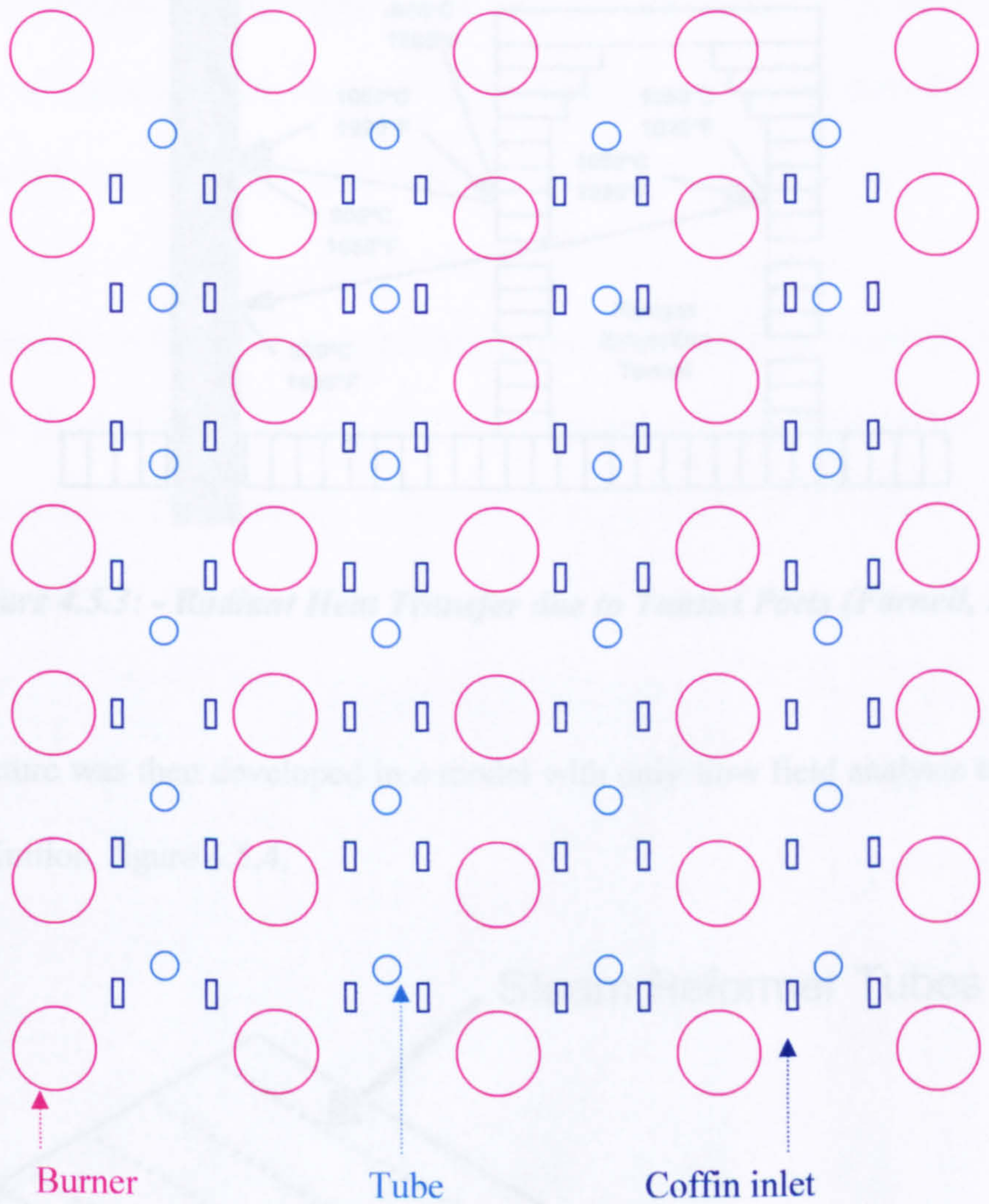

Figure 4.5.2: Overhead plot of Top-fired Primary Steam Reformer

Additionally the system by Cotton (1999) also overlooks the full coffin structure, presumably as the focus of the study was flow field analysis in the furnace. However, Farnell (1999) demonstrates that the coffin network must be included in simulations considering heat transfer as the internal coffin temperature radiates back onto the tube hence increasing the local wall temperatures; termed as the 'tunnel port effect', see figure 4.5.3.

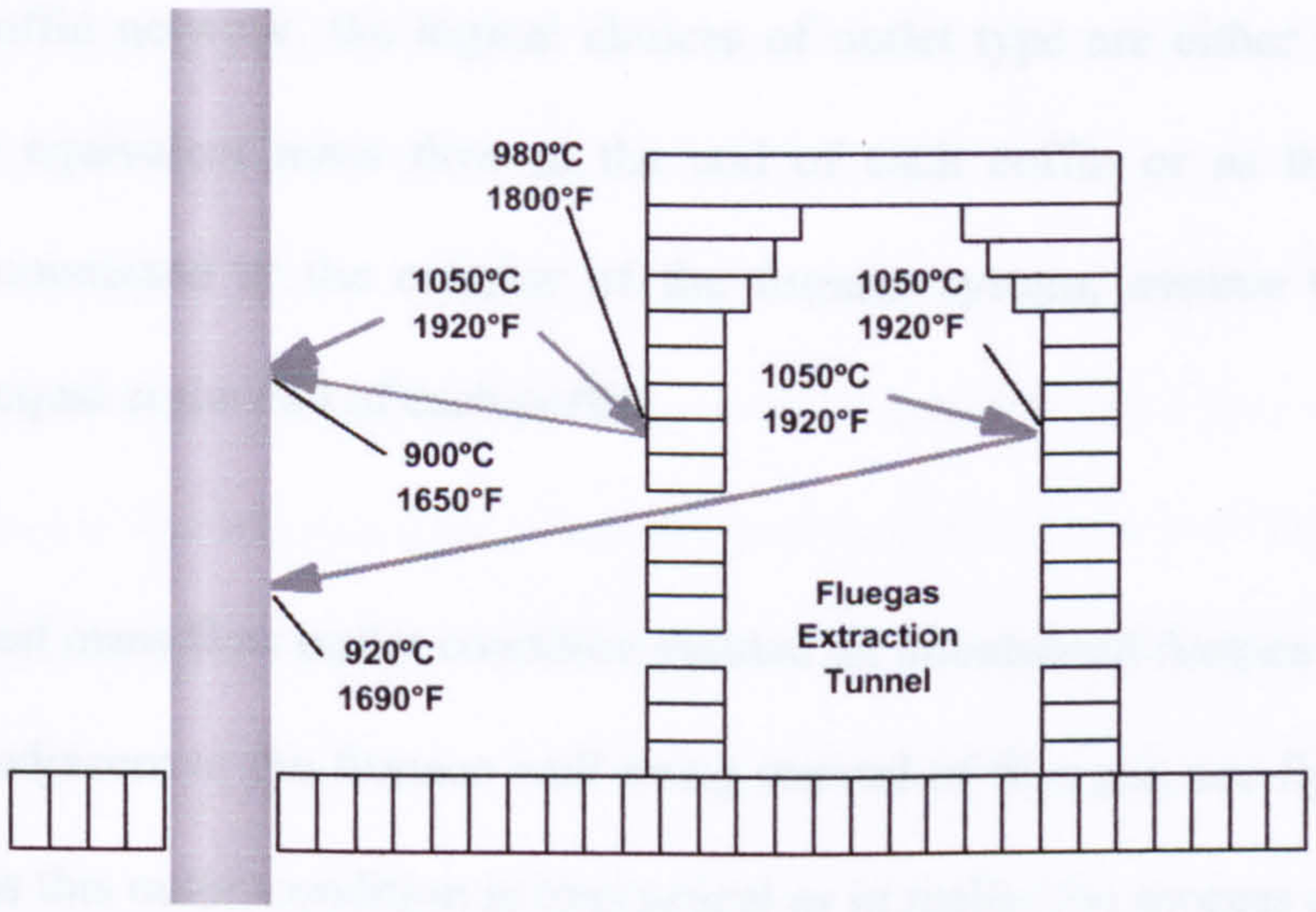

Figure 4.5.3: - Radiant Heat Transfer due to Tunnel Ports (Farnell, 1999)

This structure was then developed in a model with only flow field analysis to assess the outlet definition, figure 4.5.4.

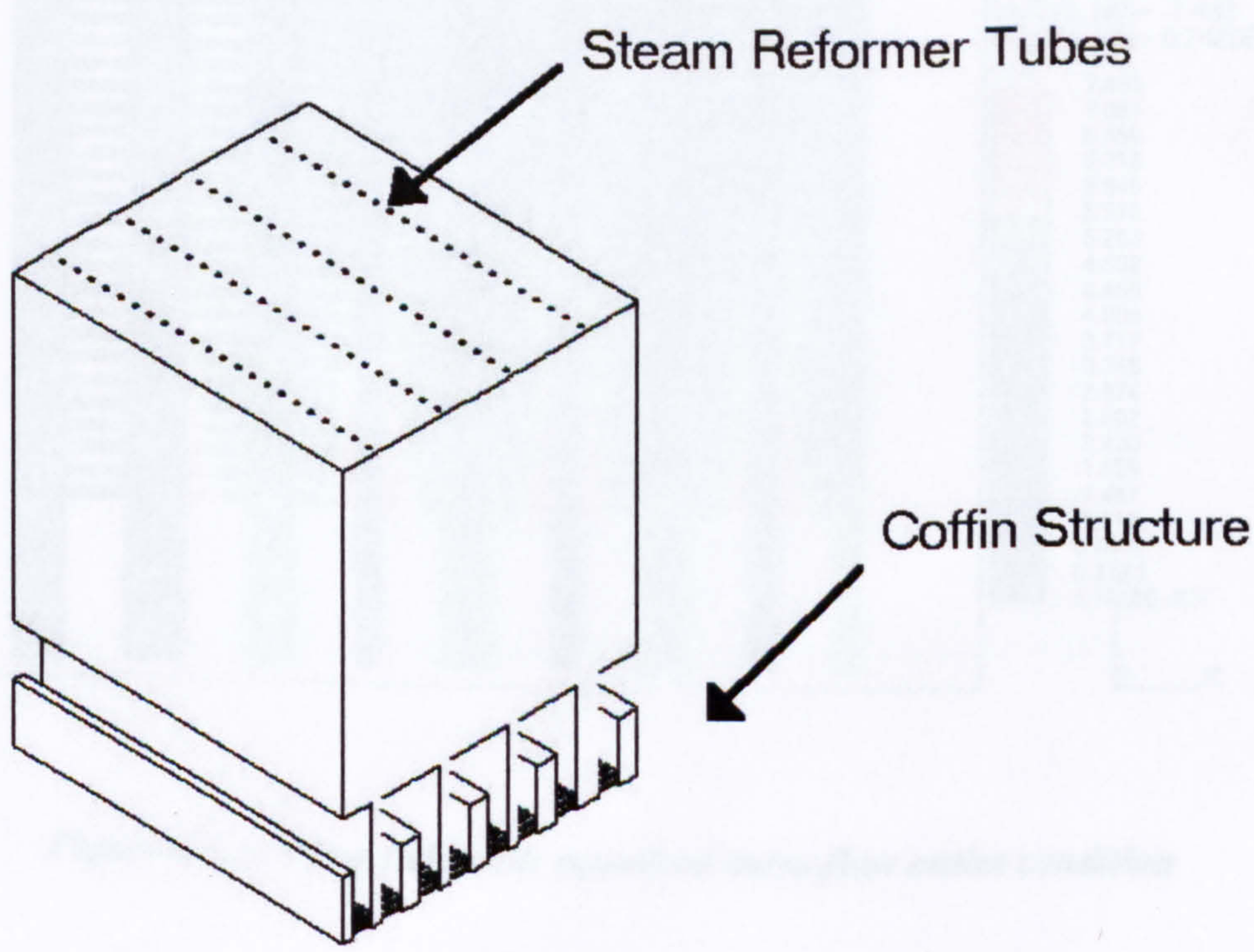

Figure 4.5.4: Model Structure - Quartered section of Top-fired Primary Steam Reformer

With the coffin network, the logical choices of outlet type are either to presume that there is an equivalent mass flow at the end of each coffin or as these coffins are ultimately connected at the exterior of the furnace system, assume that the system pressure is equal at the end of each coffin.

The equalised mass flow outlet condition yielded an imbalanced furnace flow-field with the coffins adjacent to the furnace wall being starved of flue gas, see figure 4.5.5. This result proves this outlet condition is impractical as in reality the process conditions yield a well balanced furnace.

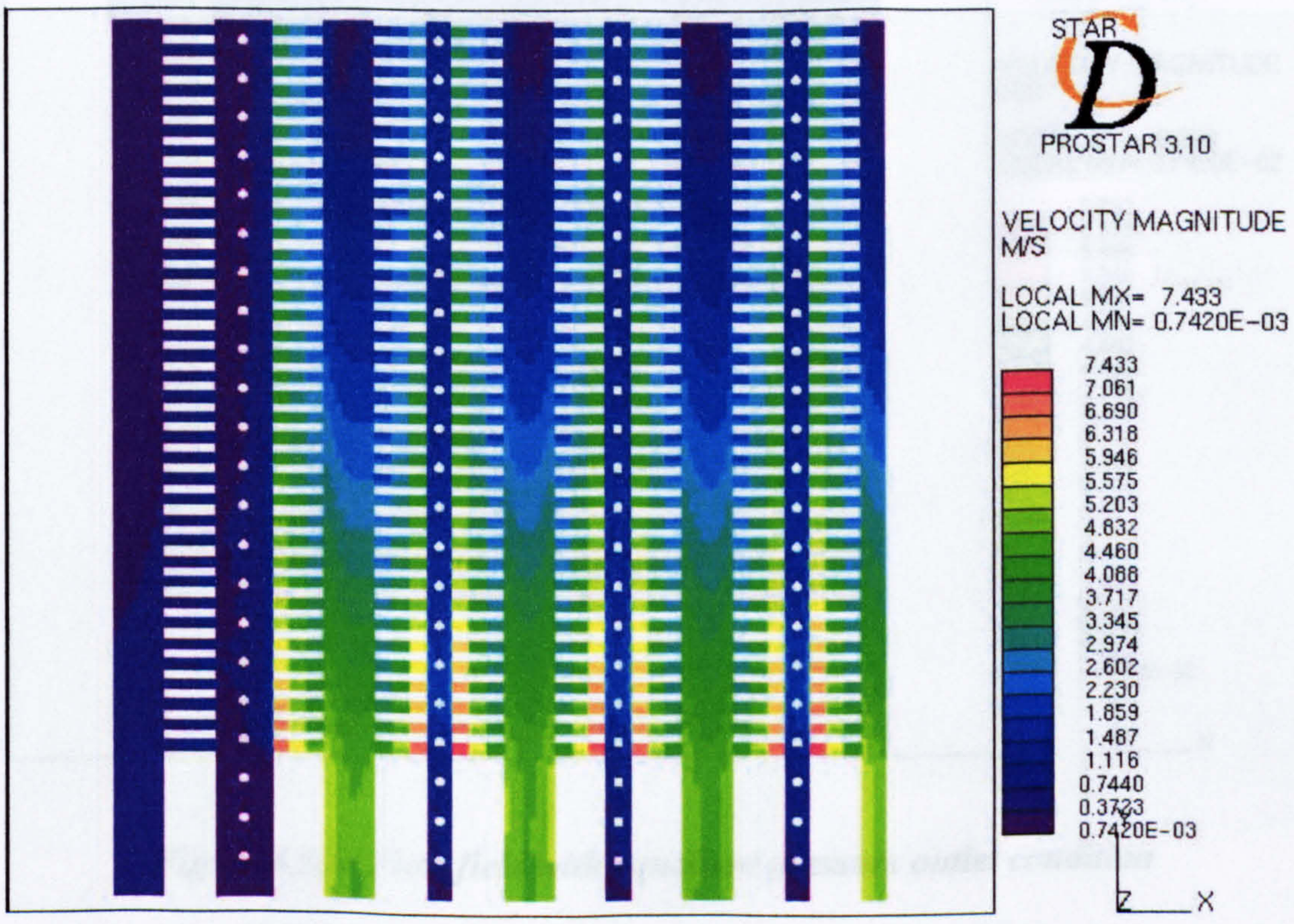

Figure 4.5.5: Flow field with equalised mass-flow outlet condition

The equalised pressure outlet condition yielded a balanced furnace flow-field, see figure 4.5.6, with the coffins adjacent to the furnace wall seeing slightly more flue gas than the internal coffins. These differences in the flue gas rates are purely due to the variation in the burner / coffin arrangement between the area adjacent to the furnace wall and the central furnace i.e. there is one row of burners positioned over each coffin but the coffin adjacent to the wall has only one set of inlets from the furnace while those in the centre have two.

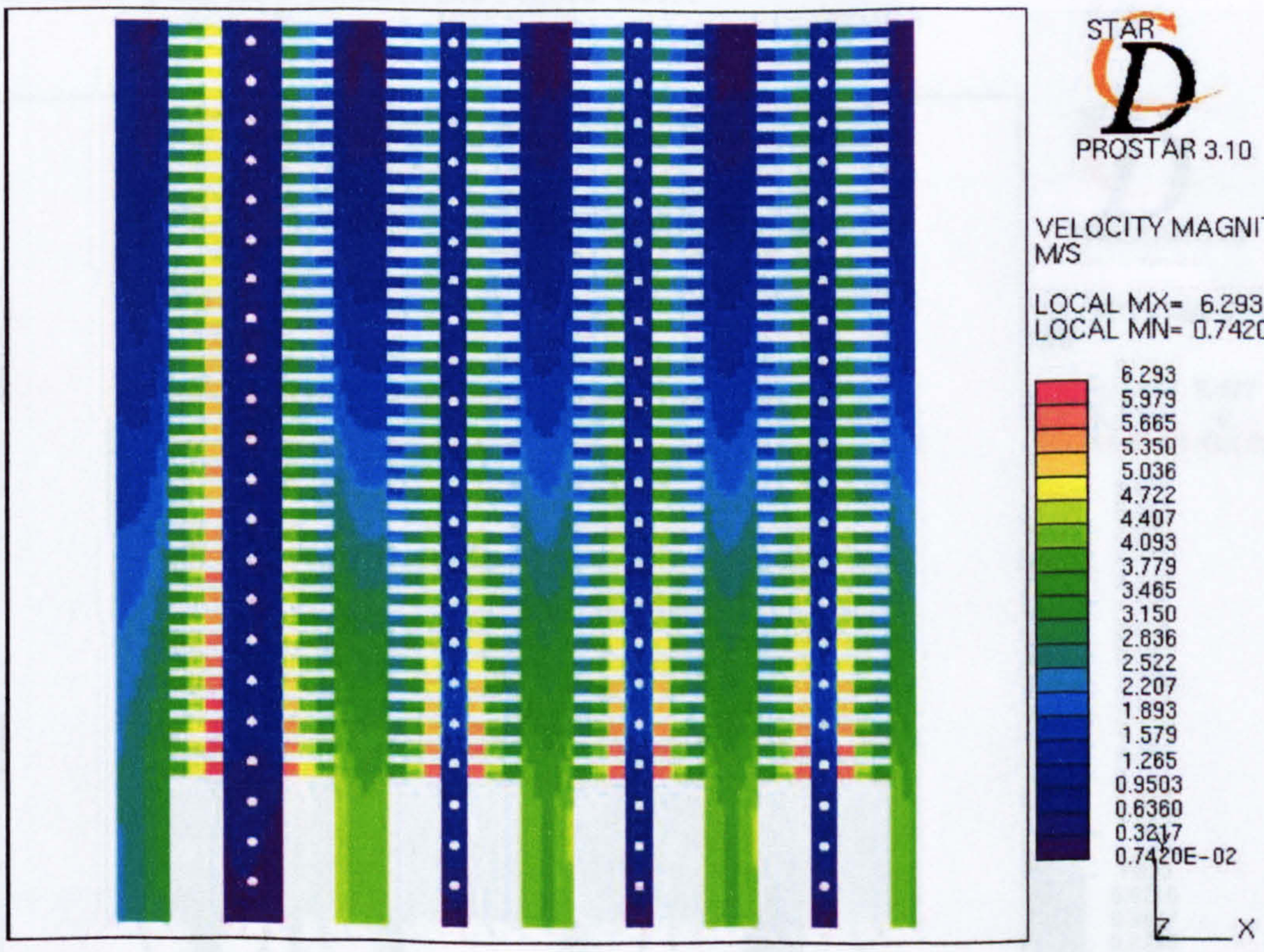

Figure 4.5.6: Flow field with equalised pressure outlet condition

Notably, even though the outlet type employed in Cotton (1999) is unclear for the chosen location by Cotton (1999), of the inlet to the coffin network, neither an equalised mass flow nor a pressure definition would yield a 'true' flow pattern.

As further evidence of the suitability of the boundary definitions employed for the flow analysis model, the burner rates were adjusted in a form of sensitivity analysis. The original flow-field was well balanced with all the flue gas predominately following the 'idealised' plug flow pattern, see Figure 4.5.7.

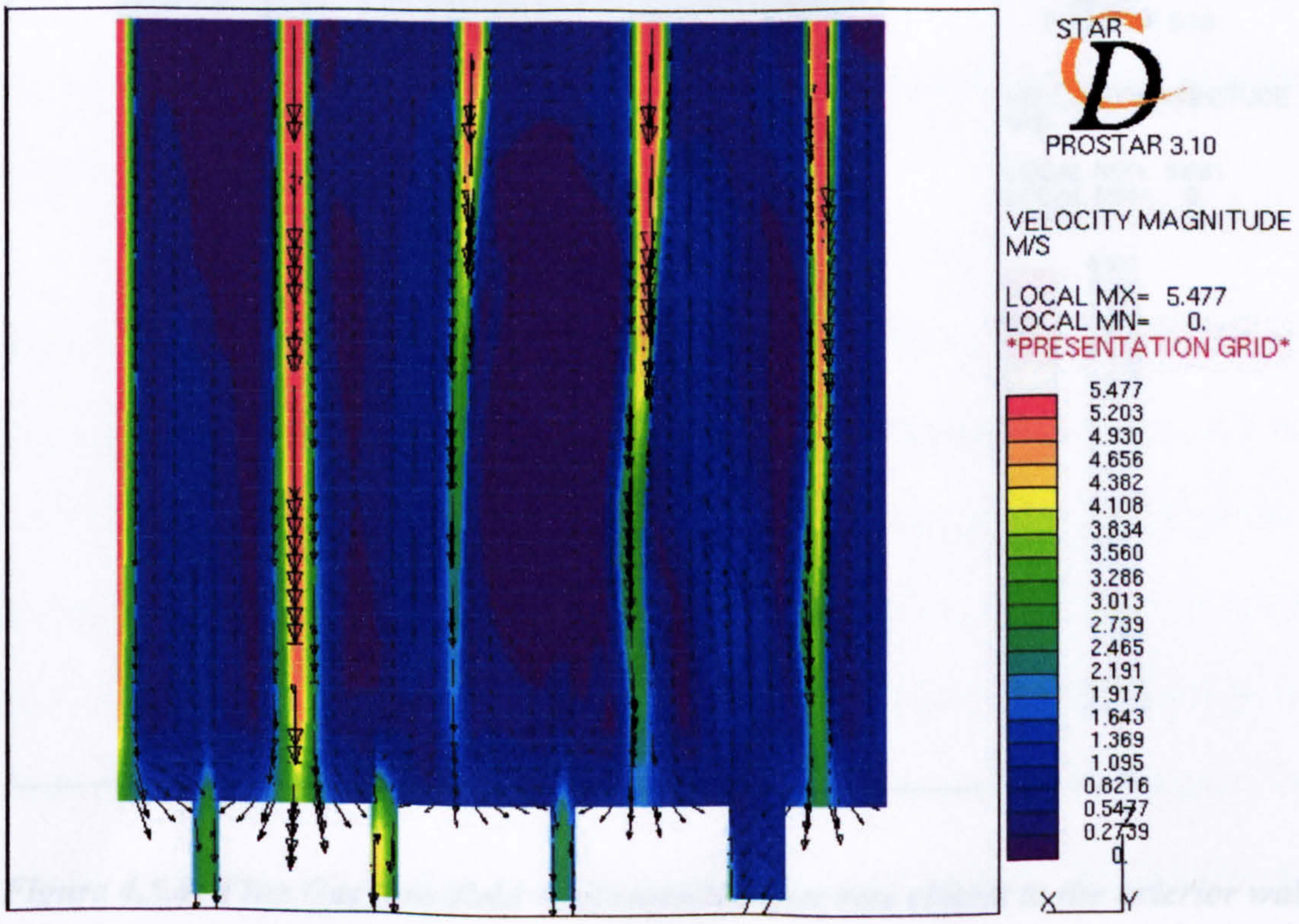

Figure 4.5.7: Flue Gas flow-field – design conditions

For the five percent increase in the burner flow rate for the burner closest to the exterior wall, clearly the effect was dramatic, see figure 4.5.8. The flow pattern has 'flipped' from a balanced plug-flow to a turbulent pattern with only a limited change in the burner rate. Adjustment of the burner rates has created a significant momentum imbalance in the furnace flow field, displayed by the large area of recirculation adjacent to the furnace wall.

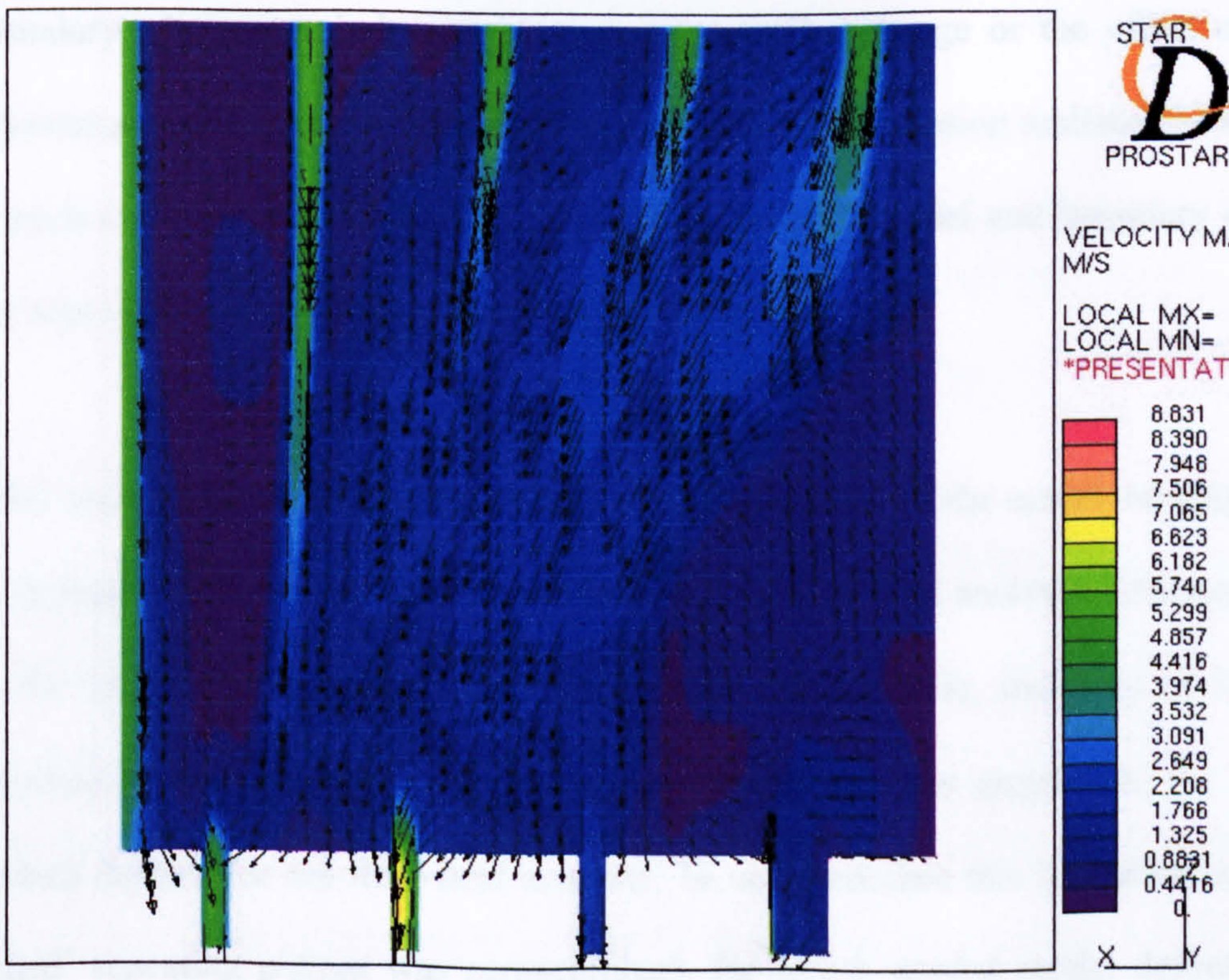

Figure 4.5.8: Flue Gas flow-field – increased burner rate closest to the exterior wall

Although, this affect may seem excessive, it concurs with the observations of the field trial reported by Cotton (1999) on a similar style of steam reformer furnace. The multiple jet interactions which define the furnace flow field yield this phenomena, with each burner essentially countering the effect of each other, see figure 4.5.7.

This technique of boundary sensitivity analysis is another method of validating the performance of both the boundary and model definitions, as quite often the affect of a boundary adjustment is known such as for an inlet change or the effect of such an adjustment can be argued from first principals. If the simulation realistically reflects the boundary change then it can be inferred that the both model and boundary definitions are representative and the linkage between them is correct.

After assessment of the system definition, the next stage of the model development was to include other physical phenomena than just the flow field analysis. Unfortunately due to the limitations of the computational equipment available, inclusion of all relevant physical phenomena for the primary steam reformers was impossible for the model system defined for the flow-field analysis. To accommodate this limitation, initially the 'ideal' repeating pattern was compromised, for which several model definitions were assessed, and then the number of cells in the mesh were reduced. Realistically the minimum repeating pattern that can be considered is of a width of two tubes, see figure 4.5.9, as unlike the system defined by Cotton (1999) each tube is not located in line with a coffin inlet, however, the coffin inlets have to be adjusted by a distance of 45 cm for the minimum pattern. With this minimum pattern and approximately a 20% reduction in the number of cells, the computational equipment was capable of performing the simulation calculations.

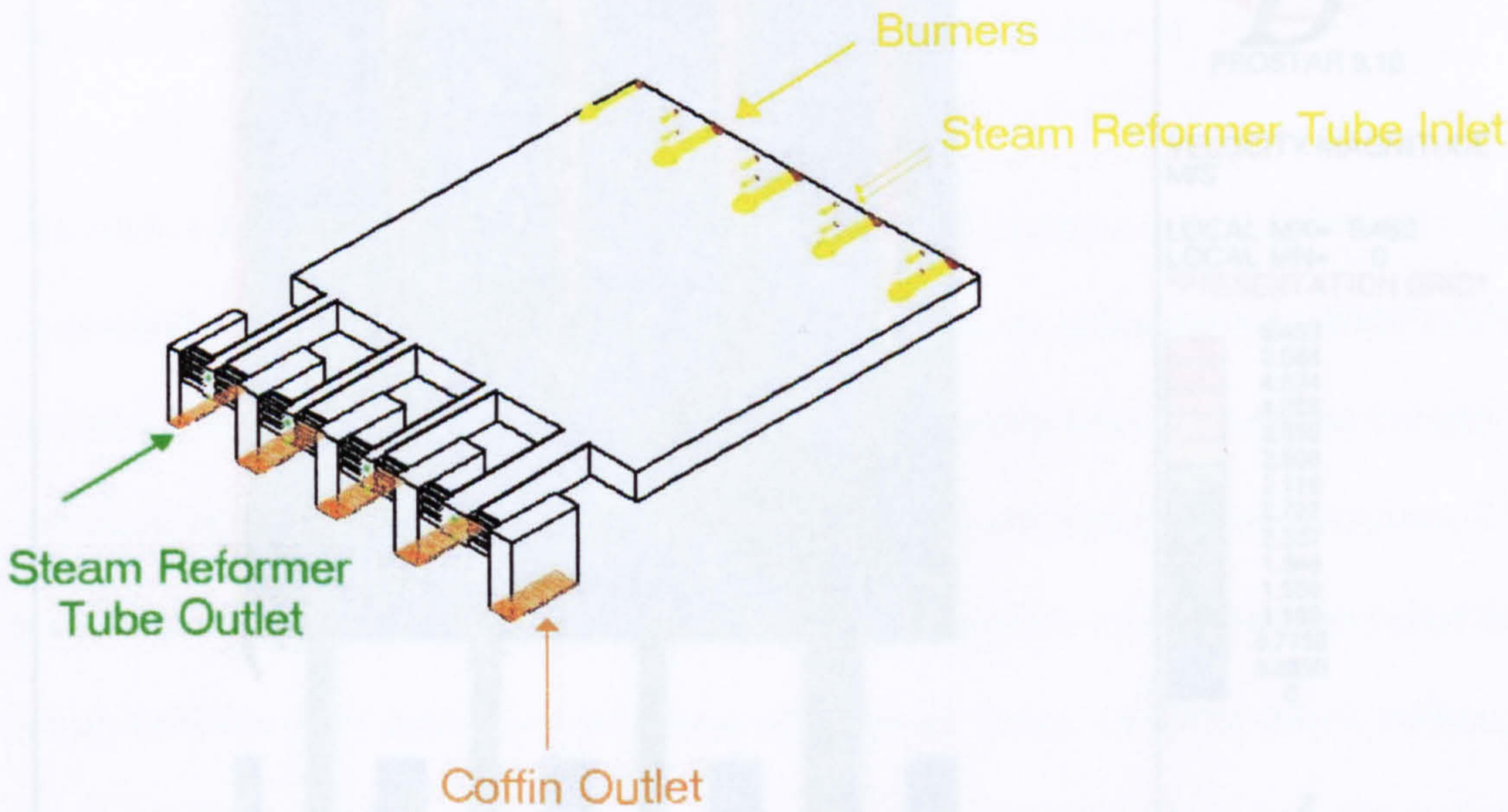

Figure 4.5.9: Model Structure - Minimum repeating pattern of Top-fired Primary Steam Reformer

However, the simulation results achieved with this model definition were unsatisfactory, as not only were the observed temperature profiles along the tube lengths not achieved but also the variation of the temperatures amongst the tubes was significantly greater than reality. Both these observations seemed to represent a furnace flow-field imbalance and this was discovered on analysis of the flow-field results, see figure 4.5.10

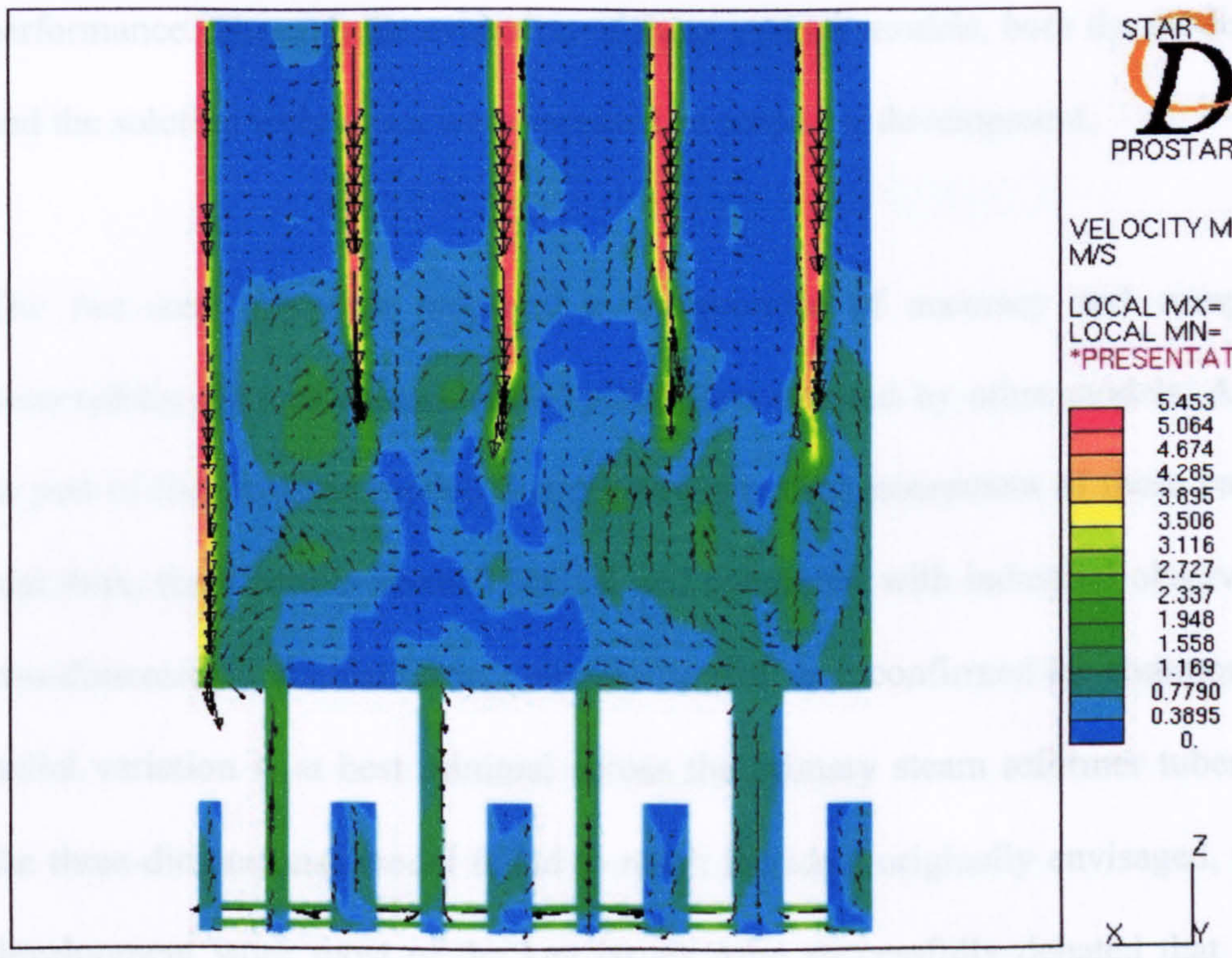

Figure 4.5.10: flow-field results

This imbalance is not due to failings in the model definition, as the same model definition produced a balanced flow-field, but the reduction in the number of cells has led to the simulation not fully converging, which is represented by the error in the simulation results. Ultimately these results reflect the "Catch 22" of creating a manageable mesh that would solve for computational equipment available and achieve a result that would reflect measured observations.

4.5.3 Conclusions

Although the primary steam reformer is a not a simplistic system, reasonably close agreement to industrial data for the overall process was achieved at various levels of modelling complexity; sensitivity analysis on these models also yielded sensible

performance. Through the evolution of these various models, both the model definition and the solution techniques were assessed as scope for development.

The two-zone approach proposed a compromise of accuracy and complexity that successfully allowed assessment of parameters ignored by other models. Additionally, as part of the dynamic model, this allowed practical assessment of these parameters in real time; these results seemed logical and concurred with industrial observations. The two-dimensional simulation was also successful, as it confirmed the common belief that radial variation is at best minimal across the primary steam reformer tubes. Although the three-dimensional model failed to reach the ideal originally envisaged, through the development work most of the key issues were successfully debated that will appear when logistical constraints are removed. Overall the development of these primary steam reformer models, highlighted such modelling topics as initialisation, numerical solvers, mesh sensitivity, scaling of variables and model partition amongst others.

Throughout these models, the clear focus of improvement, in terms of both accuracy and understanding of the process, was the inter-linking of the furnace and the reactor tubes, which is close to being achieved. Aside from furnace modelling development the next improvement should be to tackle the issues of the heavier hydrocarbons than methane that exist in 'industrial quality methane' and carbon depositions.

Chapter 5

Secondary Steam Reformers

For secondary steam reformers, due to the similarity of the reactor bed section to that of the tube section of the primary steam reformer, the same equilibrium and carbon deposition / removal assumptions can be employed at the most basic modelling level. Contrary to the primary steam reformer, for the secondary steam reformer the combustive section used to supply heat for the catalytic reaction is directly connected to the reactor bed section, so additional assumptions are required for this zone. Ravi et al. (1989) hypothesises that carbon monoxide and hydrogen will combust in preference to methane as methane has a higher activation energy, that all of the oxygen introduced into the reactor is consumed prior to reaching the reactor bed section and that the exit temperature of the combustion section is equal to the adiabatic flame temperature.

Twigg (1997) confirms that this equilibrium assumption holds for both primary and secondary steam reformers. In contrast the combustion assumptions are quite controversial, with significant disparity amongst several authors as to the reaction scheme, discussed in detail in section 5.1, and the overlooking of several key issues, highlighted in chapter 3, by effectively ignoring the geometry of the combustion section. Understanding the processes in this section and developing more representative modelling are the main focus in the research.

5.1 Simple Model

- DUNN, A.J. 1999. An expose of gPROMS and StarCD Computational Packages for Modelling an Industrial Secondary Reformer. *University of Bradford.* Bradford. UK

As for the primary steam reformer, to initiate and form a foundation for research a basic model is developed. Contrary to the primary steam reformer the number of previous modelling attempts is quite sparse, as discussed in chapter 3, but most of the models reported in published literature are similar to the model reported by Ravi et al. (1989).

The secondary steam reformer model reported by Ravi et al. (1989) and the primary steam reformer model developed in section 4.1 were used as a basis for this work. Model validation is performed against industrial data from a number of steam reformers. The general purpose modelling package of gPROMS is used in this work, which includes several features highlighted in chapter 1.

5.1.1 Model description

The construction of secondary steam reformers leads the system to be considered as two sections, a combustion section and a reactor bed section. The model description includes a section for both of these domains and also for the numerical solution of the model. A full listing of the model equations is included in Appendix 3.

Combustion Section

The assumptions of Ravi et al. (1989) for this section are employed for this model. These authors assume that only hydrogen and carbon monoxide combust due to the higher activation energy for methane, combustion is instantaneous, the combustion zone is well mixed and the temperature at the exit of the combustion zone is equal to the adiabatic flame temperature.

Reactor Bed Section

The steady-state model developed in section 4.1 was used as a basis for the reactor bed model developed in this work. Within the secondary steam reformer reactor bed, the only chemical reactions considered are,

$CH_4 + H_2O \Leftrightarrow CO + 3\ H_2$ methane steam reforming

$CO + H_2O \Leftrightarrow CO_2 + H_2$ water-gas shift

Ravi et al. (1989) hypothesises that due to differences in the catalyst found in the primary and secondary steam reformers that the selectivity of the water-gas shift reaction can be considered negligible and hence was overlooked in their model. Although no other reference in published literature comments on this selectivity difference, and in fact all other authors refer to both reactions, Ravi et al. (1989) demonstrated that with this assumption the simulation results "agree with actual plant data". Hence although far from ideal the same approach as Ravi et al. (1989) was adopted for this model.

Notably, no higher hydrocarbons than methane remain after the primary steam reformer, so no 'methane equivalent' approach is adopted. Also carbon deposition / removal is ignored as this issue does not have the same prevalence as for the primary steam reformer.

The kinetic expressions modified by Ravi et al. (1989) to allow for the differences between primary and secondary steam reforming catalyst are adopted due to the capable performance discussed previously. Radial variation is neglected for all variables and the internal heat transfer coefficient and the pressure drop expressions of Beek (1962) and Robbins (1991) respectively, are modified to take into account the shape of modern catalysts.

The same physical property expressions as for the models developed in chapter 4, were adopted i.e. polynomial expressions for the gaseous components properties and average expressions for the gaseous mixture properties except for viscosity and conductivity.

Numerical solution

The full model of the secondary reformer, results in a system of differential and algebraic equations, consisting of ninety four equations. A second order orthogonal collocation method with 12 discretisation points was applied for the solution technique as this was proven to be mesh independent. The solution strategy described in section 4.1, of initially de-coupling the heat balance and the pressure profile, was employed for this model and performed with the same robustness as discussed previously.

5.1.2 Simulation and Model Validation

The model was validated against industrial data from several secondary steam reformers. A typical industrial secondary steam reformer comprises of a burner suspended in a combustion section above a catalyst bed and associated support with a combined height of around 13 m and diameter of 5 m; typically operated at a pressure of some 30 bar and a temperature range 970 – 2000 °C. The simulation results are presented in Table 5.1.1 and Table 5.1.2, and clearly show that despite some gross simplifications the simulated data compared well to the industrial data for both sections.

Table 5.1.1 Comparison between plant and simulated data for the combustion section

	Temperature (°C)	**% Combustion of process gas**
Simulation Results	1100	23
Measured Data [Christensen et al. 1994 Farnell 1993]	~1200	20

Table 5.1.2 Comparison between plant and simulated data for the overall performance of the secondary steam reformer

		Plant data	**Calculated values**	**Deviation (%)**
Dry Mol %	CH_4	0.2	0.19	2.7
	CO	11.5	11.9	-4.1
	CO_2	8.8	9.15	-4.0
	H_2	57.1	56.1	1.7
	Inerts	22.4	22.5	-0.58

A sense check on the hypothesis of the selectivity of the water-gas shift reaction was performed by simulating with the reaction kinetics included. Consistently the simulation data showed closer agreement with this assumption. This method of assessment is not ideal as although these assumptions performed well for this data set they are not based on fundamentals of the system, so it may be coincidental or put in other words circumstances mean that two wrongs in fact make a right in this case.

5.1.3 Conclusions

A 'basic' secondary steam reformer model was developed to initiate further research of the simulation of secondary steam reformers. The model was based on previously published research with a number of small refinements.

Although not the most complicated model, in comparison to previously published simulations, the simulation results demonstrated reasonable agreement to industrial plant data. Additionally, the observations are comparable to those in published literature.

Despite the reassuring performance, this level of modelling does not approach some of the key topics for secondary steam reformers, discussed in chapter 3. Further development to include the effect of these issues is required to yield any notably beneficial information from simulation.

5.2 Three-Dimensional Model

- DUNN, A.J., MUJTABA I.M. and YUSTOS, J. 2001. Preliminary Optimisation of a Top-Fired Primary Steam Reformer using gPROMS, 2001, *University of Malaya*, Malaysia

The secondary steam reformer modelling has not seen the same amount of interest as the primary steam reformer due to several reasons including the relative lack of interest in the unit operation to that of the primary steam reformer. Despite this the 'standard' modelling complexity for secondary steam reformers is significantly greater than the primary reformer due to the specific unit issues; fundamentally the difference in the linkage of the combustion and catalyst bed sections.

5.2.1 Model description

As was highlighted in section 5.1, the construction of secondary steam reformers leads the system to be split into a combustion section and a reactor bed section. Following the "best-in-class" principle introduced in chapter 1, two simulation packages were used for the model described in this section. Overlap of the sub-models occurs in the catalyst bed, with the overall reactive flow analysis simulated using the computational fluid dynamics package StarCD and the general simulation package gPROMS employed specifically for the reactor bed. Although only the key equations are discussed in the model description a full listing is included in Appendix 3.

Combustion section

There are a number of published papers on secondary steam reformer modelling which include reactive flow simulation of the combustion section, Farnell (1992), Blanchard and LeBlanc (1993) and Christensen et al. (1994), however, the details of these systems is sparse as all are proprietary industrial simulations. The information that could be gleamed from these papers and research from similar systems was drawn upon to set the basis for this model.

As for the model in section 4.5, turbulence is represented by the time-averaged approach as it is the most validated approach; specifically Chen's κ–ε model. Additionally, Versteeg and Malalasekera (1995) note that the main alternative to the κ–ε representations, the mixing-length approach, is "completely incapable of describing flows with separation and recirculation", hence for the jet formation from the burner of the secondary steam reformer this approach would not be suitable. To enhance the accuracy of the flow-field, the affect of the near wall region on the flow is depicted; the recognised methods for the representation of the near wall region are wall functions, two-layer models and low Reynolds number models. A two-layer approach is applied, as Computational Dynamics (1998b) states this method offers "improved friction and heat transfer predictions" to wall functions, however, the mesh requirements are less than that of the low Reynolds number approach. Rodi (1991) highlights the notable variation in performance of these near-wall approaches, but the Norris and Reynolds form appears to offer the most realistic performance for a system similar to the secondary steam reformer and hence is adopted for this simulation.

As highlighted in section 4.5 and discussed in chapter 1, there is no idealistic approach to reactive flow simulation, with several approaches showing varied performance for a number of systems. The reason for the wide range of approaches and performance lies in the fundamental difficulty of simulating not only the transportation of the particles, i.e. turbulent phenomena, but also the interaction of these particles and their affects at a molecular level. Any simplification from the molecular level is effectively a generalisation reliant on assumptions that are susceptible to becoming invalid. This conundrum can be compared to the effect of diffusion in a catalyst particle, as for both the mass transport effect and the underlying kinetics must be separated and defined, however, diffusion is far easier to simulate.

Despite these complexities, there is a common consensus amongst the authors of reported secondary steam reformer simulations, that the rate of combustion is "controlled by the rate of mixing" [Farnell (1992)]; more commonly termed as the 'mixed is burnt' approach. From these industrial observations it would appear that the combustion section of the secondary steam reformer is at least on the edge of a 'fast reaction' system, defined by Bird et al. (2002) as having mixing time constants significantly greater than reaction time constants. As highlighted in chapter 1 and chapter 4 the two main approaches for reactive flow representation are the probability distribution function and the eddy break-up model.

For the probability distribution function approach the time-average value of the concentration, density and temperature are assumed to be the integral of the product of the instantaneous value of the variable, which is assumed a function of the mixture fraction, and the probability distribution function for the mixture fraction, for which the mixture fraction is calculated based on transport equations. The mixture fraction function for the variables is based upon the assumption of fast reactions, with the main approaches being to presume 'mixed is burnt', each reaction reaches equilibrium or the reactions take place at finite rates in one-dimensional transient laminar flames, for this model the 'mixed is burnt' is assumed. There are a several of forms of the probability distribution functions, however, for this model a beta function is employed.

The Eddy break-up approach hypothesises that the rate of reaction is a function of the local flow properties, namely the dissipation rate of reactants, oxygen and reaction products. The minimum of weighted versions of these rates is then defined as the reaction rate,

$$R_F = -\frac{\rho\varepsilon}{k} A_{ebu} \min\left[m_F, \frac{m_O}{s_O}, B_{ebu} \frac{m_P}{s_P} \right] \tag{5.1}$$

$$s_O = n_O M_O / n_F M_F \tag{5.2}$$

$$s_P = n_P M_P / n_F M_F \tag{5.3}$$

To allow for reaction kinetics, the kinetic reaction rate and the eddy break-up reaction rate are calculated for each cell and the minimum is hypothesised to be the reaction rate for that cell.

The possibility of an alternative form for the representation of competing reactions was investigated by returning to the basics of the problem. As Brown (2001) nicely demonstrates neither of the two idealistic approaches of plug-flow or a continuously stirred tank perform well in predicting reactor performance. However, as Fogler (1992) discusses these failings are well recognised and several approaches have been hypothesised to reflect the non-ideality. Starting with the idea that each cell in the combustion section performs closer to the continuously stirred tank ideal than the plug-flow ideal the non-ideal continuously stirred tank approach employing a dead-space and bypass was introduced, see figure 5.2.1. With each cell open on all sides it was hypothesised that the dead space and bypass could be based on the relative approach vectors of the reactive components from the surrounding cells to yield a percentage of the cell for which no reactants were not in contact and a percentage of the flow which failed to come into contact with another reactive component. Although trials with this approach yielded some confusing results that did not match those observed in reality, fundamentally if an exact method of estimating parameters could be developed this alternative would accurately predict the unit performance.

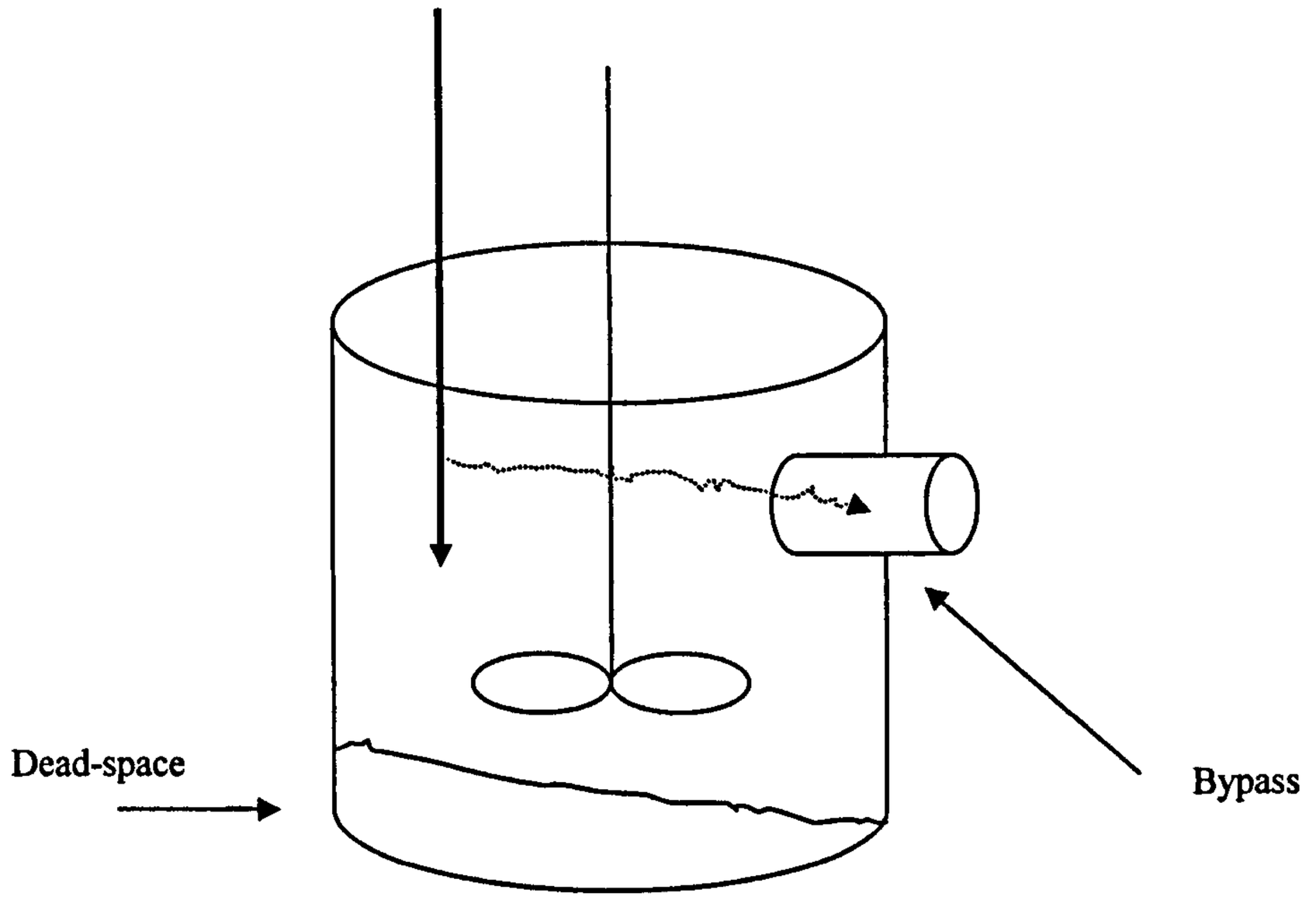

Figure 5.2.1: Continuously Stirred Tank reactor model with dead volume and bypass

The 'best practice' of the simplification of the chemical reaction scheme, employed in section 5.1, from the full component listing is adopted to limit the simulation to a manageable size. For the use of the eddy break-up approach this system of reduced reactions have to take an alternate form due to the presence of combustion products, i.e. carbon dioxide etc., in the fuel for the secondary steam reformer.

So instead of,

$$CO + 0.5\ O_2 \Longrightarrow CO_2$$

An additional passive dummy product [D] was created, with the other reaction products defined as reactants in terms of the eddy break-up approach. So the alternate takes the form of,

$$CO + 0.5\ O_2 \Longrightarrow CO_2 + D$$

This adjustment is required for the eddy break-up model, as for this approach the mass fraction of the combustion products are calculated from the mixture fraction and the fuel mass fraction. The process gas inlet to the secondary steam reformer is rich in combustion products although no combustion exists at this point as the oxygen is introduced to the system via the burner, hence the eddy break-up approach predicts negative temperatures. When these combustion products are redefined as reactants this issue is avoided, however the combustion model code requires a minimum of one product hence the passive dummy variable is introduced.

As was discussed in chapter 3, there is some contention in the reduced chemical scheme for the combustive section of the secondary steam reformer. Ravi et al. (1989) state that "the combustion of hydrogen and carbon monoxide is considered to be instantaneous whereas that of methane is neglected on account of its higher activation energy". However, Synder et al. (1986) identify methane as the main combustible with only "a small amount of hydrogen and carbon monoxide", while Orphanides (1993) states "principally hydrogen is consumed in the combustion zone together with methane and carbon monoxide" and Blanchard and LeBlanc (1993) and an ICI secondary reforming catalysts pamphlet indicate only hydrogen combustion. Farnell (1992) indeterminately states "only 20% of process gas feed is consumed in combustion" but does not define composition of combustibles.

In addition to the discrepancies in the reaction schemes also several kinetic expressions have been proposed for the combustion of methane, hydrogen and carbon monoxide at various operating conditions. Predominately, for CFD simulations simple global reaction schemes are adopted with an eddy break-up model to limit the computational intensity. From the simulations discussed in section 3.6.5, the leading kinetic expressions are taken from Dryer and Glassman (1972), Westbrook and Dryer (1981) and Yetter et al. (1986); from a brief survey of combustion simulations using computational fluid dynamics the kinetics of Westbrook and Dryer (1981) are the most consistently employed. Westbrook and Dryer (1981), however, are not without critics, such as Coffee (1985), for generalising the reaction scheme to such an extent that the combustion properties will be incorrectly simulated. Interestingly, Coffee (1985) also highlights typographical errors in the kinetics of Westbrook and Dryer (1981) which are acknowledged by these authors in a response attached to Coffee (1985), however, these errors are not acknowledged by another paper found in this literature survey.

Considering the composition of the feed streams to the reformers, see table 3.5.2, the assumption of sole hydrocarbon combustion for a secondary reformer is questionable. In reality all three reactions will occur in parallel and hence are included in the reaction scheme. The kinetics of Westbrook and Dryer (1981), with the corrections of Coffee (1985) are employed for the reaction kinetics.

Outside of the combustion processes the only other reaction speculated to occur in the combustive zone is methane steam reforming. This subject is reported in discussion notes attached to the papers of Farnell (1992) and Blanchard and LeBlanc (1993). Farnell (1992) indicates that the effect of methane steam reforming is "not so important as for oxygen-fired secondary reformers" but "some allowance" is made for the thermal effect of reforming. Blanchard and LeBlanc (1993) draws upon unreported experimental work that concluded that the reforming reaction "doesn't come into play in this system until the gas gets to the catalyst bed". As the likelihood of this reaction's occurrence and its affect are both minimal, this reaction was not considered in the overall reaction scheme.

Fundamentally the use of the eddy break-up approach for multiple reactions is significantly questionable, primarily because the reaction parameters are empirically derived for a single reaction system and it would seem logical that these parameters would require refinement with the inclusion of other reactions; this concern with the applicability to multiple reactions is shared by Brink et al. (2000). Additionally, the modification required to allow for the existence of combustion products in the unit feed offers no solace to the applicability to secondary steam reformers. In comparison for the probability distribution function approach, the main concerns are the assumption that the reaction kinetics are instantaneous and the common reliance on the accuracy of the mixture compositions. Combining these observations with the previously noted opinion of Libby and Williams (1994) on the simulation accuracy of the presumed distribution function and their reported performance by Hjertager (2001) for 'fast chemical reactions', the reduced chemical reaction scheme as part of a beta – probability distribution function model was employed.

As for the model developed in section 4.5, the thermal radiation is represented by the 'Discrete transfer method' of Lockwood and Shah (1981), for radiation in the participating media, and the radiation properties are represented by correlations from the radiation band model by Grosshandler (1993). Although the combustive sections of the primary and secondary steam reformers differ there appears to be no reason to suggest similar simulation performance to that demonstrated in fired-furnaces from being replicated in the secondary steam reformer.

Thermal conduction from the secondary steam reformer is assumed negligible as in terms of model accuracy the risk of potential errors, such as estimates of insulation thickness, outweigh the potential benefit of inclusion of this physical phenomena. Additionally, the insulation performance for secondary steam reformers can be considered to be high as external to the reactor are several layers of refractory and a water jacket.

Apart from the radiation properties, the same physical property expressions as for the steam reformer tubes were adopted i.e. polynomial expressions for the gaseous components properties and average expressions for the gaseous mixture properties except for viscosity and conductivity. However, as was highlighted in section 4.5, the full expressions for all the physical properties including the radiation properties are introduced in stages within 'operational envelopes' to limit the chances of destabilising the solution.

Reactor bed

As was discussed previously this model of the secondary steam reformer is split over two packages, the StarCD and the gPROMS packages. To provide consistency across the model the reactor bed has to be represented in both sub-models. This is to allow the interaction of the combustion section flow-field and reactor bed to be fully represented.

The StarCD model as shown in figure 5.2.3, includes the geometry of the secondary steam reformer from the vessel inlet up to the under-bed for the catalyst. The effect of the equipment outside of these bounds is negligible as on the inlet a range of flow adjustment devices is employed to provide plug-flow at the inlet and below the catalyst bed is purely a support structure which is designed to offer a minimal pressure drop; additionally published details outside these bounds are sparse.

As the catalyst bed is randomly packed an exact representation is fundamentally impossible, so alternatively the common practice is to represent its overall effect. This overall representation is termed as a distributed resistance, for which the main concern is the duplication of the catalyst bed pressure drop, for which the Ergun equation is employed,

$$\frac{dp}{L} = -\alpha u - \beta u^2 \tag{5.4}$$

where the values for α and β are defined to represent the secondary steam reformer catalyst.

Within the gPROMS sub-model all the physical phenomena of the reactor bed are included. The sub-model is based on the two-dimensional model defined in section 4.4 with only minor modifications to allow for the differences between primary and secondary steam reformers. Two-dimensional variation is only considered for the reactor bed model as the assumptions employed for the computational fluid dynamics simulation, such as plug-flow at the inlets, and the time-averaged nature of the modelling will minimise any potential variation in the third dimension. The data from the simulation is averaged in the third dimension at the interface of the reactor bed to allow for the dimensional discrepancy.

Apart from the parametrical changes required converting the model from a primary steam reformer to a secondary steam reformer, the only other changes were based on those employed for the model development in section 5.1. As for the model developed in section 5.1, the hypothesis of Ravi et al. (1989) that the selectivity of the water-gas shift reaction can be considered negligible and the modified kinetic expressions by Ravi et al. (1989) were adopted. Additionally, as for the model in section 5.1, no 'methane equivalent' approach was necessary and carbon deposition / removal was ignored. All other details of the model developed in section 4.4 were consistent for the secondary steam reformer.

Numerical solution

As for the model discussion the numerical solution is discussed separately for the StarCD and gPROMS sub-models.

As for the three-dimensional primary steam reformer models discussed in chapter 4, careful consideration and reassessment was required for the numerical solution, throughout the development of the various meshing versions. As was highlighted in section 4.5, this holds a greater prominence for these three-dimensional models as the format in which the computational fluid dynamics packages are presented allows a quick solution to be attained with only limited consideration of modelling issues.

Despite the automatic inclusion of some of the 'best practices' in the computational fluid dynamics software, such as scaling and block decomposition, as is clear from the discussion in section 4.5 there are a significant number of settings that remain with the user of the computational fluid dynamics packages. These settings are set on a basis of accuracy with some require tailoring to the initialisation strategy to assist solution stability.

With the sparse information on initialisation techniques for computational fluid dynamic modelling, the previous experience for the primary steam reformer modelling was drawn upon. As for the primary steam reformer the pre-prescribed techniques used in commercial computational fluid dynamics packages, of the predictor-corrector approach employing pressure field initialisation, were found wanting. A more considered approach was required, following the same principle of gradual introduction.

For each of the mesh arrangements employed a common approach was found for initialising the solution. Initially the model was solved for a flow-field simulation with the heat balance included. Firstly the model was solved with the SIMPLE solution technique and upwind differencing as these were found to be the most robust in achieving convergence. These results were then employed to initialise the next stage with the improved approaches of SIMPISO and higher order discretisation. Then to complete the set of the key system variables, the next step is to introduce the chemical components but without chemical reaction. With the sensitivity of the heat balance, the combustion reactions were introduced next, followed by thermal radiation over the same steps as discussed in section 4.5. Also as discussed previously, to reduce the chances of destabilising the solution the radiation properties and some of the physical properties, such as density, conductivity, specific heat and molecular viscosity, were set an 'operational envelope' of the maximum possible range of these parameters for this system as part of a staged initialisation.

As was found for the primary steam reformer research, these stages are not totally 'portable' to any computational fluid dynamic simulation, but with initial simplification of some of the complexities of the flow-field system, such as adjustment of boundary definitions, hence reducing turbulence and amount of mixing a robust solution can be achieved.

The integrity of the solution as indicated earlier in chapter 1 and section 4.5 is a key issue in the world of computational fluid dynamics due to the diversity between the 'simple' colourful nature of the results and the complexities behind achieving those results. As discussed the ideology of mesh independence is to reach a solution from the system of equations and boundaries that is not affected by changes to the mesh structure employed for the system i.e. mesh independence.

As for the model developed in section 4.5, the traditional approach of doubling the mesh density until the results showed only an insignificant change was overlooked due to its fundamental failings. In place the technique employed was the efficient deployment of cells based upon the calculation of error estimation as demonstrated in chapter 1 and section 4.5. After the simulation had solved the truncation error was estimated for each cell and the top twenty percent were refined, with this process being repeated until the error reached an insignificant level. Despite the concerns of several authors that fundamentally 'mesh independence' is an ideal that is unachievable, when considered against all other sources of error in the simulation this criticism becomes more measured.

For the gPROMS sub-model the same approach as for the two-dimensional model in section 4.4 was employed. The full model of the primary reformer results in a system of differential and algebraic equations, consisting of eighty-two equations per region. The solution techniques applied along the length was a second order orthogonal collocation finite element method with 15 discretisation points. Across the radius, the method of calculating the voidage profile essentially divides the radius into two regions, so the solution techniques applied were both second order orthogonal collocation finite element methods, with 20 discretisation points and 12 discretisation points.

Both scaling and block decomposition were immediately enforced for the primary steam reformer model. The relatively simple approach of initialising with a solution for no radial variation reached a valid solution despite the significant radial variation found for the secondary steam reformer.

5.2.2 Simulation and model validation

As was highlighted in chapter 3, data is sparser for secondary steam reformers than for the primary steam reformers particularly system geometry and dimensions; with no completely consistent set of data available in published literature. This fundamentally poses a difficulty for defining a simulation and validating the results. As there was no other option the best attempt was made at gleaning a set of system parameters from several authors, notably Rocha de Avila and Neto (1993) and Singh and Patel (1995), and a set of unit conditions were assumed from Elvers et al. (1989).

Apart from the lack of consistent data, none of data sources provided any geometrical details of the internals of the secondary steam reformer, e.g. burner shape, size and location. To rectify this the most basic burner form of a single tube coaxial to the process gas inlet was adopted, see figure 5.2.2

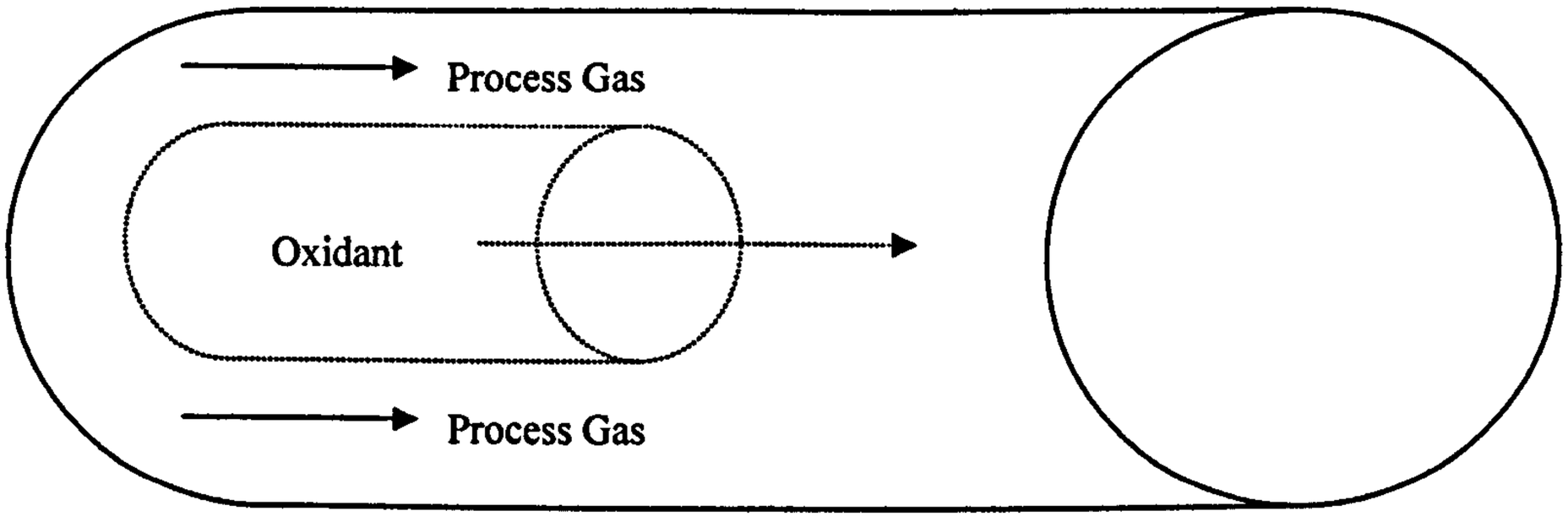

Figure 5.2.2: Burner design

Drawing from the observations of several studies of coaxial jet mixing, notably Thring and Newby (1953) and Beer and Chigier (1972), the burner was designed to perform at the unit conditions.

The model was validated against industrial data from a secondary steam reformer within the ammonia processes reported by Elvers (1989). The 'melting pot' secondary steam reformer design was 10m in length etc with the burner.

Despite the concerns of the assumptions employed to define the secondary steam reformer the overall results reflect the general performance of the reported unit, see table 5.2.1.

Table 5.2.1 Comparison between plant and simulated data for the overall performance of the secondary steam reformer

		Plant data	Calculated values	Deviation (%)
Dry Mol %	CH_4	0.2	0.196	2.1
	CO	11.5	11.8	-3.2
	CO_2	8.8	9.07	-3.1
	H_2	57.1	56.4	1.3
	Inerts	22.4	22.5	-0.44

Additionally, the simulation results for the distribution of methane composition and temperature, see figure 5.2.3, and distribution of the methane composition across the bed, see figure 5.2.4, show no obvious anomalies and appear logical showing limited variation across the bed and two sections of mixing.

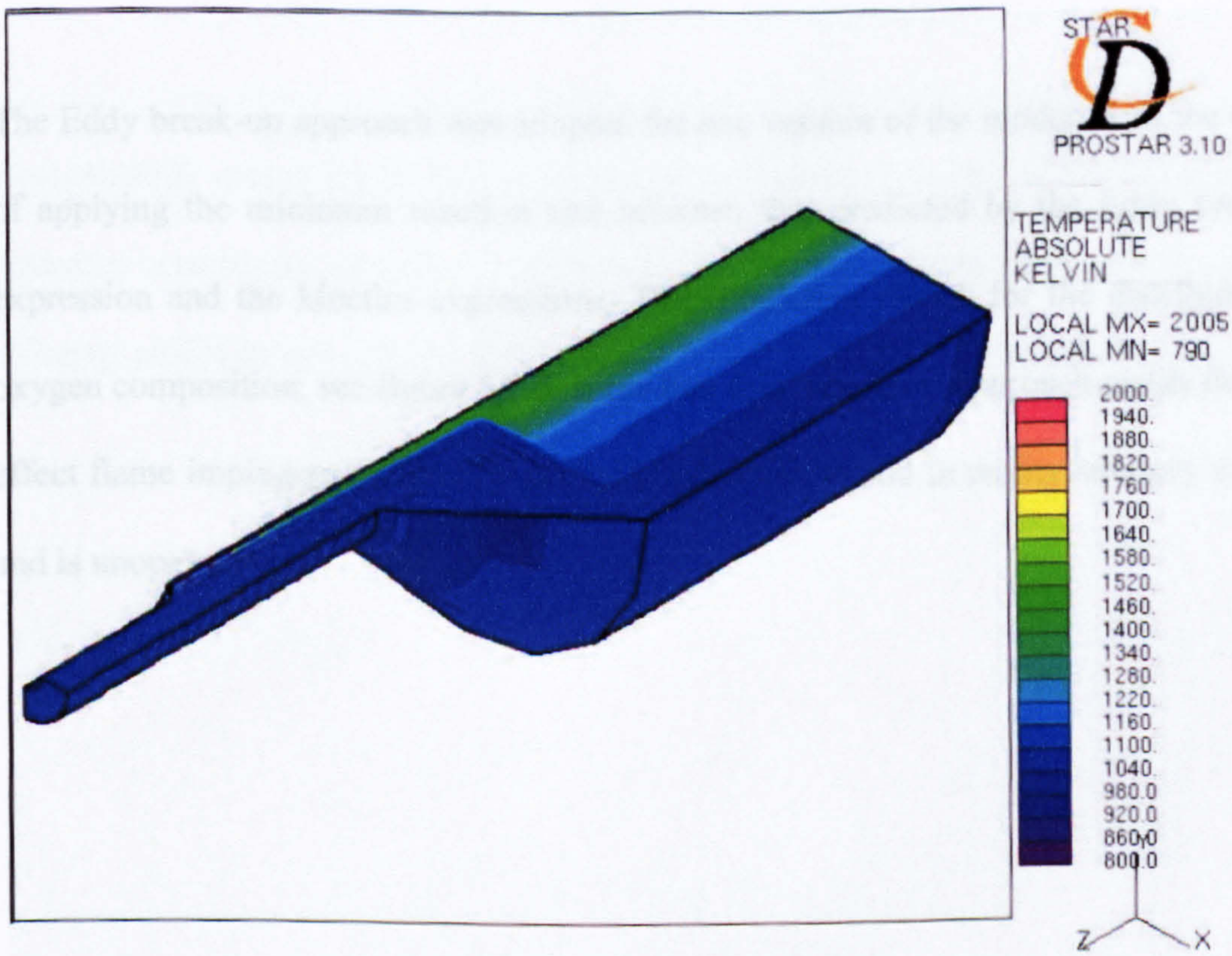

Figure 5.2.3: Temperature Distribution [Quarter section]

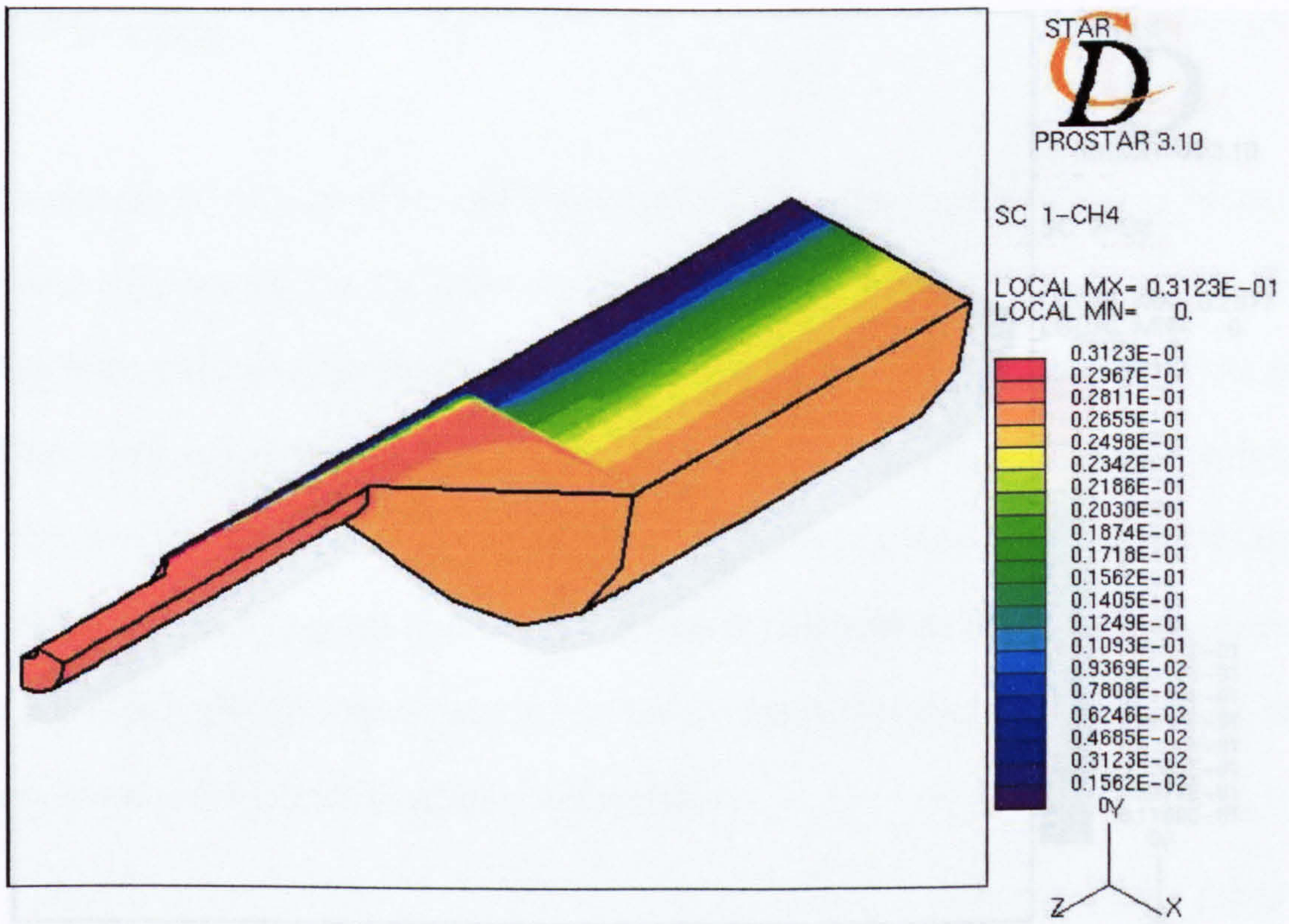

Figure 5.2.4: Methane Distribution [Quarter Section]

The Eddy break-up approach was adopted for one version of the model, with the option of applying the minimum reaction rate between that predicted by the Eddy break-up expression and the kinetics expressions. The simulation results for the distribution of oxygen composition, see figure 5.2.5, show that this 'negative' approach yields the false effect flame impingement into the catalyst bed which would in reality severely damage and is unoperational.

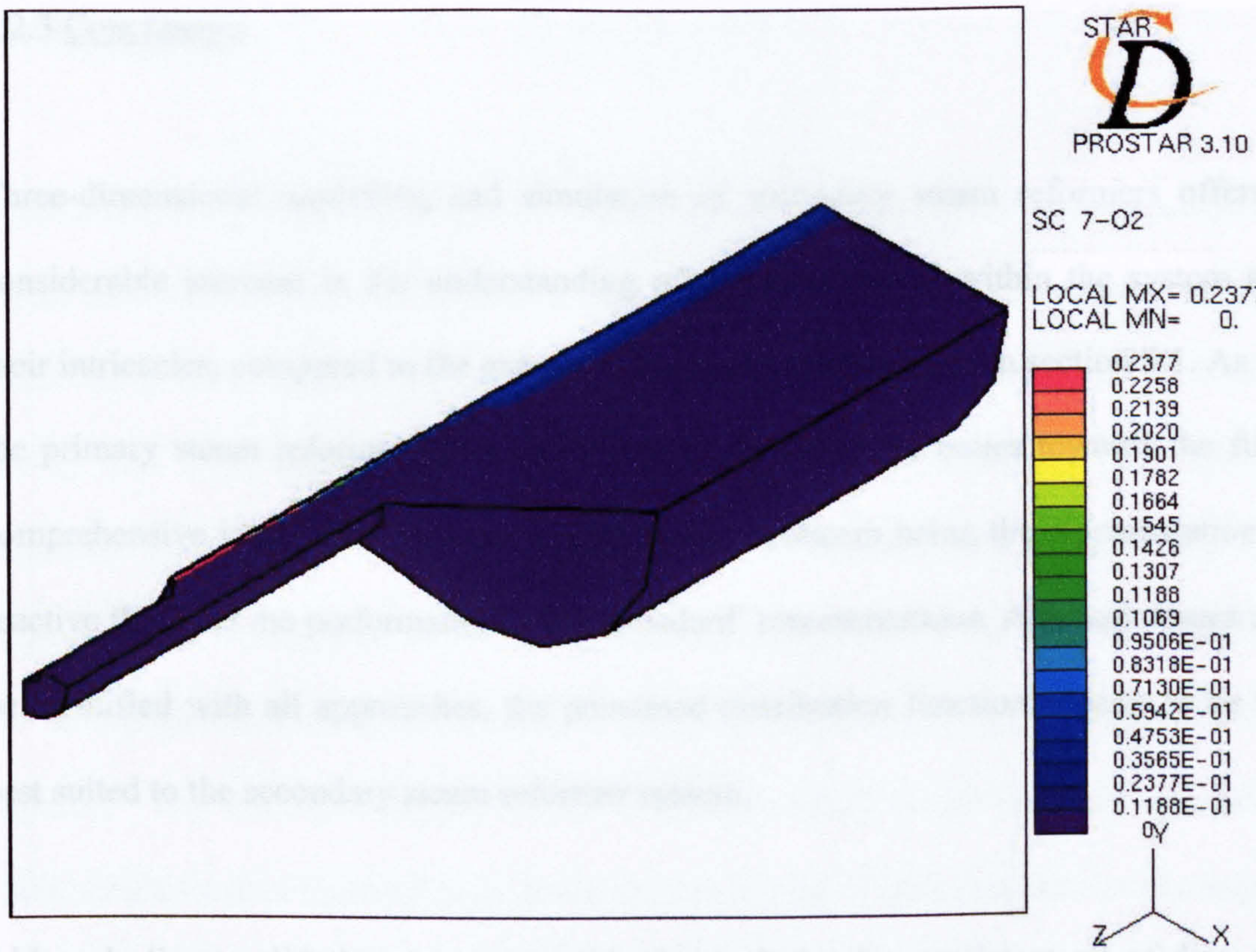

Figure 5.2.5: Distribution of oxygen [Quarter section]

Unfortunately due to the lack of information on step changes in unit performance, the boundary sensitivity technique employed for the three-dimensional primary steam reformer model would offer no further solace to the accuracy of this model.

5.2.3 Conclusions

Three-dimensional modelling and simulation of secondary steam reformers offers a considerable increase in the understanding of the mechanisms within the system and their intricacies, compared to the extremely basic model developed in section 5.1. As for the primary steam reformer, through the model development issues towards the fully comprehensive ideal have been aired. The primary concern being the representation of reactive flow and the performance of the 'standard' representations. Although issues can be identified with all approaches, the presumed distribution function appears to be the best suited to the secondary steam reformer system.

Although direct validation was impossible due to lack of a consistent set of data, the model concurred with results from industrial plant reported in open literature and showed no anomalies. A complete set of validation data would be required to confirm the choice of reaction representation. Uniquely for this set of steam reformer models reported in chapter 4, the simulation combines both the gPROMS and StarCD simulation packages.

5.3 Summary

Despite the complex nature of the secondary steam reformer system even a simplistic model performs well against industrial data for the overall process; a complete data set would have been ideal. This seems to offer endorsement of the opinion of Farnell (1992) that from underlying industrial experience and knowledge of the system, simplified models can be employed for the design of secondary steam reformers. This opinion is only valid when the unit is in the area of 'operational knowledge' and there are no unusual circumstances; otherwise thorough modelling of the system would be required. The three-dimensional model of the secondary steam reformer appears to reach such a level of thoroughness, however, due to lack of data it cannot be thoroughly assessed.

The primary concern for the three-dimensional model is that of representation of reactive flow and the performance of the 'standard' approaches. It was shown that although all approaches have failings, the presumed distribution function appears to be the best suited to the secondary steam reformer system. Overall the development of these secondary steam reformer models, highlighted such modelling topics as initialisation, numerical solvers, mesh sensitivity, scaling of variables and model partition amongst others.

Chapter 6

Optimisation Cases

The natural progression once a model is developed and confidence is established in the simulation results is to try and improve on the unit performance. This improvement study is generally labelled as optimisation although its complexity can vary greatly. This chapter includes a number of optimisation studies of varying level of complexity completed as part of this research. These studies employ models developed in chapter 4 and draw on the discussions on optimisation from chapter 2 to demonstrate the functionality of optimisation for primary and secondary steam reformers.

6.1 Primary Steam Reformers

As discussed previously, see chapter 3, the primary steam reformer is the first stage of possibly a multiple stage steam reforming section for several important production schemes. Steam reforming converts hydrocarbons with steam to form a mixture of hydrogen and carbon oxides, which are major chemical building blocks. Primary steam reformers are traditionally a furnace with suspended catalyst filled tubes and burners in various firing arrangements. The top-fired furnace is the most popular firing arrangement of industrial steam reformers, see figure 6.1.1.

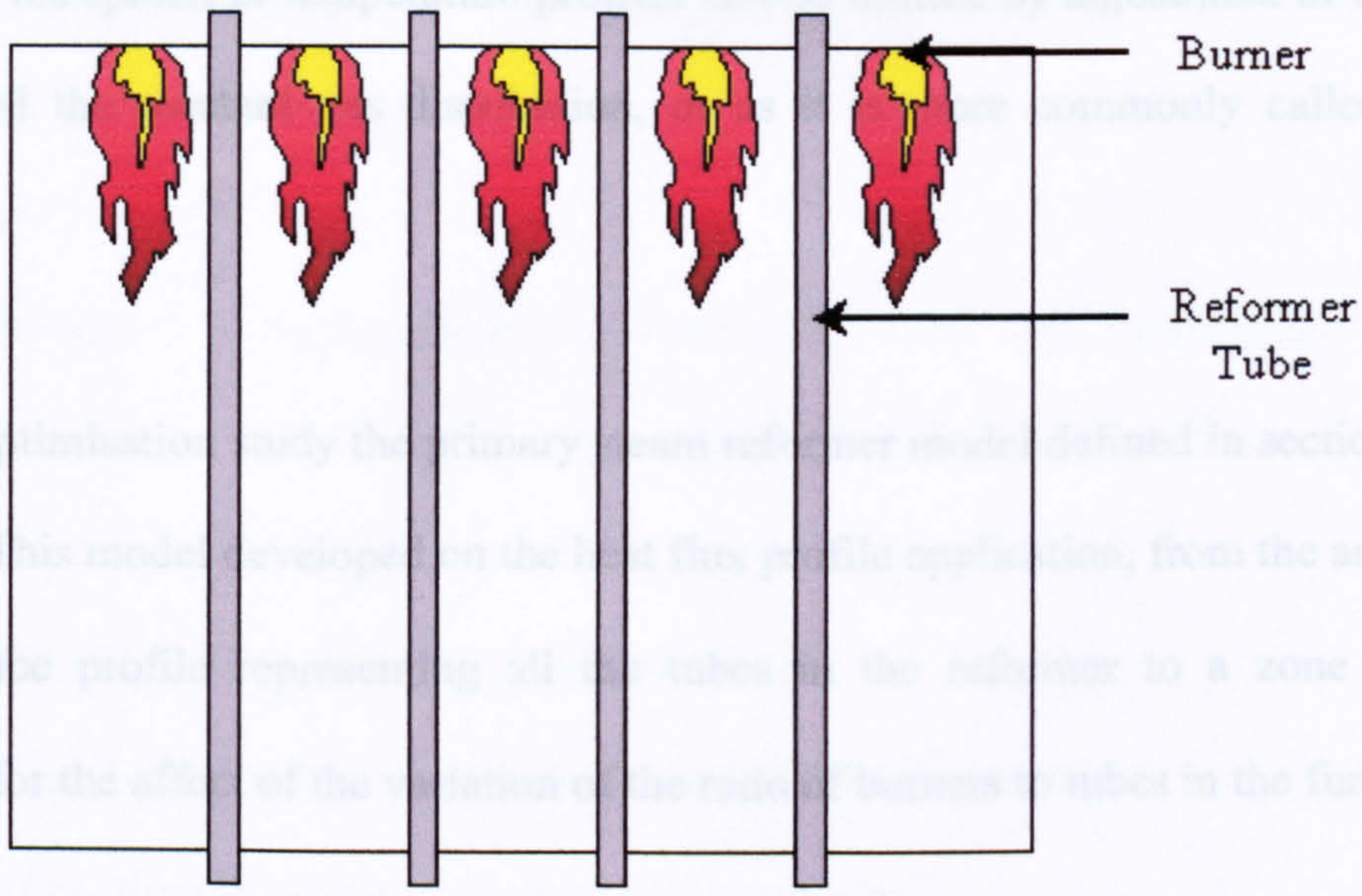

Figure 6.1.1 Layout of a Top-Fired Primary Reformer.

There have been a number of optimisation studies for primary steam reformers, see chapter 2, though primarily these have concentrated on the operating conditions within the reformer tubes. Other conditions are of at least comparable interest in operational terms and this is the focus for the optimisation studies in this chapter.

6.1.1 Two Zone Optimisation

- DUNN, A.J., MUJTABA I.M. and YUSTOS, J., 2002, Modelling and Simulation of a Top-Fired Primary Steam Reformer using gPROMS, Dev. in Chem. Eng. & Mineral Proces. Journal., Vol. 10, No. 1 & 2, pp 77 – 87

The operational lifetime of a primary steam reformer tube is fundamentally dependent on the maximum temperature experienced. Ideally both for ease of maintenance and to avoid operating the furnace with reduced capacity, the furnace should have a consistent tube lifetime or equivalently a uniform temperature profile. For top-fired steam

reformers the spread of temperature profiles can be limited by adjustment of the burner profile and the reactant gas distribution, or as it is more commonly called furnace balancing.

For this optimisation study the primary steam reformer model defined in section 4.1.2 is adopted. This model developed on the heat flux profile application, from the assumption of one tube profile representing all the tubes in the reformer to a zone approach allowing for the affect of the variation of the ratio of burners to tubes in the furnace.

An optimisation problem formulation is developed for both methods of furnace balancing.

a) Furnace balancing via adjustment of the burner profile. The optimisation problem can be expressed as,

$$\text{Minimize} \qquad \textit{Difference}(\mathbf{u}) = (\text{'Outer Zone' Tube Wall Temperature} - \text{'Inner Zone' Tube Wall Temperature})^2$$

where $\mathbf{u}$ = {Ratio of Fuel Gas Flowrate between Zones}; subject to $0.5 < \mathbf{u} < 1.5$

'Outer Zone' Outlet Pressure = 'Inner Zone' Outlet Pressure

b) Furnace balancing via adjustment of the reactant gas distribution. The optimisation problem can be expressed as,

Minimize *Difference*(**u**) = ('Outer Zone' Tube Wall Temperature – 'Inner Zone' Tube Wall Temperature)^2

where **u** = {Orifice Plate Diameter}; subject to 0.5 < **u** < 2.3

'Outer Zone' Outlet Pressure = 'Inner Zone' Outlet Pressure

Orifice Plate Diameter < Internal Pipe Diameter

The successive quadratic programming method is employed for this optimisation problem based on the recommendations from the previous discussion in chapter 2. In order to avoid arriving at the local optima rather than the global optima the optimisation was initialised from the boundaries of each **u** definition, the optimal point arrived at from the extremes, and at intervals of ten percent between the extremes. For each initialisation point, the optimisation yielded the same result, within numerical tolerance, without anomaly.

Implementing optimisation, for the burner profile and the reactant gas distribution between the two zones, reduced the difference in the temperature profiles (Figure 6.1.2 and 6.1.3). Both methods enhanced the 'balance' of the furnace, however, adjustment of the reactant gas distribution offers a smoother influence on the overall tube profile in comparison to the burner profile.

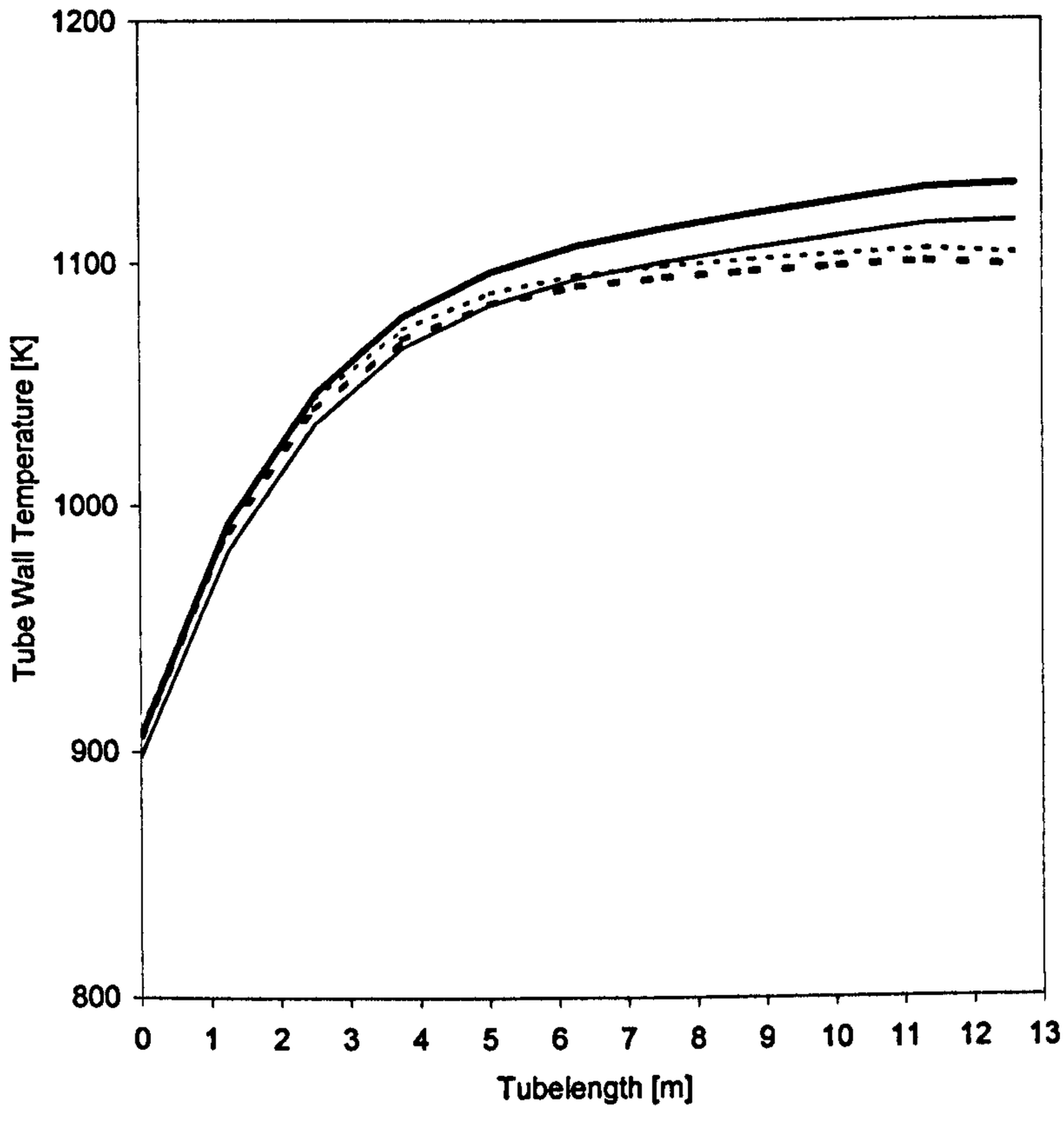

Figure 6.1.2 Comparison of inner and outer zones' tube wall temperature profiles. Furnace balancing via adjustment of the burner profile. Optimal Ratio of Fuel Gas Flowrate between Zones = 1.05 CPU time = 130 seconds.

Although the optimisation results from the zone approach are logical, it should be noted that the implications of the operational changes, particularly the affect on the flow field in the furnace are not fully portrayed by the heat flux profile representation. To accurately display these effects a full flow simulation of the furnace would be required. Cotton (1999) demonstrates that adjustment of the burner profile has to be considered carefully as it can significantly alter the furnace flow-field and hence the furnace performance. This issue is discussed and demonstrated in more depth in chapter 4.

However, from first principles, adjustment of the burner profile would seam to have a more significant effect on the furnace flow-field.

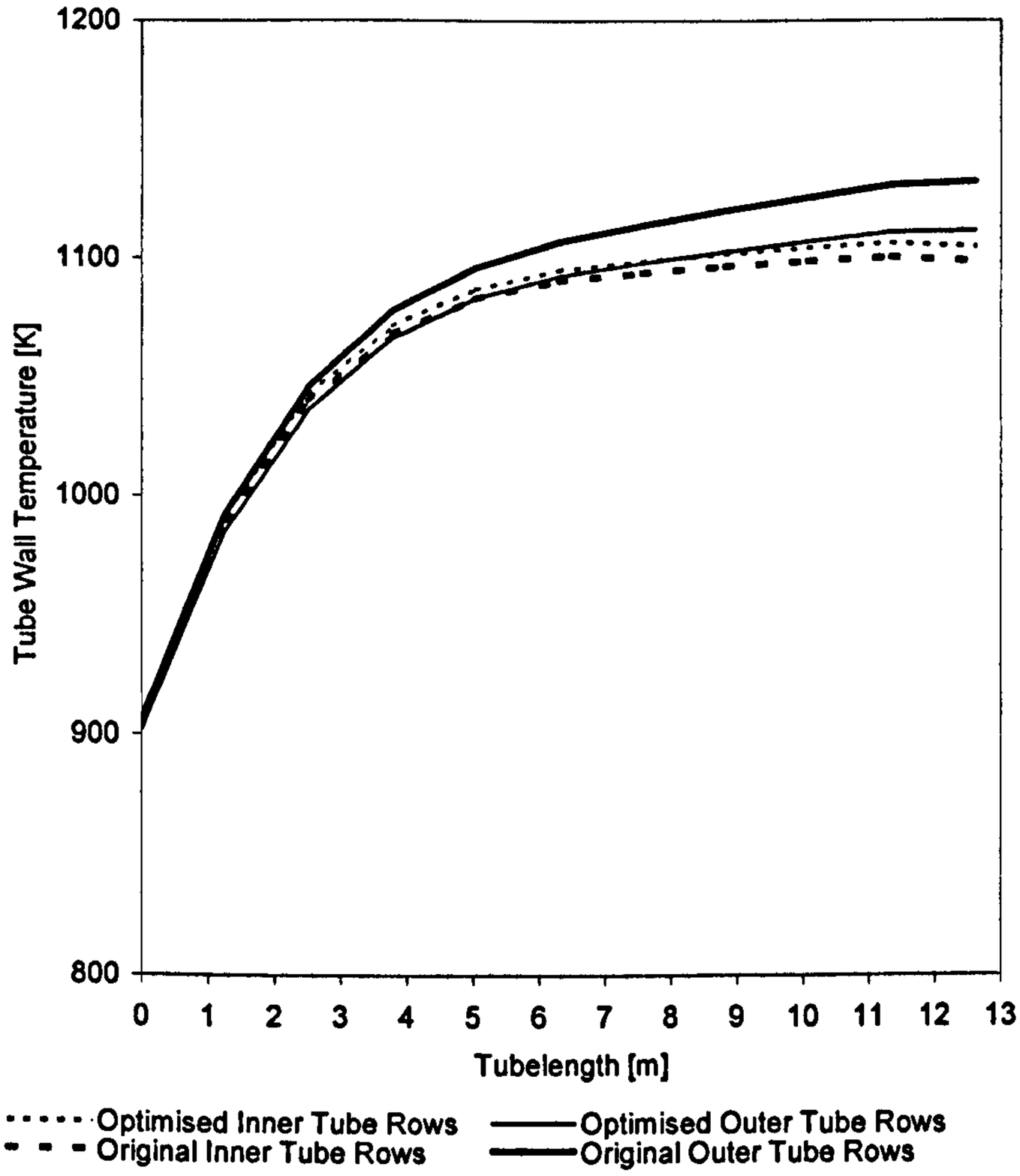

Figure 6.1.3 Comparison of inner and outer zones' tube wall temperature profiles. Furnace balancing via adjustment of the reactant gas distribution. Optimal Orifice Plate Diameter Ratio = 1.3. CPU time = 390 seconds.

During the design phase it is industrial practice, for this style of Top-Fired steam reformer, to perform balancing via reactant gas distribution; to limit the effect of flow field issues and simplify the furnace balancing. Over the operational life of the catalyst charge disturbances will occur and unequivocally the performance of the reactor will

change, however, adjustment of the orifice plates is an unrealistic operational practice so furnace balancing via adjustment of the burner profile is performed. Ultimately, using both balancing techniques reduces the extent of balancing via the burner profile.

Optimisation of the burner profile and reactant gas distribution, between the zones, reduced the difference of the tube wall temperature profiles. This is a significant operational condition overlooked by defining an average reformer tube.

6.1.2 Dynamic Two Zone Optimisation

- DUNN, A.J., MUJTABA I.M. and YUSTOS, J. 2001. Preliminary Optimisation of a Top-Fired Primary Steam Reformer using gPROMS. *6th World congress of Chemical Engineering*. Melbourne. Australia

Over the operational life of the catalyst charge and reformer tubes, the process will experience several changes, predominately the cause will be process disturbances, however, unequivocally the performance of the reactor will alter. The process operators will be required to respond to these changes, some of which can seriously effect the furnace balance, to maintain the performance of the unit. As was discussed previously in chapter 4, industrial practice is to balance the furnace solely via adjustment of the burner profile once operational, which is reflected in this optimisation study.

For this optimisation study the primary steam reformer model defined in section 4.1.3 is adopted. This model developed a dynamic version of model defined in section 4.1.2; the zonal approach to the affect of the variation of the ratio of burners to tubes in the furnace.

A major operational disturbance which could significantly affect the furnace balance is a composition change of burner feedstock; highlighted in chapter 4. This situation could arise for a number of reasons, however, we will consider that the fuel gas is supplied from a gas field and that the steam reformer operators have been informed of the impending step change. Over an operating period of one hour, the specific gravity can be considered to shift to a new operating condition, see figure 6.1.4.

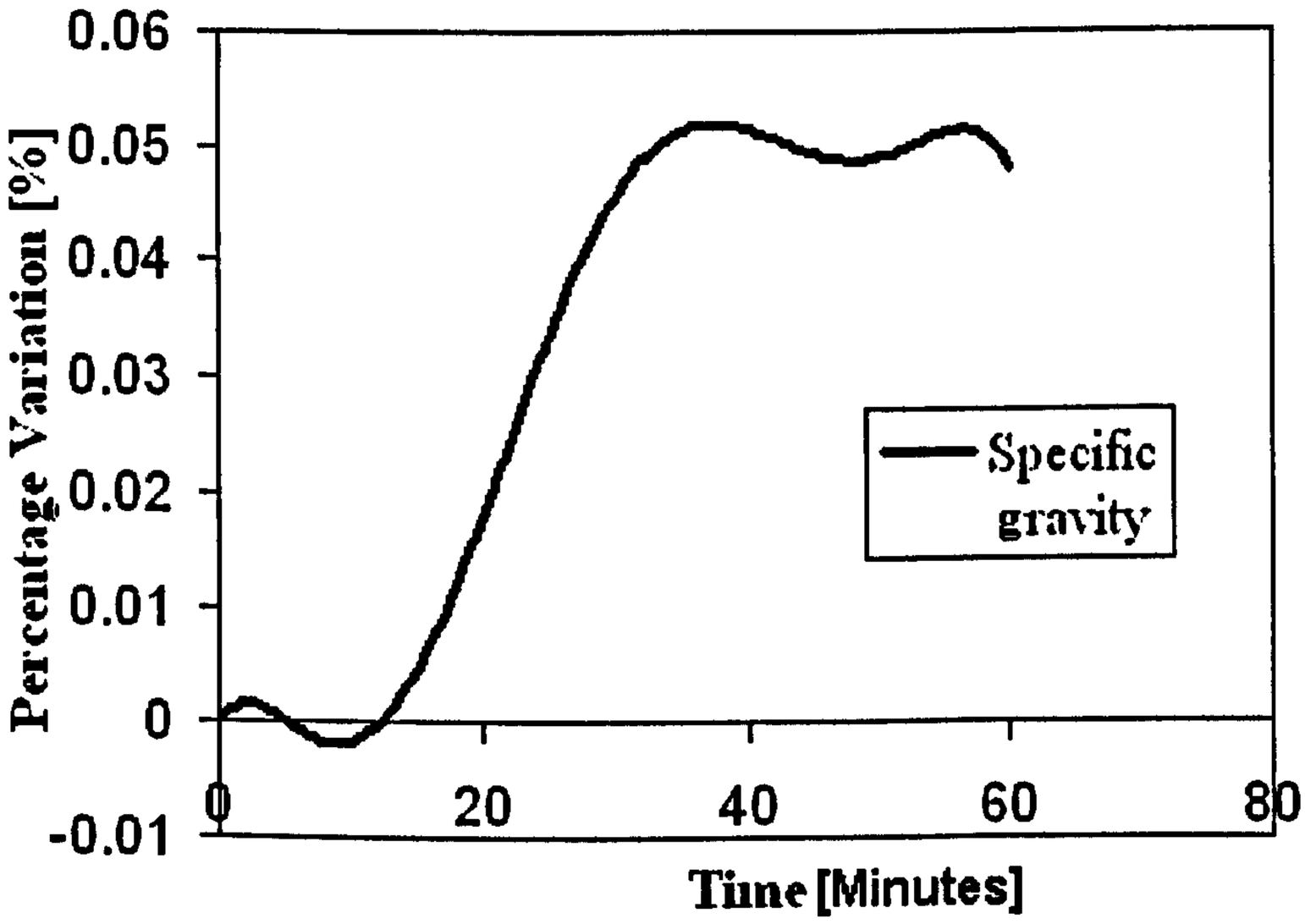

Figure 6.1.4 Burner fuel specific gravtity profile

Zidan (2001) reports that industrial practice is to respond with initially manual feedforward contol, of reducing the burner rates, followed by staged manual feedback control (Figure 6.1.5). Optimisation of the burner profile to limit the maximum heat flux

and tube wall temperature produces an "ideal" response (Figure 6.1.5). The optimisation problem can be expressed as,

$$\text{Min } \textit{Difference}(u) = \int \text{('Outer Zone' Outlet Pressure} - \text{'Inner Zone' Outlet Pressure)}^2 \; \text{dTime}$$

where $\mathbf{u}$ = { Fuel Gas Burner Rate}

Tube Wall Temperature < Tube Wall Temperature Limit

Heat Flux < Heat Flux Limit

As for the optimisation study in section 6.1.1, the successive quadratic programming method is employed for this optimisation problem based on the recommendations from the previous discussion in chapter 2. The practice of initialising the optimisation from several points to avoid arriving at the local optima is also employed. The optimisation was initialised from the 'normal' fuel gas burner rate, at the extremes of half and double the fuel gas burner rate, at the optimal point arrived at from the extremes and then at intervals of ten percent between the extremes. For each initialisation point, the optimisation yielded the same result, within numerical tolerance, without anomaly.

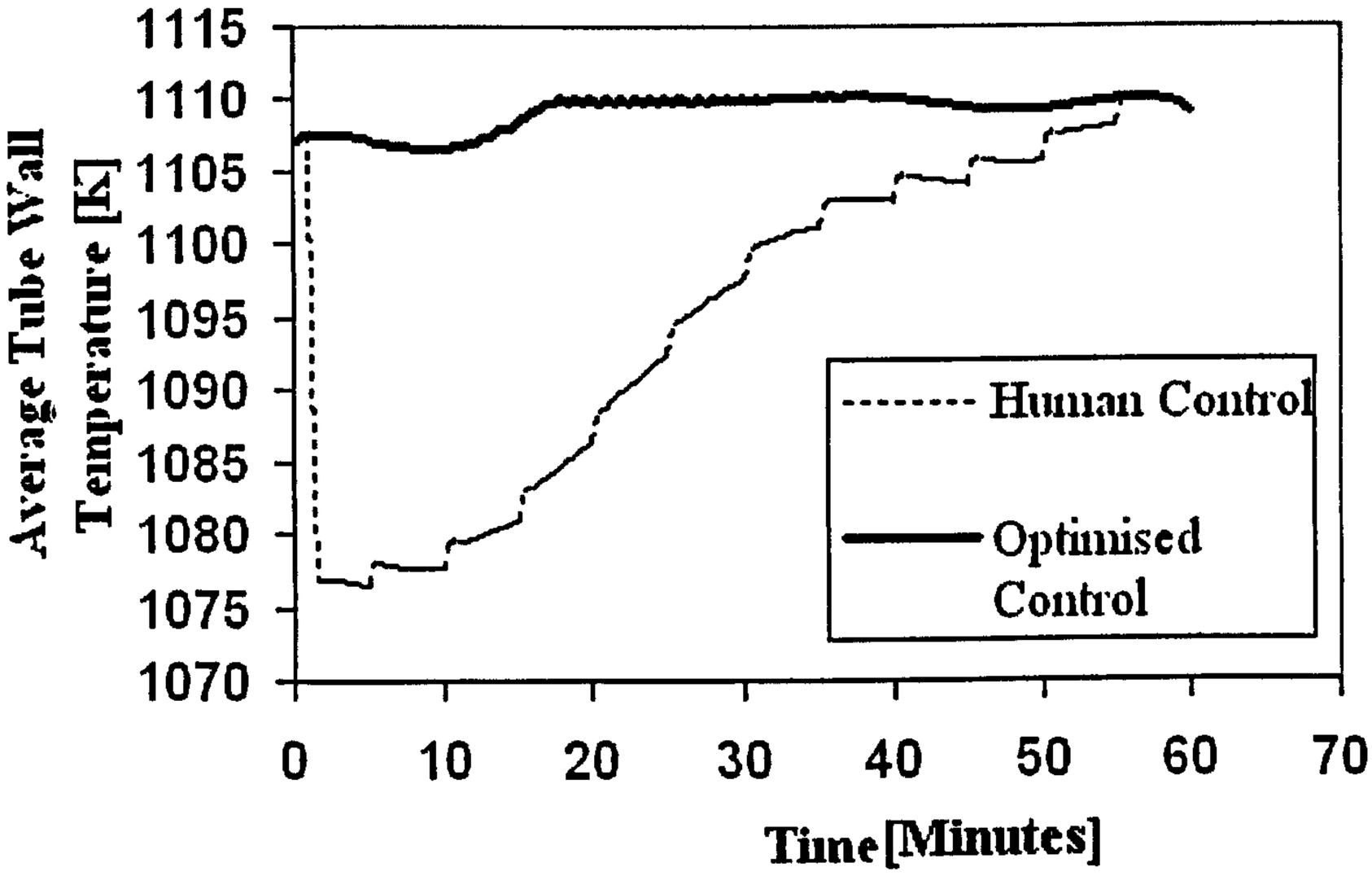

Figure 6.1.5 Response of Average Tube Wall Temperature to variation in the fuel specific gravity

The optimised strategy clearly offers the best strategy as the effect on the outlet composition is limited, see figure 6.1.6. Throughout the period of change of burner fuel composition the 'balance' of the furnace deviates only slightly and produces a very limited scope for adjustment of the burner profile across the zones.

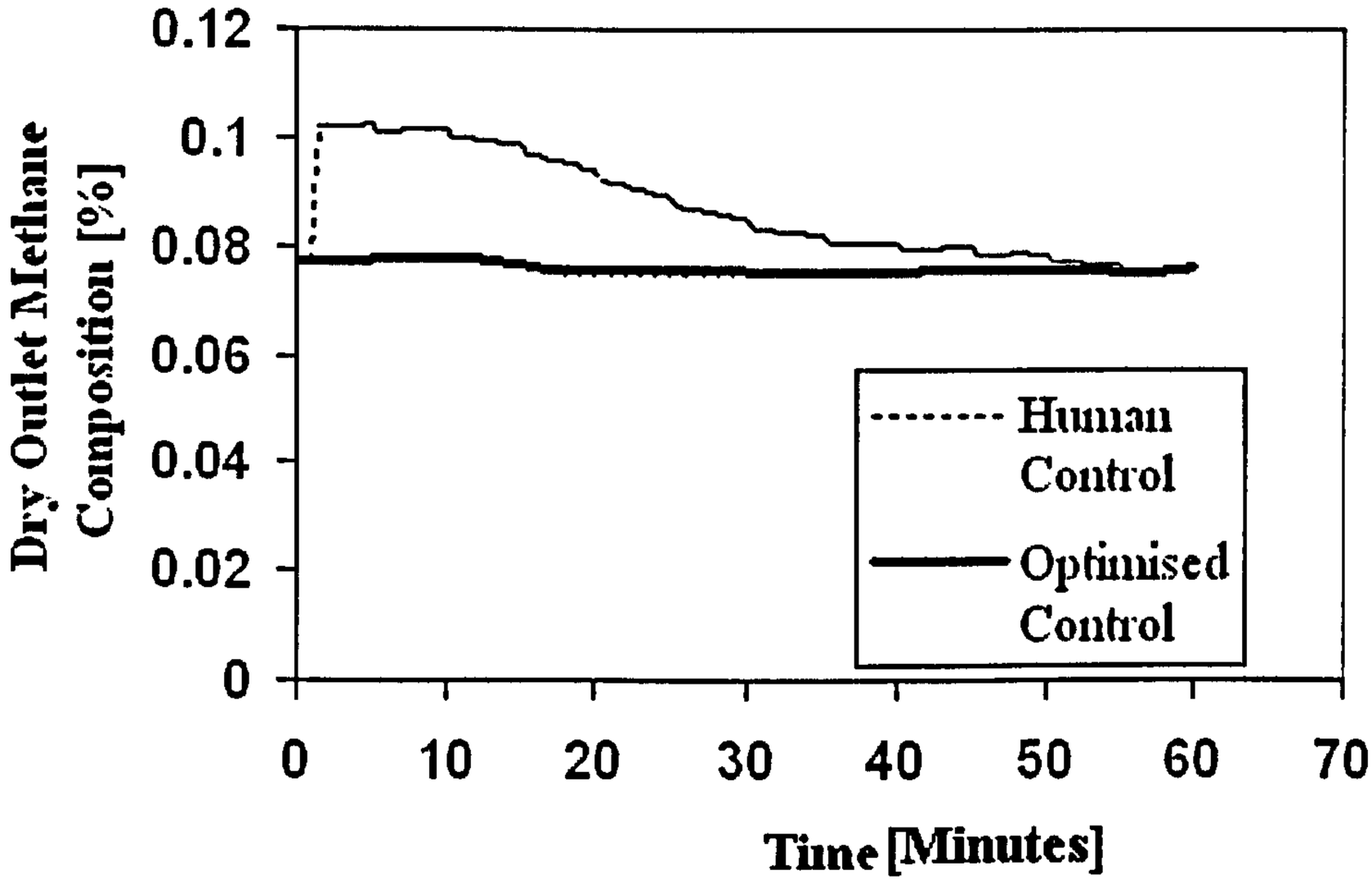

Figure 6.1.6 Response of outlet methane composition to variation in the fuel specific gravity

For typical operational changes experienced by a primary steam reformer, optimisation of the reactant gas distribution and burner rate not only reduced the difference of the tube wall temperature profiles but also limited the impact of the operational shifts. This study has demonstrated both that furnace balancing is a significant operational condition that requires consideration throughout a process campaign and also vindicates the industrial practice of furnace balancing initially via reactant gas distribution and then via burner adjustment. Defining an average reformer tube would not allow the assessment of the furnace performance.

6.1.3 Conclusions

Optimisation was successfully performed on significant operational parameters for top-fired primary steam reformers, which has been overlooked by other optimisation studies. These results concurred with industrial observations for both steady-state and dynamic representations and showed the potential to be developed for real time optimisation. Although comparisons were not made with other techniques, for both cases, of differing structure, the successive quadratic programming technique demonstrated notable performance in arriving at an optimal solution, on a par to that suggested in the discussions in chapter 2.

6.2 Secondary Steam Reformers

As discussed previously, see chapter 3, the secondary steam reformer is the last stage of possibly a multiple stage steam reforming section for several important production schemes. Secondary steam reformers partially oxidise their feedstock of primary steam reformer products to provide the energy to convert the remaining feedstock and combustion products to a mixture of hydrogen and carbon oxides of increased purity; also can act as the introduction point for elemental nitrogen if air used as oxidant in the burner. Secondary steam reformers are often considered as two sections, a combustion section and a reactor bed section, with the simplest form being a coaxial jet burner, see figure 6.2.1.

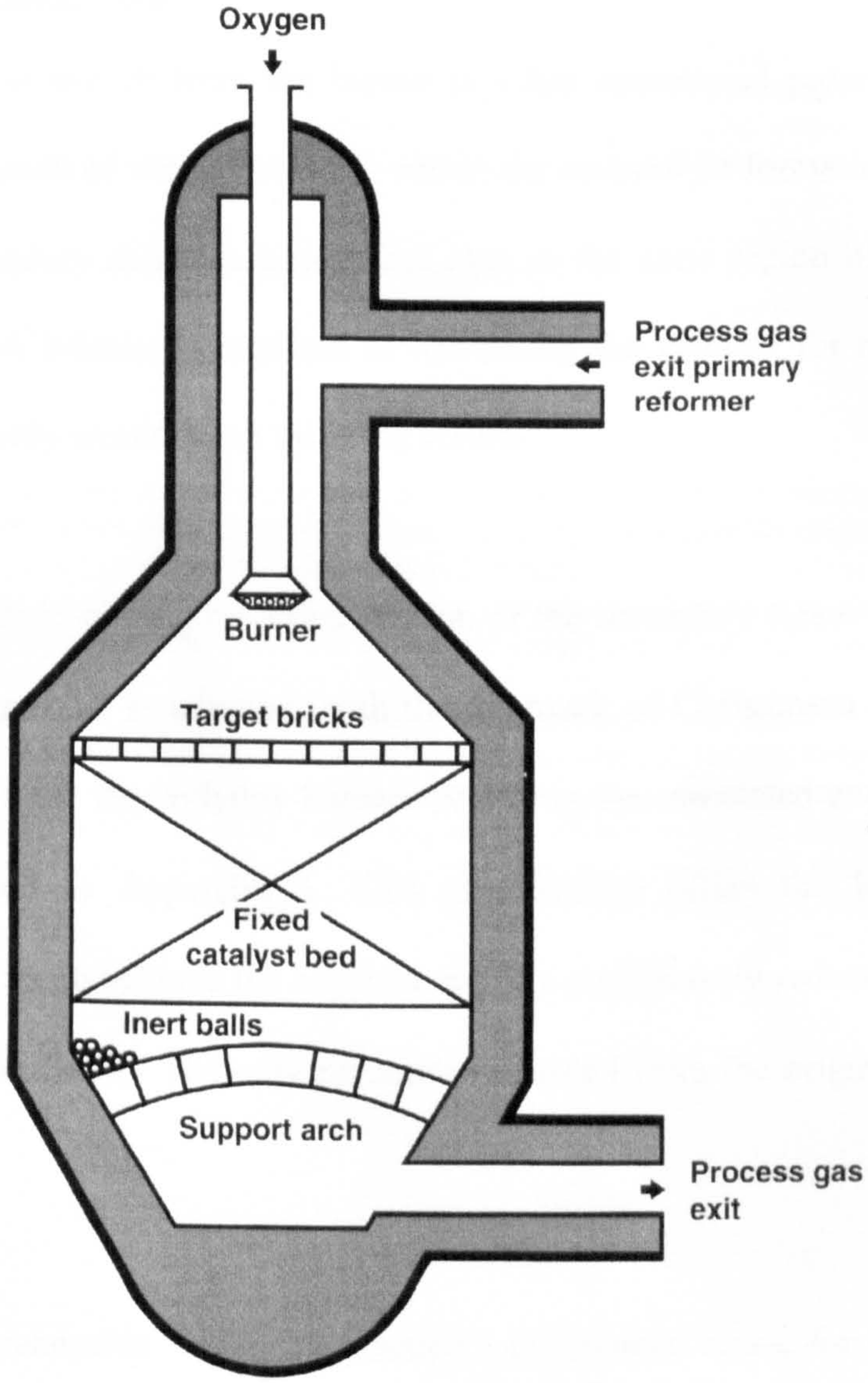

Figure 6.2.1. Layout of a Secondary Reformer. [Farnell (1993)]

In contrast to the primary steam reformer there is a lack of optimisation studies of the secondary steam reformer, with only one other reported optimisation study and the details of this study are at best vague. This situation is primarily due to the perception, referred to in chapter 2, that CFD is not suitable for optimisation studies, however, as was the case in the past for less intricate modelling this perception is being challenged. Two examples are given to demonstrate the potential of optimisation for secondary steam reformers when fluid flow analysis is included.

6.2.1 Burner Velocity Work

The jet velocity of the air from the burner is a key operational parameter, as it will determine the amount of mixing not only within the co-axial jet formation region, in the neck of the secondary steam reformer, but also in the cone region of the secondary steam reformer. A balance is required as optimising the velocity for mixing in either region independently would reach differing results.

For this optimisation study a modified version of the secondary steam reformer model defined in section 4.2.2 is adopted, with the approach of Christensen et al. (1994) to chemical reaction and the enthalpy balance replacing the associated expressions; a full listing is included in Appendix 3. This modification offers the least impact on simulation accuracy to achieve the requirement of a significantly reduced solution time for practical optimisation. The only parameter adjusted from the original model is the burner velocity.

Defining a comprehensive "objective function", in financial terms, for the implications of adjusting the burner velocity would create the unwanted situation of a highly complex response to the burner velocity, discussed in chapter 2, which will increase the likelihood of achieving a sub-optimal result. So the unit performance target of yielding the greatest performance from the catalyst bed was adopted, within practical limits on the burner velocity and a fixed mass flux constraint. The ideal performance from the catalyst bed occurs when an even temperature and compositional distribution occurs across the inlet of the catalyst bed. The optimisation problem can be expressed as,

$$\text{Min } \textit{Difference}(\mathbf{u}) = \Sigma(X(i) - X(i)_{mean})^2 + \Sigma(T - T_{mean})^2$$

$$\text{Burner Mass flux} = \text{Initial Burner Mass Flux}$$

where $\mathbf{u}$ = { Normalised Burner Velocity}; subject to $0.8 < \mathbf{u} < 1.2$

X(i) is the inlet composition for chemical species i to the catalyst bed

T is the inlet temperature to the catalyst bed

The Newton-Raphson method is employed, with the recommendations for non-exact derivatives of Fletcher (1987) highlighted in chapter 2, for this optimisation problem.

As for the cases from section 6.1, in order to avoid arriving at the local optima rather than the global optima the optimisation was initialised from several locations. The optimisation was initialised from the 'normal' burner velocity and then at the extremes of the burner velocity, see Table 6.2.1.

Table 6.2.1: Optimisation results from multiple points of initialisation

Run Number	Initialisation Point	Optimal Point
1	1	0.912
2	0.8	0.836
3	1.2	1.05

This optimiser initially appears to find a 'unique' optimum, however, when the practice of initialising the optimisation from several points was employed, the optimum was found to be inconsistent. These multiple optima are due to the rugged response to a change in burner velocity, or "noise" of the objective function.

In addition to the inconclusive optima, the benefit of the optimisation is also of concern as the improvement in the reduction of variation at the catalyst bed inlet is not significant in comparison to the accuracy of the simulation results, see Table 6.2.2. This cost/benefit consideration for optimisation with computational fluid dynamics has increased the popularity of optimisation techniques such as Genetic Algorithms, which offer no mathematical guarantee of the achieving the optima, however, will highlight the general area of the optimum conditions often with lower computational costs.

Table 6.2.2: Radial variation objective function results from each optimisation run

Run Number	Optimal Point	Objective Function
1	0.912	3567.23
2	0.836	3606.25
3	1.05	3743.23

Out of interest the optimisation was changed so that the mass flux constraint was relaxed. This optimisation case yielded what initially appeared as strange inclinations, with the optimiser continually minimising the inlet velocity to zero; suggesting that a lower velocity created more mixing! Logically the optimiser is correct, as if there is only one inlet to the reactor, then the inlet of the catalyst bed will have no variation of composition or temperature; this phenomena of poor objective function formulation was highlighted in chapter 2.

This optimisation study of the burner velocity has demonstrated the key issues for optimisation with computational fluid dynamics. The main issues are the difficulty that the often irregular response of the objective function posses to finding a global optimum and the balance of the benefit of any such optima against the simulation accuracy. These issues are fundamental to the lack of optimisation studies with computational fluid dynamics and the move towards less mathematically rigorous techniques for optimisation.

6.2.2 Ratio of Length of Cylindrical Zone to Height of Cone Zone.

As for this optimisation study reported in 6.2.1 the same modified version of the secondary steam reformer model defined in section 4.2.2 is adopted. The only parameter adjusted from the original model is the ratio of the length of the neck to the height of the cone section.

As was discussed in section 6.2.1 and chapter 2, the definition of comprehensive objective functions, in financial terms, are more likely to achieving a sub-optimal result as their response to parameters changes can be highly complex; this can also be considered as the objective function is too noisy and the optimiser would not be able "to see the wood for the trees". Instead as for the optimisation in section 6.2.1 the unit performance target of yielding the greatest performance from the catalyst bed was adopted. The optimisation problem can be expressed as,

Min *Difference*(**u**) = $\Sigma(X(i) - X(i)_{mean})^2 + \Sigma(T - T_{mean})^2$

Velocity magnitude across the bed inlet < Maximum velocity to avoid horizontal displacement of the catalyst in the catalyst bed

where **u** = { Ratio of Height of Cone and Cylindrical sections}; subject to $0.9 < \mathbf{u} < 1.1$

X(i) is the Inlet composition for chemical species i

T is the Inlet Temperature

The Newton-Raphson method is employed, with the recommendations for non-exact derivatives of Fletcher (1987) highlighted in chapter 2, for this optimisation problem. This relocation of the cone / cylinder intersection involved the complicated task of balancing the mixing for both sections to maximise the overall mixing performance. As was highlighted in chapter 3, to avoid excessive movement of the catalyst in the catalyst bed, there is a maximum allowable velocity across the top of the catalyst bed.

As for the previous optimisation cases, in order to avoid arriving at the local optima rather than the global optima the optimisation was initialised from several locations. The optimiser, initialised from several locations, reached a consistent optimum at the maximum tube length limit, which coincidentally from the data appears to be at approximately a minimum velocity magnitude across the catalyst bed inlet, see Table 6.2.3 and Table 6.2.4.

Table 6.2.3: Optimisation results from multiple points of initialisation

Run Number	Initialisation Point	Optimal Point
1	1	0.963
2	0.9	0.956
3	1.1	0.965
4	0.960	0.961

Table 6.2.4: Optimisation results from multiple points of initialisation

Ratio of Height of Cone and Cylindrical sections	Maximum Relative Velocity Magnitude across the catalyst bed inlet
0.9	1.745
0.93	1.230
0.961	0.967
1	1
1.1	1.211

With both the constraints on the ratio and the maximum velocity ignored, the optimiser continued to increase the tube section length until the cone section is totally removed. However, by this stage the maximum velocity constraint is significantly violated. This identifies that if the maximum velocity constraint could be overcome the geometry of the secondary steam reformer could be considerably simplified. This seems to suggest that the cone section was introduced in the design for the secondary steam reformers to correct this issue of catalyst movement.

The ratio of the cylindrical section length to the cone section height is an interesting design issue. The optimisation study clearly demonstrates that optimisation with computational fluid dynamics can not only develop practical results i.e. quantifiable, but also offer a more in depth understanding of the issues within a process which can in turn generate novel design changes. This is an interesting contrast to the previous optimisation case.

6.2.3 Conclusions

Despite the added complexities with the secondary steam reformer system and the employment of optimisation with computational fluid dynamics, some success was achieved in the optimisation studies.

Although the first case only served to highlight the main issues of optimisation with computational fluid dynamics, the secondary steam reformer design has been refined over several decades and the burner velocity has probably been optimised through trial and error to at least the general area of the global optimum. Hence the limited benefit shown in optimal results.

Due to the impracticality of adjusting the ratio of the length of the cylindrical section to the height of the cone section, this probably will have seen less adjustment over the development of the designs and hence the scope of optimisation highlighted in the second case. This optimisation case also clearly highlighted the impact of the velocity limit across the top of the bed.

Although comparisons were not made with other optimisation techniques, the Newton-Raphson method demonstrated that within the confidence of the model accuracy the optimal region can be found. This follows the observations of other authors, that until the hardware is capable of optimising computational fluid dynamics models of notable accuracy less mathematically robust techniques can be employed.

6.3 Conclusions

Overall the performance of the optimisation techniques recommended in chapter 2 were shown to be positive, despite the varying nature of the processes and the models employed, and a number of the issues highlighted in chapter 2 were exhibited. Although concerns still remain with optimisation on computational fluid dynamics models these are diminishing as the model packages are evolving. These cases clearly demonstrate that even for mature processes such as the primary and secondary steam reformers there still remains scope for optimisation.

Chapter 7

Conclusions and Recommendations

Computer modelling is both a very powerful and sometimes highly complex tool, which should be used cautiously as it does not come without pitfalls and challenges. These tools have over recent years seen great advancement in terms of their capabilities and notable progress towards addressing key modelling issues. Optimisation, as for modelling, also has a number of key issues, however, the potential benefits of optimisation are immense. With the advancement in computer power, however, although more powerful optimisation techniques have been developed, the ultimate prize of a universal optimiser is still illusive, with techniques being chosen to suit the circumstances.

Steam reforming is currently, and will remain for some time, a significant industrial process, due to the importance of synthesis gas and hydrogen. No doubt the process will develop, however, the trend appears to be towards the combined reformer structure, which appear to be predominately based on secondary steam reformers. Despite previous research resolving some of the modelling complications for steam reformers, this is by no means a 'closed book'.

Several models of differing levels of complexity were developed which have successfully modelled both steam reformer systems, in terms of the overall process. Through this development the modelling of all the key phenomena of chemical engineering were evaluated for their representation in the steam reformer systems; the phenomena included fluid flow, heat transfer, mass transfer and chemical reaction. As is the crux of any engineering problem, compromises were required in the modeling, with some improvements implemented on previously perceived 'best practices'. Additionally, the purpose of simulation was expanded from the 'basics' of validation to include assessment of previously overlooked or indistinct unit issues.

For the primary steam reformers a reasonably close agreement to industrial data for the overall process was achieved at various levels of modelling complexity. Most notably through these versions the compromise of two-zone approach was developed and demonstrated assessment of parameters ignored by other models, both in steady-state and dynamic form. Despite the logistical limitation on the three-dimensional model, the development work appears to have resolved most of the key modelling issues.

For the secondary steam reformer system, as for the primary steam reformer models, a reasonably close agreement to industrial data for the overall process was achieved at various levels of modelling complexity. Despite the lack of a complete set of validation data, the model evolution has allowed some analysis of the modelling issues, while developing the only three-dimensional model secondary steam reformer model in open publication.

Overall the development of the primary and secondary steam reformer models, highlighted such modelling topics as initialisation, numerical solvers, mesh sensitivity, scaling of variables and model partition amongst others.

The optimisation studies both demonstrated a positive performance for the identified optimisation techniques and demonstrated a number of the issues associated with optimisation, although optimisation with computational fluid dynamics models is still controversial. Clearly even for mature processes such as the primary and secondary steam reformers there still remains scope for optimisation.

Despite the progress reported in this thesis, there still remains scope for further research for both primary and secondary steam reformers.

For the primary steam reformer, when the logistical constraints are overcome, the fully inter-linked furnace and reactor model should be employed as this will significantly improve the model accuracy and allow for a comprehensive assessment of the understanding of the process; including assessment of assumptions in simplified models such as the two-zone approach. Aside from the furnace modelling development another improvement should be to tackle the issues of the heavier hydrocarbons than methane that exist in 'industrial quality methane' and the kinetic representation of carbon depositions.

For the secondary steam reformers, although the systems are similar the research is not as widespread as for the primary steam reformers. .Primarily further assessment is required for the reaction schemes and kinetics both above and within the catalyst bed. A complete data set is still required for rigorous model validation.

With these recommended developments there is further scope for optimisation cases for both the primary and secondary steam reformers. Additionally, the benefit of optimisation with computational fluid dynamic models is still disputed due to concerns over accuracy and cost in terms of time to undertake such a study. Developments in these areas are required for an acceptance of fluid flow optimisation in the process industries.

Appendix 1

Analysis of the influence of pressure on gas viscosity

As is shown in Figure A1.1 that even at the highest pressures and lowest temperatures within the operational range of steam reformers, the effect of pressure on viscosity may be neglected.

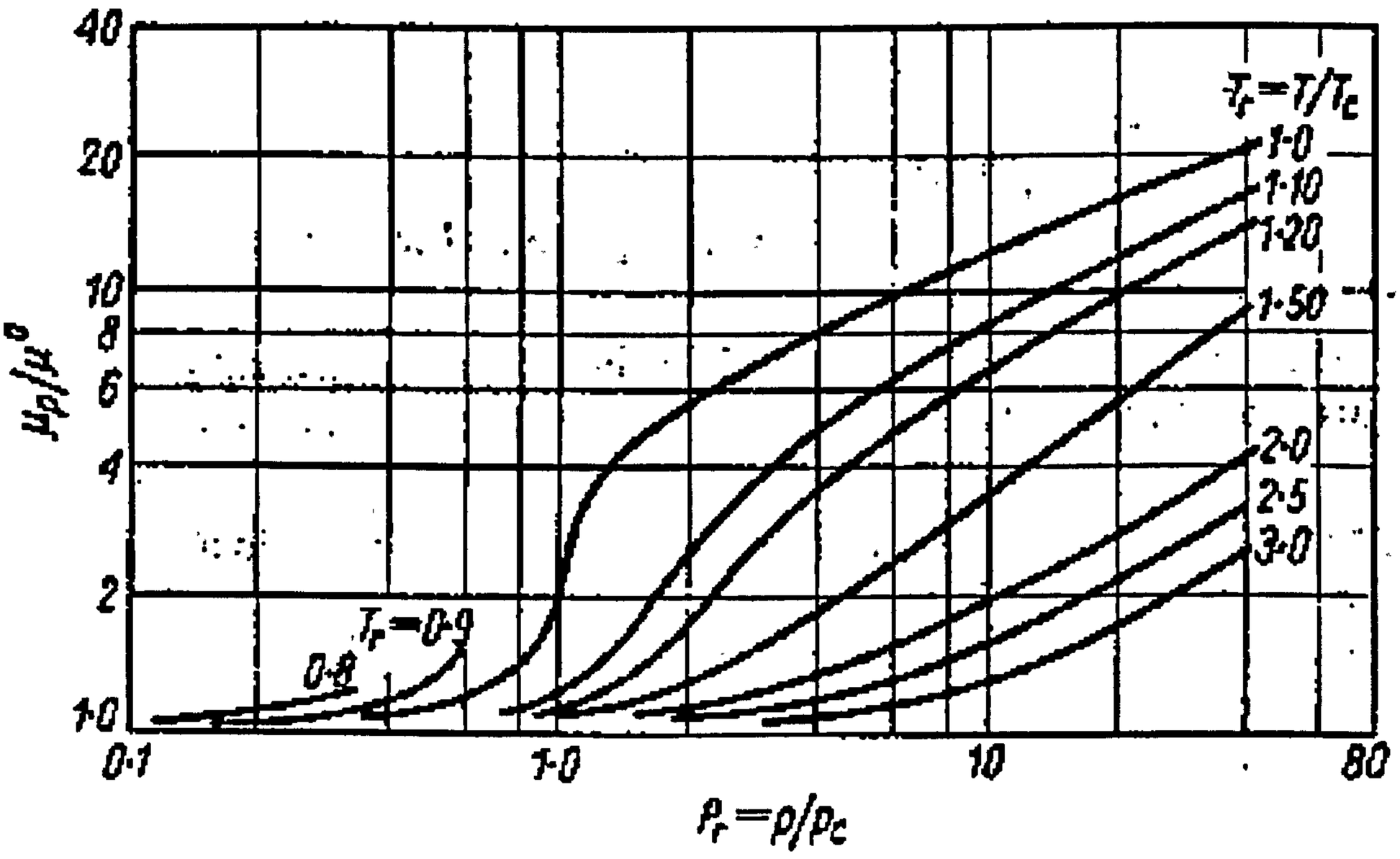

Figure A1.1: Ratio of the viscosity at high pressure to the viscosity at moderate pressure and at the same temperature, as a function of T_r and P_r: Position of the chemical species involved. [Bretsznajder, 1971]

Analysis of the influence of pressure on gas conductity

As is shown in Figure A1.2 that even at the highest pressures and lowest temperatures within the operational range of steam reformers, the effect of pressure on conductivity may be neglected.

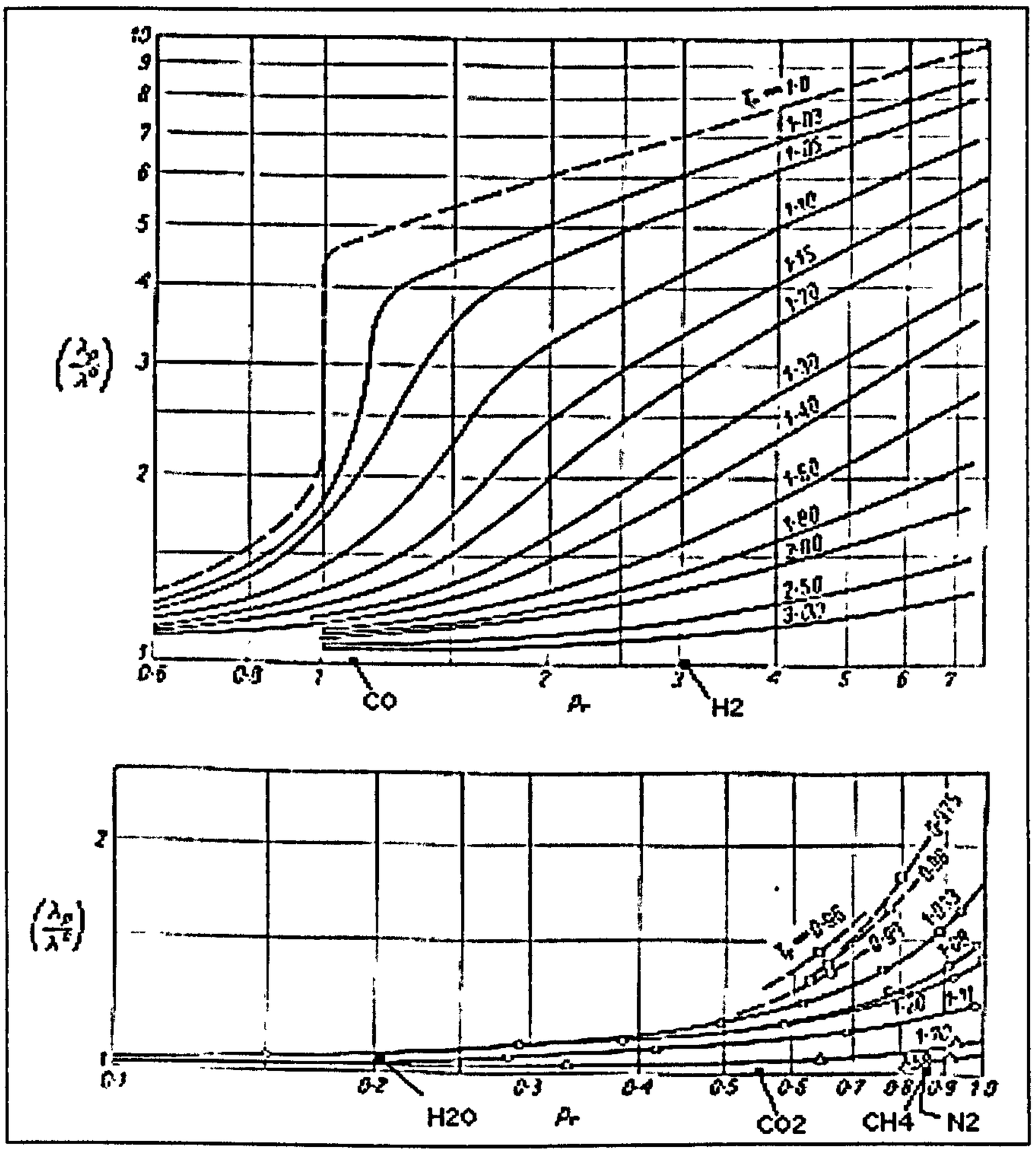

Figure A1.2: Ratio of the conductivity at high pressure to the conductivity at moderate pressure and at the same temperature, as a function of T_r and P_r: Position of the chemical species involved. (Bretsznajder, 1971)

Analysis of the influence of pressure on heat capacity

Using Data from Hilsenrath (1960) the influence of pressure on the heat capacity of the components in the steam reformer system are shown in figures A1.3 – A1.7.

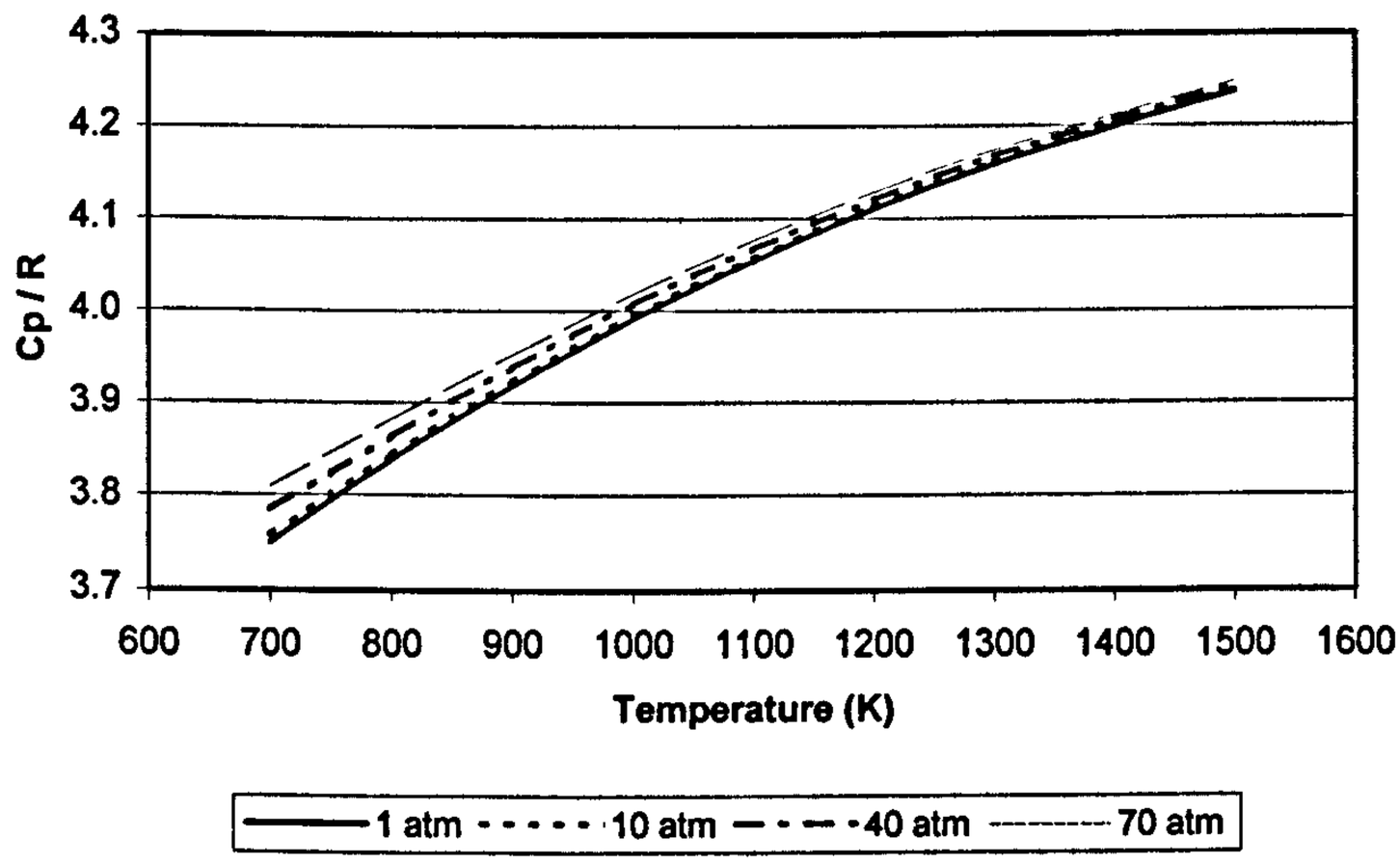

Figure A1.3: Influence of pressure on heat capacity of CO

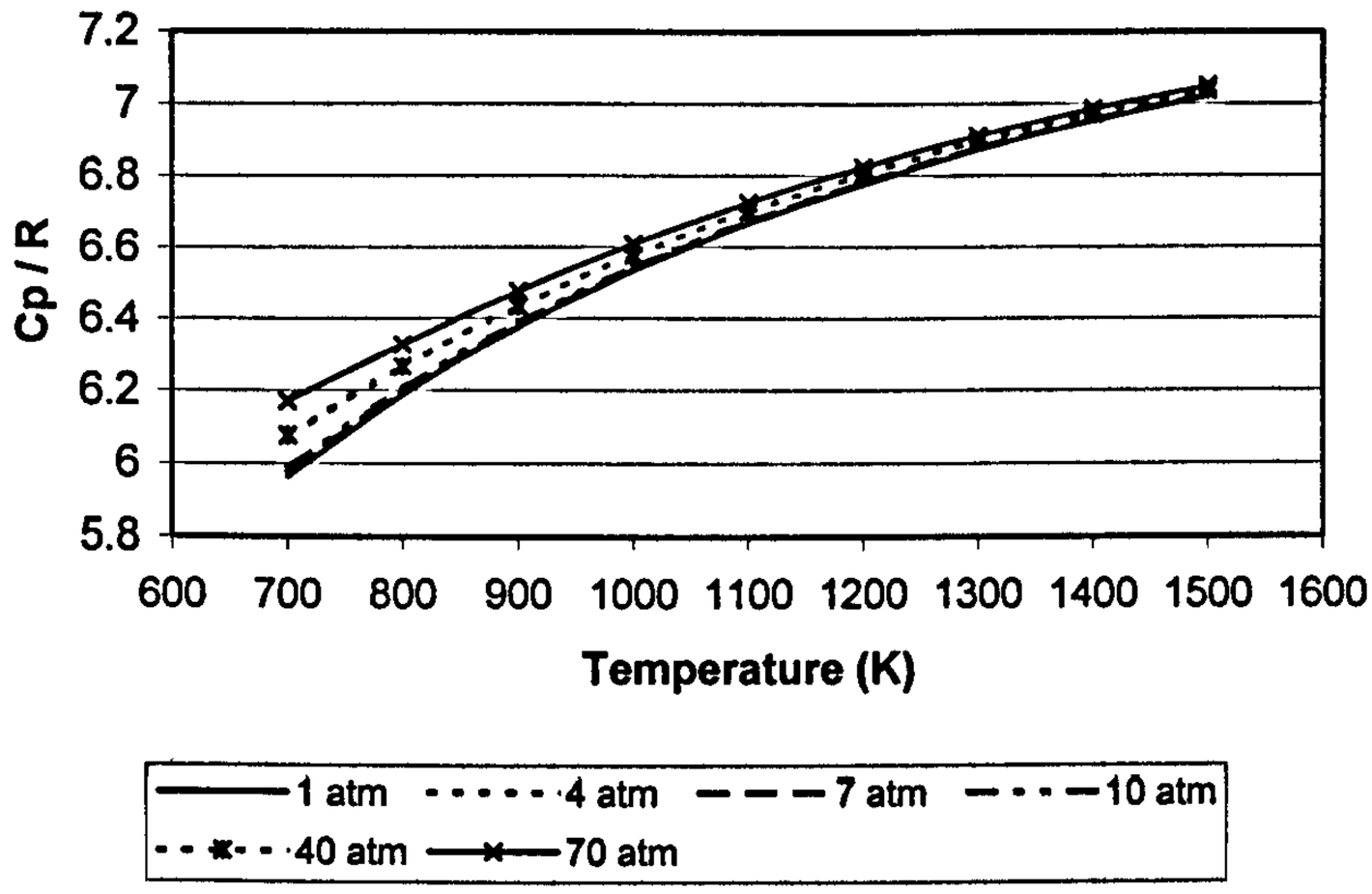

Figure A1.4: Influence of pressure on heat capacity of CO_2

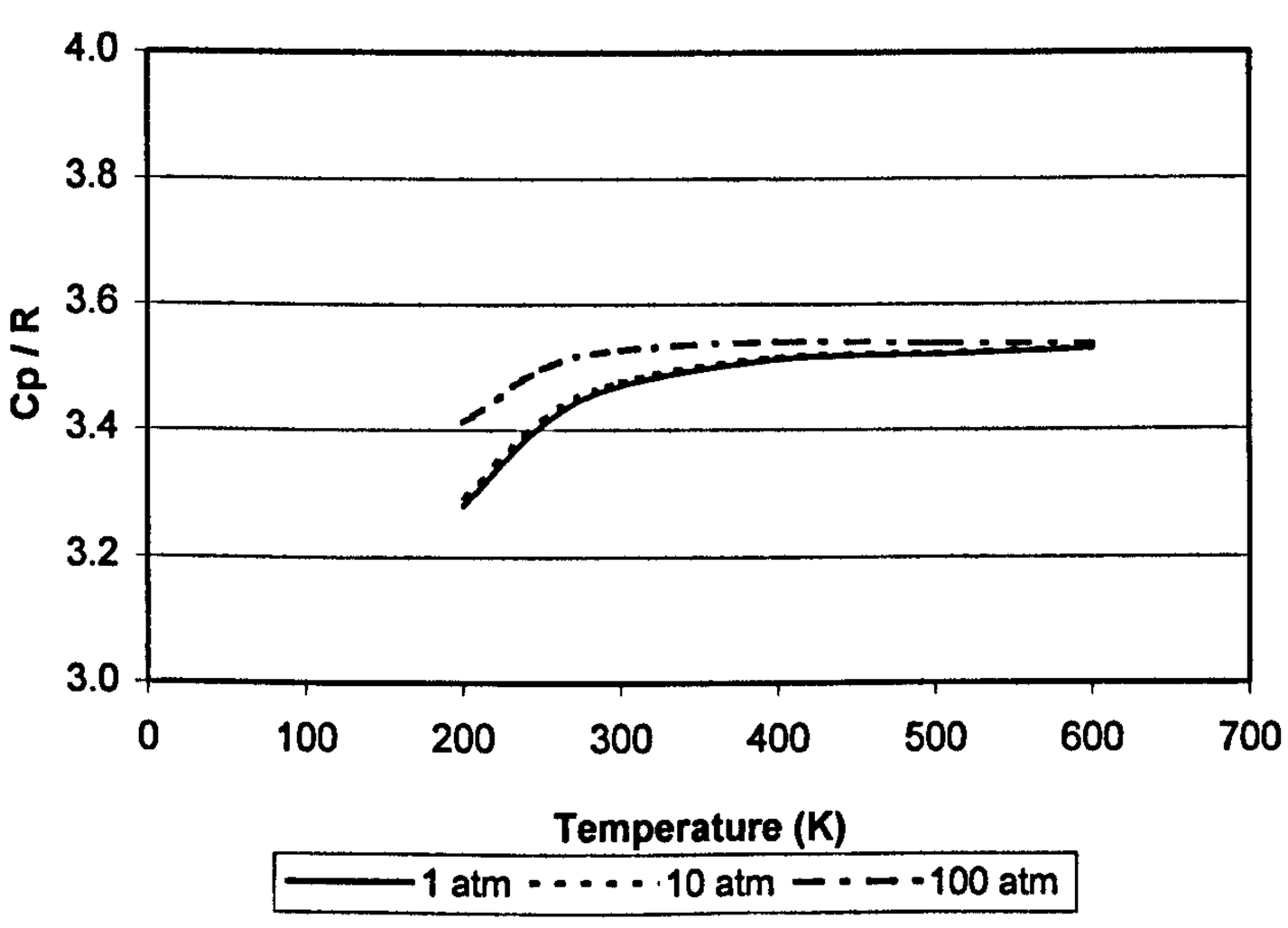

Figure A1.5: Influence of pressure on heat capacity of H_2

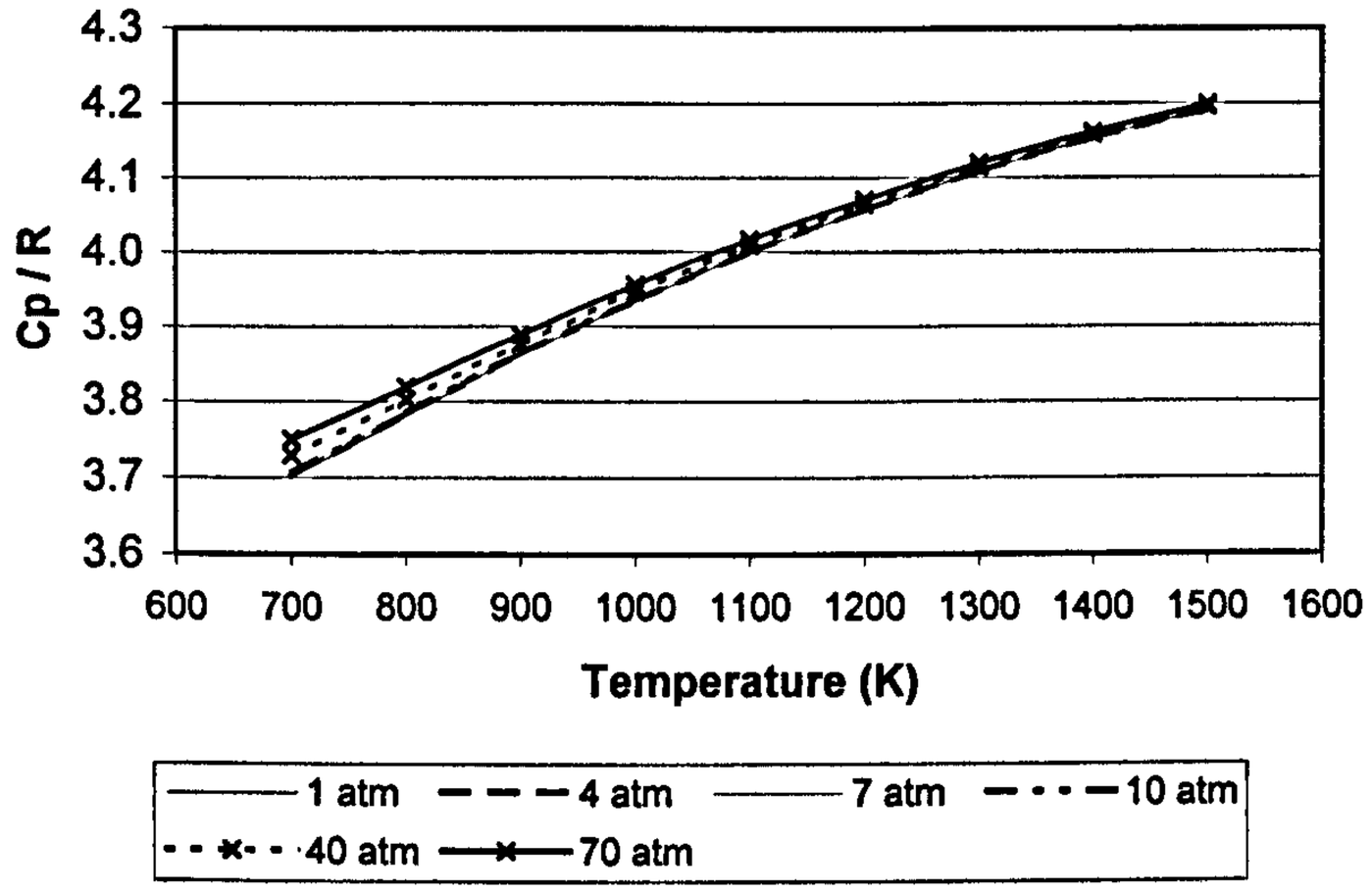

Figure A1.6: Influence of pressure on heat capacity of N_2

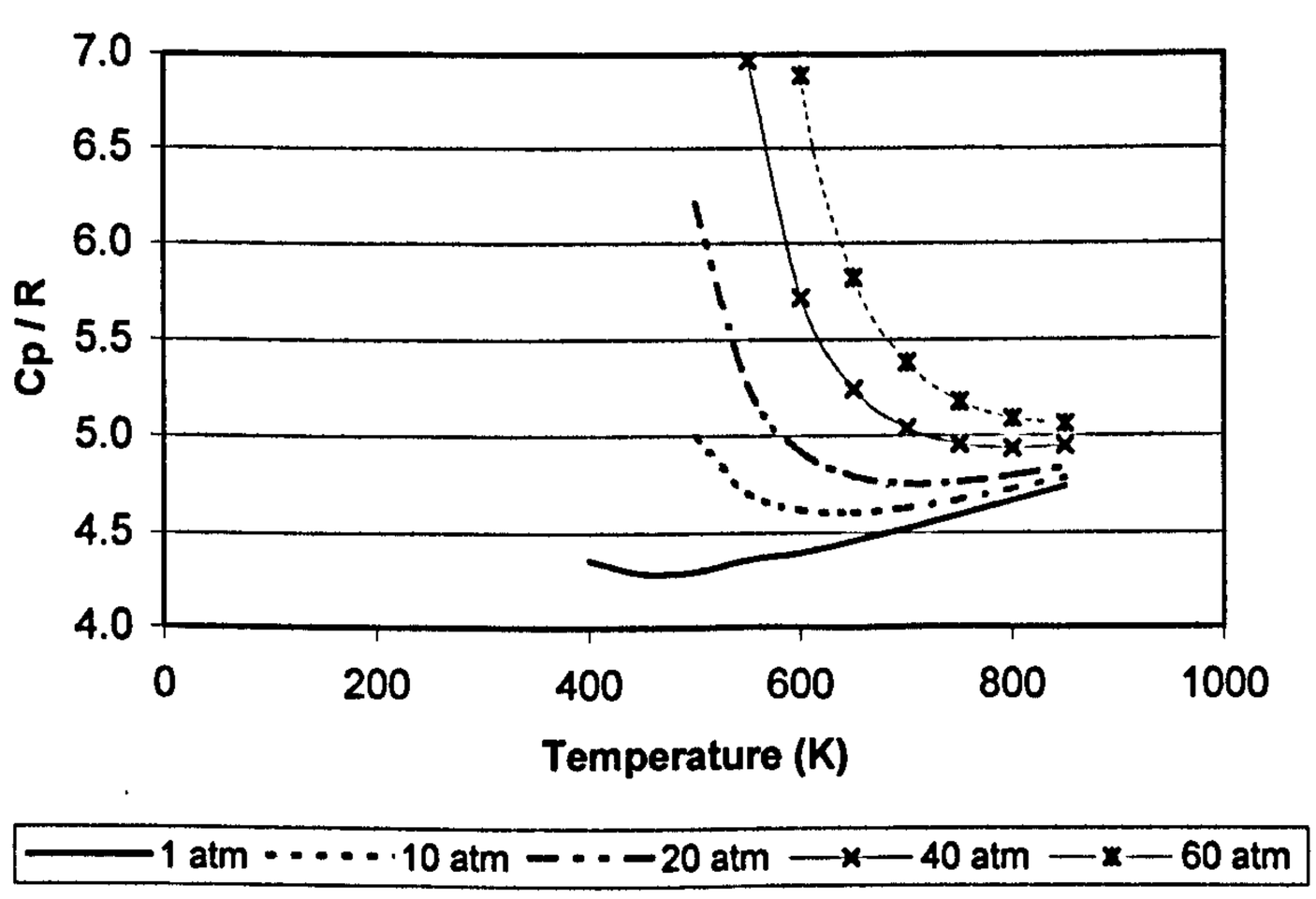

Figure A1.7: Influence of pressure on heat capacity of Steam

Appendix 2

Values of the mixture viscosity according to different expressions:

For the viscosity of the gas mixture, different expressions can be found in the literature. The Wilke expression is reported in general texts by Reid et al. (1977) and Perry et al. (1997)

$$\mu_m = \sum_{i=1}^{NC} \frac{x_i \mu_i}{\sum_{k=1}^{NC} x_k \phi_{ik}} \quad \text{, where} \qquad \text{(A2.1)}$$

$$\phi_{ik} = \frac{\left[1+\left(\frac{\mu_i}{\mu_k}\right)^{0.5}\left(\frac{M_k}{M_i}\right)^{0.25}\right]^2}{\left[8\left(1+\left(\frac{M_i}{M_k}\right)\right)\right]^{0.5}} \qquad \text{(A2.2)}$$

while Alatiqi et al. (1989) reported the following expression as part of a primary steam reformer model

$$\mu_m = \sum_{i=1}^{NC} x_i \mu_i \qquad \text{(A2.3)}$$

and Davies (1971) reported the following expression as part of a primary steam reformer model

$$\mu_m = \frac{\sum_{i=1}^{NC} x_i \mu_i M_i^{0.5}}{\sum_{i=1}^{NC} x_i M_i^{0.5}} \qquad \text{(A2.4)}$$

All three expressions give very similar results when the molar fraction of hydrogen is very small at the reactor inlet, see Table A2.1. However, at the reactor outlet when the hydrogen composition increases, the differences are noticeable, see Table A2.1. and a rigorous equation like (A2.1) must be used.

	equation A2.1	equation A2.3	equation A2.4
Viscosity of the mixture at the inlet of the tube ($N.s/m^2$)	2.5753E-05	2.5827E-05	2.5900E-05
Viscosity of the mixture at the outlet of the tube ($N.s/m^2$)	3.5141E-05	3.2583E-05	3.7114E-05

Table A.2.1. Values of the mixture viscosity according to different expressions.

Values of the mixture conductivity according to different expressions:

For the gas conductivity of the mixture, Bretsznajder (1971) reports there are a number of different proposed expressions. Reid et al. (1977) recommends the Wassiljewa expression.

$$\lambda_m = \sum_{i=1}^{NC} \frac{x_i \lambda_i}{\sum_{k=1}^{NC} x_k A_{ik}} \qquad \text{(A2.5)}$$

In this expression, the approximation of Mason and Saxena reported by Reid et al. (1977) is applied, where $A_{ik} = \phi_{ik}$ in the same form as equation A2.2.

Alatiqi et al. (1989) reported the following expression as part of a primary steam reformer model

$$\lambda_m = \sum_{i=1}^{NC} x_i \lambda_i \qquad \text{(A2.6)}$$

$$\lambda_m = \frac{1}{\sum_{i=1}^{NC} \frac{x_i}{\lambda_i}} \qquad \text{(A2.7)}$$

The Brokaw expression is an average of the two following expressions, A2.6 and A2.7, where the influence of hydrogen is taken into account by A2.9.

$$\lambda_m = a\left(\sum_{i=1}^{NC} x_i \lambda_i\right) + (1-a)\left(\frac{1}{\sum_{i=1}^{NC} \frac{x_i}{\lambda_i}}\right) \qquad \text{(A2.8)}$$

$$a = 0.40705 x_{H_2}^2 + 0.04072 x_{H_2} + 0.33274 \qquad \text{(A2.9)}$$

Davies (1971) reported the following expression as part of a primary steam reformer model

$$\lambda_m = \frac{\sum_{i=1}^{NC} x_i \lambda_i M_i^{0.333}}{\sum_{i=1}^{NC} x_i M_i^{0.333}} \qquad \text{(A2.10)}$$

As was demonstrated for the viscosity, the expressions give similar results at the inlet of the steam reformer, however, significant differences occur when the fraction of hydrogen increases. Hence the rigorous expression A2.5 recommended by Reid et al. (1977) was adopted.

	Mixture conductivity at the inlet (W/m.K)	Mixture conductivity at the outlet (W/m.K)
equation A2.5	0.0721194	0.31593
equation A2.6	0.0712831	0.250702
equation A2.7	0.0673775	0.147878
equation A2.8	0.068677	0.190621
equation A2.10	0.0709234	0.189851

Table A.2.2. Values of the mixture conductivity according to different expressions.

Appendix 3

Equations for model [section 4.1.1]

Steam Reformer Tubes

$$\frac{\partial F_i}{\partial z} = A\rho \sum_{1}^{nc} \left(Nu_{i1} R_1 + Nu_{i2} R_2 \right)$$

$$R_1 = 127\sqrt{P} \exp\left(\frac{-8780}{R_g T}\right)\left(x_{CH_4} - \frac{x_{H_2}^3 x_{CO} P^2}{K_{eq1} x_{H_2O}}\right)$$

$$R_2 = \exp\left(\frac{-13880}{R_g T} + 8.23\right)\sqrt{P}\left(x_{CO} - \frac{x_{H_2} x_{CO_2}}{K_{eq2} x_{H_2O}}\right)$$

$$K_{eq1} = \exp\left(\frac{A_{K11}}{T} + A_{K12}\right)$$

$$K_{eq2} = \exp\left(\frac{A_{K21}}{T} + A_{K22}\right)$$

$$\frac{\partial T}{\partial Z} = \frac{A\rho_C \sum_{1}^{nr} R_{nr} \Delta H_{nr} + \pi D_i Q}{\sum_{1}^{nc} F_i C_{Pi}}$$

$$K_M * = {P_{H_2}}^2 \Big/ P_{CH_4}$$

$$K_B * = P_{CO_2} \Big/ {P_{CO}}^2$$

$$\frac{1}{U} = \frac{1}{h_i} + \frac{D_i \ln\left(D_o / D_i\right)}{2\lambda_w}$$

$$\frac{h_i D_p}{\lambda_m} = htfactor\left(2.58\,\mathrm{Re}_p^{1/3}\,\mathrm{Pr}^{1/3} + 0.094\,\mathrm{Re}_p^{0.8}\,\mathrm{Pr}^{0.4}\right)$$

$$\frac{dP}{dz} = -3.026 \cdot 10^{-7} Fpd\rho^3 u^2$$

$$Q = U\left(T_{wall} - T\right)$$

Furnace model

$$Q = F_G SG\left(a + bz + cz^2 + dz^3 + ez^4\right)\eta$$

Physical Properties

$$c_{pi} = \sum_{i}^{n} \left(a_m\right)_i T^{i-1}$$

$$\mu_i = \sum_{i}^{n} \left(a_m\right)_i T^{i-1}$$

$$\lambda_l = \sum_{i}^{n} \left(a_m\right)_i T^{i-1}$$

$$\mu_m = \sum_{i=1}^{NC} \frac{x_i \mu_i}{\sum_{k=1}^{NC} x_k \phi_{ik}}$$

$$\phi_{ik} = \frac{\left[1 + \left(\frac{\mu_i}{\mu_k}\right)^{0.5} \left(\frac{M_k}{M_i}\right)^{0.25}\right]^2}{\left[8\left(1 + \left(\frac{M_i}{M_k}\right)\right)\right]^{0.5}}$$

$$\lambda_m = \sum_{i=1}^{NC} \frac{x_i \lambda_i}{\sum_{k=1}^{NC} x_k A_{ik}}$$

$$A_{ik} = \phi_{ik}$$

notation:

A	Cross-sectional area
A_{Kii}	coefficient
A_{ik}	mixture conductivity parameter
a,b,c,d,e	polynomial coefficients
a_m	polynomial coefficient
C_{Pi}	Specific heat capacity for component i
D_i	Internal diameter
D_o	External diameter
D_P	Particle diameter
F_i	Molar flow rate of component i
F_G	Fuel gas flow rate
Fpd	coefficient
h_i	internal heat transfer coefficient
htfactor	coefficient
K_{eqi}	equilibrium constant for reaction i
K_M*	threshold constant for methane cracking
K_B*	threshold constant for Boudouard coking
M_i	molar mass of component i
P	Pressure
P_i	Partial pressure of component i
Pr	Prandtl number

Q	Heat flow from furance
R_i	Reaction rate for reaction i
R_g	Universal gas constant
Re_p	Reynold's number of the particle
S_G	specific gravity
T	Temperature
T_{wall}	wall temperature
u	gas velocity
U	Overall heat transfer coefficient
x_i	molar fraction
z	Axial distance
ΔH_i	enthalpy of reaction i
ϕ_{ik}	Wilke's parameter for mixture viscosity
λ_i	gaseous conductivity of component i
λ_m	average gaseous conductivity
λ_w	steel conductivity
μ_i	gaseous viscosity of component i
μ_m	average gaseous viscosity
ρ	density
ρ_c	catalyst density
η	unit efficiency

Equations for model [section 4.2.1]

Steam Reformer Tubes

$$\frac{\partial F_i}{\partial z} = A\rho \sum_{1}^{nc} \left(\eta_i Nu_{i1} R_1 + \eta_i Nu_{i2} R_2 + \eta_i Nu_{i3} R_3\right)$$

$$R_1 = \frac{k_1}{p_{H_2}^{2.5}} \left(p_{CH_4} p_{H_2O} - \frac{p_{H_2}^3 p_{CO}}{K_{eq1}} \right) \Big/ (DEN)^2$$

$$R_2 = \frac{k_2}{p_{H_2}} \left(p_{CO} p_{H_2O} - \frac{p_{H_2} p_{CO_2}}{K_{eq2}} \right) \Big/ (DEN)^2$$

$$R_3 = \frac{k_3}{p_{H_2}^{3.5}} \left(p_{CH_4} p_{H_2O}^2 - \frac{p_{H_2}^4 p_{CO_2}}{K_{eq3}} \right) \Big/ (DEN)^2$$

$$DEN = 1 + Ka_{CO} p_{CO} + Ka_{H_2} p_{H_2} + Ka_{CH_4} p_{CH_4} + Ka_{H_2O} p_{H_2O} / p_{H_2}$$

$$K_{eqi} = \exp\left(\frac{A_{Ki1}}{T} + A_{Ki2} \right)$$

$$\frac{\partial T}{\partial Z} = \frac{A\rho_C \sum_{1}^{nr} \eta_i R_{nr} \Delta H_{nr} + \pi D_i Q}{\sum_{1}^{nc} F_i C_{Pi}}$$

$$K_M * = {P_{H_2}}^2 \Big/ P_{CH_4}$$

$$K_B * = P_{CO_2} \Big/ {P_{CO}}^2$$

$$\frac{1}{U} = \frac{1}{h_i} + \frac{D_i \ln\left(D_o / D_i\right)}{2\lambda_w}$$

$$\frac{h_i D_p}{\lambda_m} = htfactor\left(2.58\,\mathrm{Re}_p^{1/3}\,\mathrm{Pr}^{1/3} + 0.094\,\mathrm{Re}_p^{0.8}\,\mathrm{Pr}^{0.4}\right)$$

$$\frac{dP}{dz} = -3.026 \cdot 10^{-7} Fpd\rho^3 u^2$$

$$Q = U(T_{wall} - T)$$

$$\frac{\partial^2 D_i^e p_i}{d\omega^2} = \rho_C R_{fi} R T l_c^{\,2}$$

$$\eta_i = \int_0^1 r_i \, d\omega / r_{ib}$$

$$\frac{1}{D_i^e} = \frac{1}{D_{ik}^e} + \sum_{\substack{j=1 \\ j \neq i}}^{n} \left[y_j - y_i \left(R_{fj} \Big/ R_{fi} \right) \right] \Big/ D_{ij}^e$$

$$G = \frac{C_D A_0}{v_2} \sqrt{\frac{2 P_1 v_1 \ln\left(\frac{P_1}{P_2}\right)}{1 - \left(\frac{v_1 A_0}{v_2 A_1}\right)^2}}$$

Furnace model

$$Q = F_G SG(a + bz + cz^2 + dz^3 + ez^4)\eta$$

Physical Properties

$$c_{pi} = \sum_i^n (a_m)_i T^{i-1}$$

$$\mu_i = \sum_i^n (a_m)_i T^{i-1}$$

$$\lambda_i = \sum_i^n (a_m)_i T^{i-1}$$

$$\mu_m = \sum_{i=1}^{NC} \frac{x_i \mu_i}{\sum_{k=1}^{NC} x_k \phi_{ik}}$$

$$\phi_{ik} = \frac{\left[1 + \left(\frac{\mu_i}{\mu_k}\right)^{0.5}\left(\frac{M_k}{M_i}\right)^{0.25}\right]^2}{\left[8\left(1 + \left(\frac{M_i}{M_k}\right)\right)\right]^{0.5}}$$

$$\lambda_m = \sum_{i=1}^{NC} \frac{x_i \lambda_i}{\sum_{k=1}^{NC} x_k A_{ik}}$$

$A_{ik} = \phi_{ik}$

notation:

A	Cross-sectional area
a,b,c,d,e	polynomial coefficients
A_{ik}	mixture conductivity parameter
A_{Kii}	coefficient
a_m	polynomial coefficient
C_D	discharge coefficient
C_{Pi}	Specific heat capacity for component i
D_i	Internal diameter
D_o	External diameter
D_P	Particle diameter
D_i^e	effective diffusivity of component i
D_{ik}^e	knudsen diffusivity of component i
DEN	Xu's parameter for reaction rate
F_i	Molar flow rate of component i

F_G	Fuel gas flow rate
Fpd	coefficient
G	mass flow rate of gas
h_i	internal heat transfer coefficient
htfactor	coefficient
K_{eqi}	equilibrium constant for reaction i
k_i	rate constant for reaction i
K_M*	threshold constant for methane cracking
K_B*	threshold constant for Boudouard coking
Ka_i	adsorption constant for component i
l_C	characteristic length of catalyst
M_i	molar mass of component i
P	Pressure
P_i	Partial pressure of component i
Pr	Prandtl number
Q	Heat flow from furance
R_{fi}	rate of change of component i
R_g	Universal gas constant
R_i	Reaction rate for reaction i
r_{ib}	rate of reaction i in bulk
Re_p	Reynold's number of the particle

S_G	specific gravity
T	Temperature
T_{wall}	wall temperature
U	Overall heat transfer coefficient
u	gas velocity
x_i	molar fraction
z	Axial distance
ΔH_i	enthalpy of reaction i
ϕ_{ik}	Wilke's parameter for mixture viscosity
λ_i	gaseous conductivity of component i
λ_m	average gaseous conductivity
λ_w	steel conductivity
μ_l	gaseous viscosity of component i
μ_m	average gaseous viscosity
ρ_c	catalyst density
ρ	density
η	unit efficiency
η_i	effectiveness factor of reaction I
υ	volume per unit mass of fluid
ω	dimensionless co-ordinate in catalyst pellet

Equations for model [section 4.3.1]

Steam Reformer Tubes

$$\frac{\partial F_i}{\partial t} = v\left(A\rho \sum_{1}^{nc} \left(Nu_{i1} R_1 + Nu_{i2} R_2 \right) - \frac{\partial F_i}{\partial z} \right)$$

$$R_1 = 127\sqrt{P} \exp\left(\frac{-8780}{R_g T} \right) \left(x_{CH_4} - \frac{x_{H_2}^3 x_{CO} P^2}{K_{eq1} x_{H_2O}} \right)$$

$$R_2 = \exp\left(\frac{-13880}{R_g T} + 8.23 \right) \sqrt{P} \left(x_{CO} - \frac{x_{H_2} x_{CO_2}}{K_{eq2} x_{H_2O}} \right)$$

$$K_{eq1} = \exp\left(\frac{A_{K11}}{T} + A_{K12} \right)$$

$$K_{eq2} = \exp\left(\frac{A_{K21}}{T} + A_{K22} \right)$$

$$\frac{\partial T}{\partial t} = u \left(\frac{A\rho_C \sum_{1}^{nr} R_{nr} \Delta H_{nr} + \pi D_i Q}{\sum_{1}^{nc} F_i C_{Pi}} - \frac{\partial T}{\partial Z} \right)$$

$$K_M * = {P_{H_2}}^2 \Big/ P_{CH_4}$$

$$K_B * = P_{CO_2} \Big/ {P_{CO}}^2$$

$$\frac{1}{U} = \frac{1}{h_i} + \frac{D_i \ln\left(D_o / D_i \right)}{2\lambda_w}$$

$$\frac{h_i D_p}{\lambda_m} = htfactor\left(2.58\,\mathrm{Re}_p^{1/3}\,\mathrm{Pr}^{1/3} + 0.094\,\mathrm{Re}_p^{0.8}\,\mathrm{Pr}^{0.4} \right)$$

$$\frac{dP}{dz} = -3.026 \cdot 10^{-7} Fpd\rho^3 u^2$$

$$Q = U(T_{wall} - T)$$

$$G = \frac{C_D A_0}{v_2} \sqrt{\frac{2P_1 v_1 \ln\left(\frac{P_1}{P_2}\right)}{1-\left(\frac{v_1 A_0}{v_2 A_1}\right)^2}}$$

Furnace model

$$Q = F_G SG\left(a + bz + cz^2 + dz^3 + ez^4\right)\eta$$

Physical Properties

$$c_{pi} = \sum_i^n (a_m)_i T^{i-1}$$

$$\mu_i = \sum_i^n (a_m)_i T^{i-1}$$

$$\lambda_i = \sum_i^n (a_m)_i T^{i-1}$$

$$\mu_m = \sum_{i=1}^{NC} \frac{x_i \mu_i}{\sum_{k=1}^{NC} x_k \phi_{ik}}$$

$$\phi_{ik} = \frac{\left[1 + \left(\frac{\mu_i}{\mu_k}\right)^{0.5} \left(\frac{M_k}{M_i}\right)^{0.25}\right]^2}{\left[8\left(1 + \left(\frac{M_i}{M_k}\right)\right)\right]^{0.5}}$$

$$\lambda_m = \sum_{i=1}^{NC} \frac{x_i \lambda_i}{\sum_{k=1}^{NC} x_k A_{ik}}$$

$$A_{ik} = \phi_{ik}$$

notation:

A	Cross-sectional area
A_{ik}	mixture conductivity parameter
A_{Kii}	coefficient
a_m	polynomial coefficient
a,b,c,d,e	polynomial coefficients
C_D	discharge coefficient
C_{Pi}	Specific heat capacity for component i
D_i	Internal diameter
D_o	External diameter
D_P	Particle diameter
F_i	Molar flow rate of component i
F_G	Fuel gas flow rate
Fpd	coefficient
G	mass flow rate of gas
h_i	internal heat transfer coefficient
htfactor	coefficient
K_{eqi}	equilibrium constant for reaction i
K_M*	threshold constant for methane cracking
K_B*	threshold constant for Boudouard coking
M_i	molar mass of component i
P	Pressure
P_i	Partial pressure of component i

Pr	Prandtl number
Q	Heat flow from furance
R_g	Universal gas constant
R_i	Reaction rate for reaction i
Re_p	Reynold's number of the particle
S_G	specific gravity
T	Temperature
T_{wall}	wall temperature
U	Overall heat transfer coefficient
u	gas velocity
x_i	molar fraction
z	Axial distance
ΔH_i	enthalpy of reaction i
ϕ_{ik}	Wilke's parameter for mixture viscosity
η	unit efficiency
λ_I	gaseous conductivity of component i
λ_m	average gaseous conductivity
λ_w	steel conductivity
μ_i	gaseous viscosity of component i
μ_m	average gaseous viscosity
ρ	density
ρ_c	catalyst density
υ	volume per unit mass of fluid

Equations for model [section 4.4.1]

Steam Reformer Tubes

$$u\frac{\partial C_i}{\partial z} = D_{er}\left(\frac{\partial^2 C_i}{\partial r^2} + \frac{1}{r}\frac{\partial C_i}{\partial r}\right) + \rho_C \sum_1^{nc}\left(Nu_{i1}R_1 + Nu_{i2}R_2\right)$$

$$R_1 = 127\sqrt{P}\exp\left(\frac{-8780}{R_g T}\right)\left(x_{CH_4} - \frac{x_{H_2}^3 x_{CO} P^2}{K_{eq1} x_{H_2O}}\right)$$

$$R_2 = \exp\left(\frac{-13880}{R_g T} + 8.23\right)\sqrt{P}\left(x_{CO} - \frac{x_{H_2} x_{CO_2}}{K_{eq2} x_{H_2O}}\right)$$

$$K_{eq1} = \exp\left(\frac{A_{K11}}{T} + A_{K12}\right)$$

$$K_{eq2} = \exp\left(\frac{A_{K21}}{T} + A_{K22}\right)$$

$$\sum_1^{nc} F_i C_{Pi}\frac{\partial T}{\partial Z} = K_{eff}\left(\frac{\partial^2 T}{\partial r^2} + \frac{1}{r}\frac{\partial T}{\partial r}\right) + \rho_C \sum_1^{nr} R_{nr}\Delta H_{nr}$$

$$K_M * = {P_{H_2}}^2 \Big/ P_{CH_4}$$

$$K_B * = P_{CO_2} \Big/ {P_{CO}}^2$$

$$\frac{1}{U} = \frac{1}{h_i} + \frac{D_i \ln\left(D_o / D_i\right)}{2\lambda_w}$$

$$\frac{h_i D_p}{\lambda_m} = htfactor\left(2.58\,\mathrm{Re}_p^{1/3}\,\mathrm{Pr}^{1/3} + 0.094\,\mathrm{Re}_p^{0.8}\,\mathrm{Pr}^{0.4}\right)$$

$$\frac{dP}{dz} = -3.026\cdot 10^{-7} Fpd\rho^3 u^2$$

$$Q = U\left(T_{wall} - T\right)$$

$$D_{er} = \frac{u_s[1-\varepsilon]D_p}{10}\left[1+19.4\left(\frac{D_p}{d_t}\right)^2\right]$$

$$\lambda_{er} = \frac{0.00255}{1+120\left(\frac{D_p}{d_t}\right)^2}\frac{u_s[1-\varepsilon]\rho_g D_p}{\mu}$$

$$\varepsilon = 1-\frac{h'}{g_i}\sum_{j_1}^{j_2} n_j v_{ij}$$

$$h' = \frac{N_T}{\pi\Delta r^2 L}$$

$$g_i = 2am-2i+1$$

Furnace model

$$Q = F_G SG\left(a+bz+cz^2+dz^3+ez^4\right)\eta$$

Physical Properties

$$c_{pl} = \sum_i^n (a_m)_i T^{i-1}$$

$$\mu_l = \sum_i^n (a_m)_i T^{i-1}$$

$$\lambda_l = \sum_i^n (a_m)_i T^{i-1}$$

$$\mu_m = \sum_{i=1}^{NC}\frac{x_i\mu_i}{\sum_{k=1}^{NC} x_k\phi_{ik}}$$

$$\phi_{ik} = \frac{\left[1+\left(\frac{\mu_i}{\mu_k}\right)^{0.5}\left(\frac{M_k}{M_i}\right)^{0.25}\right]^2}{\left[8\left(1+\left(\frac{M_i}{M_k}\right)\right)\right]^{0.5}}$$

$$\lambda_m = \sum_{i=1}^{NC} \frac{x_i \lambda_i}{\sum_{k=1}^{NC} x_k A_{ik}}$$

$$A_{ik} = \phi_{ik}$$

notation:

A	Cross-sectional area
A_{Kii}	coefficient
A_{ik}	mixture conductivity parameter
a_m	polynomial coefficient
a,b,c,d,e	polynomial coefficients
a	aspect ratio
C_i	Molar concentration of component i
C_{Pi}	Specific heat capacity for component i
D_{er}	effective radial diffusivity
D_i	Internal diameter
D_o	External diameter
D_P	Particle diameter
d_t	tube diameter
F_i	Molar flow rate of component i
F_G	Fuel gas flow rate
Fpd	coefficient
h_i	internal heat transfer coefficient
htfactor	coefficient

K_{eqi}	equilibrium constant for reaction i
K_M*	threshold constant for methane cracking
K_B*	threshold constant for Boudouard coking
L	length of bed
M	radius equivalent number of concentric cylindrical channels [CCCs]
M_i	molar mass of component i
N_T	total number of spheres in bed
P	Pressure
P_i	Partial pressure of component i
Pr	Prandtl number
Q	Heat flow from furance
R_g	Universal gas constant
R_i	Reaction rate for reaction i
Re_p	Reynold's number of the particle
S_G	specific gravity
T	Temperature
T_{wall}	wall temperature
U	Overall heat transfer coefficient
u	gas velocity
u_s	superficial velocity
v_{ij}	volume of solid in the i^{th} concentric cylindrical channel [CCC] due to sphere with centre in j^{th} CCC

x_i	molar fraction
z	Axial distance
ε	voidage
ΔH_i	enthalpy of reaction i
Δr	thickness of concentric cylindrical channels [CCCs]
ϕ_{ik}	Wilke's parameter for mixture viscosity
η	unit efficiency
λ_{er}	effective radial thermal conductivity
λ_I	gaseous conductivity of component i
λ_m	average gaseous conductivity
λ_w	steel conductivity
μ_i	gaseous viscosity of component i
μ_m	average gaseous viscosity
ρ	density
ρ_c	catalyst density
ρ_g	gas density

Equations for model [section 4.5.1]

Steam Reformer Tubes

$$\frac{\partial F_i}{\partial z} = A\rho\sum_{1}^{nc}\left(Nu_{i1}R_1 + Nu_{i2}R_2\right)$$

$$R_1 = 127\sqrt{P}\exp\left(\frac{-8780}{R_g T}\right)\left(x_{CH_4} - \frac{x_{H_2}^3 x_{CO} P^2}{K_{eq1} x_{H_2O}}\right)$$

$$R_2 = \exp\left(\frac{-13880}{R_g T} + 8.23\right)\sqrt{P}\left(x_{CO} - \frac{x_{H_2} x_{CO_2}}{K_{eq2} x_{H_2O}}\right)$$

$$K_{eq1} = \exp\left(\frac{A_{K11}}{T} + A_{K12}\right)$$

$$K_{eq2} = \exp\left(\frac{A_{K21}}{T} + A_{K22}\right)$$

$$\frac{\partial T}{\partial Z} = \frac{A\rho_C\sum_{1}^{nr} R_{nr}\Delta H_{nr} + \pi D_i Q}{\sum_{1}^{nc} F_i C_{Pl}}$$

$$K_M * = {P_{H_2}}^2 \Big/ P_{CH_4}$$

$$K_B * = P_{CO_2} \Big/ {P_{CO}}^2$$

$$\frac{1}{U} = \frac{1}{h_i} + \frac{D_i \ln\left(D_o / D_i\right)}{2\lambda_w}$$

$$\frac{h_i D_p}{\lambda_m} = htfactor\left(2.58\,\mathrm{Re}_p^{1/3}\,\mathrm{Pr}^{1/3} + 0.094\,\mathrm{Re}_p^{0.8}\,\mathrm{Pr}^{0.4}\right)$$

$$\frac{dP}{dz} = -3.026\cdot 10^{-7} Fpd\rho^3 u^2$$

$$Q = U(T_{wall} - T)$$

Steam Reformer Tubes: Physical properties

$$c_{pi} = \sum_{i}^{n} (a_m)_i T^{i-1}$$

$$\mu_i = \sum_{i}^{n} (a_m)_i T^{i-1}$$

$$\lambda_i = \sum_{i}^{n} (a_m)_i T^{i-1}$$

$$\mu_m = \sum_{i=1}^{NC} \frac{x_i \mu_i}{\sum_{k=1}^{NC} x_k \phi_{ik}}$$

$$\phi_{ik} = \frac{\left[1 + \left(\frac{\mu_i}{\mu_k}\right)^{0.5} \left(\frac{M_k}{M_i}\right)^{0.25}\right]^2}{\left[8\left(1 + \left(\frac{M_i}{M_k}\right)\right)\right]^{0.5}}$$

$$\lambda_m = \sum_{i=1}^{NC} \frac{x_i \lambda_i}{\sum_{k=1}^{NC} x_k A_{ik}}$$

$$A_{ik} = \phi_{ik}$$

Steam Reformer Tubes: notation:

A	Cross-sectional area
A_{Kii}	coefficient
A_{ik}	mixture conductivity parameter
a,b,c,d,e	polynomial coefficients
a_m	polynomial coefficient

C_{Pi}	Specific heat capacity for component i
D_i	Internal diameter
D_o	External diameter
D_P	Particle diameter
F_G	Fuel gas flow rate
F_i	Molar flow rate of component i
Fpd	coefficient
h_i	internal heat transfer coefficient
htfactor	coefficient
K_{eqi}	equilibrium constant for reaction i
K_M*	threshold constant for methane cracking
K_B*	threshold constant for Boudouard coking
M_i	molar mass of component i
P	Pressure
P_i	Partial pressure of component i
Pr	Prandtl number
Q	Heat flow from furance
R_g	Universal gas constant
R_i	Reaction rate for reaction i
Re_p	Reynold's number of the particle
S_G	specific gravity
T	Temperature
T_{wall}	wall temperature

U	Overall heat transfer coefficient
u	gas velocity
x_i	molar fraction
z	Axial distance
ΔH_i	enthalpy of reaction i
ϕ_{ik}	Wilke's parameter for mixture viscosity
η	unit efficiency
λ_i	gaseous conductivity of component i
λ_m	average gaseous conductivity
λ_w	steel conductivity
μ_i	gaseous viscosity of component i
μ_m	average gaseous viscosity
ρ_c	catalyst density
ρ	density

Furnace model

$$\frac{1}{\sqrt{g}}\frac{\partial}{\partial t}\left(\sqrt{g}\rho\right)+\frac{\partial}{\partial x_j}\left(\rho\tilde{u}_j\right)=s_m$$

$$\frac{1}{\sqrt{g}}\frac{\partial}{\partial t}\left(\sqrt{g}\rho u_i\right)+\frac{\partial}{\partial x_j}\left(\rho\tilde{u}_j u_i-\tau_{ij}\right)=-\frac{\partial p}{\partial x_i}+s_i$$

$$\tau_{ij}=2\mu s_{ij}-\frac{2}{3}\mu\frac{\partial u_k}{\partial x_k}\delta_{ij}-\overline{-\rho u_i' u_j'}$$

$$\frac{1}{\sqrt{g}}\frac{\partial}{\partial t}\left(\sqrt{g}\rho H\right)+\frac{\partial}{\partial x_j}\left(\rho\tilde{u}_j H-F_{h,j}-u_i\tau_{ij}\right)=\frac{1}{\sqrt{g}}\frac{\partial}{\partial t}\left(\sqrt{g}\rho\right)-\frac{\partial}{\partial x_j}\left(u_{c_j}p\right)+s_i u_i+s_h$$

$$F_{h,j} = k\frac{\partial T}{\partial xj} - \overline{\rho u_j' h'} + \sum_m h_m \rho D m \frac{\partial m_m}{\partial x_j}$$

$$F_{m,j} = \rho D_m \frac{\partial m_m}{\partial x_j} - \overline{\rho u_j' m_m'}$$

$$\frac{1}{\sqrt{g}}\frac{\partial}{\partial t}\left(\sqrt{g}\rho k\right) + \frac{\partial}{\partial x_j}\left(\rho \tilde{u}_j k - \frac{\mu_{eff}}{\sigma_k}\frac{\partial k}{\partial x_j}\right) = \mu_t\left(P + P_B\right) - \rho\varepsilon - \frac{2}{3}\left(\mu_t \frac{\partial u_i}{\partial x_i} + \rho k\right)\frac{\partial u_i}{\partial x_i}$$

$$\frac{1}{\sqrt{g}}\frac{\partial}{\partial t}\left(\sqrt{g}\rho\varepsilon\right) + \frac{\partial}{\partial x_j}\left(\rho \tilde{u}_j \varepsilon - \frac{\mu_{eff}}{\sigma_\varepsilon}\frac{\partial \varepsilon}{\partial x_j}\right) = \frac{\varepsilon}{k}\left[\mu_t\left(C_{\varepsilon 1}P + C_{\varepsilon 3}P_B\right) - \frac{2}{3}\left(\mu_t \frac{\partial u_i}{\partial x_i} + \rho k\right)\frac{\partial u_i}{\partial x_i}\right]$$

$$\mu_{eff} = \mu + \mu_t$$

$$\mu_t = f_\mu \frac{C_\mu \rho k^2}{\varepsilon}$$

$$P = 2 s_{ij} \frac{\partial u_i}{\partial x_j}$$

$$P_B = -\frac{g_i}{\sigma_{h,t}}\frac{1}{\rho}\frac{\partial \rho}{\partial x_i}$$

$$\varepsilon = \frac{k^{3/2}}{l}\left(1 + \frac{C_\varepsilon}{\mathrm{Re}_y}\right)$$

$$f_\mu = 1 - \exp\left(-\frac{1}{A_\mu}\mathrm{Re}_y\right)$$

$$\mathrm{Re}_y = \frac{\sqrt{k}y}{\nu}$$

$$l = \kappa C_\mu^{-0.75} y$$

$$S_R = \sum_{np}\sum_{nbj} S_j^i$$

$$S_j^i = \left(I_{n+1} - I_n\right)\underline{\Omega^i}.d\underline{A_j^i}\partial\underline{\Omega^i}$$

$$I_{n+1} = I_n e^{-ds^*} + \frac{E^*}{\pi}\left(1 - e^{-ds^*}\right)$$

$$I_i = \sum_j F_{ji} J_j$$

$$J_i = \varepsilon_r E_{B,i} + \rho_r I_i$$

$$F_{ij} = \sum_{k=1}^{N_{L,i}} \alpha_k f_{ij}$$

$$s^* = k_e s$$

$$k_e = k_a + k_s$$

$$E^* = \frac{1}{k_e}\left(k_a E_g + \frac{k_s}{4}\int_{4\pi} p\left(\underline{\Omega}, \underline{\Omega'}\right) I\left(\underline{\Omega'}\right) d\underline{\Omega'}\right)$$

$$\frac{\partial(\rho e)}{\partial t} = \frac{\partial}{\partial x_i}\left(k\frac{\partial T}{\partial x_i}\right) + s_e$$

$$\phi = \int_0^1 \hat{\phi}(f) P(f) df$$

$$P(f) = \frac{f^{a-1}(1-f)^{b-1}}{\int_0^1 f^{a-1}(1-f)^{b-1} df}$$

$$a = \frac{f}{g_f}\left[f(1-f) - g_f\right]$$

$$b = \frac{(1-f)}{f} a$$

Physical properties

$$\rho = \frac{p}{RT}\left(\sum_m \frac{m_m}{M_m}\right)$$

$$\left(\frac{c_p}{R}\right)_m = \sum_i^n (a_m)_i T^{i-1}$$

$$\ln(\Phi_m) = \sum \frac{(a_m)_i}{(\ln T^{i-1})}$$

$$\phi = \sum_{m \neq bg} m_m \phi_m + \left(1 - \sum_{m \neq bg} m_m\right)\phi_{bg}$$

$$(\varepsilon_p)_m = \sum_i^n (a_m)_i T^{i-1}$$

notation:

a_m	polynomial coefficients
c_p	specific heat capacity
$C_{\varepsilon x}, \sigma_k, \sigma_\varepsilon$	turbulence model coefficients
D_m	molecular diffusivity
E_g	black-body emissive power of gas at temperature T_g
$F_{h,j}$	diffusional energy flux in direction x_j
$F_{m,j}$	diffusional flux component in direction x_j
f_{ij}	view factor
$\sqrt{g}$	determinant of metric tensor
H	chemico-thermal enthalpy
h, h_m	static enthalpy
I_i	incident flux

J_i	total radiation flux
k	thermal conductivity
k	turbulence energy
k_a	gas absorption coefficient
k_s	gas scattering coefficient
m_m	mass fraction of mixture constituent m
M_m	molar mass of mixture constituent m
p	piezometric pressure
$p(\underline{\Omega}, \underline{\Omega}')$	probability that the radiation incident in direction $\underline{\Omega}'$ will be scattered to within $d\underline{\Omega}$ of $\underline{\Omega}$
P(f)	presumed probability density function
p_r	surface reflectivity
R	universal gas constant
s_h	energy source
s_i	momentum source components
s_m	mass source
T	temperature
t	time
u_i	absolute fluid velocity in direction x_i
$\tilde{u}_j$	relative velocity between fluid and local coordinate frame that moves
x_i	cartesian coordinate
a_m	polynomial coefficient

ε	turbulence energy dissipation rate
ε_r	surface emissivity
Φ_m	thermal conductivity or molecular viscosity of component m
ϕ_m	local mixture viscosity, thermal conductivity or mean specific heat capacity
ϕ_{bg}	background mixture viscosity, thermal conductivity or mean specific heat capacity
ϕ	temperature, density or species concentration
μ_t	turbulent viscosity
ρ	density
τ_{ij}	stress tensor components

Equations for model [section 5.1.1]

Combustion Section

$$\frac{K_3(T_C)}{K_4(T_C)} = \frac{(F_{H_2O} + 2X_3)[F_{CO} - 2(F_{air}x_{O_2} - X_3)]}{(F_{H_2} - 2X_3)[F_{CO_2} + 2(F_{air}x_{O_2} - X_3)]}$$

$$\sum_j F_j^2 \int_{T_{PR}}^{T_C} C_{pj}\,dT + \sum_{overall\ m} F_m^2 \int_{T_{air}}^{T_C} C_{pm}\,dT = (-\Delta H_{H_2})T_C 2X_3 + (-\Delta H_{CO})T_C 2(F_{air}x_{o_{2,air}} - X_3)$$

notation:

C_{Pj} molar heat capacity of component j

F_i molar flow rate of component i

K equilibrium constant

T temperature

T_C combustion temperature

T_{PR} temperature at inlet of reformer

X_i number of moles of oxygen

x_i mole fraction of component i

ΔH_R enthalpy of reaction R

Reactor Bed Section

$$\frac{\partial F_i}{\partial z} = A\rho \sum_{1}^{nc} \left(Nu_{i1} R_1 \right)$$

$$R_1 = \frac{k_m k_r}{k_m + k_r} \left(P_{CH_4} - P^e_{CH_4} \right)$$

$$K_{eq1} = \exp\left(\frac{A_{K11}}{T} + A_{K12} \right)$$

$$\frac{\partial T}{\partial Z} = \frac{A\rho_C \sum_{1}^{nr} R_{nr} \Delta H_{nr} + \pi D_i Q}{\sum_{1}^{nc} F_i C_{Pi}}$$

$$\frac{1}{U} = \frac{1}{h_i} + \frac{D_i \ln\left(D_o / D_i \right)}{2\lambda_w}$$

$$\frac{h_i D_p}{\lambda_m} = htfactor\left(2.58\,\mathrm{Re}_p^{1/3}\,\mathrm{Pr}^{1/3} + 0.094\,\mathrm{Re}_p^{0.8}\,\mathrm{Pr}^{0.4} \right)$$

$$\frac{dP}{dz} = -3.026 \cdot 10^{-7} Fpd\rho^3 u^2$$

$$Q = U\left(T_{wall} - T \right)$$

Reactor Bed Section: Physical Properties

$$c_{pi} = \sum_{i}^{n} \left(a_m \right)_i T^{i-1}$$

$$\mu_i = \sum_{i}^{n} \left(a_m \right)_i T^{i-1}$$

$$\lambda_i = \sum_{i}^{n} \left(a_m \right)_i T^{i-1}$$

$$\mu_m = \sum_{i=1}^{NC} \frac{x_i \mu_i}{\sum_{k=1}^{NC} x_k \phi_{ik}}$$

$$\phi_{ik} = \frac{\left[1 + \left(\frac{\mu_i}{\mu_k}\right)^{0.5} \left(\frac{M_k}{M_i}\right)^{0.25}\right]^2}{\left[8\left(1 + \left(\frac{M_i}{M_k}\right)\right)\right]^{0.5}}$$

$$\lambda_m = \sum_{i=1}^{NC} \frac{x_i \lambda_i}{\sum_{k=1}^{NC} x_k A_{ik}}$$

$A_{ik} = \phi_{ik}$

Reactor Bed Section: notation

A	Cross-sectional area
A_{Kii}	coefficient
A_{ik}	mixture conductivity parameter
a_m	polynomial coefficient
a,b,c,d,e	polynomial coefficients
C_{Pi}	Specific heat capacity for component i
D_i	Internal diameter
D_o	External diameter
D_P	Particle diameter
F_i	Molar flow rate of component i
F_G	Fuel gas flow rate
Fpd	coefficient

h_i	internal heat transfer coefficient
htfactor	coefficient
K_{eqi}	equilibrium constant for reaction i
k_m	Sherwood constant
k_r	reaction rate constant
M_i	molar mass of component i
P	Pressure
P_i	Partial pressure of component i
$P^e_{CH_4}$	equilibrium partial pressure of component i
Pr	Prandtl number
Q	Heat flow from furance
R_g	Universal gas constant
R_i	Reaction rate for reaction i
Re_p	Reynold's number of the particle
S_G	specific gravity
T	Temperature
T_{wall}	wall temperature
U	Overall heat transfer coefficient
u	gas velocity
x_i	molar fraction
z	Axial distance
ΔH_i	enthalpy of reaction i
ϕ_{ik}	Wilke's parameter for mixture viscosity

η	unit efficiency
λ_i	gaseous conductivity of component i
λ_m	average gaseous conductivity
λ_w	steel conductivity
μ_i	gaseous viscosity of component i
μ_m	average gaseous viscosity
ρ_c	catalyst density
ρ	density

Equations for model [section 5.2.1]

Combustion Section

$$\frac{1}{\sqrt{g}}\frac{\partial}{\partial t}\left(\sqrt{g}\rho\right)+\frac{\partial}{\partial x_j}\left(\rho\tilde{u}_j\right)=s_m$$

$$\frac{1}{\sqrt{g}}\frac{\partial}{\partial t}\left(\sqrt{g}\rho u_i\right)+\frac{\partial}{\partial x_j}\left(\rho\tilde{u}_j u_i-\tau_{ij}\right)=-\frac{\partial p}{\partial x_i}+s_i$$

$$\tau_{ij}=2\mu s_{ij}-\frac{2}{3}\mu\frac{\partial u_k}{\partial x_k}\delta_{ij}-\overline{-\rho u_i' u_j'}$$

$$\frac{1}{\sqrt{g}}\frac{\partial}{\partial t}\left(\sqrt{g}\rho H\right)+\frac{\partial}{\partial x_j}\left(\rho\tilde{u}_j H-F_{h,j}-u_i\tau_{ij}\right)=\frac{1}{\sqrt{g}}\frac{\partial}{\partial t}\left(\sqrt{g}\rho\right)-\frac{\partial}{\partial x_j}\left(u_{c_j}p\right)+s_i u_i+s_h$$

$$F_{h,j}=k\frac{\partial T}{\partial xj}-\overline{-\rho u_j' h'}+\sum_m h_m\rho Dm\frac{\partial m_m}{\partial x_j}$$

$$F_{m,j}=\rho D_m\frac{\partial m_m}{\partial x_j}-\overline{-\rho u_j' m_m'}$$

$$\frac{1}{\sqrt{g}}\frac{\partial}{\partial t}\left(\sqrt{g}\rho k\right)+\frac{\partial}{\partial x_j}\left(\rho\tilde{u}_j k-\frac{\mu_{eff}}{\sigma_k}\frac{\partial k}{\partial x_j}\right)=\mu_t\left(P+P_B\right)-\rho\varepsilon-\frac{2}{3}\left(\mu_t\frac{\partial u_i}{\partial x_i}+\rho k\right)\frac{\partial u_i}{\partial x_i}$$

$$\frac{1}{\sqrt{g}}\frac{\partial}{\partial t}\left(\sqrt{g}\rho\varepsilon\right)+\frac{\partial}{\partial x_j}\left(\rho\tilde{u}_j\varepsilon-\frac{\mu_{eff}}{\sigma_\varepsilon}\frac{\partial\varepsilon}{\partial x_j}\right)=\frac{\varepsilon}{k}\left[\mu_t\left(C_{\varepsilon 1}P+C_{\varepsilon 3}P_B\right)-\frac{2}{3}\left(\mu_t\frac{\partial u_i}{\partial x_i}+\rho k\right)\frac{\partial u_i}{\partial x_i}\right]$$

$$\mu_{eff}=\mu+\mu_t$$

$$\mu_t=f_\mu\frac{C_\mu\rho k^2}{\varepsilon}$$

$$P=2s_{ij}\frac{\partial u_i}{\partial x_j}$$

$$P_B=-\frac{g_i}{\sigma_{h,t}}\frac{1}{\rho}\frac{\partial\rho}{\partial x_i}$$

$$\varepsilon = \frac{k^{3/2}}{l}\left(1+\frac{C_\varepsilon}{\mathrm{Re}_y}\right)$$

$$f_\mu = 1-\exp\left(-\frac{1}{A_\mu}\mathrm{Re}_y\right)$$

$$\mathrm{Re}_y = \frac{\sqrt{k}y}{\nu}$$

$$l = \kappa C_\mu^{-0.75} y$$

$$S_R = \sum_{np}\sum_{nbj} S_j^i$$

$$S_j^i = \left(I_{n+1} - I_n\right)\underline{\Omega}^i . d\underline{A}_j^i \partial\underline{\Omega}^i$$

$$I_{n+1} = I_n e^{-ds^*} + \frac{E^*}{\pi}\left(1-e^{-ds^*}\right)$$

$$I_i = \sum_j F_{ji} J_j$$

$$J_i = \varepsilon_r E_{B,i} + \rho_r I_i$$

$$F_{ij} = \sum_{k=1}^{N_{L,i}} \alpha_k f_{ij}$$

$$s^* = k_e s$$

$$k_e = k_a + k_s$$

$$E^* = \frac{1}{k_e}\left(k_a E_g + \frac{k_s}{4}\int_{4\pi} p\left(\underline{\Omega},\underline{\Omega}'\right) I\left(\underline{\Omega}'\right) d\underline{\Omega}'\right)$$

$$\phi = \int_0^1 \hat{\phi}(f) P(f) df$$

$$P(f) = \frac{f^{a-1}(1-f)^{b-1}}{\int_0^1 f^{a-1}(1-f)^{b-1} df}$$

$$a = \frac{f}{g_f}\left[f(1-f) - g_f\right]$$

$$b = \frac{(1-f)}{f} a$$

Reactor bed

$$\frac{dp}{L} = -\alpha u - \beta u^2$$

$$u\frac{\partial C_i}{\partial z} = D_{er}\left(\frac{\partial^2 C_i}{\partial r^2} + \frac{1}{r}\frac{\partial C_i}{\partial r}\right) + \rho_C \sum_{1}^{nc}\left(Nu_{i1} R_1\right)$$

$$R_1 = \frac{k_m k_r}{k_m + k_r}\left(P_{CH_4} - P^e_{CH_4}\right)$$

$$K_{eq1} = \exp\left(\frac{A_{K11}}{T} + A_{K12}\right)$$

$$\sum_{1}^{nc} F_i C_{Pi}\frac{\partial T}{\partial Z} = K_{eff}\left(\frac{\partial^2 T}{\partial r^2} + \frac{1}{r}\frac{\partial T}{\partial r}\right) + \rho_C \sum_{1}^{nr} R_{nr}\Delta H_{nr}$$

$$K_M * = {P_{H_2}}^2 \Big/ P_{CH_4}$$

$$K_B * = P_{CO_2} \Big/ {P_{CO}}^2$$

$$\frac{1}{U} = \frac{1}{h_i} + \frac{D_i \ln\left(D_o / D_i\right)}{2\lambda_w}$$

$$\frac{h_i D_p}{\lambda_m} = htfactor\left(2.58\,\mathrm{Re}_p^{1/3}\,\mathrm{Pr}^{1/3} + 0.094\,\mathrm{Re}_p^{0.8}\,\mathrm{Pr}^{0.4}\right)$$

$$\frac{dP}{dz} = -3.026\cdot 10^{-7} Fpd\rho^3 u^2$$

$$Q = U\left(T_{wall} - T\right)$$

$$D_{er} = \frac{u_s[1-\varepsilon]D_p}{10}\left[1+19.4\left(\frac{D_p}{d_t}\right)^2\right]$$

$$\lambda_{er} = \frac{0.00255}{1+120\left(\frac{D_p}{d_t}\right)^2}\frac{u_s[1-\varepsilon]\rho_g D_p}{\mu}$$

$$\varepsilon = 1-\frac{h'}{g_i}\sum_{j_1}^{j_2} n_j v_{ij}$$

$$h' = \frac{N_T}{\pi \Delta r^2 L}$$

$$g_i = 2am - 2i + 1$$

Reactor bed: Physical Properties

$$c_{pi} = \sum_i^n (a_m)_i T^{i-1}$$

$$\mu_i = \sum_i^n (a_m)_i T^{i-1}$$

$$\lambda_i = \sum_i^n (a_m)_i T^{i-1}$$

$$\mu_m = \sum_{i=1}^{NC} \frac{x_i \mu_i}{\sum_{k=1}^{NC} x_k \phi_{ik}}$$

$$\phi_{ik} = \frac{\left[1+\left(\frac{\mu_i}{\mu_k}\right)^{0.5}\left(\frac{M_k}{M_i}\right)^{0.25}\right]^2}{\left[8\left(1+\left(\frac{M_i}{M_k}\right)\right)\right]^{0.5}}$$

$$\lambda_m = \sum_{i=1}^{NC} \frac{x_i \lambda_i}{\sum_{k=1}^{NC} x_k A_{ik}}$$

$$A_{ik} = \phi_{ik}$$

Reactor bed: notation:

A	Cross-sectional area
A_{Kii}	coefficient
A_{ik}	mixture conductivity parameter
a_m	polynomial coefficient
a,b,c,d,e	polynomial coefficients
a	aspect ratio
C_i	Molar concentration of component i
C_{Pi}	Specific heat capacity for component i
D_{er}	effective radial diffusivity
D_i	Internal diameter
D_o	External diameter
D_P	Particle diameter
d_t	tube diameter
F_i	Molar flow rate of component i
F_G	Fuel gas flow rate
Fpd	coefficient
h_i	internal heat transfer coefficient
htfactor	coefficient
K_{eqi}	equilibrium constant for reaction i

K_M*	threshold constant for methane cracking
K_B*	threshold constant for Boudouard coking
k_m	Sherwood constant
k_r	reaction rate constant
L	length of bed
m	radius equivalent number of concentric cylindrical channels [CCCs]
M_i	molar mass of component i
N_T	total number of spheres in bed
P	Pressure
P_i	Partial pressure of component i
$P^e_{CH_4}$	equilibrium partial pressure of component i
Pr	Prandtl number
Q	Heat flow from furance
R_g	Universal gas constant
R_i	Reaction rate for reaction i
Re_p	Reynold's number of the particle
S_G	specific gravity
T	Temperature
T_{wall}	wall temperature
U	Overall heat transfer coefficient
u	gas velocity
u_s	superficial velocity

v_{ij}	volume of solid in the i^{th} concentric cylindrical channel [CCC] due to sphere with centre in j^{th} CCC
x_i	molar fraction
z	Axial distance
α, β	coefficients
ε	voidage
ΔH_i	enthalpy of reaction i
Δr	thickness of concentric cylindrical channels [CCCs]
ϕ_{ik}	Wilke's parameter for mixture viscosity
η	unit efficiency
λ_{er}	effective radial thermal conductivity
λ_i	gaseous conductivity of component i
λ_m	average gaseous conductivity
λ_w	steel conductivity
μ_i	gaseous viscosity of component i
μ_m	average gaseous viscosity
ρ	density
ρ_c	catalyst density
ρ_g	gas density

Physical properties

$$\rho = \frac{p}{RT}\left(\sum_m \frac{m_m}{M_m}\right)$$

$$\left(\frac{c_p}{R}\right)_m = \sum_i^n (a_m)_i T^{i-1}$$

$$\ln(\Phi_m) = \sum \frac{(a_m)_i}{(\ln T^{i-1})}$$

$$\phi = \sum_{m \neq bg} m_m \phi_m + \left(1 - \sum_{m \neq bg} m_m\right)\phi_{bg}$$

$$(\varepsilon_p)_m = \sum_i^n (a_m)_i T^{i-1}$$

notation:

a_m	polynomial coefficient
$C_{\varepsilon x}, \sigma_k, \sigma_\varepsilon$	turbulence model coefficients
c_p	specific heat capacity
D_m	molecular diffusivity
E_g	black-body emissive power of gas at temperature T_g
$F_{h,j}$	diffusional energy flux in direction x_j
$F_{m,j}$	diffusional flix component in direction x_j
f_{ij}	view factor
$\sqrt{g}$	determinant of metric tensor
H	chemico-thermal enthalpy
h, h_m	static enthalpy

I_i	incident flux
J_i	total radiation flux
k	thermal conductivity
k	turbulence energy
k_a	gas absorption coefficient
k_s	gas scattering coefficient
m_m	mass fraction of mixture constituent m
p	pressure
$p(\underline{\Omega}, \underline{\Omega}')$	probability that the radiation incident in direction $\underline{\Omega}'$ will be scattered to within $d\underline{\Omega}$ of $\underline{\Omega}$
p_r	surface reflectivity
P(f)	presumed probability density function
R	universal gas constant
s_h	energy source
s_i	momentum source components
s_m	mass source
p	piezometric pressure
T	temperature
t	time
u_i	absolute fluid velocity in direction x_i
$\tilde{u}_j$	relative velocity between fluid and local coordinate frame that moves
x_i	cartesian coordinate

ε	turbulence energy dissipation rate
ε_r	surface emissivity
Φ_m	thermal conductivity or molecular viscosity of component m
ϕ_m	local mixture viscosity, thermal conductivity or mean specific heat capacity
ϕ_{bg}	background mixture viscosity, thermal conductivity or mean specific heat capacity
ϕ	temperature, density or species concentration
μ_t	turbulent viscosity
ρ	density
τ_{ij}	stress tensor components

Equations for model [section 6.2.1 and 6.2.2]

Combustion Section

$$\frac{1}{\sqrt{g}}\frac{\partial}{\partial t}\left(\sqrt{g}\rho\right)+\frac{\partial}{\partial x_j}\left(\rho\tilde{u}_j\right)=s_m$$

$$\frac{1}{\sqrt{g}}\frac{\partial}{\partial t}\left(\sqrt{g}\rho u_i\right)+\frac{\partial}{\partial x_j}\left(\rho\tilde{u}_j u_i-\tau_{ij}\right)=-\frac{\partial p}{\partial x_i}+s_i$$

$$\tau_{ij}=2\mu s_{ij}-\frac{2}{3}\mu\frac{\partial u_k}{\partial x_k}\delta_{ij}-\overline{-\rho u_i' u_j'}$$

$$\eta=\sum_i^n\left(a_m\right)_i {f_m}^{i-1}$$

$$\frac{1}{\sqrt{g}}\frac{\partial}{\partial t}\left(\sqrt{g}\rho H\right)+\frac{\partial}{\partial x_j}\left(\rho\tilde{u}_j H-F_{h,j}-u_i\tau_{ij}\right)=\frac{1}{\sqrt{g}}\frac{\partial}{\partial t}\left(\sqrt{g}\rho\right)-\frac{\partial}{\partial x_j}\left(u_{c_j}p\right)+s_i u_i+s_h$$

$$F_{h,j}=k\frac{\partial T}{\partial xj}-\overline{-\rho u_j' h'}+\sum_m h_m\rho Dm\frac{\partial m_m}{\partial x_j}$$

$$F_{m,j}=\rho D_m\frac{\partial m_m}{\partial x_j}-\overline{-\rho u_j' m_m'}$$

$$\frac{1}{\sqrt{g}}\frac{\partial}{\partial t}\left(\sqrt{g}\rho k\right)+\frac{\partial}{\partial x_j}\left(\rho\tilde{u}_j k-\frac{\mu_{eff}}{\sigma_k}\frac{\partial k}{\partial x_j}\right)=\mu_t\left(P+P_B\right)-\rho\varepsilon-\frac{2}{3}\left(\mu_t\frac{\partial u_i}{\partial x_i}+\rho k\right)\frac{\partial u_i}{\partial x_i}$$

$$\frac{1}{\sqrt{g}}\frac{\partial}{\partial t}\left(\sqrt{g}\rho\varepsilon\right)+\frac{\partial}{\partial x_j}\left(\rho\tilde{u}_j\varepsilon-\frac{\mu_{eff}}{\sigma_\varepsilon}\frac{\partial\varepsilon}{\partial x_j}\right)=\frac{\varepsilon}{k}\left[\mu_t\left(C_{\varepsilon 1}P+C_{\varepsilon 3}P_B\right)-\frac{2}{3}\left(\mu_t\frac{\partial u_i}{\partial x_i}+\rho k\right)\frac{\partial u_i}{\partial x_i}\right]$$

$$\mu_{eff}=\mu+\mu_t$$

$$\mu_t=f_\mu\frac{C_\mu\rho k^2}{\varepsilon}$$

$$P=2s_{ij}\frac{\partial u_i}{\partial x_j}$$

$$P_B=-\frac{g_i}{\sigma_{h,t}}\frac{1}{\rho}\frac{\partial\rho}{\partial x_i}$$

Reactor bed

$$\frac{dp}{L} = -\alpha u - \beta u^2$$

Physical properties

$$\rho = \frac{p}{RT}\left(\sum_m \frac{m_m}{M_m}\right)$$

$$\left(\frac{c_p}{R}\right)_m = \sum_i^n (a_m)_i T^{i-1}$$

$$\ln(\Phi_m) = \sum \frac{(a_m)_i}{(\ln T^{i-1})}$$

$$\phi = \sum_{m \neq bg} m_m \phi_m + \left(1 - \sum_{m \neq bg} m_m\right)\phi_{bg}$$

notation:

a_m	polynomial coefficient
$C_{\varepsilon\alpha}, \sigma_k, \sigma_\varepsilon$	turbulence model coefficients
D_m	molecular diffusivity
c_p	specific heat capacity
$F_{h,j}$	diffusional energy flux in direction x_j
$F_{m,j}$	diffusional flix component in direction x_j
f_m	mixture fraction
h, h_m	static enthalpy
$\sqrt{g}$	determinant of metric tensor
H	chemico-thermal enthalpy

k	thermal conductivity
k	turbulence energy
m_m	mass fraction of mixture constituent m
p	piezometric pressure
R	universal gas constant
s_h	energy source
s_i	momentum source components
s_m	mass source
T	temperature
t	time
u_i	absolute fluid velocity in direction x_i
$\tilde{u}_j$	relative velocity between fluid and local coordinate frame that moves
x_i	cartesian coordinate
ε	turbulence energy dissipation rate
Φ_m	thermal conductivity or molecular viscosity of component m
ϕ_m	local mixture viscosity, thermal conductivity or mean specific heat capacity
ϕ_{bg}	background mixture viscosity, thermal conductivity or mean specific heat capacity
η	temperature or molar fraction of component
μ_t	turbulent viscosity
ρ	density
τ_{ij}	stress tensor components

References

Adris, A.M., Pruden, B.B., Lim, C.J., and Grace, J.R., 1996, On the Reported Attempts to Radically Improve the Performance of the Steam Methane Reforming Reactor, Canadian J. of Chem, Eng., 74, 177-186

Alatiqi, M.A., Meziou, A.M., and Gasmelseed, G.A., 1989, Modelling, Simulation and Sensitivity Analysis of Steam Methane Reformers, Int. J. Hydro. Energy, 14 241-256

Alatiqi, I.M., and Meziou, A.M., 1991, Dynamic Simulation and Adaptive Control of an Industrial Steam Gas Reformer, Computers and Chemical Engineering, Vol. 15, No. 3, pp 147-155

Barbieri, G., and Di Maio, F.P., 1997, Simulation of the Methane Steam Re-forming Process in a Catalytic Pd-Membrane Reactor, Ind. Eng. Chem. Res., Vol. 36, pp 2121-2127

Basini, L., and Piovesan, L., 1998, Reduction on Synthesis Gas Costs by Decrease of Steam/Carbon and Oxygen/Carbon Ratios in the Feedstock, Ind. Eng. Chem. Res., Vol. 37, pp 258 – 266

Beaton, C.F. and Hewitt, G.F., 1989, Physical Property Data for the Design Engineer, Hemisphere Publishing Corporation, New York

Beek, J., 1962, Advances in Chemical Engineering 3, Academic Press, New York

Beer, J.M., and Chigier, N.A., 1972, Combustion Aerodynamics, Applied Science Publishers Ltd

Biegler, L.T. and Hildebrandt, D., 1995, Synthesis Of Chemical Reactor Networks, AIChE Symposium Series, Vol. 91, No. 304, pp 52-67

Binder, J.D., 1997, CFD: More Than Pretty Pictures, Aerospace America, Vol. 35, No.11, pp 17-19

Bird, R.B., Stewart, W.E. and Lightfoot, E.N., 2002, Transport Phenomena, 2nd edition, John Wiley & Sons, New York

Blanchard, K.L. and LeBlanc, J.R., 1994, Application of Combustion Chambers in Secondary Reformers, AIChE Ammonia Plant Safety, Vol. 34, pp 195-204

Bretsznajder, S., 1971. Prediction of Transport and other Physical Properties of Fluids. International Series of Monographs in Chemical Engineering, Vol. 11, pp 43 - 48

Brink, A., Mueller, C., Kilpinen, P. and Hupa, M., 2000, Possibilities and Limitations of the Eddy Break-up Model, Combustion and Flame, Vol. 123, pp 275 – 279

Brown, P.N., Hindmarsh, A.C., and Petzold, L.R., 1998, Consistent Initial Condition calculation for differential-algebraic systems, SIAM J. Sci. Stat. Comput., Vol. 19, No. 5, pp 1495-1512

Bunday, B., Basic optimisation Methods, Edward Arnold, 1985, London, England

Chang, C.L., and Liou., C.T., 1987, Development of a Hydrogen Plant Simulation Model via Process Simulation, Journal of Chinese Institute of Chemical Engineers, Vol. 18, Parts 4, pp 203-207

Chapra, S.C., and Canale, R.P., 1998, Numerical Methods for Engineers: with programming and software applications, 3ed., McGraw-Hill, Singapore

Chen, C.L., 1988, A class of successive quadratic programming methods for flowsheet optimisation, PhD. Thesis, Imperial College of Science and Technology, London

Cheung, S., Aaronson, P. and Edwards, T., 1995, CFD Optimisation Of A Theoretical Minimum-Drag Body, Journal of Aircraft, Vol. 32, No. 1, pp 193-198

Christensen, T.S., Dybkjaer, Ib., Hansen, L. and Primdahl, I.I., 1994, Design and Performance of Secondary and Autothermal Reforming Burners, AIChE Ammonia Plant Safety, Vol. 35, pp 205-215

Christensen, T.S., and Primdahl, I.L., 1994, Improve syngas production using autothermal reforming, Hydrocarbon Processing, Vol. 73, No. 3, pp 39 - 46

Coffee, T.P., 1985, On the simplified reaction mechanisms by oxidation of hydrocarbon fuels in flames by C.K. Westbrook, and F.L. Dryer, Combust. Sci. Tech, Vol. 43, pp 333-339

Collatz, L., 1966, The numerical treatment of differential equations, 3rd edition, 2nd printing, Springer-Verlag, Berlin, Germany

Cotton, W., 1999, Fluegas Flow Patterns in Top-Fired Steam Reforming Furnaces, IMTOF99, Billingham, UK

Computational Dynamics, 1998a, StarCD Version 3.05 Methodology, Computational Dynamics, London

Computational Dynamics, 1998b, StarCD Version 3.05 User Guide, Computational Dynamics, London

COMPUTATIONAL DYNAMICS. 2002. Software Platforms [online]. London: Computational Dynamics. http://www.cd-adapco.com/products/platforms.htm [accessed 22 July 2002]

Connaughton, G.E. and Clark, R.W., 1984, Secondary Reformer Catalyst Support Dome: Failure and Repair, AIChE Ammonia Plant Safety, Vol. 25, pp 73-78

Craig, K.J., De Kock, D.J., and Snyman, J.A., 1999, Using CFD and Mathematical Optimization to investigate Air Pollution due to Stacks, International Journal for Numerical Methods in Engineering, Vol. 44, pp 551-565

Cromarty, B.J., 1990, Carbon formation and removal in the primary reforming process, ICI Catalysts Customer Symposium Thaicat 90, Bangkok, Thailand

Cromarty, B.J., and Farnell, P.W., 1993, Steam Reformer Catalyst Loading, IMTOF '93, London, UK

Cuthrell, J.E. and Biegler, L.T., 1987, On The Optimisation Of Differential-Algebraic Process Systems, AIChE Journal, Vol. 33, No. 8, pp 1257-1270

Cuthrell, J.E. and Biegler, L.T., 1989, Simultaneous Optimization And Solution Methods For Batch Reactor Control Problems, Computers and Chemical Engineering, Vol. 13, No. 1/2, pp 49-62

Dadone, A. and Grossman, B., 2000, Progressive optimization of inverse fluid dynamic design problems, Computers & Fluids, Vol. 29, pp 1 – 32

Davies, J. and Lihou, D.A., 1971, Optimal Design of Methane Steam Refomer, Chem. Process Eng., Vol. 21, No.4, pp 71 – 80

Deen, N.G., Solberg T. and Hjertager, B.H., 2001, Large Eddy Simulation of the Gas-Liquid flow in a square cross-sectioned bubble column, Chem. Eng. Sci., Vol. 56, pp 6341 - 6349

Delmas, H. and Froment G.F.,1988, A simulation model accounting for structural radial nonuniformities in fixed bed reactors, Chem. Eng. Sci., Vol. 43, No. 8, pp 2281-2287

Dennis Jr., J.E. and Schnabel, R.B., 1983, Numerical methods for unconstrained optimisation and nonlinear optimisation, Prentice-Hall, New Jersey, USA

Detemmerman, T. and Froment, F., 1998, Three Dimensional Coupled Simulation of Furnaces and Reactor Tubes for the Thermal Cracking of Hydrocarbons, Rev. de L'Instuit Francais ou Petrole, 53, pp 181-194.

Dombrowski, N., Mahmud, T., Talaee, S., and Ahmad, A., 1996, Numerical Simulation Of Sprays From Pressure Nozzles In The Pressence Of Hot Gas, IChemE Research Event, 2nd European Conference for young researches, pp 645-647

Dryer, F.L., and Glassman, I., 1972, High-Temperature Oxidation of CO and CH_4, 14th Symposium on Combustion, Pennsylvania University, Pennsylvania, pp 987, 989, 1000

Dryer, F.L. and Glassman, I., 1973, High-Temperature Oxidation of CO and CH_4, Fourteen International Symposium on Combustion, Combustion Institute, Pittsburgh, pp 987 - 1002

Duffy, D.G., 1986, Solutions of partial differential equations, 1st Edition, TAB Books Inc., Blue Ridge Summit, USA

Dybkjaer, Ib., 1995, Tubular Reforming and Autothermal Reforming of Natural Gas – An Overview of Available Processes, Fuel Processing Technology, Vol. 42, Parts 2-3, pp 85-107

Edgar, T.F., and Himmelblau, D.M., 1989, Optimization of Chemical Processes, McGraw-Hill, Singapore

Elnashaie, S.S.E.H., Al-Ubaid., A.S., Solimanm M.A., and Adris, A.M., 1988, On the kinetics and reactor modelling of the Steam Reforming of Methane – A Review, Journal of Engineering Sciences, Vol. 14, Parts 2, pp 247-273

Elnashaie, S.S.E.H., Adris, A.M., Soliman, M.A. and Al-Ubaid, A.S., 1992, Digital Simulation of Industrial Steam Reformers for Natural Gas using Heterogeneous Models, Canadian Journal of Chemical Engineering, Vol. 70, pp 786-793

Elnashaie, S.S.E.H, Abdalla, B.K. and Hughes, R., 1993, Simulation of the Industrial Fixed Bed Catalytic Reactor for the Dehydrogenation of Ethylbenzene to Styrene: Heterogeneous Dusty Gas Model, Ind. Eng. Chem. Res., Vol. 32, pp 2537 – 2541

Elvers, B., Hawkins, S., Ravenscroft, M., Rounsaville, J.F., and Schulz, G., 1989a, Ullmann's Encyclopaedia of Industrial Chemistry, Volume A12, 5th Edition, VCH Verlagsgesellschalft mbH, Weinheim, Germany, pp 202-204

Elvers, B., Hawkins, S., Ravenscroft, M., Rounsaville, J.F., and Schulz, G., 1989b, Ullmann's Encyclopaedia of Industrial Chemistry, Volume A13, 5th Edition, VCH Verlagsgesellschalft mbH, Weinheim, Germany, pp 329-330

Farnell, P.W., 1992, Secondary Reforming: Theory and Application, AIChE Ammonia Plant Safety, Vol. 33, pp 24-33

Farnell, P.W., 1993, Secondary Reforming: Theory and Application, AIChE Ammonia Plant Safety, 1993, Vol. 32, pp 24 – 33

Farnell, P.W., 1996, Modern techniques for optimization of Primary Reformer Operation, AIChE Ammonia Plant Safety, Vol. 35, pp 32 – 38

Farnell, P.W., 1999a, The Tunnel Port Effect : Validation by Monte Carlo Simulation, IMTOF99, Billingham, UK

Farnell, P.W., 1999b, Investigation and Resolution of a Secondary Reformer Burner Failure, IMTOF99, Billingham, UK

Feinberg, M., 1999, Recent results in optimal reactor synthesis via attainable region theory, Chemical Engineering Science, Vol. 54, pp 2535-2543

Ferschneider, G., and Mege, P., 1993, Numerical simulation of Fixed-Bed Catalytic Reforming Reactions: Hydrodynamics/Chemical Kinetics Coupling, Revue de L'Institut Francais du Petrole, Vol. 48, No. 6, pp 711-721

Finlayson, B., 1972, The method of weighted residuals and variational principles, Academic Press, New York, USA

Fletcher, C.A.J., 1984, Computational Galerkin methods, Springer-Verlag, New York, USA

Fletcher, R.F., 1987, Practical methods of optimisation, 2nd Edition, John-Wiley and Sons, Chichester, UK

Fogler, H.S., 1992, Elements of Chemical Reaction Engineering, 2nd Edition, Prentice-Hall, New Jersey

Foumney, E.A., 1996, Computational Fluid Dynamics: Theory And Trends, IChemE Research Event, 2nd European Conference for young researches, pp 6-11

Fradette, L., Li, H.Z., Choplin, L. and Tanguy, P., 1998, 3D Finite Element Simulation Of Fluid Flow Through A SMX Static Mixer, Computers and Chemical Engineering, Vol. 22, Suppl., pp S759-S761

Fraga, E.S., 1998, The Generation and use of Partial Solutions in Process Synthesis, Trans IChemE, Vol. 76, Part A, IChemE, pp 45-54

Froment, G.F., De Deken, J.C. and Devos, E.F., 1982, Steam Reforming of Natural Gas: Intrinsic kinetics, diffusional influences and reactor design, American Chem. Soc., Vol. 43, pp 181 – 197

Froment, G.F., and Bischoff, K.B., 1990, Chemical Reactor Analysis and Design, 2ed, John Wiley and Sons, Singapore

Gani, L., and Rajan, S.D., 1999, Use of Fracture Mechanics and Shape Optimization for Component Designs, AIAA, Vol. 37, No. 2, pp 255-260

Gill, P.E., Murray, W., and Wright, M.H., 1981, Practical optimisation, Academic Press, London, UK

Goff, S.P., and Wang, S.I., 1985, Syngas Production by Reforming, 6th International Conference : Large Chemical Plants, Antwerp, Belgium

Goldstone, P. and Malik, N., 1999, Air Products improves burner performance, CFX Update, No. 17, pp 7

Govindarao, V.M.H. and Froment, G.F., 1986, Voidage profiles in packed beds of spheres, Chem. Eng. Sci., Vol. 41, No. 3, pp 533-539

Govindarao, V.M.H. and Ramrao, K.V.S., 1988, Prediction of location of particles in the wall region of a randomly packed bed of spheres, Chem. Eng. Sci., Vol. 43, No. 9, pp 2544-2545

Govindarao, V.M.H., Subbanna, M., Rao, A.V.S and Ramrao, K.V.S., 1990, Voidage profile in packed beds by multi-channel model: effects of curvature of the channels, Chem. Eng. Sci., Vol. 45, No. 1, pp 362-364

Grosshandler, W.L., 1993, RADCAL: A Narrow-Band Model for Radiation Calculations in a Combustion Environment, NIST Technical Note 1402, National Institute of Standards and Technology, Gaithersburg, USA

Gulijk, C., 1998, Using CFD To Calculate Transversal Dispersion In A Structured Packed Bed, Computers and Chemical Engineering, Vol. 22, Suppl., pp S767-S770

Ha, J. and Zhu, Z., 1998, Computation of turbulent reactive flows in industrial burners, Appl. Math. Mod., Vol. 22, pp 1059-1070

Harris, C.K., Roekaerts, D., Rosendal, F.J.J., Buitendijk, F.G.J., Daskopoulous, Ph., Vreenegoor, A.J.N. and Wang, H., 1996, Computational Fluid Dynamics For Chemical Reactor Engineering, Chemical Engineering Science, Vol. 51, No. 10, pp 1569-1594

Hilsenrath, J., 1960, Tables of Thermodynamic and Transport Properties of Air, Argon, Carbon Dioxide, Carbon Monoxide, Hydrogen, Nitrogen, Oxygen, and Steam. Pergamon Press, Oxford

Hjertager, L.K., Hjertager, B.H. and Solberg, T., 2001, CFD Modeling of Fast Chemical Reactions in Turbulent Liquid Flows, ESCAPE – 11, Copenhagen, pp 159 - 164

Hoek,W., and Schittkowski, K., 1981, Test examples for nonlinear programming codes, lecture notes in economics and mathematical systems 187, Springer-Verlag, Berlin

Hohmann, F.W., 1996, Improve steam reformer performance, Hydrocarbon Processing, Vol. 3, pp 71 -74

Holiday, S.O., Dombrowski, N. and Foumeny, E.A., 1996, The Design Optimisation Of Jet Mixers, IChemE Research Event, 2nd European Conference for young researches, pp 874-876

Holiday, S.O., 1996, Characterisation of flow in coaxial jet mixers, University of Leeds, Leeds, England

Hoomans, B.P.B, Kuipers, J.A.M., Briels, W.J., and van Swaaij, W.P.M., 1998, Comments and reply by authors on the paper "Numerical Simulation Of The Gas-Solid Flow In A Fluidized Bed By Combining Discrete Particle Method With Computational Fluid Dynamics" by B.H.Xu and A.B. Yu, Chemical Engineering Science, Vol. 53, No. 14, pp 2645-2646

Hossain, M.A., 1988, Best conditions to make syngas, Hydrocarbon Processing, Vol. 67, No. 5, pp 76-A – 76-C

Hottel, H.C. and Sarofim, A.F., 1967, Radiative Transfer, Mc Graw-Hill, New York

ICI, 1996, Operating Manual: Catalysis for steam reforming natural gas, ICI Katalco, 73W/055/2/CAT57, Billingham, UK

Hyman, M.H., 1968, Simulate Methane Reformer Reactions, Hydrocarbon Process., 47, 131-137

Jang, D.S., Jetli, R. and Acharya, S., 1986, Comparison of the PISO, SIMPLER and SIMPLEC Algorithms for the Treatment of the Pressure-Velocity Coupling in Steady Flow Problems, Numer. Heat Transfer, Vol. 19, pp 209 – 228

Jaworski, Z. and Dudczak, J., CFD Modelling Of Turbulent Macromixing In Stirred Tanks. Effect Of The Probe Size And Number On Mixing Indices, Computers and Chemical Engineering, Vol. 22, Suppl., 1998, pp S293-S298

Kee, R.J., Rupley, F.M. and Miller, J.D., 1990, The Chemkin thermodynamic data base, Sandia Report, SAND 87-8215B.UC-4

Koenig, J., Kontopoulos, A.J., Dybkjaer, Ib., and Rostrup-Nielsen, T., 1997, Capacity increase of Ammonia Plants: Two Options, , AIChE Ammonia Plant Safety, Vol. 38, pp 206-215

Kosek, J., Stepanek, F., Novak, A., Grof, Z. and Marek, M., 2001, Multi-scale modelling of growing polymer particles in heterogeneous catalytic reactors, European Symposium on Computer Aided Process Engineering - 11, Kolding, Denmark, Elsevier, 177 - 182

Knight, D.D., 1997, Automated Optimal Design Using Cfd And High Performance Computing, Lecture Notes in Computer Science, Vol. 1215, pp 198-221

Kulasekaran S., Linjewile T.M. and Agarwal,. P.K., 1999, Mathematical modelling of fluidised bed combustion 3. Simultaneous combustion of char and combustible gases, Fuel, Vol. 78, pp 403 – 417

Kvamsdal, H.M., Svendesen, H.F., Hertzberg, T., and Olsvik, O., 1999, Dynamic Simulation and Optimisation of catalytic steam reformer, Chem. Eng. Sci., Vol. 54, pp 2697 – 2706

LeBlanc, J.R., Schneider III, R.V, Wright, K.W., and Lai, B., 1995, Simple, Safe and Reliable KRES: First Commercial Application, AIChE Ammonia Plant Safety, Vol. 36, pp 38-51

LeBlanc, J.R., Schneider III, R.V., Wright, K.W. and Lai, B., 1996, Simple, Safe and Reliable KRES: First Commercial Application, AIChE Ammonia Plant Safety, Vol. 35, pp 38 – 51

Levent, M., Budak, G., and Karabulut, A., 1998, Estimation of concentration and temperature profiles for methane-steam reforming reaction in a porous catalyst, Fuel Processing Technology, Vol. 55,No. 3, pp 251-263

Libby, P.A. and Williams, F.A., 1994, Turbulent Reacting Flows, Academic Press, London

Lockwood, F.C. and Shah, N.G., 1981, A new radiation solution method for incorporation in general combustion prediction procedures, Eighteenth International Symposium on Combustion, Combustion Institute, Pittsburgh, pp 625 – 632

Logsdon, J.S. and Biegler, L.T., 1992, Accurate Determination Of Optimal Reflux Policies For The Maximum Distillate Problem In Batch Distillation, National AIChE Meeting, New Orleans, April 1992, Paper 61 d

McKenna, T.F., Cokljat, D. and Wild, P., 1998, CFD Modelling Of Heat Transfer During Gas Phase Olefin Polymerisation, Computers and Chemical Engineering, Vol. 22, Suppl., pp S285-S292

McKetta, J.J, and Cunningham, W.A., 1977, McKetta Encyclopaedia of Chemical Processing and Design, Volume 3, Marcel Dekker Inc., New York, USA

McKetta, J.J, 1994, McKetta Encyclopaedia of Chemical Processing and Design, Volume 47, Marcel Dekker Inc., New York, USA

Maggioris, D., Goulas, A., Alexopoulos, A.H., Chatzi, E.G. and Kiparissides, C., 1998, Use Of CFD In Prediction Of Particle Size Distribution In Suspension Polymer Reactors, Computers and Chemical Engineering, Vol. 22, Suppl, pp S315-S322

Manickam, M., Schwarz, M.P. and Perry, J., 1998, CFD modelling of Waste Heat Recovery Boiler, Appl. Math. Model, Vol. 22, pp 823 – 840

Maskan, F., Wiley, D.E., and Clements, D.J., 2001, Optimisation of Reverse Osmosis Membrane System Using Gradient-Based and Evolutionary Computation Methods: A Comparison, 6th World Congress of Chemical Engineering, Melbourne, Australia

MET OFFICE. 2004. The great storm of 1987 [online]. London: Met Office. http://www.metoffice.com/education/historic/1987.html [accessed 27 May 2004]

Miyasugi, T., Kosaka, S., Kawai, T. and Suzuki, A., 1984, A Heat-Exchanger Type Steam Reformer for Ammonia Production, AIChE Ammonia Plant Safety, Vol. 25, pp 64-68

Moe, J.M. and Gerrard, E.R., 1965, Chemical Reaction and Heat Transfer Rates in the Steam Methane Reaction, AIChE 56th National Meeting, San Fransico, California

Morton, W., 1998, Department of Chemical Engineering, University of Edinburgh, Private Communication

Murdoch, R. and Still K., 1996, Elimination of Carbon Formation in Secondary Reformer System, AIChE Ammonia Plant Safety, Vol. 35, pp 82 – 89

Murray, A.P. and Snyder, T.S., 1985, Steam-Methane Reformer Kinetic Computer model with heat transfer and geometry options, Ind. Eng. Chem. Process Des. Dev., Vol. 24, pp 286 – 294

Nagy, Z., Agachi, S., Allgower, F., Findeisen, R., Diehl, M., Bock, H.G., and Schloder, J.P., 2001, Using genetic algorithms in robust nonlinear model predictive control, ESCAPE-11, Kolding, Denmark, pp 711 - 716

Ng, K.M., 2001, A Multiscale-Multifaceted to process synthesis and development, European Symposium on Computer Aided Process Engineering - 11, Kolding, Denmark, Elsevier, 41 - 54

Nithiarasu, P., and Zienkiewicz, O.C., 2000, Adaptive mesh generation for fluid mechanics problems, Int. J. Numer. Meth. Engng., Vol. 47, p 629 - 662

Noble, R., Tremayne, D., and Green, A., 1998, Thrust – Through the Sound Barrier, Transworld Publishers, London, UK

Oh, P.P., Rangaiah, G.P. and Ray, A.K., 2001, Optimal Design and Operation of an Industrial Hydrogen Plant for Multiple Objectives, *In:* Luss, R., Recent Developments in Optimization and Optimal Control in Chemical Engineering, Research Signposts, 2002, Trivandrum, India

Oh, S.C., and Yeo, Y.K., 1998, Adaptive Predictive Control of Steam-Reforming Plant Using Bilinear Model, Journal of Chemical Engineering of Japan, Vol.31, No.6, pp 1007-1013

Omtveit, T., Tanskanen, J. and Lien, K.M., 1994, Graphical Targeting Procedures For Reactor Systems, Computers and Chemical Engineering, Vol. 18, Suppl., pp S113-S118

Oran, E.S., and Boris, J.P., 2001, Numerical Simulation of Reactive Flow, 2nd Edition, Cambridge University Press, New York

Orphanides, P., 1993, Developments in Natural Gas Reforming Technology for Syngas, AIChE Ammonia Plant Safety, Vol. 34, pp 292-312

Pandiella, S.S., Garcia, L.A., Diaz, M. and Webb, C., 1996, Simulation Of The Fluid Dynamics In A Bubble Column Using CFD: Analyis Of The Solution Procedure, IChemE Research Event, 2nd European Conference for young researches, pp 961-963

Papageorgiou, J.N. and Froment, G.F., 1995, Simulation Models Accounting for Radial Voidage Profiles in Fixed-Bed Reactors, Chem. Eng. Sci., Vol. 50, No. 19, pp 3043 - 3056

Pantelides C.C., 1988, The consistent initialization of differential-algebraic systems, SIAM J. Sci. Stat. Comput., Vol. 9, No. 2, pp 213 - 231

Perry, R.H., Green, D.W. and Maloney, J. O., 1997, Perry's Chemical Engineer's Hanbook, 7th edition, McGraw-Hill, New York

Pierce, C.D. and Moin, P., 1998, Method For Generating Equilibrium Swirling Inflow Conditions, AIAA, Vol. 36, No. 7, pp 1325-1327

Pipilis, K.G., 1990, Higher order moving finite element methods for systems described by partial differential-algebraic equations, Imperial College of Science, Technology and Medicine

Plehiers, P.M. and Froment, G.F., 1989, Coupled Simulation of Heat Transfer and Reaction in a Steam Reforming Furnace, Chem. Eng. Tech., 12, 20-26

Poloni, C., 2001, Frontier System : A state of the art tool for multidisciplinary design optimisation, London, UK

Press, W.H., Teukolsky, S.A., Vetlerling, W.T., and Flannery, B.P., 1992, Numerical Recipies In Fortran, 2ed, Cambridge university press, USA

PROCESS SYSTEMS ENTERPRISE. 2002. Lifecycle Analysis [online]. London: Process Systems Enterprise.
http://www.psenterprise.com/products_gproms_lifecycle_modelling.html [accessed 22 July 2002]

Rajesh, J.K., Gupta, S.K., Rangaiah, G.P. and Ray, A.K., 2000, Multiobjective Optimization of Steam Reformer Performance Using Genetic Algorithm, Ind. Eng. Chem. Res., Vol. 39, pp 706 – 717

Rase, H.F., 1990, Fixed-Bed Reactor Design and Diagnostics: Gas Phase Reactions, Butterworths, London, UK

Ravi, K., Joshi, Y.K., Dhingra, S.C. and Guha, B.K., 1989, Simulation of Primary and Secondary Reformers for Improved Energy Performance of an Ammonia Plant, Chem. Eng. Tech., 12, 358-364

Razinsky, E. and Brighton, J.A., 1971, Confined Jet Mixing for Nonseparating Conditions, Journal of Basic Engineering, Vol. 12, pp 333 – 349

Reid, R.C., Prausnitz, J.M. and Sherwood, T.K., 1977, The Properties of Gases and Liquids, 3 ed. McGraw-Hill, New York

Reklaitis, G.V., Ravindran, A., and Ragsdell, K.M., 1983, Engineering optimisation, John-Wiley and Sons, New York, USA

Richardson, J.A., 1983, Boudouard Carbon and Metal Dusting in Steam Reforming Plants, ICI Katalco, Billingham, UK

Robbins, L.A., 1991, Improve Pressure-Drop Prediction with a New Correlation, Chem. Eng. Prog., 87, pp.87-91

Rocha de Avila, P.R. and Neto, A.S., 1993, Secondary Reformer Air Mixture Failure, AIChE Ammonia Plant Safety, Vol. 34, pp 229-235

Rodi, W., 1991, Influence of Buoyancy and Rotation on equations for Turbulent Length Scale, Second Symposium on Turbulent Shear Flows, New York

Roesler, F.C., 1967, Theory of Radiative Heat Transfer in Co-current Tube Furnaces, Chem. Eng. Sci., 22, 1325-1336

Rosen, M.A., 1991, Thermodynamic investigation of hydrogen production by Steam Methane Reforming, International Journal of Hydrogen Energy, Vol. 16, No. 3, pp 207 – 217

Rosen, M.A., 1996, Thermodynamic comparison of Hydrogen Production Processes, Int. J. Hydrogen Energy, Vol. 21, No. 5, pp 349-365

Rosen, O. and Luus, R., 1991, Evaluation of Gradients for Piecewise Constant Optimal Control, Comp. Chem. Engng., Vol.15, No. 4, pp 273-281

Rostrup-Nielsen, J.R., 1975, Steam reforming catalysts, Danish technical press Inc., Copenhagen, Denmark

Rostrup-Nielsen, J.R. and Tottrup, P.B., 1979, Steam Reforming of Heavy Feedstocks, Proc. Symposium on Science of Catalysis and its application in industry, pp 379

Rostrup-Nielsen, J.R., 1984, Catalytic Steam Reforming, Catalysis – Science and Technology, Vol 5., Anderson A.R. and Boudart, M. :eds, Springer, Berlin

Seddon, D., 1994, Technology and Economics of Gas Utilisation: Methanol, SPE - Asia Pacific Oil and Gas Conference, pp 473-484

Shaw, G., de Wet, H., and Hohmann, F., 1994, Commissioning of World's Largest Oxygen Blown Secondary Reformer, AIChE Ammonia Plant Safety, Vol. 35, pp 315-335

Siminiceanu, I, and Ungureanui, F., 1997, Methanol Steam Reforming : A Thermodynamic Study, Revista de Chimie, Vol. 48, No. 9, pp 785-791

Singh, J. and Patel, J.J., 1995, Equipment Performance of Ammonia Plant at 120% Load, AIChE Ammonia Plant Safety, Vol. 36, pp 198-206

Singh, J. and Patel, J.J., 1996, Equipment Performance of Ammonia Plant at 120% Load, AIChE Ammonia Plant Safety, 1996, Vol. 35, pp 198 – 206

Singh, C.P.P. and Saraf, D.N., 1979, Simulation of Side Fire Steam-Hydrocarbon Reformers, Ind. Eng. Chem. Proc. Design and Develop., 18, 1-7

Singh, C.P.P. and Saraf, D.N., 1981, Process Simulation of Ammonia Plant, Ind. Eng. Chem. Proc. Design and Develop., Vol. 20, 425 – 433

Slooff, J.W., and Schmidt, W., 1994, Advisory group for Aerospace research and development (AGARD) Computational Aerodynamics based on the Euler Equations, Canada Communication Group, Hull (Quebec), Canada

Slooff, J.W. and Schmidt, W., 1994, Advisory group for Aerospace research and development (AGARD) Appraisal of the suitability of turbulence models in flow calculations, Canada Communication Group, Hull (Quebec), Canada

Smith, E.M.B, and Pantelides, C.C., 1995, Global optimisation of general process models, Grossmann, I.E., Global Optimisation in Engineering Design, Boston (in press)

Snyder, G.D., Wang, S.I., and Palmer, B.L., 1986, Hydrogen plant expansion using Oxygen Secondary Reforming, National Petroleum Refiners Association, AM-86-47, pp 1-27

Soliman, M.A., El-Nashaie, S.S.E.H, Al-Ubaid, A.S. and Adris, A., 1988, Simulation of Steam Reformers for Methane, Chemical Engineering Science, Vol. 43, No. 8, pp 1801-1806

Srinivasan R.A., Sriramulu, S., Kulasekaran, S. and Agarwal, P.K., 1998, Mathematical modelling of fluidised bed combustion – 2: combustion of gases, Fuel, Vol. 77, No. 9/10, pp 1033 – 1049

Sun, Y., Pantelides, C.C., and Chalabi, Z.S., 1995, Mathematical Modelling and Simulation of Near-Ambient Grain Drying, Comp. Electr. Agric., 13, 243-271

Svenningsen, S.H., Madsen, J.I., Hassing, N.H., and Pauker, W.H., 1996, Optimisation Of Flow Geometries Applying Quasianalytical Sensitivity Analysis, Applied Mathematical Modelling, Vol. 20, March, pp 214-224

Teixeira, A.C.S.C and Giudici, R., 1999, Deactivation of steam reforming catalysts by sintering: experiments and simulation, Chem Eng. Sci., Vol. 54, pp 3609 – 3618

Thring, M.W., and Newby, M.P., 1953, Combustion length of enclosed Turbulent Jet Flames, 4th Symposium (International) on Combustion, Williams and Wilkins, pp 789-796

Tillack, D.J. and Guthrie, J.E., 1999, Select the Right Alloys for Refineries and Petrochemical Plants, Chem. Eng. Prog., Vol. 39, pp 59 - 66

Trimm, D.L., 1997, Coke formation and minimisation during steam reforming reactions, Catalysis Today, Vol. 37, pp 233-238

Twigg, M.V., 1997, Catalyst Handbook, Manson Publishing, London

Ucer, A.S., 1994, Advisory group for Aerospace research and development (AGARD) Turbomachinery design using CFD, Canada Communication Group, Hull (Quebec), Canada

Upreti, S.R. and Deb, K., 1997, Optimal Design Of An Ammonia Synthesis Reactor Using Genetic Algorithms, Computers and Chemical Engineering, Vol. 21, No. 1, pp 87-92

Vasantharajan, S. and Biegler, L.T., 1990, Simultaneous Strategies For Optimization Of Differential-Algebraic Systems With Enforcement Of Error Criteria, Computers and Chemical Engineering, Vol. 14, No. 10, pp 1083-1100

Venkatasubramanian, V., Chan, K., Sundaram, A. and Caruthers, J.M., 1995, Designing Molecules With Genetic Algorithms, AIChE Symposium Series, Vol. 91, No. 304, pp 270-275

Versteeg, H.K., and Malalasekera, W., 1995, An introduction to Computational Fluid Dynamics: The finite Volume Method, Longham Scientific and Technical, Harlow, England

Vick, K.A., 1987, Inspection and Repair of a Secondary Reformer, AIChE Ammonia Plant Safety, Vol. 27, pp 113 – 117

Vieira, R.C., and Biscaia Jr., E.C., 2001, Direct methods for consistent initialization of DAE systems, Comp. Chem. Eng., Vol. 25, pp 1299 - 1311

Villadsen, J. and Michelsen, M.L., 1978, Solution of Differential equation models by polynomial approximation, Prentice-Hall Inc., Englewood Cliffs, New Jersey, USA

Vortmeyer, D. and Haidegger, E., 1991, Discrimination of three approaches to evaluate heat fluxes for wall-cooled fixed bed chemical reactors, Chem. Eng. Sci., Vol. 46, No. 10, pp 2651-2660

Wagner, E.S., and Froment, G.F., 1992, Steam reforming analyzed, Hydrocarbon Processing, Vol. 71, No. 7, pp 69 - 77

Wesenberg, M.H., Grislingas, A., and Grevskott, S., 2001, Heat Transfer in Steam Reformer Tubes, 6th World Congress of Chemical Engineering, Melbourne, Australia

Westbrook, C.K. and Dryer, F.L, 1981, Simplified Reaction Mechanisms for the Oxidation of Hydrocarbon Fuels in Flames, Comb. Sci. & Tech., Vol. 27, pp 31-43

Winkel, M.L., Zullo, L.C., Verheijen, P.J.T., and Pantelides, C.C., 1995, Modelling and Simulation of the Operation of an Industrial Batch Plant Using gPROMS, Comp. Chem. Eng., 19, S571-S576

Wujek, B.A. and Renaud, J.E., 1998a, New Adaptive Move-Limit Management Strategy For Approximate Optimisation, Part 1, AIAA, Vol. 36, No. 10, pp 1911-1921

Wujek, B.A. and Renaud, J.E., 1998b, ,New Adaptive Move-Limit Management Strategy For Approximate Optimisation, Part 2, AIAA, Vol. 36, No. 10, pp 1922-1934

Xu, J., and Froment, G.F., 1989a, Methane Steam Reforming, Methanation and Water-Gas Shift: I. Intrinsic Kinetics, AIChE J., Vol. 35, No.1, pp 88-96

Xu, J., and Froment, G.F., 1989b, Methane Steam Reforming, Methanation and Water-Gas Shift: II. Diffusional Limitations and Reactor Simulation, AIChE J., Vol. 35, No.1, pp 97-103

Yetter R.A., Dryer, F.L. and Rabitz, H.,1986, Complications of one-step kinetics for moist CO-oxidation, Twenty first International Symposium on Combustion, Combustion Institute, Pittsburgh, pp 749-760

Yossefi, D., Belmont, M.R., Ashcroft, S.J., Abraham, M., Thurley, R.W.F. and Maskell, S.J., 1995, Early Stages Of Combustion In Internal Combustion Engines Using Linked CFD And Chemical Kinetics Computations And Its Applications To Natural Gas Burning Engines, Combustion Science and Technology, Vol. 130, No. 1-6, pp 171-200

Yossefi, D., Belmont, M.R., Ashcroft, S.J., Abraham, M., Thurley, R.W.F. and Maskell, S.J., 1997, Early stages of Combustion in Internal Combustion Engines Using Linked CFD and Chemical Kinetics Computations and its Applications to Natural Gas Burning Engines, Combust. Sci. & Tech., Vol. 130, pp 171-200

Yule A.J., Damou, M. And Kostopoulos, D., 1993, Modelling confined jet flow, International Journal of Heat and Fluid Flow, Vol. 14, No. 1, pp 10 – 16

Yustos, J., 1999, Modelling and Simulation of a Primary Steam Reformer Using gPROMS, Internal Report, University of Bradford, Bradford, UK

Zhang, D. and Frankel, S.H., 1998, A numerical study of natural gas combustion in a lean burn engine, Fuel, Vol. 77, No. 12, pp 1339-1347

Zhang, S., and Yu., Y., 1995, Simulation analysis and optimisation of Steam Reforming Process for a large-scale Ammonia Plant, Chinese Journal of Chemical Engineering, Vol. 3, Parts 4,pp 223-232

Zidan, M.S., 2001, Private Communication, Sirte Oil Company Ltd., Brage, Libya

Zwillinger, D., 1989, Handbook of Differential Equations, 3rd edition, Academic Press, New York, USA